N° d'ordre Année 2012

Thèse

Mélanges de polymères à base de Poly(acide lactique) : Relation Structure/ rhéologie/ procédés de mise en forme

Présentée devant
L'institut national des sciences appliquées de Lyon

Pour obtenir
Le grade de docteur

Ecole doctorale : Ecole doctorale matériaux de Lyon
Spécialité : Matériaux polymères

Par
Racha AL-ITRY
(Ingénieur)
Soutenance prévue le 27 Novembre 2012 devant la Commission d'examen

Jury

N. BILLON	Professeur	Rapporteur
Y. GROHENS	Professeur	Rapporteur
M. BOUSMINA	Professeur	Examinateur
C. CARROT	Professeur	Examinateur
K. LAMNAWAR	Maître de conférences	Co-encadrant de thèse
A. MAAZOUZ	Professeur	Directeur de thèse

Ingénierie des Matériaux Polymères (UMR 5223)
Laboratoire des Matériaux Macromoléculaires (INSA de Lyon)

Mélanges de polymères à base de Poly (acide lactique) : Relation structure/ rhéologie/ procédés de mise en forme

Résumé

Ce travail de thèse porte sur l'étude des relations structure/procédés de mise en forme/propriétés finales de matériaux polymères à base de PLA/PBAT. Ces derniers sont destinés à l'emballage alimentaire en vue de remplacer le polyéthylène téréphtalate (PET). Cependant le PLA a certaines limites de processabilité par les technologies de la plasturgie. Le renforcement de ses propriétés à l'état fondu a été obtenu grâce à l'introduction d'un époxyde multifonctionnel capable de réagir avec les bouts de chaînes des polyesters. Aussi, des mélanges à base de PLA/PBAT ont été mis en œuvre en vue de conférer la ductilité au matériau final.

La première étape consiste en la compréhension des mécanismes de dégradation thermique et hydrolytique des deux polymères PLA et PBAT au cours des processus de mise en œuvre. En effet, la réaction d'extension des chaînes couplée au branchement induits par l'époxyde multifonctionnel palie cette dégradation. Les mécanismes d'extension de chaînes et de branchements sous-jacents ont été mis en évidence par l'analyse des énergies d'activation, des spectres de relaxation à l'état fondu ainsi que celle des grandeurs physico-chimiques en solution. En outre, les représentations de Van-Gurp-Palmen confirment la co-existence de chaînes macromoléculaires linéaires et aléatoirement branchées.

La seconde étape de ce travail a été dédiée à la compatibilisation des mélanges PLA/PBAT par ce même époxyde multifonctionnel. Des études expérimentales modèles basées sur la détermination de la tension interfaciale et la modélisation rhéologique ont montré le rôle majeur de compatibilisant induit par cet agent réactif. Ainsi, la diminution de la tension interfaciale confère à ces matériaux une meilleure cohésion interfaciale et une morphologie fine et homogène de la phase dispersée, accompagnée par l'amélioration des propriétés mécaniques.

L'étude des propriétés rhéologiques en cisaillement et en élongation des matériaux modifiés a permis de montrer une meilleure tenue mécanique à l'état fondu. Ainsi, une meilleure aptitude à l'extrusion gonflage a été démontrée en élargissant leurs cartes de stabilité.

Parallèlement à ces travaux, des études de bi-étirage des polymères seuls, de leurs homologues modifiés et de leurs mélanges montrent un durcissement structural, dû à la cristallisation induite sous déformation. Les morphologies cristallines ont été analysées finement par des méthodes calorimétriques et spectroscopiques.

Enfin, ces études ont été transposées à l'élaboration et à la compréhension des comportements d'une formulation industrielle complexe à base de PLA, PBAT et de farine céréalière plastifiée.

Mots-Clés: Poly (acide lactique) (PLA), Extension de chaînes, Branchement, Compatibilisation, Rhéologie, étirage bi-axial, Extrusion-gonflage.

Blends based on Poly (lactic acid): Structure/ rheology/ processing relationship

Abstract

The ultimate aim of the present thesis focuses on the structure/processing/properties relationship of the PLA/PBAT materials. The latters are intended for food packaging in order to replace poly (ethylene terephthalate (PET). However, PLA has a limited processability in conventional technologies of plastics industry. The strengthening of its melt properties has been achieved through the incorporation of a multifunctional epoxide, able to react with the end chains of polyesters. Furthermore, PLA/PBAT blends were prepared to make the final material more ductile.

The first part of the study consists on the understanding of thermal and hydrolytic degradation mechanisms of neat PLA and PBAT polymers upon processing. Indeed, the degradation was overcome through the chain extension reaction coupled to branching, induced by the multifunctional epoxide.

The chain extension and branching mechanisms were highlighted by the analysis of the activation energy and the relaxation spectra in the molten state as well as the physico-chemical properties in solution. Moreover, the Van-Gurp-Palmen plots confirm the co-existence of linear and randomly branched macromolecular chains.

The second part has been dedicated to the compatibilization of PLA/PBAT blends by the multifunctional epoxide. Experimental models studies, based on the assessment of the interfacial tension, and the rheological modeling showed the major role of the reactive epoxide agent as a compatibilizer. Thus, the decrease of the interfacial tension gives a better cohesive interface with finer and homogenous morphology of the dispersed phase, accompanied with an improvement of the mechanical properties.

The study of the shear and elongation rheological properties of modified materials showed an enhancement of their melt strength. Therefore, a better ability to be blown has been demonstrated, by expanding their stability maps.

Besides, biaxial stretching studies of neat polymers, their modified counterparts as well as their blends show a structural strain hardening, due to a strain-induced crystallization. The crystalline phases were analyzed thanks to calorimetric and spectroscopic methods.

Finally, the present studies have been used to elaborate and understand the behavior of a complex industrial formulation based on PLA, PBAT and thermoplastic cereal flour.

Mots-Clés: Poly(lactic acid) (PLA), Chain extension, Branching, Compatibilization, Rheology, bi-axial stretching, blowing extrusion.

INSA Direction de la Recherche - Ecoles Doctorales – Quinquennal 2011-2015

SIGLE	ECOLE DOCTORALE	NOM ET COORDONNEES DU RESPONSABLE
CHIMIE	**CHIMIE DE LYON** **http://www.edchimie-lyon.fr** Insa : R. GOURDON	M. Jean Marc LANCELIN Université de Lyon – Collège Doctoral Bât ESCPE 43 bd du 11 novembre 1918 69622 VILLEURBANNE Cedex Tél : 04.72.43 13 95 directeur@edchimie-lyon.fr
E.E.A.	**ELECTRONIQUE, ELECTROTECHNIQUE, AUTOMATIQUE** **http://edeea.ec-lyon.fr** Secrétariat : M.C. HAVGOUDOUKIAN eea@ec-lyon.fr	M. Gérard SCORLETTI Ecole Centrale de Lyon 36 avenue Guy de Collongue 69134 ECULLY Tél : 04.72.18 60 97 Fax : 04 78 43 37 17 Gerard.scorletti@ec-lyon.fr
E2M2	**EVOLUTION, ECOSYSTEME, MICROBIOLOGIE, MODELISATION** **http://e2m2.universite-lyon.fr** Insa : H. CHARLES	Mme Gudrun BORNETTE CNRS UMR 5023 LEHNA Université Claude Bernard Lyon 1 Bât Forel 43 bd du 11 novembre 1918 69622 VILLEURBANNE Cédex Tél : 04.72.43.12.94 e2m2@biomserv.univ-lyon1.fr
EDISS	**INTERDISCIPLINAIRE SCIENCES-SANTE** **http://ww2.ibcp.fr/ediss** Sec : Safia AIT CHALAL Insa : M. LAGARDE	M. Didier REVEL Hôpital Louis Pradel Bâtiment Central 28 Avenue Doyen Lépine 69677 BRON Tél : 04.72.68 49 09 Fax :04 72 35 49 16 Didier.revel@creatis.uni-lyon1.fr
INFOMATHS	**INFORMATIQUE ET MATHEMATIQUES** http://infomaths.univ-lyon1.fr	M. Johannes KELLENDONK Université Claude Bernard Lyon 1 INFOMATHS Bâtiment Braconnier 43 bd du 11 novembre 1918 69622 VILLEURBANNE Cedex Tél : 04.72. 44.82.94 Fax 04 72 43 16 87 infomaths@univ-lyon1.fr
Matériaux	**MATERIAUX DE LYON** Secrétariat : M. LABOUNE PM : 71.70 –Fax : 87.12 Bat. Saint Exupéry Ed.materiaux@insa-lyon.fr	M. Jean-Yves BUFFIERE INSA de Lyon MATEIS Bâtiment Saint Exupéry 7 avenue Jean Capelle 69621 VILLEURBANNE Cédex Tél : 04.72.43 83 18 Fax 04 72 43 85 28 Jean-yves.buffiere@insa-lyon.fr
MEGA	**MECANIQUE, ENERGETIQUE, GENIE CIVIL, ACOUSTIQUE** Secrétariat : M. LABOUNE PM : 71.70 –Fax : 87.12 Bat. Saint Exupéry mega@insa-lyon.fr	M. Philippe BOISSE INSA de Lyon Laboratoire LAMCOS Bâtiment Jacquard 25 bis avenue Jean Capelle 69621 VILLEURBANNE Cedex Tél :04.72.43.71.70 Fax : 04 72 43 72 37 Philippe.boisse@insa-lyon.fr
ScSo	**ScSo*** M. OBADIA Lionel Sec : Viviane POLSINELLI Insa : J.Y. TOUSSAINT	M. OBADIA Lionel Université Lyon 2 86 rue Pasteur 69365 LYON Cedex 07 Tél : 04.78.69.72.76 Fax : 04.37.28.04.48 Lionel.Obadia@univ-lyon2.fr

*ScSo : Histoire, Geographie, Aménagement, Urbanisme, Archéologie, Science politique, Sociologie, Anthropologie

Remerciements

Ce travail a été essentiellement effectué à l'IMP@INSA, ingénierie des matériaux polymères de l'INSA de Lyon. Maintenant que cette thèse a reçu sa forme définitive, il me reste à dire combien je suis redevable à tous ceux qui m'ont aidé dans son élaboration. D'abord, je tiens à exprimer ma gratitude à l'ancien directeur de l'IMP@INSA, M. **Jean François GERARD**, de m'avoir accueilli au sein de cette structure. Je remercie également le directeur actuel, M. **Etienne FLEURY**, pour sa participation scientifique dans le projet.

Cette thèse a été effectuée sous la direction de M. **Abderrahim MAAZOUZ**, professeur à l'INSA de Lyon et M. **Khalid LAMNAWAR**, maître de conférences à l'INSA de Lyon, mon encyclopédie vivante. Je leur adresse mes sincères remerciements pour avoir assuré la direction de ces travaux avec intérêt et compétence. La pertinence de leurs remarques m'ont permis de progresser et de réaliser ce travail. Je tiens également à les remercier pour l'agréable ambiance de travail qu'ils ont su instaurer. Je leur serai reconnaissante à vie.

Je voudrais ensuite remercier mon jury de thèse, en commençant par Mme **Noëlle BILLON** et M. **Yves GROHENS** qui ont eu la gentillesse de lire mon manuscrit. Mes remerciements s'adressent aussi à M. **Christian CARROT** et M. **Mosto BOUSMINA** qui m'ont fait l'honneur de faire partie de ce jury.

Je ne saurais oublier les partenaires industriels pour leur soutien, tant scientifique que financier en leur exprimant mes remerciements sincères, et, en particulier M. **Claude JANIN**, Mme **Nadège LIBE** et Mme **Valérie LACRAMPE** pour leurs conseils tout au long de cette étude et pour l'intérêt qu'ils ont porté à ce travail.

Que **M. Pierre ALCOUFFE** soit vivement remercié pour sa gentillesse et sa participation active à la partie caractérisation morphologique. Je tiens aussi à remercier **Mme Christelle COMBEAUD** et **M. Gabriel MONGE** pour leur aide précieuse pour approfondir des points rédhibitoires dans cette thèse, en particulier la diffraction des rayons X. Qu'ils en soient remerciés.

Un grand merci également à toutes les personnes, que j'ai rencontrées à la fois à l'IMP@INSA et au site de la plasturgie à Bellignat. Je pense en particulier à mes

collègues du bureau, Florent, Gino, Thibault, Mohamed, Floriane et Marie. C'est en amitié que je remercie également Amir, Ali, Serife, Molka, Nora, Hua gui, Julien et bien d'autres encore. Ils ont su rendre mon séjour agréable et enrichissant du point de vue humain et scientifique. Mention spéciale à « la communauté libanaise » en France (Mira Jaafar, Maya Omar, Mohamad Alwan, Mayssa Hachem, Myrna Nachabeh, Rami tadmouri, Amanda Oueini, Julie Oueini, Aziz Oueini, Georgio Bassil, Rami Abou Naccoul et Salam Moubarak…). Un immense merci à Marie-Rose Frangieh, pour sa présence, ses encouragements, son soutien, pour tout ce qu'elle m'apporte et pour tout ce que nous partageons.

Enfin, je ne saurais conclure mes remerciements sans exprimer ma profonde reconnaissance et mon affection à mon mari et ma famille, plus particulièrement à ma mère et mon père, pour leur amour, leur soutien moral inconditionnel et leur patience jusqu'au bout. Cette thèse vous est dédiée.

Table of contents

CHAPTER 3
CHAIN EXTENSION/BRANCHING BALANCE OF MODIFIED PLA AND PBAT POLYMERS WITH A MULTIFUNCTIONAL EPOXIDE: RHEOLOGICAL AND SOLUTION PROPERTIES

CHAPTER 4
RHEOLOGICAL INVESTIGATION AND INTERFACIAL TENSION PROPERTIES OF PLA/PBAT/ MULTIFUNCTIONAL EPOXIDE BLENDS

CHAPTER 5
EXTRUSION BLOWN FILM OF POLY (LACTIC ACID) AND ITS BLENDS: IMPROVEMENT OF PROCESSING STABILITY

CHAPTER 6
BIAXIAL ORIENTATION OF MATERIALS BASED ON POLY (LACTIC ACID): STRUCTURE AND PROPERTIES

PART A- NEAT AND MODIFIED PLA, PBAT AND THEIR BLENDS WITH MULTI-FUNCTIONAL EPOXIDE

PART B- PLA, PBAT AND THERMOPLASTIC CEREAL FLOUR BLENDS: AN EXAMPLE OF AN INDUSTRIAL FORMULATION

LIST OF FIGURES

LIST OF TABLES

INTRODUCTION GENERALE

Dans un contexte où le développement durable apparaît comme une priorité majeure dans le domaine des matériaux polymères, la mise au point de polymères issus de ressources renouvelables est en pleine croissance. En effet, l'intérêt écologique de ces matériaux réside dans le fait qu'ils contiennent intrinsèquement la solution de leur élimination du fait qu'ils peuvent être assimilés directement par les micro-organismes du sol. Quant aux retombées économiques, l'emballage alimentaire présente à titre d'exemple un fort potentiel de développement.

Le poly (acide lactique) (PLA) est un des polymères biodégradables synthétisés à partir des monomères issus de ressources renouvelables (l'acide lactique). Il peut être extrait à partir des matières végétales (maïs, betterave, pommes de terre). Les applications de ce polymère ou de ses mélanges sont nombreuses. En effet le poly (acide lactique) suscite un grand engouement de la part de la communauté des scientifiques et industrielle puisqu'il est biodégradable, compostable et biocompatible.

Les verrous de développement d'un tel polymère résident dans l'élargissement de sa fenêtre de processabilité et le rehaussement de ses propriétés thermomécaniques. Dernièrement, l'intérêt s'est accru pour l'utilisation du PLA pour produire des emballages alimentaires biodégradables. Le rehaussement des propriétés de ce polymère en vue d'améliorer sa mise en forme suscite un intérêt scientifique et industriel majeur.

Dans ce contexte, les travaux de cette thèse s'inscrivent dans un programme de recherche supporté par deux pôles de compétitivité, Plastipolis et Céréales Vallée et financés par la direction générale de la compétitivité, de l'industrie et des services (DGCIS). Le but ultime est la démonstration industrielle de films en bio-polymères d'où l'acronyme de ce projet : Difex-Bio. Aussi, il s'agit de développer un matériau totalement ou partiellement bio-sourcé à base de matrice biodégradable et/ou compostable. Nous avons également choisi le Poly (butylène-adipate-co-téréphtalate), PBAT pour la ductilité qu'il peut conférer aux mélanges à base de PLA.

Etant donné la pluridisciplinarité de ce travail, nous avons opté pour une présentation sous forme de chapitres/publications en anglais ayant chacun son propre état de l'art et sa propre bibliographie.

Pour éviter les redondances, le premier chapitre a été consacré à la présentation d'une manière sommaire des caractéristiques des matériaux de base et des techniques expérimentales. Il présente également l'élaboration et la mise en forme des différentes formulations par extrusion réactive. Les matériaux obtenus sont caractérisés à leur tour par différentes techniques physico-chimiques et rhéologiques.

Le deuxième chapitre est consacré au rehaussement de la tenue mécanique à l'état fondu des polymères de base. A cet effet, nous avons choisi un époxyde multifonctionnel (Joncryl ADR®) susceptible de réagir avec les bouts de chaînes de chaque polymère et jouer le

rôle d'allongeur de chaîne. En outre, cet agent réactif pali la dégradation thermique et hydrolytique de ses deux polyesters et de leur mélange. Ainsi, les mécanismes réactionnels ont été mis en évidence par des analyses spectroscopiques et confortés par des études rhéologiques à l'état fondu et en solution.

Le troisième chapitre porte sur l'élaboration des mélanges à base de PLA/PBAT. Nous avons abordé les concepts fondamentaux liés aux propriétés de ces mélanges. En effet, ces études ont permis d'élucider les mécanismes d'allongement et/ou branchement de chaînes induits par le Joncryl.

Dans le quatrième chapitre, nous avons montré qu'outre le caractère d'allongeur et/ou branchement des chaines, le Joncryl joue le rôle d'agent compatibilisant des mélanges PLA/PBAT. Ainsi, on assiste à une évolution remarquable de la tension interfaciale. En outre, des expérimentations sur des systèmes modèles (rétraction de la gouttelette déformée) ont été mises en œuvre pour évaluer de manière directe la tension interfaciale. L'évolution de cette dernière corrobore parfaitement la modélisation rhéologique. Les valeurs obtenues sont en parfait accord avec les prédictions du modèle de Palierne.

Dans les cinquième et sixième chapitres, les études rhéologiques en élongation et en cisaillement des polymères modifiés et de leurs mélanges ont montré une meilleure aptitude à la transformation par les procédés de la plasturgie tels que l'extrusion gonflage et le biétirage. Nous avons étudié plus particulièrement l'influence de l'allongement de chaîne sur la stabilité des différentes formulations au cours du procédé. Enfin, les propriétés morphologiques, structurales et mécaniques des matériaux finaux ont été étudiées. La cristallisation induite par la présence du Joncryl et par le process ainsi que son influence sur ces propriétés a été étudiée de manière exhaustive.

Le dernier chapitre de ce manuscrit a pour objectif la transposition de l'étude à la réalisation de films à base de formulations industrielles contenant du PLA, PBAT et de farine plastifiée. Cette dernière a été développée par les partenaires dans le cadre du consortium. L'objectif est de substituer par la farine, l'amidon présent dans des grades commerciaux à base de PLA et de PBAT.

Chapter 1
Materials and Experimental Methods

1

For the clarity of the present manuscript, an experimental part, including the materials and the various methods, is presented here. Other methods, used for a specific characterization (the blowing extrusion set-up, for instance) are presented in the corresponding chapter.

I Materials

I.1 Polymers used

PLA (Grade: 4032D) was purchased from Natureworks and consisted of 2% D-lactide units. PBAT (Grade: Ecoflex FBX 7011) was obtained from BASF. Commercial multi-functional styrene-acrylic oligomers (BASF, Joncryl ADR®-4368) accepted by the Food & Drug Administration (FDA) for food packaging were used. The main characteristics of the polymers used in this study are listed in Table I-1. The chemical structures of PLA, PBAT and Joncryl ADR® were shown in Figure I-1.

Table I-1 Main Characteristics of the used polymers and of Joncryl ADR®-4368

Material	Grade/Supplier	Melt temperature (°C)	Glass Temperature (°C)	Molecular weight (g/mol)
PLA	NW 4032D (2% D-Lactide)	168°C	~ 60	100.000
PBAT	Ecolflex FBX 7011	110-120°C	-30	40.000

Characteristics_Joncryl ADR®-4368
Functionality: f ~ 9
Glass transition temperature: 54°C
EEW (epoxy equivalent weight): 285 g/mol
Molecular weight (Mw): ~ 6800g/mol

(a): PLA

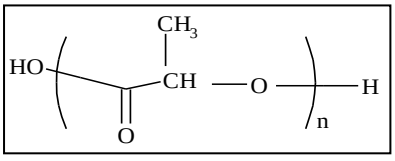

(b): PBAT

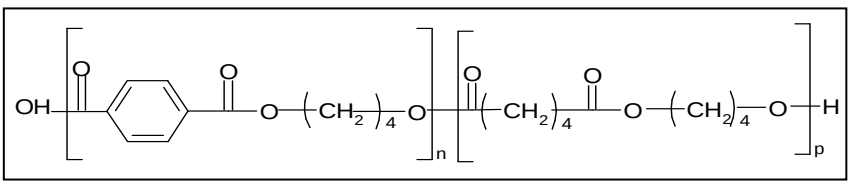

(c): General structure of the styrene–acrylic multi-functional oligomeric chain extenders. Where R1–R5 are H, CH3, a higher alkyl group, or combinations of them; R6 is an alkyl group, and x, y and z are each between 1 and 20.

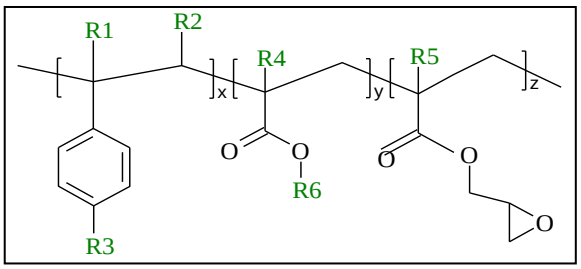

Figure I-1 Chemical structure of (a): PLA, (b): PBAT and (c): Joncryl ADR®-4368

I.2 Processing and blend preparation

Before compounding, both PBAT and PLA pellets were dried under vacuum at 80°C for 12 hours to remove moisture. Moreover, Joncryl ADR® was dried under vacuum at 40°C.
A PRISM TTW 16/25D corotating twin-screw extruder (TSE) with a screw diameter of 16mm (Thermo Electron Polylab System Rhecord RC400P) was used for i) the processing of the neat polymers at different temperatures, shear rate and residence time, ii) the reactive extrusion to investigate the role of various amount of Joncryl ADR® on controlling the degradation of both PLA and PBAT iii) the elaboration of uncompatibilized and compatibilized PLA/PBAT blends.
The PRISM 16mm twin screw extruder had a clam shell barrel design with a length to diameter ratio of 25:1 (cf. Figure I-2). The mixing was conducted under a nitrogen atmosphere at a rotation speed of 40 rpm until the stabilization of the torque. The temperature profile was set to 140,190,190,180 and 180°C from the feed zone to the die. After the melt blending, each extrudate was quenched in a cold water bath and granulated.

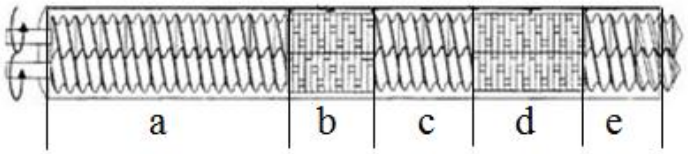

Figure I-2 The 16 mm diameter corotating twin-screw extruder. The numbers 1–8 at the top of the extruder indicate the sampling positions. All dimensions are given in mm: a = 9*16 mm+1*8mm forwarding conveying elements, b= 14*4 mm Kneading blocks (60°offset), c = 4*16 mm forwarding conveying elements, d = 18*4 mm Kneading blocks (60°offset), e= 4*14 mm forwarding conveying elements plus, f = Vent ports (closed)

Various amounts of Joncryl ADR® i.e from 0 to 1 wt% were used for PLA, PBAT and their PLA/PBAT (80/20) blends. An amount of 1%wt was only used for the academic approach. Notations and compositions of the overall studied materials are given in Table I-2.

Table I-2 Compositions of the unmodified and the modified PLA, PBAT and their blends

a) Sample name	wt % of neat polymer in the blends	Wt % of Joncryl in the blends
	Neat & Modified PLA	
PLA_0	100	0
PLA_0.25	99,75	0.25
PLA_0.5	99,5	0.5
PLA_1	99	1
	Neat & Modified PBAT	
PBAT_0	100	0
PBAT_0.25	99,75	0.25
PBAT_0.5	99,5	0.5
PBAT_1	99	1

b) Sample name	PLA (wt%)	PBAT (wt%)	Joncryl (wt%)
PLA_PBAT_0	80	20	0
PLA_PBAT_0.25	79,8	19,95	0.25
PLA_PBAT_0.5	79,6	19,9	0.5
PLA_PBAT_1	79,2	19,8	1

II Experimental Methods

II.1 Physico-chemical characterizations

II.1.1 Acid value Analysis

Titration of the acid value of neat and processed PLA and PBAT has been performed with the help of an automatic Mattler-Toledo T70 titrator. The solution was obtained by dissolving 3 grams of polymer in 60 ml of Chloroform. KOH in MeOH solution (2.03*10-2 mol.L-1) was used for the titration of the carboxylic groups. A PH sensor was used to follow the evolution of the solution acidity and to determinate the equivalent volume Ve as follow (Eq.1):

Equation 1

$$AV = \frac{Ve \times C(KOH) \times M(KOH)}{m}$$

Where Ve (mL) is the equivalent volume corresponding to the equilibrium PH plateau, C (KOH) is the molar concentration ($mol.L^{-1}$) of KOH, M (KOH) is the molar mass ($g.mol^{-1}$) of KOH and m is the weight (g) of the dissolved polymer.

II.1.2 Molecular Weight Measurements

II.1.2.1 Intrinsic viscosity measurements

The inherent and reduced viscosities were measured using an Ubbelhode-type capillary viscometer at 25°C. This temperature was controlled using a thermo regulated chamber. Chloroform was used as solvent. The flow time was measured at different concentrations (0,5g/100ml- 0,25g/100ml- 0,16g/100ml- 0,125g/100ml) for each sample. The introduction of the solution was done carefully and quickly in the viscosimeter which is integrated in the adequate visco'clock® system in order to avoid evaporation of the chloroform and keep constant the concentration of the solution. The experiments are checked more than three times.
The intrinsic viscosity, characteristic radii (hydrodynamic and gyration radii) were determined. Moreover, the Huggins constant (K') was calculated.

II.1.2.2 Size Exclusion-chromatography

The average molecular weight, the average molecular number and the polydispersity index of PLA, as well as for PBAT, before and after processing at different temperatures were measured using size exclusion chromatography (SEC). SEC analyses were performed in THF (0,5 ml/min) at room temperature, using a VARIAN prostar chromatograph. It is made of a RHEODYNE injector, two Mixed- PL gel columns (G4000 HXL to G1000 HXL) with porosity about 50 – 100000A° and a RI-101 refractive index detector. Monodisperse poly (styrene) was used as calibration standards. The PLA and PBAT solutions were prepared at concentrations of 5mg/ml in THF, with a flow rate of 0.5 ml/min.

II.1.3 Fourier transformation infrared spectroscopy (FTIR)

Infrared spectra of neat and processed PLA and PBAT were obtained with an FTIR Nicolet iS10 thermo scientific spectrometer in attenuated total reflectance (ATR) mode with a diamond crystal collecting 32 scans. Each spectrum was obtained within the range of 4000-650 cm^{-1} with a wavelength resolution of 4 cm^{-1}.

II.2 Thermo-mechanical characterizations

II.2.1 Thermal gravimetric analysis (TGA)

TGA measurements were performed using a TGA-Q500 thermogravimetric analyzer from TA instruments. Samples of 10 mg were heated from room temperature to 550°C at 10°C/min under nitrogen atmosphere. The effect of the environment was firstly validated and degradation was more pronounced under air. For the clarity purpose, only results under nitrogen will be shown here.

II.2.2 Non isocthermal Crystallization

The thermal properties of neat and processed PLA, PBAT and their blends were investigated with the help of a differential scanning calorimeter Q10® DSC (TA) equipped with a liquid nitrogen cooling system (LNCS). The DSC cell was constantly purged with nitrogen at a flow rate of 50 ml/min. A set of heating/cooling ramps was carried out following a three step process; the samples were firstly heated to 200°C and kept in the molten state for 2 min to erase the thermal history of the material.

They were then cooled down to 25°C at 10°C/min to evaluate the ability of PLA component to crystallize upon cooling. After cooling treatment, the samples were heated back to 200°C at 10°C/min. The percent crystallinity was calculated upon the second heating by using the following equation (Eq.2):

Equation 2

$$X_c(\%) = 100 * \frac{\Delta H_m - \Delta H_{cc}}{f * \Delta H_{m\infty}}$$

Where "ΔH_m" is the measured heat of fusion, ΔH_{cc} the cold crystallization enthalpy (J/g) , "f" is the weight fraction of PLA or PBAT in the blend and "$\Delta H_{\infty m}$ "is the enthalpy of fusion for a crystal having infinite crystal thickness (93J.g^{-1} for PLA and 114 J.g^{-1} for PBAT)

II.2.3 Thermo-mechanical analysis

The investigation of the thermo-mechanical properties was conducted through dynamic mechanical thermal analysis (DMTA) performed on a RSA II (TA instruments). Oscillating tensile-compressions tests under a strain of 0.2% at a fixed oscillatory frequency of 1Hz were performed during temperature sweeps from -80°C up to 110°C at a rate of 3°C/min.

II.2.4 Mechanical properties

Mechanical tests were carried out using an Instron machine under room temperature (23°C) with a cross head speed at 5 mm/min. The specimen dimension was 20×4×2 (in mm) denoting respectively the length, breadth and the height samples. Prior to testing, the samples were dried in a vaccum oven at 60°C for only 2 hours and kept in sealed dessicators until tests.

II.3 Rheological characterizations

II.3.1 Dynamic shear rheology

After a 12h drying stage performed at 80°C under vacuum, the pellets were molded into disks of 25 mm diameter with a thickness of about 2mm. These disks were subsequently dried in a vaccum at 40°C oven overnight before analysis.

Small amplitude shear measurements (SAOS) were investigated with an Advanced Rheometric Expansion system (ARES) using a parallel plates geometry with a plate diameter of 25mm and a gap inferior to 2mm. The heated chamber at 180°C was continuously purged with nitrogen to avoid thermal degradation. Prior to experiments, dynamic strain sweep tests with a maximum angular frequency amplitude of 100 rad/s was performed. Hence, the strain value is set at 5% to validate the linear viscoelastic region.

The following rheological measurements were carried out:

- Dynamic time sweep test to verify the thermal stability of neat PLA and PBAT at lower angular frequency in linear regime
- Dynamic frequency sweep tests over an angular frequency range of 0.05-100 rad/s

The viscoelastic parameters based on G′, G″, η′ and η″ were used to plot the Cole-Cole diagrams, relaxation spectra and the flow curves.

II.3.2 Capillary flow rheology

Experimental runs with a non-isothermal flow were performed by using a pressure – controlled CEAST capillary rheometer at 180°C through a die with a 180° entry angle and various L/D ratios to obtain Bagley corrections. The capillary measurements were conducted in a closed environment under nitrogen atmosphere. The elongation viscosity was determined by Cogswell model.

II.4 Morphological properties

To investigate the phase morphology of PLA/PBAT (80/20) blends with various amounts of Joncryl ADR®, fractured surfaces at room temperature of the blends were observed by transmission electron microscopy (TEM) after being gold coated. Scanning electron microscopy was applied to characterize the morphology of unmodified PLA/PBAT blend. The cryo-fractured sample surface was with thin layer gold, and then scanned at an accelerating voltage of 8 KV.

Chapter 2
Improvement of thermal stability, rheological and mechanical properties of PLA, PBAT and their blends by reactive extrusion with functionalized epoxy

2

I Abstract

The aim of this study has been to gain a fundamental understanding of the mechanisms and conditions governing thermal degradation of poly (lactic acid) (PLA), poly (butylene-adipate-co-terephtalate) (PBAT) and their blends upon processing conditions. Thermal degradation of biodegradable PLA and PBAT polymers was investigated firstly by thermal analysis and size-exclusion chromatography (SEC). It is shown that the neat polymers degrade upon processing thus the decreasing of the molecular weight, rheological and mechanical properties. Secondly, the reactive extrusion of polymers was performed with various amounts of chain extension/branching agent, containing about nine Glycidyl methacrylate (GMA)/Epoxide functions, named Joncryl ADR®-4368. The incorporation of the multi-functional oligomer showed an improvement of their thermal stability. SEC and intrinsic viscosity measurements of these modified PLA and PBAT confirmed the increase of viscosity and molecular weight, probably related to the formation of extended and branched chains. Rheological investigation of extended/branched PLA and PBAT as well as compatibilized PLA/PBAT (80/20) (wt/wt) blends with various concentrations of GMA reactive functions exhibited higher viscosity and storage modulus compared to the unmodified samples. This increase becomes more pronounced as the concentration of Joncryl ADR® increases. Viscoelastic properties were assessed and related to the molecular structure of modified polymers. Hence, the mechanisms of degradation, chain extending with GMA/Epoxide functions and their competition have been proposed. The effect of reactive compatibilization on the PLA/PBAT blends has been confirmed using transmission electron microscopy (TEM), scanning electron microscopy (SEM) observations and tensile tests by the improvement of phase dispersion and the increasing both of Young's modulus and strain at break.

Keywords: Biodegradable polymers-thermal stability-chain extender-reactive extrusion-viscoelastic properties- molecular weight measurements

II Introduction

Natural polymers, biopolymers and synthetic polymers based on annually renewable resources are the basis for the twenty-first-century portfolio of sustainable, eco-efficient plastics. The interest on these polymers is considerable in the prospect to decrease of the world resources in oil and in a concern to limit the contribution of plastics to the waste disposal. The subject is vast and hence it is a daunting task to summarize their remarkably rich and multi-faced area related to these biopolymers fields.

Polylactide or poly(lactic acid) (PLA) is the front runner in the emerging bio-plastics market with the best availability and the most attractive cost structure. PLA is linear, aliphatic thermoplastic polyester with rigidity and clarity similar to polystyrene (PS) and poly (ethylene terephthalate) (PET). It is biodegradable for different applications ranging from medical to packaging, resorbable and biodegradable under industrial composting conditions [1]. It can be produced by condensation directly from its basic building block lactic acid, which is derived by fermentation of sugars

from carbohydrate sources (corn, sugarcane, tapioca…). But, higher molecular weights of PLA are achieved by ring-opening-polymerization (ROP) of cyclic lactide dimer [2]. Generally, PLA is made into useful items using thermal processes like injection molding and extrusion. Therefore, its rheological properties, especially its shear viscosity, have important effects on thermal processes. Despite all its advantages, some properties of PLA such as inherent brittleness, poor melt strength; narrow processing window and low thermal stability pose considerable scientific challenges and limit their large scale-applications (film blowing or injection molding) [3-29-30]. Recently, some developments in modification of PLA including copolymerization, blending, compounding and additives were highlighted to improve its relevant properties [4-5-6-7]. It has been reported that the thermal degradation of PLA, upon thermal processing, predominantly consists of random main-chain scission and unzipping depolymerization reaction [8]. The random degradation reaction involves hydrolysis, oxidative degradation, cis-elimination, intramolecular and intermolecular trans-esterification [9-10-11]. Depending on processing conditions, one of these several undesired reactions is dominant. For example, trans-esterification was found as a dominant degradation mechanism of PLA and high temperatures (above 200°C) leading to the formation of cyclic oligomers [12]. Moreover, the melt degradation of PLA at temperatures above 180°C was studied [13]. A random main-chain scission in such temperatures seems to be responsible of the melt degradation. Almost all the active chain-end groups, residual catalysts, residual monomers and other impurities enhance the thermal degradation of PLA [14]. As a consequence, an undesired molecular weight reduction and weight loss occur from 180°C to 220°C. It is proved that the modification of the polymer to get long and branched structures by using chain extenders is an efficient approach to control the degradation of PLA [7-15]. Consequently, many authors have shown the interest of using a chain extender which is able to reconnect cleaved chains by increasing molecular weight of polymer, strength of melt and also can be used as a reactive compatibilizer in blends [16-17-31]. The chain extenders are generally poly-functional, thermally stable and easily available. Some of the extenders reported in literature are di and multi-functional epoxies [18], diisocyanate compound [19], dianhydride [20], bis-oxazolines, tris (nonyl-phenyl) phosphate (TNPP) [7] and polycarbodiimide (PCDI). Multi-functional epoxy compounds have been extensively used as chain extenders for polyesters. In this case, the epoxy functions can react with both nucleophilic end groups –OH and –COOH of PLA leading to high molecular weight polymer. Branched but less cross-linked PLA could be obtained for more than 1.5%wt of a multifunctional epoxide [21]. The branched polymers not only increase the molecular weight, but have many different properties compared with linear polymers. In the light of previous works, the addition of such a chain extender with the aim of enhancing the extrusion and injection foamability of PLA was investigated [22-32]. With the same objective, a similar chain extender on amorphous and crystalline PLA(s) was also studied [23].

Meanwhile, blending PLA with other flexible polymers (PCL, PBS, PBAT…) was also investigated [24-25-26]. In our study, Poly (butylene-adipate-co-terephtalate) (PBAT) is selected. It is aliphatic-aromatic copolyester, which is fully biodegradable, a flexible plastic designed for film extrusion. In the view of its high toughness and biodegradability, PBAT is considered as a good candidate for the toughness of PLA [27]. Based on previous work on PLA/PBAT blends, it was discussed the incorporation of Glycidyl methacrylate (GMA) functions in such a blend in order to investigate the mechanical properties of PLA/PBAT/GMA (80/20/GMA) blends [24]. The surprising elongation at break value (3%) is obtained for PLA/PBAT/GMA blends. It is lower than those of PLA (4.5%) and PBAT (500%) respectively. The better understanding of the polymer stability is an interesting approach to explain this strange obtained result. Despite the interesting nature of the kind of research, few efforts have been dedicated to the study of the thermal degradation of PBAT and no study was dedicated to the effect of chain extender on the PBAT under processing. Compared to PLA, the onset temperature of thermal degradation started much later for PBAT [28]. It was also reported that no significant chain modification of PBAT occurred upon processing up to 200°C [14].

This paper represents the approach to obtain thermo-stable PLA and PBAT polymers upon melt processing and investigates the effect of their thermal stability on the structural, rheological, mechanical and morphological properties of modified PLA, PBAT and their compatibilized blends. Hence, the mechanisms of degradation, chain extending with epoxy and their competition will be discussed.

III Results and discussions

III.1 Highlighting of PLA, PBAT thermal degradation: Effect of processing conditions

In this paragraph, the thermal stability of PLA and PBAT upon processing was investigated; for both polymers, a processing under an increased temperature (180,190 and 200°C) and/or a higher residence time exhibits a lower final torque, as well as a reduced viscosity, making the melt more flowing. Moreover, it was noted that nitrogen atmosphere is more effective in preventing polymer degradation compared to air atmosphere.
The processing parameters were thus set in order to minimize the thermal degradation of the studied polymers while maintaining a high quality of extrudate. Consequently, a processing temperature below 200°C, an inert atmosphere and a lower residence time (3 minutes) were required.
Hence, the effect of these processing conditions on the thermal stability of neat polymers has been investigated by the molecular weight and intrinsic viscosity measurements at different steps of the process. The relative observations and the degradation mechanism for both PLA and PBAT will be discussed in the next sections.

III.2 Molecular weight measurements

III.2.1 Intrinsic viscosity

As it is common, the value of the intrinsic viscosity provides a measure of the ability of an isolated and Gaussian polymer single chain to increase the viscosity of the solvent in the absence of intermolecular interactions between polymer molecules. The intrinsic viscosity, [η] was determined by extrapolation of reduced and inherent viscosities to zero concentration (cf. Figure II-1).
These two viscosities were plotted respectively by using Huggins (Eq.3) [33] and Kraemer (Eq.4) [34] [35] approaches:

Equation 3

$$\eta_{red} = \frac{\eta_{sp}}{C} = \frac{1}{C} * \left(\frac{t - t_0}{t_0} \right) = [\eta] + K'[\eta]^2 * C$$

Equation 4

$$\eta_{inh} = \frac{\mathrm{Ln}(\eta_{rel})}{C} = \frac{1}{C} * \left(Ln \frac{t}{t_0} \right) = [\eta] + K''[\eta]^2 * C$$

Where "t" and "t_o" denote respectively the efflux time of the solution and solvent, K′ the Huggins constant and K″ the Kramer constant. The magnitude of K′ increasing can be related to the breadth of the molecular weight distribution or branching of the solute. K′ values for PLA (K′=0.3) and PBAT (K′=0.93) showed that the chloroform represents a good solvent for the studied polyesters, indicating that the hydrodynamic volume of the polymer chain shrinks with favorable interaction between polymer and solvent [35].

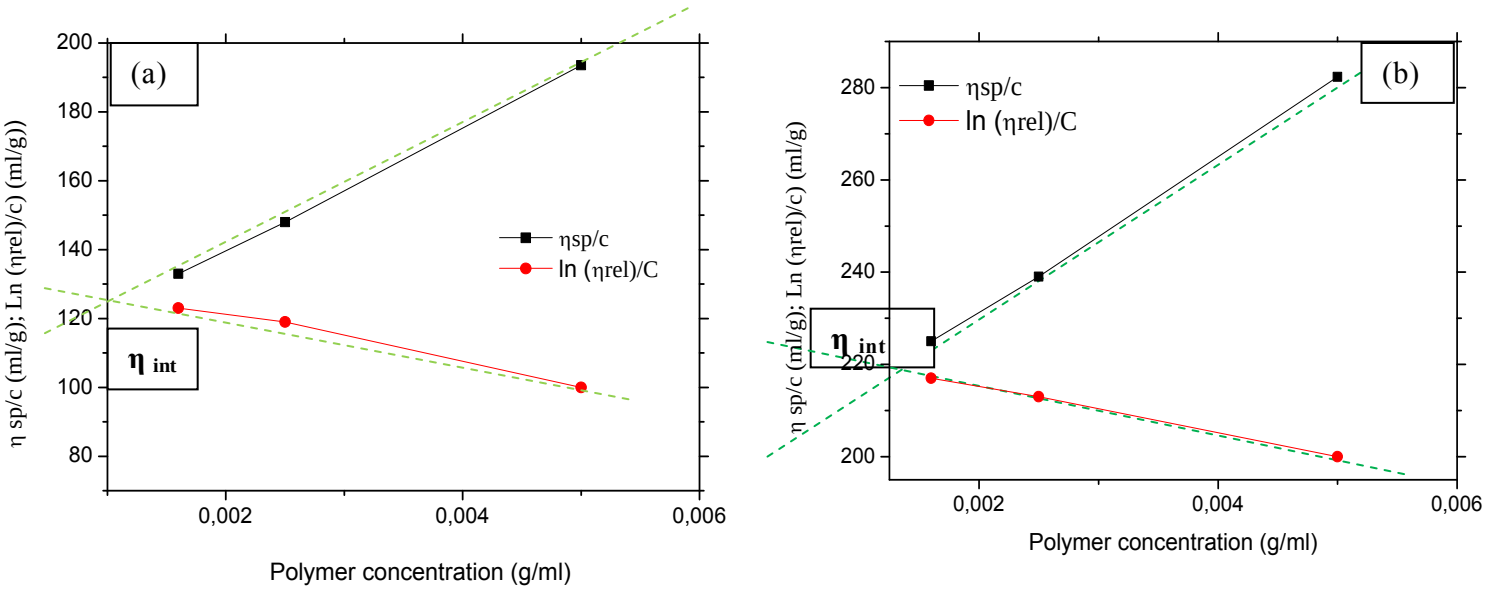

Figure II-1 Examples of plots of the reduced viscosity (ηsp/c) and inherent viscosity as a function of polymer concentration solutions in chloroform for (a): Neat PLA and (b): chain extended/branched PLA

Intrinsic viscosities values of different solution in chloroform are summarized in Table II-1.

Table II-1 Characteristic molecular weights obtained by SEC and intrinsic viscosity measurements of different samples at various temperatures

Samples	$\overline{M_\omega}$ (g/mol)	$\overline{M_n}$ (g/mol)	DPI	K (degradation parameter)	Intrinsic viscosity (ml/g)
Pristine PLA	100.000	57000	1.75		125
PLA_extruded 180°C	94.000	48000	1.95	1.18	115
PLA_extruded 190°C	93.000	47500	1.96	1.2	111
PLA_extruded 200°C	92.000	46900	1.96	1.21	112
Pristine PBAT	45.000	19800	2.27		91
PBAT_extruded 180°C	43.000	19600	2.19	1.01	79.5
PBAT_extruded 190°C	39.000	18500	2.11	1.07	77
PBAT_extruded 200°C	34.000	16100	2.11	1.23	75

The reported results show a decrease on intrinsic viscosity when both PLA and PBAT were extruded during 3 minutes. These changes can be related to the cleavage of the chains to shorter ones via the degradation mechanisms (hydrolysis, random main-scission reaction, transesterification reactions, β-scission…) accompanied by a significant increase of carboxyl and hydroxyl end groups, as can be seen in Table II-2 [36-37].

Table II-2 Acid value of neat and processed PLA and PBAT

Samples	Acid Value (mg KOH/g polymer)
Pristine PLA	1,3
PLA_extruded 180°C	1,41
Pristine PBAT	0,45
PBAT_extruded 180°C	0,588

III.2.2 Average molecular weight

To deeper investigate the effect of temperature factor, size exclusion chromatography tests were performed on the processed samples. Moreover, we evaluate a parameter "K" (Eq.5) as the degradation factor [14].

Equation 5

$$K = \frac{\bar{M}_{n(\,pellets)}}{\bar{M}_{n(\mathrm{Processed-polymers})}}$$

Where $\overline{M_n}$ (pellets) is the average number molecular weight of pristine polymer and $\overline{M_n}$ (processed polymers) is the average number molecular weight of processed polymers at temperature T. Interestingly, "K" values for both PLA and PBAT increased as processing temperature increased indicating a decrease of their average number molecular weight (Table II-1). Moreover, it is found that these two polymers showed a thermal degradation under 180°C and 200°C at 3 minutes. PLA and PBAT pellets had got a slight reduction of molecular weight, as starting from dried samples and working under nitrogen flow, which is related to temperature-mechanical shear combination during processing [36-37]. The decrease of average molecular weight confirms the decrease of intrinsic viscosity. These changes can be related to the cleavage of the long chains via the degradation mechanisms.
The decrease in molecular weight of PLA after processing is not drastic, thus indicating that degradation by hydrolysis is limited. Normally, hydrolysis (in the presence of moisture) leads to a very significant molecular weight reduction. Chain scission was thus responsible for that decrease. Hence the mechanisms of PLA and PBAT degradation can be proposed in the next sections.

III.3 Thermal analysis

TGA was carried out to investigate the effect of processing on the thermal decomposition of PLA and PBAT under nitrogen atmosphere. Table II-3 summarizes the characteristic temperature of the thermal decomposition. The onset temperature of the decomposition of PLA slightly decreases with the extrusion process. This change could be originated from the degradation of the polymer,

leading to the presence of shorter polymer chains and an increase in the number of chain ends per mass.

Table II-3 Thermogravimetric analysis for pristine and processed polymers

Samples	T_{onset} (°C)	T_{10} (°C)	$T_{maximum\ degradation}$ (°C)	Samples	T_{onset} (°C)	T_{10} (°C)	$T_{maximum\ degradation}$ (°C)
PLA_Pellets	328	354	383	PBAT_Pellets	356	393	424
Processed PLA	300	343	381	Processed PBAT	343	382	425

Chain ends then promote the depolymerization by back-bitting (intramolecular transesterification) considering that is the dominant degradation pathway at the temperature range of 270-360°C [38-41]. The same trend was observed for neat and processed PBAT. However, the onset static temperature (T_{onset}) of thermal decomposition of PBAT started later than in the PLA, which is 30°C higher than PLA. The higher decomposition temperature of the polymers corroborates with literature [28]. But, TGA measurements are not representative to the real decomposition during processing and cannot gives rising any information about the real mechanism governing this phenomenon under processing conditions (temperature, shear rate, residence time).
Meanwhile, compared to PLA pellets, the extruded PLA showed an increase of its crystallinity (Cf. Table II-4; Figure II-2) level while increasing the temperature. PLA degradation can be once again evocated to explain this phenomenon.

Table II-4 Crystallinity values or Pristine PLA, processed PLA at 180°C and at 190°C

Samples	Xc (%)
PLA pellets	1.7
PLA_extruded 180°C	35
PLA_extruded 190°C	39

The products of the degradation (Oligomers for example) would then act as nucleating agent allowing a reduced cold crystallization temperature [36]. It is shown that the thermal analysis was corroborated with molecular weight measurements which highlighted a reduction on the average molecular weight. However, DSC was not efficient to show the thermal degradation of PBAT.

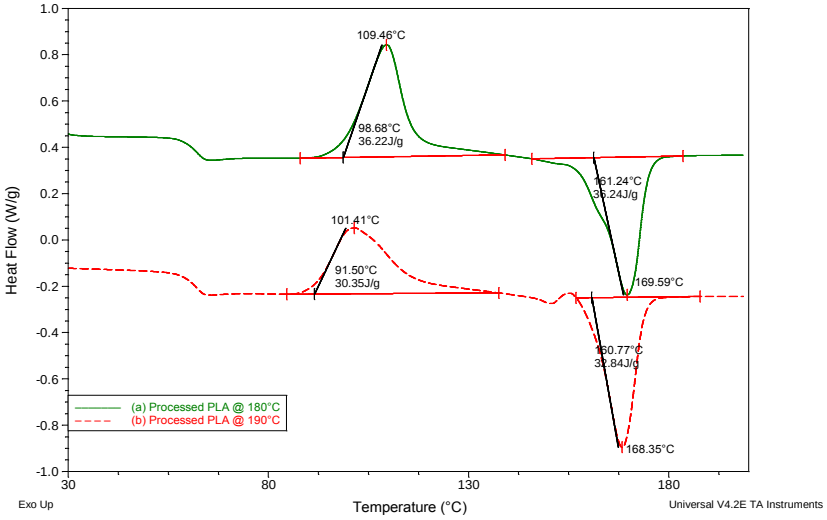

Figure II-2 DSC thermograms (second heating cycle) of (a): PLA extruded at 180°C (b): PLA extruded at 190°C

Therefore, in order to deeply understand the thermal degradation of PLA and PBAT, the rheological properties of both polymers were investigated.

III.4 Rheological investigation

The rheological investigation is used as a suitable tool to evaluate the thermal stability of PLA and PBAT upon processing at increasing temperature from 180°C to 200°C. It is shown in Figure II-3 that the viscosity values of PBAT and PLA decreased from 5000 Pa.s to 2800 Pa.s and from 3500 Pa.s to 1250 Pa.s respectively. According to the literature [39], the decrease in viscosity corresponds to a loss in molecular weight. This was caused mainly by the breaking down of the chain length of both polymers due to the strong shear forces. Moreover, the processing temperature had larger influence on the viscosities values of PLA during time, which decreased from at constant frequency. The viscosity-frequency curves of PLA melts display a maximum instead of a horizontal plateau. This unusual behavior can be related to a thermal degradation process at long residence times in the rheometer despite using nitrogen [60]. Furthermore, the complex viscosity, normalized by its initial values at t=0, is presented as a function of time for PLA and PBAT, as it is shown in Figure II-4.

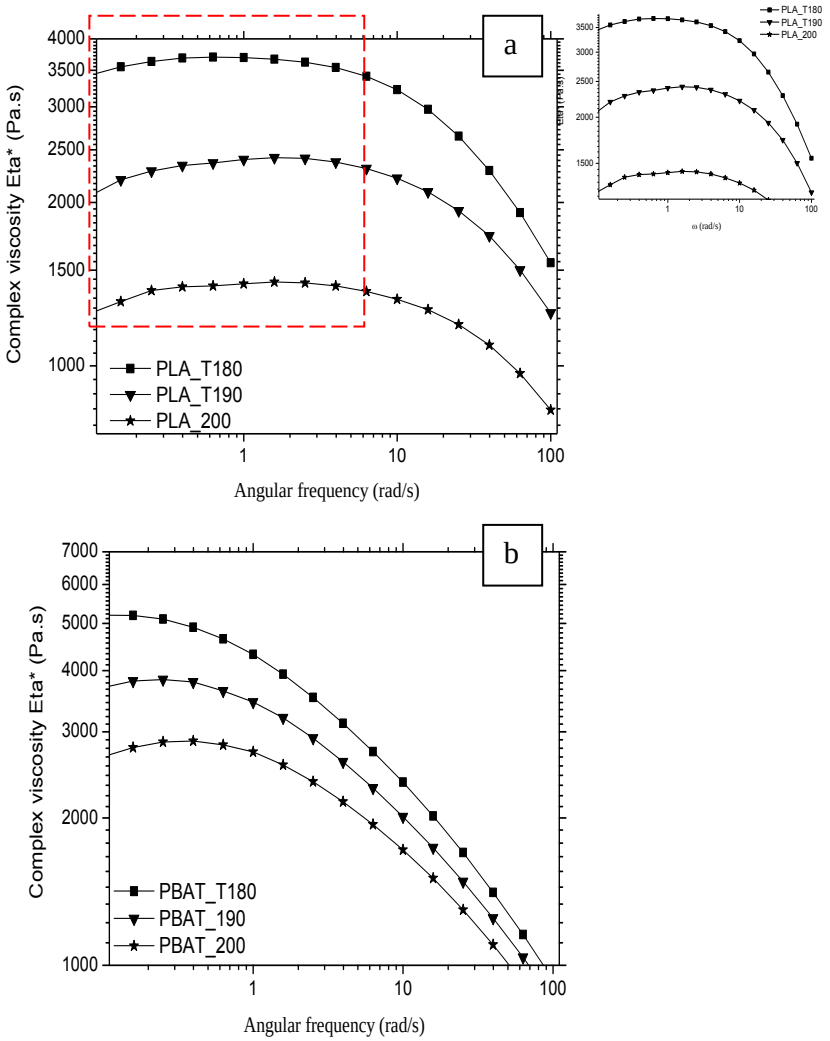

Figure II-3 Rheological behavior of (a): PLA and (b): PBAT at different temperatures, under inert atmosphere

For these two polymers, a significant reduction in viscosity over time was observed. This drastic decrease also confirms the possible thermal degradation occurring during processing.

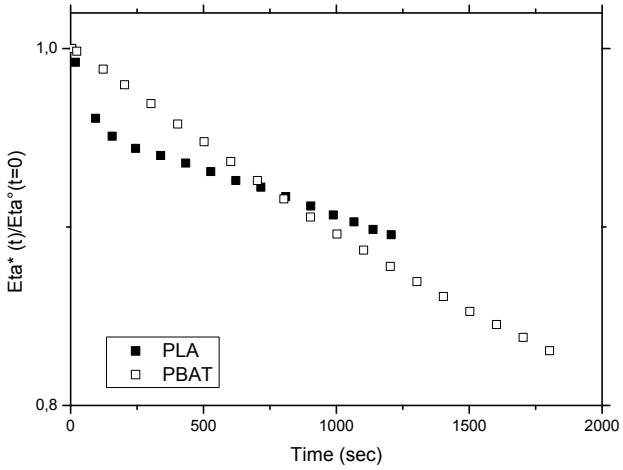

Figure II-4 Evolution of Eta*(t)*/Eta°(t=0) versus time of PLA and PBAT at 180°C

Thermal instability of PLA at high temperatures in the extrusion process has been broadly investigated [40-42-43-46]. Numerous researches reveal that the degradation reactions can occur during processing. Their identification seems to be complicated. On the other hand, few efforts have been dedicated to the study of the thermal degradation of PBAT. It was reported that no significant chain modification of PBAT occurred upon processing up to 200°C [14]. In case of polyesters, many several degradation mechanisms can happen depending on the processing conditions. Hydrolysis of the ester linkage, water-based degradation mechanism, randomly takes place in the polymer. The rate of such a mechanism depends on water concentration, acid or base catalyst, morphology of the polymer and temperature [40-44]. Based on the study performed by Witzke (1997), hydrolysis is the dominant degradation mechanism at a temperature between 150-215°C [45]. Other study showed that the thermal degradation was also found to proceed by random main-chain scission at temperatures above 180°C [13]. The chain end groups contribute also to the degradation.

a) Proposed hydrolytic mechanism of PLA

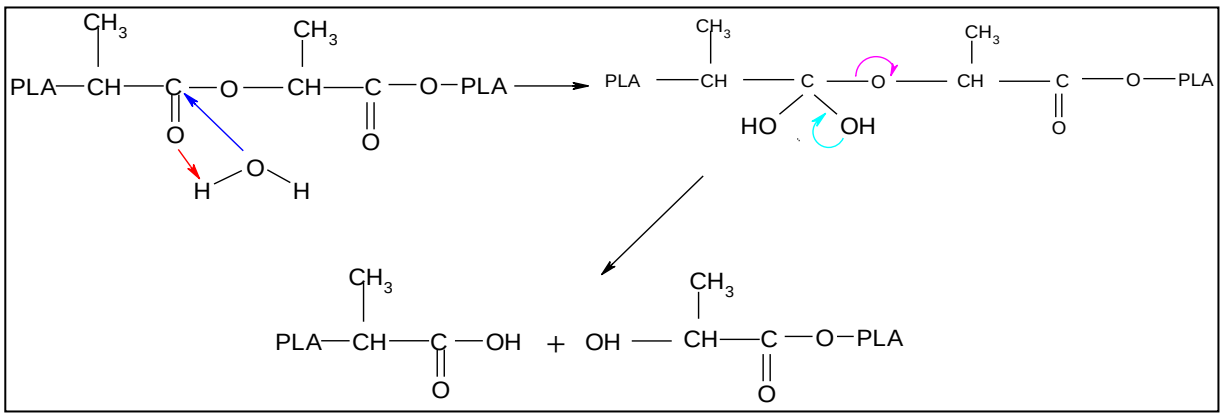

b) β-C-H Hydrogen transfer of PLA

Figure II-5 Proposed degradation mechanisms of PLA

Their contribution is more pronounced in the temperature range of 270°C-360°C [41]. Gupta et al [8] reported that, in polyesters case, there are three possible linkages i.e. carbon-Oxygen ether linkage (β-H-C hydrogen transfer), Carbonyl Carbon-Carbon linkage and Carbonyl Carbon-Oxygen linkage which can undergo scission linkages. The Carbonyl Carbon-Oxygen linkage would be cleaved in the early stage of PLA thermal degradation. Tranesterification, cis-elimination and thermo-oxidative reaction can not occur in our case; Trans-esterification mechanism was found as a dominant degradation mechanism of PLA at high temperatures (above

200°C), leading to the formation of cyclic oligomers [12-41-51]. Cis-elimination and thermo-oxidative reactions also occur at high temperature range (300-500°C) [41-12]. Based on these observations, the possible mechanisms of the thermal degradation of PLA as well as PBAT in our study were determined, as shown in Figures II-5 and II-7 [49]. They include hydrolysis and random main-chain scission (a β-C-H hydrogen transfer reaction, leading to a vinyl ester and acid end groups was presented).

The hydrolytic degradation of PLA and PBAT is primarily due to hydrolysis of the ester linkages, which occurs more or less randomly along the backbone of the polymer. It requires the presence of water according to the following reaction (Reaction (II-5a) and (II-5b)). In PBAT case, only one proposed mechanism is showed. Water can also react with the Carbonyl functions close to the benzene ring. It can be neglected in our case.

FTIR spectra of neat and processed PLA are represented in Figure II-6. According to Ibrahim et al. very strong and broad peaks in the range 3200-3600 cm^{-1} are due to stretching vibrations of O-H groups and the two peaks at around 2800-3000 cm^{-1} are clearly associated with the symmetric stretching vibration of the axial CH groups in saturated hydrocarbons. The lower intensity peaks in the range 2100-2300 cm^{-1} are also related to O-H stretching vibrations in carboxyl acids groups. The intensive peak originating from C=O stretching vibrations is located at around 1720 cm^{-1}.

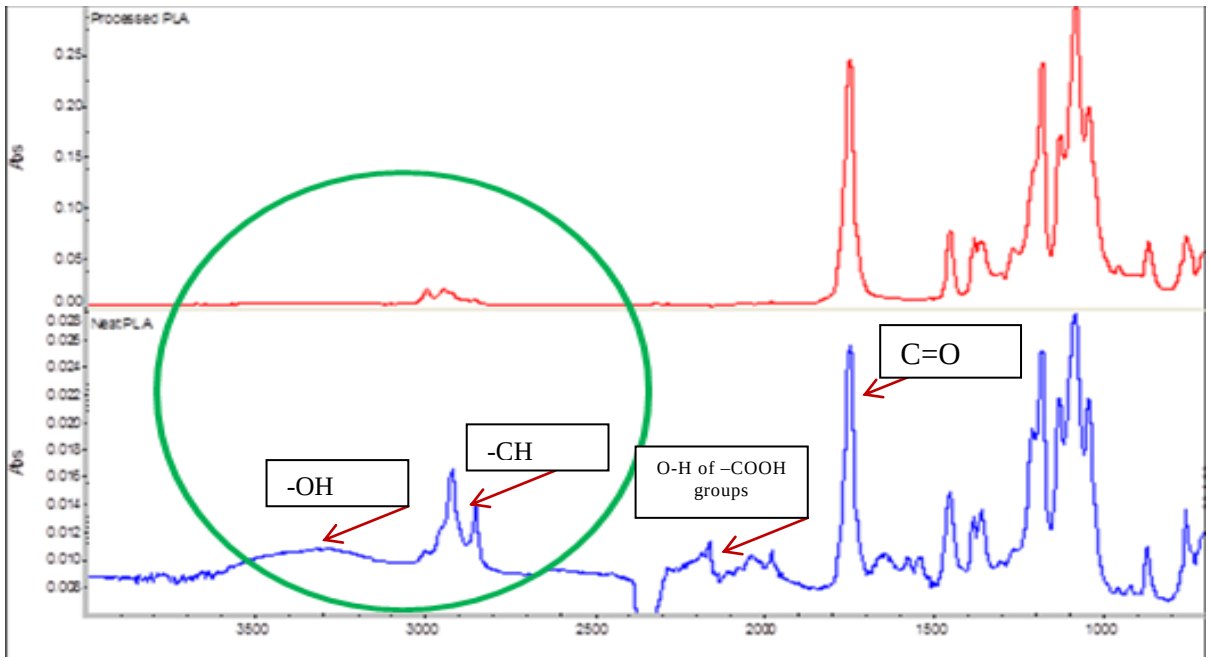

Figure II-6 FT-IR spectra of neat and processed PLA

Many weaker peaks in the range 1250-1050 cm^{-1} are assigned to C-O from carboxyl groups and C-O-C stretching vibrations. Three peaks at 1300-1500 cm^{-1} may be attributed to the vibration of C-H in CH3 groups. The peak at around 1630 cm^{-1} may correspond to H-O-H bending vibrations. There is no hint of this peak in the infrared spectrum of processed PLA. The absence of this peak could explain the occurrence of thermal chain scission at C-O bond [47], as proposed by Holland et al for PET polymer [62]. Hence, the β-C-H hydrogen transfer of PLA was proposed (cf. Fig. II-5b).

a) Proposed hydrolytic mechanism of PBAT

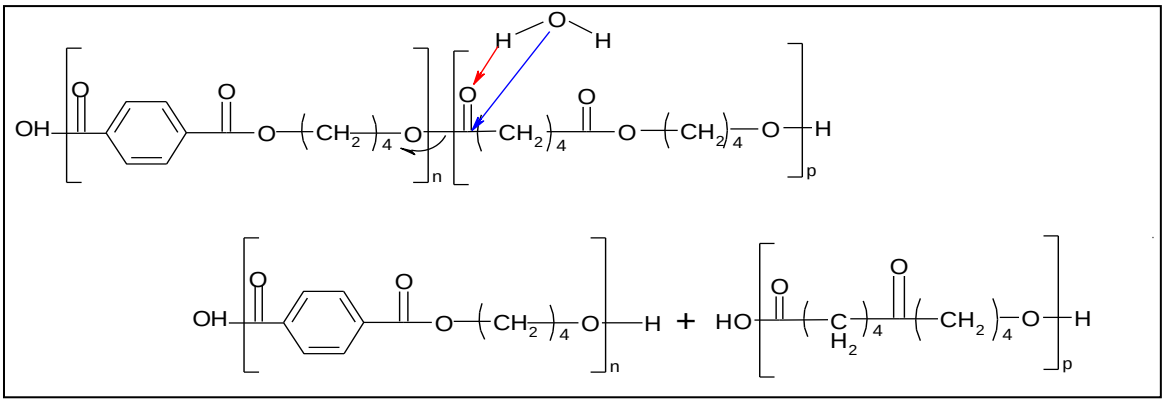

b) Main chain scissions degradation

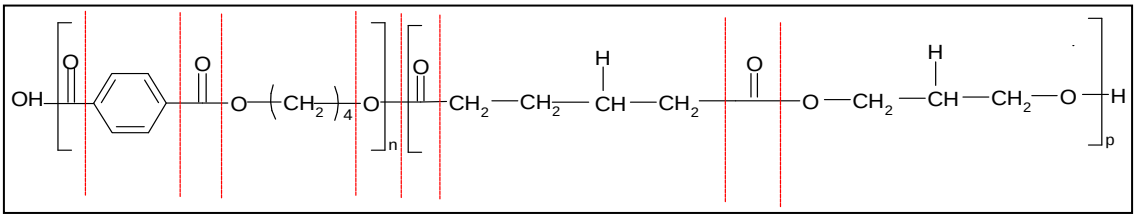

c) β-C-H Hydrogen transfer of PBAT

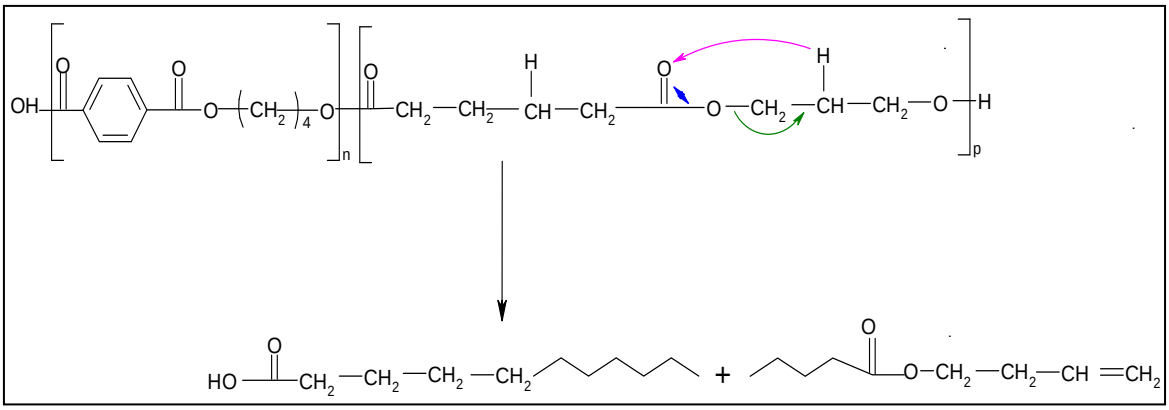

Figure II-7 Proposed degradation mechanisms of PBAT

In the other hand, few are the works dealing with the thermal degradation of PBAT. Some authors reported that the thermal behavior of PBAT shows two stages corresponding to the degradation of PBAT, which may due to the maximum decomposition of aliphatic copolyester adipic acid and 1,4-butanediol) at 340–400°C and the maximum decomposition of aromatic copolyester (terephthalic acid) at 520–600°C [48]. Others studies highlighted a β-scission occurrence on PBAT chains in the presence of dicumyl peroxide (DCP) at 180°C [49]. It was also reported that main chain scission could occur following a photodegradation [50] (Cf. Figure II-7b). According to these observations, we believe that, as PLA, a β-C-H hydrogen transfer reaction can also happened.

Figure II-8 represents the FTIR spectra of neat and processed PBAT. The functional groups of both PBAT(s) can be described as: peaks at around 3000 cm^{-1} representing C-H stretching in ali-

phatic and aromatic portions; at around 1710 cm^{-1} representing carbonyl groups (C=O) in the ester linkage; at 1267 cm^{-1} representing C-O in the ester linkage; and a sharp peak at 720 cm^{-1} representing four or more adjacent methylene (-CH2-) groups. Bending peaks of the benzene substitutes are located at wave numbers between 700 and 900 cm^{-1}. FTIR is not an efficient tool to detect the occurred thermal degradation of PBAT [50]. Titrations of functional groups before and after processing may represent a reliable method, as mentioned by Coltelli et al [37]. The titrations results demonstrated an increase of –COOH groups of PBAT.

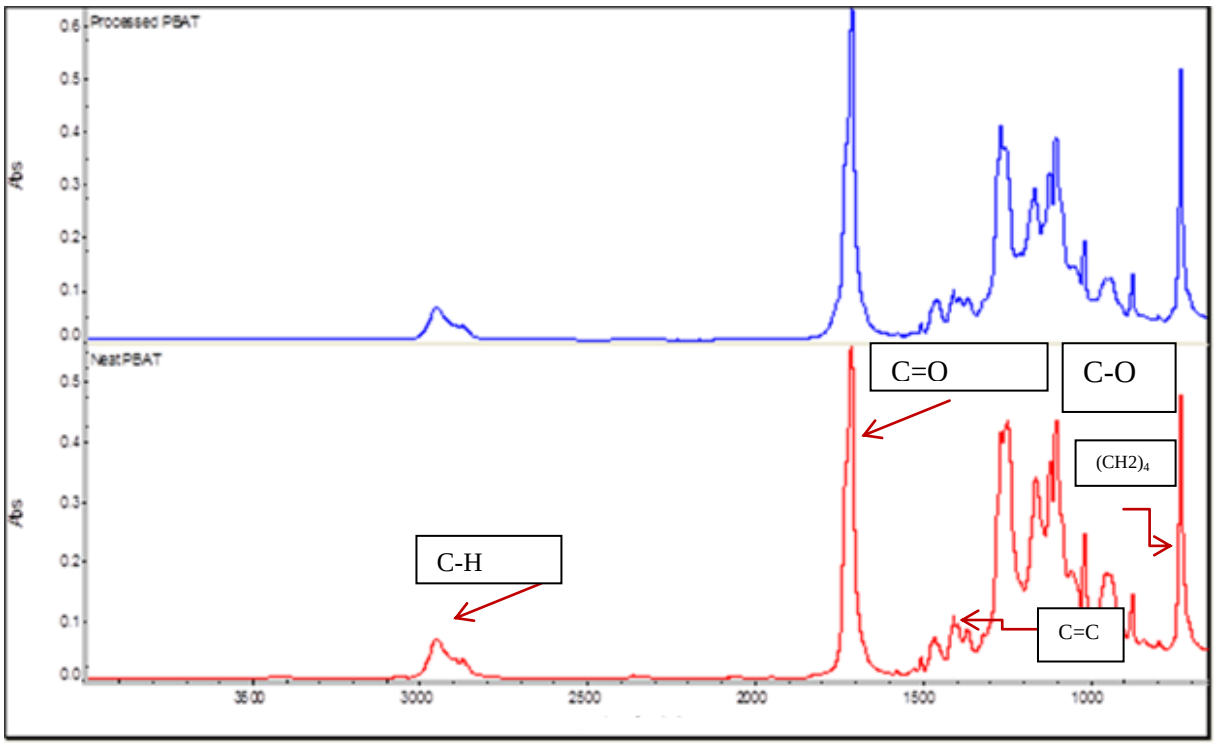

Wave number (cm^{-1})

Figure II-8 FT-IR spectra of neat and processed PBAT

III.6 Reactive extrusion of PLA, PBAT and their blends with functionalized epoxy

Table I-2 summarizes the compositions of different polymers/Joncryl blends. The preparation of these blends was discussed in Chapter I, processing & blend preparation paragraph.

III.6.1 Reactive processing of PLA, PBAT and PLA/PBAT/Joncryl blends

To compensate for such chain scission reactions, a chain extender, named Joncryl ADR®, is incorporated. According to the literature, the epoxide groups of Joncryl ADR® can theoretically react with both hydroxyl and carboxyl groups of the polyesters. Japon et al allow differentiating between the reaction of carboxylic acid and hydroxyls groups with epoxide, since epoxide groups are known to react differently with –COOH and –OH groups (Table II-5) [18-52-53].

Table II-5 Comparison between the reaction rate of Carboxylic acid/Epoxide and Hydroxyl/Epoxide

Reactive pair	Reaction rate
Carboxylic acid/epoxide	18
Primary Hydroxyl/epoxide	1.2
Secondary hydroxyl/epoxide	1

In the case of polyesters, glycidyl esterification of carboxylic acid end groups precedes hydroxyl end group etherification. This latter reaction competes with etherification of secondary hydroxyl groups and main chain transesterification. The resultant couplings involve epoxy ring-opening reactions and the creation of covalent bonds via hydroxyl side group formation. The proposed mechanism of reaction is shown here (Figure II-9). The resultant (polymer-GMA functions) system represents a complex set of concurrent reactions due to the degradation/chain extension/branching balance.

a) Predicted mechanism of the reaction between PLA and Joncryl

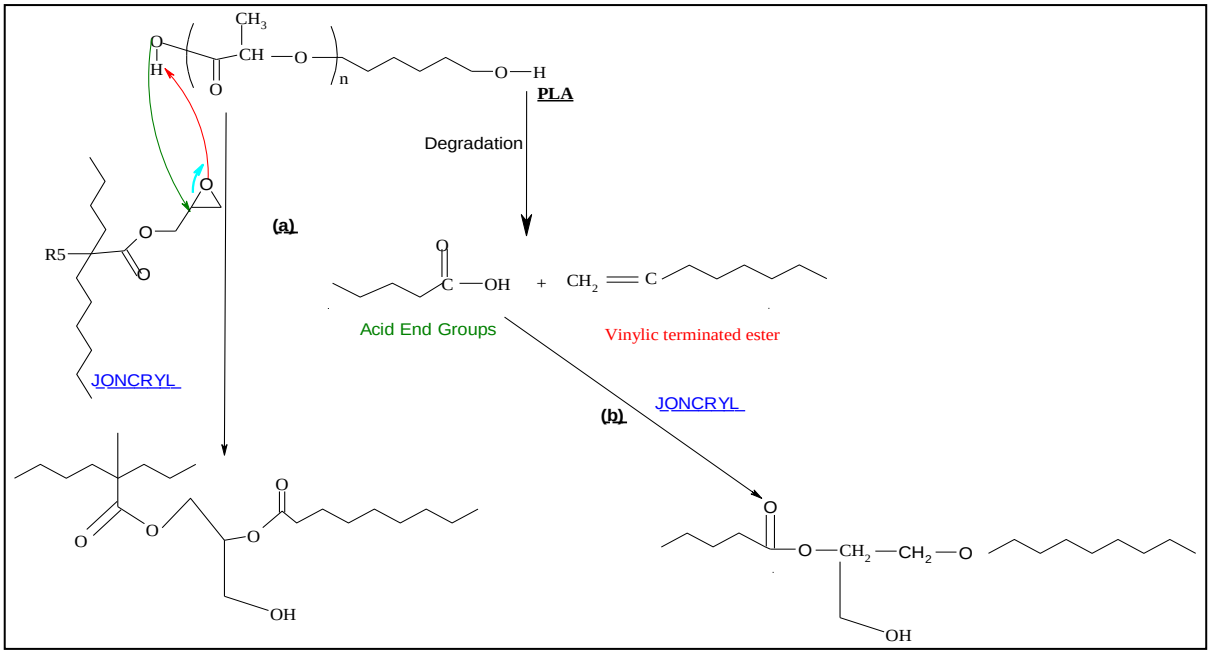

b) Predicted mechanism of the reaction between PBAT and Joncryl

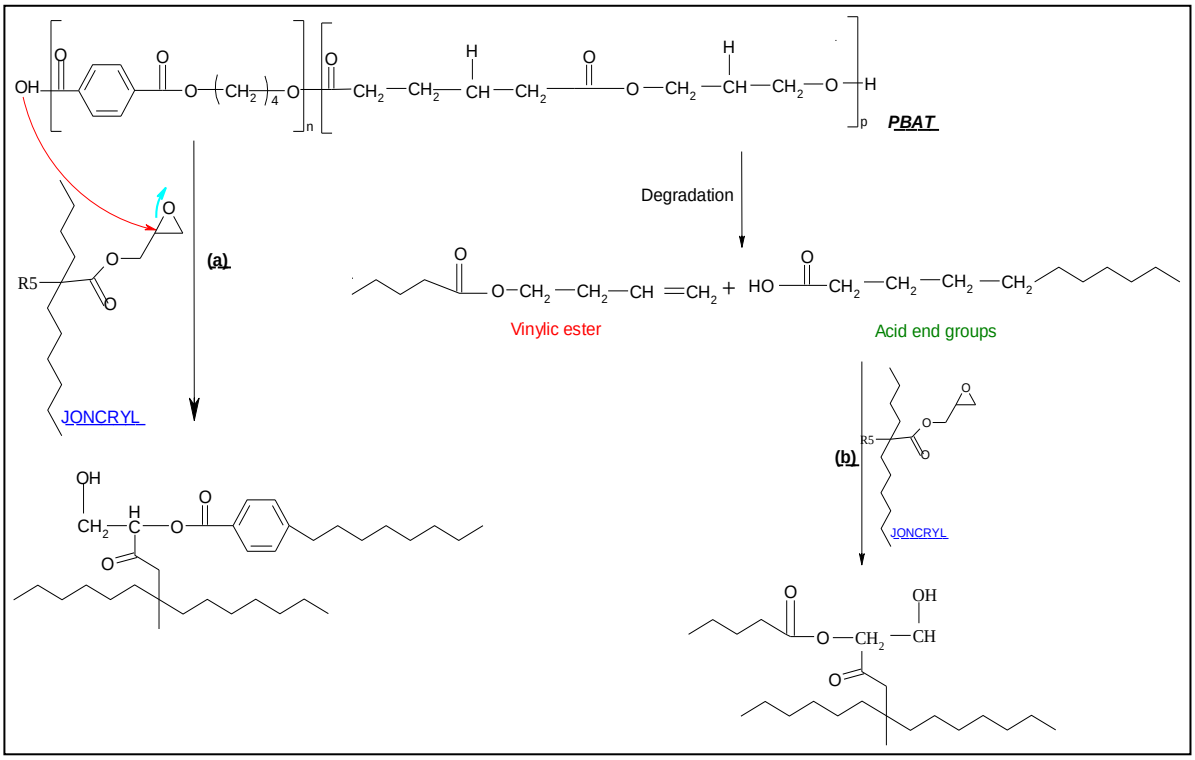

Figure II-9 Predicted reaction between polyesters and epoxy functions

III.6.1.1 Rheological investigations of modified PLA and PBAT systems

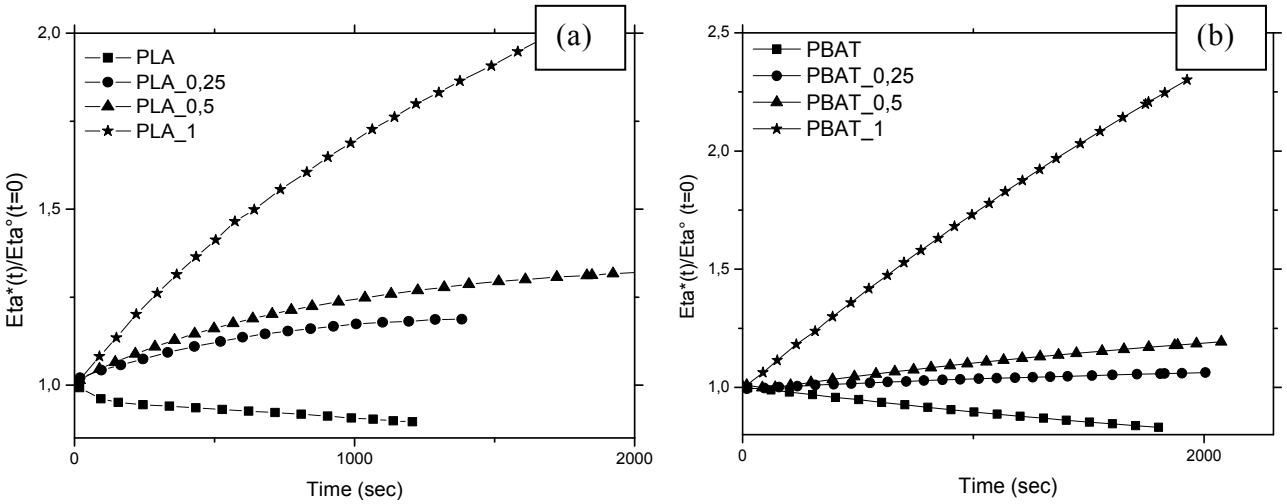

Figure II-10 Eta*(t)/Eta° (t=0) evolution versus time for (a) neat and modified PLA (b) neat and modified PBAT at 180°C

As discussed before, the results of rheological tests of neat PLA and PBAT at 180°C demonstrated a monotonous decreasing viscosity over time, highlighting therefore the occurrence of thermal degradation. This latter phenomenon is related to the decrease of intrinsic viscosity and the average molecular weight. Figure II-10 shows that the incorporation of Joncryl ensures viscosity's stabilization during time, depending on its amount. For both

polymers, at 0,25 and 0,5%wt, the viscosity takes less time to stabilize compared to the 1%wt of Joncryl where a drastic increase of relative viscosity was observed.
This could indicate significant branched structures in addition to linear ones. The initial viscosity further increases until remains constant, confirming that no significant change takes place during the rheological tests.

For both polymers, the complex viscosity modulus gradually decreases with angular frequency which is typical shear-thinning behavior, as it can be seen in Figure II-11. Thus, the incorporation of Joncryl ADR® ratio enhance the shear thinning behavior of both PLA and PBAT and consequently shifts the Newtonian plateau to lower angular frequencies [36].

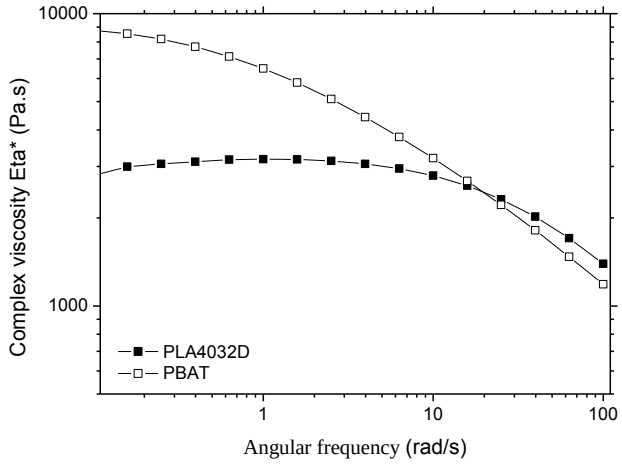

Figure II-11 Complex viscosity versus angular frequency (at 180°C) for the neat PLA and PBAT

Moreover, respective viscosities converge at high angular frequency. Chain orientation and thermal energy dissipation would be responsible for these close results. In addition, an enhancement of storage modulus G' values steadily over the whole frequency range was observed, more pronounced at lower angular frequency. The introduction of chain branches due to chain extending reactions could explain the improvement of melt elasticity. According to the literature simple star or linear structures cannot result in such a pronounced increase on elasticity of material [7-55-56]. The work is in progress to investigate the real chains topology of modified PLA and PBAT. Storage modulus become less shear sensitive when chain extension/branching agent content is increased thus revealing a cohesive network viscosity (cf. Figure II-12).

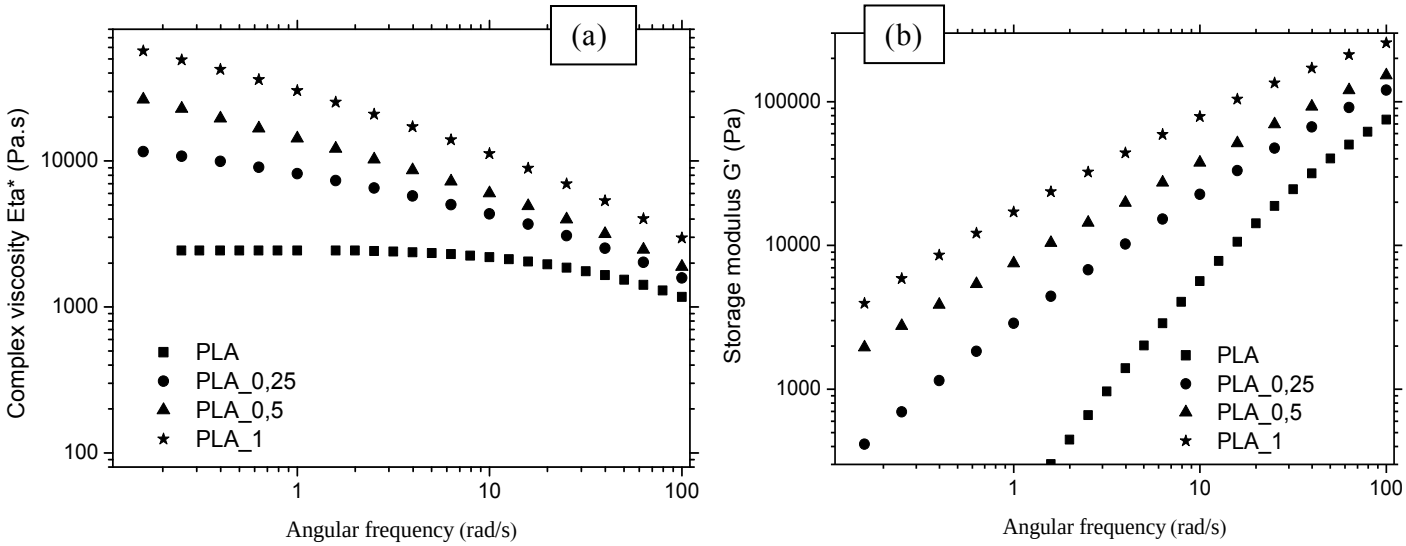

Figure II-12 (a) The complex viscosity and (b) the storage modulus angular frequency dependence at 180°C for neat and modified stable PLA with chain extender

Using a chain extender, as Joncryl ADR®, increases the viscosity and the storage modulus. It facilitates further processing since high melt viscosity and elasticity are required in processes such as thermoforming and foaming. Furthermore, the weight relaxation spectrums (λH (λ)) were also plotted to probe the effect of chain extension/branching agent on the linear viscoelastic behavior of our modified polyesters. The linear relaxation spectrum H (λ), using the plots of **G'**and ***G"*** data's, is plotted as follow (Eq. 6) [36]:

Equation 6

$$G^*(\omega,\lambda) = \int_{-\infty}^{+\infty} \frac{H(\lambda)i\omega\lambda}{\lambda(1+i\omega\lambda)} d\lambda$$

Where ω is the frequency and λ is the relaxation time. The time distribution of chains relaxation for neat and modified PLA and PBAT is reflected in Figure II-13. It is observed that the neat polymers present only one relaxation time, corresponding to this of one component, which is the pure polymer. However, in the case of modified polymers, two main relaxation times can be clearly identified, which were interpreted by the simultaneous occurrence of two relaxation processes.

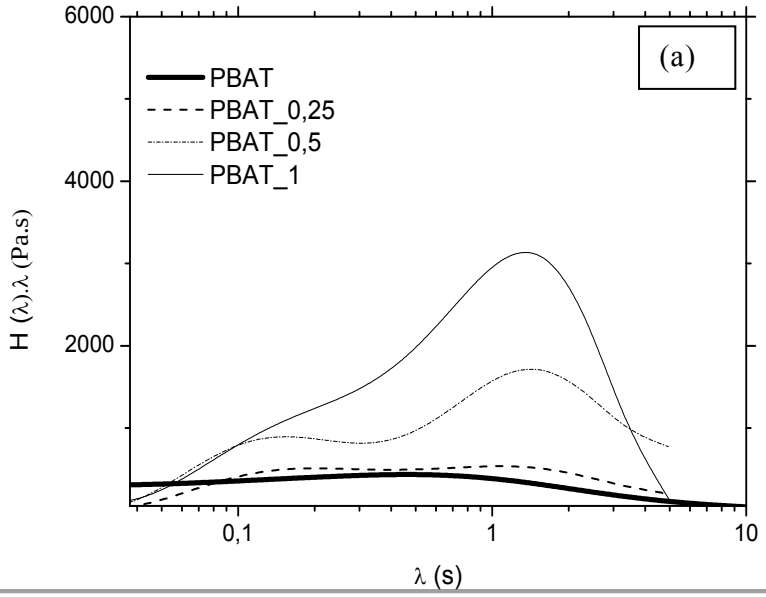

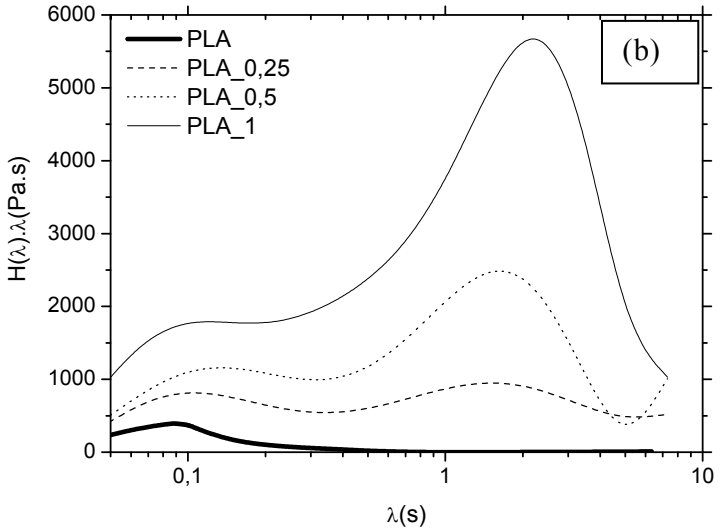

Figure II-13 Relaxation spectra of the neat and modified stable polymers
(a): PBAT (b): PLA

The same double time relaxation distribution has already been observed by Wood-Adams for long chain branched PE [57]. The high values of relaxation time λ correspond to the relaxation of the long, heavy and branched chains due to the presence of epoxy functions which restricts the chain mobility of neat polymers and retards the overall relaxation of modified polymers. The lower ones are related to the relaxation of short chains. The presence of branching, the improvement of molecular weight $\overline{M_\omega}$ and intrinsic viscosity could explain the remarkable increase of λ.

III.6.2 Molecular weight measurements and rheological investigation of modified PLA and PBAT systems upon processing

III.6.2.1 Molecular weight measurements

To fully understand the chain extension/branching balance occurring during reactive processing, the intrinsic viscosity [η] and the measurements of average molecular weight have been carried out. The incorporation of GMA/Epoxide functions into PLA and PBAT during processing significantly increases the "$\overline{M_\omega}$" and the intrinsic viscosity (Table II-7; Figure II-14). The change of molecular weight of studied systems was a direct evidence for chain extension which can be considered as the recuperation to the decrease of the molecular weight during melt extrusion, which is more pronounced for PLA. The measurements of intrinsic viscosity corroborate thus the obtained one of SEC experiments. We believe that the increase of K' values with the incorporation of reactive GMA functions is caused by the lower solubility of polymer chains, probably due to branching chain (cf. Table II-6) [35].

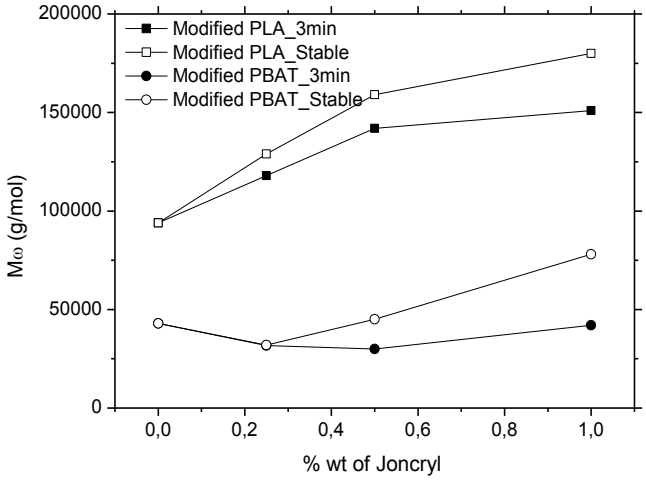

Figure II-14 Evolution of the average molecular weight "$\overline{M_\omega}$ "for polymers at 3 min upon processing and stable modified polymers

In other words, the polymer–solvent interactions are decreasing, but the polymer–polymer interactions, or association, are increasing with the ionic strength. It is clearly evident to notice that the branching reactions at such Joncryl ADR® concentrations did not reach the point of heavy cross-linking or gel formation. Recently, some authors [21] reported that when the ratio of Joncryl reached 1.5 wt%, the sample was slightly cross-linking. It was also showed that the reaction of crosslinking of epoxy functions starts at high temperatures [54].

Table II-6 K' values for neat and modified stable polymers

Samples	K'	Samples	K'
PLA_0	0,3	PBAT_0	0,93
PLA_0,25_stable	0,42	PBAT_0,25_stable	1,8
PLA_0,5_stable	0,5	PBAT_0,5_stable	1,44
PLA_1_stable	0,54	PBAT_1_stable	3,42

A careful study of rheological behavior and thermal stability of these materials will provide more information for processing PLA/PBAT blends in proper conditions and thus avoid the irreversible structure changes under non optimized melt processing conditions.

Table II-7 Characteristic molecular weights obtained by SEC and intrinsic viscosity measurements for different modified materials at 180°C

Samples	Intrinsic viscosity (ml/g)	$\overline{M_\omega}$ (g/mol)
PLA_0,25_3min upon processing	165	118000
PLA_0,5_3min upon processing	197	142000
PLA_1_3min upon processing	209	151000
PLA_0,25_stable	178	129000
PLA_0,5_stable	220	159000
PLA_1_stable	250	180000

Samples	Intrinsic viscosity (ml/g)	$\overline{M_\omega}$ (g/mol)
PBAT_0,25_3min upon processing	70	31700
PBAT_0,5_3min upon processing	65	30000
PBAT_1_3min upon processing	93	42000
PBAT_0,25_stable	71	42000
PBAT_0,5_stable	100	45000
PBAT_1_stable	170	78000

III.6.3 Thermal stability investigations of PLA/PBAT blends

We have demonstrated previously the competition of several mechanisms (degradation, chain extension, branching) over time in the presence of Joncryl ADR®. The balance between these occurred phenomena enhanced the thermal stability of PLA and PBAT. The improvement of the thermal stability of these polymers should affect the final properties of their blends. Despite the interesting nature of the kind of research, few efforts have been dedicated to this subject. Kumar et al. reported that the incorporation of GMA functions into PLA/PBAT blends in order to investigate the mechanical properties of 80/20/GMA (Glycidyl methacrylate) blends [24]. The surprising strain at break value (3%) of PLA/PBAT/GMA blends, lower than those of PLA (4.5%) and PBAT (500%) was observed. The better understanding of the polymer stability could be an interesting approach to explain this strange value. Figure II-15 showed a reduced thermal degradation for PLA/PBAT blends. The co-existence of these two polymers leads to a reduction of the terminal –COOH and –OH in the PLA molecular chain due to a condensation reaction [58].

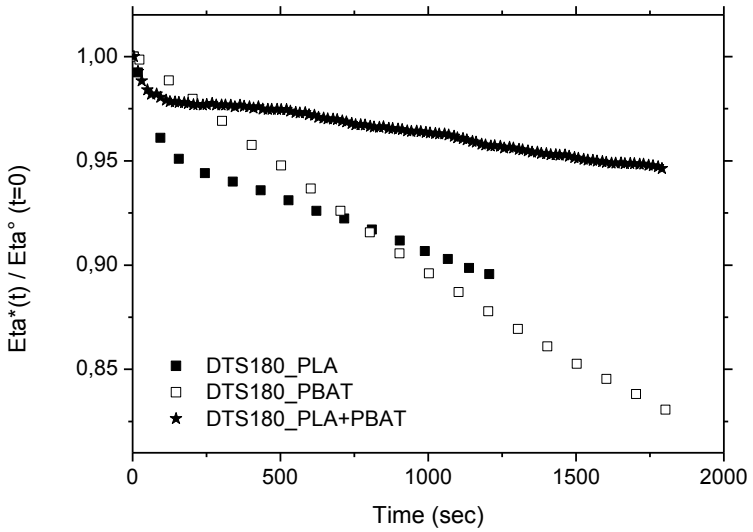

Figure II-15
Eta*(t) /Eta° (t=0) evolution versus time for PLA/PBAT (80/20) at 180°C

Meanwhile, PLA/PBAT blends showed stronger shear-thinning behavior in the whole frequency range compared to neat PLA. This trend becomes more pronounced with the increasing of PBAT contents as well PBAT present a more pronounced pseudoplastic behavior (cf. Figure II-16) [61].

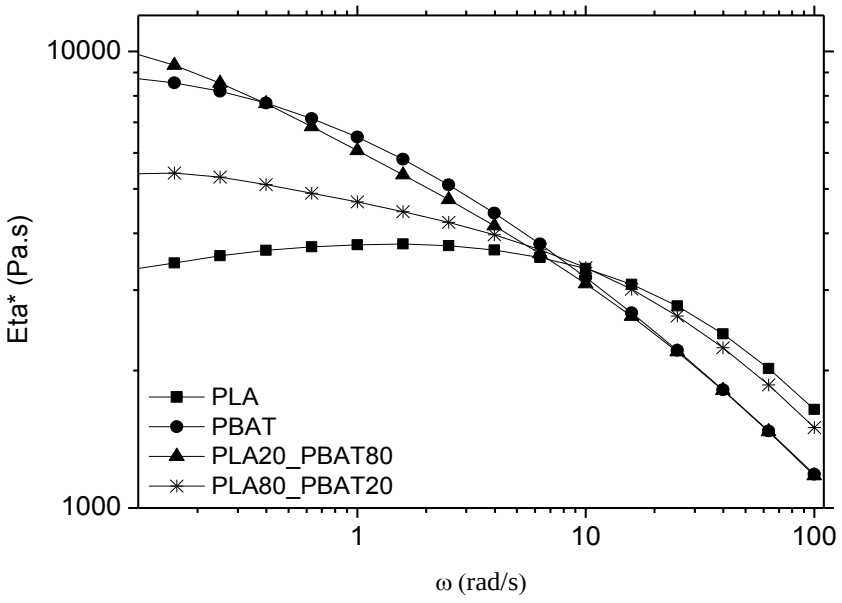

Figure II-16 The angular frequency dependence of the complex viscosity at 180°C for PLA, PBAT and PLA/PBAT blends with two different ratios of PLA/PBAT, 80/20 and 20/80

The complex viscosity of PLA/PBAT blends increased significantly compared with pure PLA. This fully proves the effectiveness of PBAT in improving melt viscosity and elasticity of PLA [59]. But, binary unmodified PLA/PBAT blend exhibit the typical morphological feature of in-

compatible systems with a poor interfacial adhesion between matrix and dispersed phase. For the clarity purpose, more details will be given in chapter IV.
However, it has demonstrated that the presence of the chain extension/branching agent in blends avoids any thermal degradation and provides the stabilization of the blends, probably due to ester linkage at the interface PLA/PBAT, as it can be seen in Figure II-17.
The mechanisms of interfacial reaction of PLA/PBAT blends with epoxy functions is demonstrated here (Figure II-18)

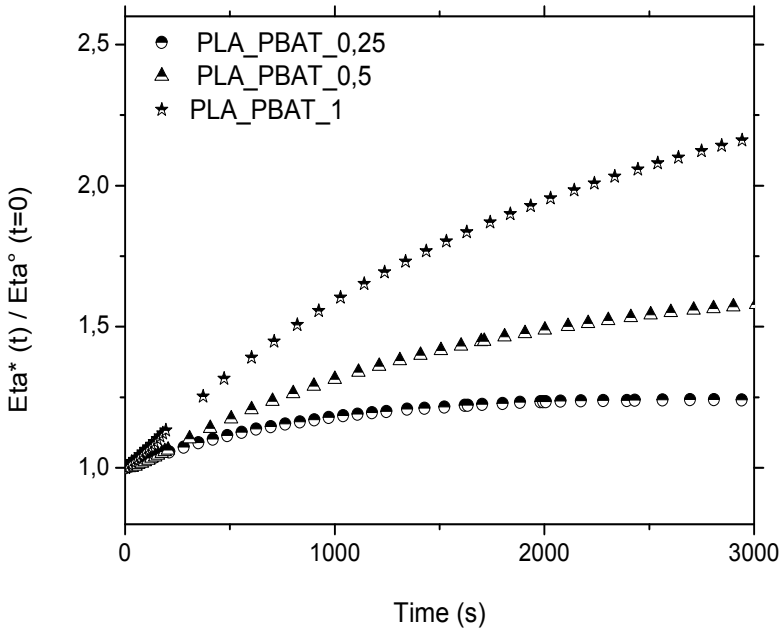

Figure II-17 Eta*(t) /Eta° (t=0) evolution versus time for PLA/PBAT/Joncryl with various concentrations of Joncryl at 180°C

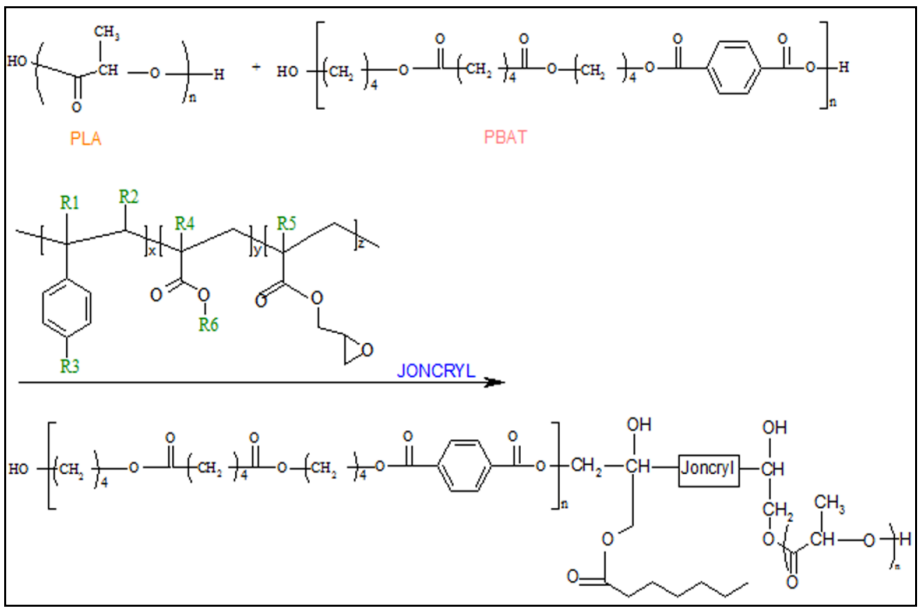

Figure II-18 Predicted reaction between Joncryl and polyesters

III.7 Mechanical properties of PLA / PBAT blends

Once the reactive stable blends were prepared, the tensile properties were being performed. The tensile mechanical properties (tensile modulus, stress at break and elongation at break) of PLA/PBAT blends are summarized in Table II-8. The results showed that the brittle properties of PLA can be modified by the addition of PBAT. The elongation at break increases from 14% (pure PLA) to 50% (PLA/PBAT blends) under processing conditions unlike Kumar et al's study [24].

Table II-8 Mechanical properties (tensile modulus, Stress at break and elongation at break) of virgin PLA, unmodified and modified PLA/PBAT blends

Samples	Tensile modulus (MPa)	Stress at break (MPa)	Elongation at break (%)
PLA_180°C	1350±90	68,5±5	14±3
PLA_PBAT_0_stable	820±70	48±2	50±10
PLA_PBAT_0.25 _stable	822±65	37±2	116±4
PLA_PBAT_0.5_stable	1095±60	47±2	135±9

It is probably related to the presence of soft elastomeric phase. The reducing of brittleness is also highlighted by the decrease of the tensile modulus from 1350 MPa to 820 MPa. Hence, the elongation at break of PLA/PBAT (80/20) blends with 0,25 and 0,5 %wt Joncryl ADR® achieved 116% and 135% respectively, higher than that for pure PLA (14%). The tensile modulus increases with the incorporation of GMA functions from 1350 MPa for PLA pure to 1095MPa for PLA/PBAT/0.5 which indicates a reactivity control at the interface due to the formation of ester linkages between PLA, PBAT and Joncryl ADR®. Therefore, the improvement of mechanical properties like elongation at break and tensile modulus was highlighted by the effect of compatibilization of Joncryl. The obtained properties have been corroborated with TEM microscopy.

IV Conclusions

Throughout this work, the thermal degradation was firstly demonstrated and quantified of the neat PLA and PBAT by using thermal and rheological tools coupled to the measurements of the average molecular weight and intrinsic viscosity. Secondly, it was shown that the reactive extrusion gives raise a more stable and modified PLA and PBAT. Finally, the PLA/PBAT 80/20 (wt/wt) blend was also prepared and its structural, rheological and improved mechanical properties was compared the unmodified one and discussed in the bases of the real mechanisms of degradation/chain extension of the polymers. Many observations were derived:

The assessment of thermal degradation for both PLA and PBAT showed that these two polymers degrade under temperature. The occurred thermal degradation of PLA and PBAT was assessed by the decrease of molecular weight and intrinsic viscosity. Moreover, the present thermal degradation was confirmed by the rheological investigation, where the viscosity decreased at very high residence time.

The incorporation of a chain extension/branching agent (Joncryl ADR-4368), by reaction extrusion, into both PLA and PBAT showed an improvement of their thermal stability. This property is thus strongly dependent on the amount of GMA functions and on the reaction time because of the competing branching and degradation reactions. It is demonstrated throughout this paper that the epoxy reactive functions have been successfully used in increasing the molar mass, intrinsic viscosity, shear thinning and elasticity during melt processing probably due to the formation of branching chains.

Hence, the mechanisms of degradation, chain extending, branching with GMA functions and their competition have been proposed.

Moreover, it was demonstrated that the incorporation of the multifunctional epoxide enhance the thermal stability of the PLA/PBAT (80/20) (w/w) blends. Compared to the unmodified samples, the presence of reactive epoxy functions showed an increase in the tensile modulus (from 820 MPa (PLA/PBAT blends) to 1095 MPa (PLA/PBAT/GMA)) and the elongation at break (from 50% (PLA/PBAT blends) to 135% (PLA/PBAT/GMA)) which contradicts the results presented by Kumar and al. where a low elongation at break value (3%) was obtained. However, in our study, the improved mechanical properties indicate a reactivity control at the interface due to the formation of ester linkages between PLA, PBAT and Joncryl ADR®.

References

[1] Gupta AP, Kumar V. New emerging trends in synthetic biodegradable polymers – Polylactide: A critique. European Polymer Journal. 43(10):4053-4074. 2007.
[2] Garlotta D. A Literature Review of Poly (Lactic Acid). Journal of Polymers and the Environment. 9(2):63-84. 2001.
[3] Alexandre M, Dubois P. Polymer-layered silicate nanocomposites: preparation, properties and uses of a new class of materials. Materials Science and Engineering: R: Reports. 28(1-2):1-63. 2000.
[4] Anderson KS, Lim SH, Hillmyer MA. Toughening of polylactide by melt blending with linear low-density polyethylene. Journal of Applied Polymer Science. 2003, 89(14):3757–3768. 2003.
[5] Martino VP, Jimenez A, Ruseckaite RA. Processing and characterization of poly(lactic acid) films plasticized with commercial adipates. Journal of Applied Polymer Science. 112 (4):2010-2018. 2009.
[6] Ogata N., Jimenez G., Kawai H., Ogihara T. Structure and thermal/mechanical properties of poly(*l*-lactide)-clay blend. Journal of Polymer Science Part B: Polymer Physics. 35(2):389-396. 1997
[7] Lehermeier HJ, Dorgan JR. Melt rheology of poly(lactic acid): Consequences of blending chain architectures. Polymer Engineering & Science. 41(12):2172- 2184. 2001.
[8] Gupta MC, Deshmukh VG. Thermal oxidative degradation of poly-lactic acid Part II: Molecular weight and electronic spectra during isothermal heating. Colloid & Polymer Science. 260(5):514–517. 1982.
[9] Kopinke FD, Remmler M, Mackenzie K, Moder M, Wachsen O. Thermal decomposition of biodegradable polyesters-II.Poly(lactic acid). Polymer Degradation and Stability. 53(3):329–342. 1996.
[10] Taubner V, Shishoo R. Influence of processing parameters on the degradation of poly(L-lactide) during extrusion. Journal of Applied Polymer Science. 79(12):2128–2135. 2001.
[11] Hyon SH, Jamshidi K, Ikada Y. Effects of residual monomer on the degradation of DL-lactide polymer. Polymer International. 46(3):196–202. 1998.
[12] Wachsen O, Platkowski K, Reichert KH. Thermal degradation of poly-L-lactide-studies on kinetics, modelling and melt stabilization. Polymer degradation and stability. 57(1):87–94. 1997.
[13] Sodergard A, Nasman JH. Stabilization of poly(L-lactide) in the melt. Polymer degradation and stability. 46(1):25–30. 1994.
[14] Signori F, Coltelli MB, BroncoS. Thermal degradation of poly(lactic acid) (PLA) and poly(butylene adipate-*co*-terephthalate) (PBAT) and their blends upon melt processing. Polymer degradation and stability. 94(1): 74-82. 2009.
[15] Mantia FL. Handbook of plastic recycling: Rapra Technology Limited. 2002.
[16] Di Y, Iannace S, Di Maio E, Nicolais L. Reactively modified poly(lactic acid) : Properties and foam processing. Macromolecular materials and engineering. 290(11):1083-1090. 2005.
[17] Kylma J, Seppala JV. Synthesis and characterization of a biodegradable Thermoplastic poly(ester-urethane) elastomer. Macromolecules. 30(10):2876-2882. 1997.
[18] Villalobos M, Awojulu A, Greeley T, Turco G, Deeter G. Oligomeric chain extenders for economic reprocessing and recycling of condensation plastics. Energy. 31(15):3227-3234. 2006.
[19] Li BH, Yang MC. Improvement of thermal and mechanical properties of poly(L-lactic acid) with 4,4-methylene diphenyl diisocyanate. Polymers for Advanced Technologies. 17(6):439-443. 2006.
[20] Awaja F, Daver F, Kosior E. Cser F. The effect of chain extension on the thermal behaviour and crystallinity of reactive extruded recycled PET. Journal of thermal analysis and calorimetry. 78(3):865–884. 2004.
[21] Yuanliang W, Chunhua F, Yongxiang L, Changshun R, Yaoyao Z, Ya F. Melt synthesis and characterization of poly(L-lactic acid) chain linked by multifunctional epoxy compound. Journal of Wuhan University of Technology-Material Science Edition. 25(5):774-779. 2010.

[22] Pilla S, Kim Seong G, Auer George K, Gong S, Park Chul B. Microcellular extrusion-foaming of polylactide with chain-extender. Polymer Engineering & Science. 49(8):1653-1660. 2009.
[23] Mihai M, Huneault MA, Favis BD. Rheology and Extrusion Foaming of Chain-Branched. Poly(lactic acid). Polymer Engineering and Science. 50(3) :629-642. 2010.
[24] Kumar M, Mohanty S, Nayak SK, Parvaiz M Rahail. Effect of glycidyl methacrylate (GMA) on the thermal, mechanical and morphological property of biodegradable PLA/PBAT blend and its nanocomposites. Bioresource technology. 101(21): 8406-8415. 2010.
[25] Biresaw G, Carriere CJ. Interfacial tension of poly(lactic acid)/polystyrene blends. Journal of Polymer Science Part B: Polymer Physics. 40 (19): 2248–2258. 2002.
[26] Huneault MA, Li H. Morphology and properties of compatibilized polylactide/thermoplastic starch blends. Polymer. 48 (1):270-280. 2007.
[27] Gu SY, Zhang K, Ren J, Zhan H. Melt rheology of polylactide/poly(butylene adipate-co-terephthalate) blends. Carbohydrate polymers. 74(1):79-85. 2008.
[28] Ko SW, Hong MK, Park BJ, Gupta RK, Choi HJ, Bhattacharya SN. Morphological and rheological characterization of multi-walled carbon nanotube/PLA/PBAT blend nanocomposites. Polymer bulletin. 63(1):125-134. 2009.
[29] Maazouz A, Lamnawar K, Mallet B. Compounding and processing of biodegradable materials based on PLA for packaging applications: In greening the 21st century materials world Frontiers in Science and Engineering: 1-44. 2011.
[30] Lamnawar K, Maazouz A, Mallet B. International patent C08J5/10, C08L67/00,FR2941702. 2010.
[31] Frenz V, Scherzer D, Villalobos M, Awojulu A.A., Edison M, and van der Meer R. Multifunctional Polymers as Chain Extenders and Compatibilizers for Polycondensates and Biopolymers. Page 1-5. 2008.
[32] Corre YM, Duchet J, Maazouz A, Reignier J. Batch foaming of chain extended PLA with supercritical CO_2: Influence of the rheological properties and the process parameters on the cellular structure. The Journal of Supercritical Fluids. 58 (1): 177-188. 2011.
[33] Huggins ML. The Viscosity of Dilute Solutions of Long-Chain Molecules. IV. Dependence on Concentration. Journal of the American Chemical Society. 64 (11): 2716–2718. 1942.
[34] Kraemer EO. Molecular Weights of Celluloses and Cellulose Derivates. Industrial and Engineering Chemistry. 30(10): 1200–1203. 1938.
[35] Cho J, Heuzey MC, Begin A, Carreau PJ. Viscoelastic properties of chitosan solutions: Effect of concentration and ionic strength. Journal of Food Engineering. 74 (4): 500 515. 2006.
[36] Corre YM, Duchet J, Maazouz A, Reignier J. Melt strengthening of poly (lactic acid) through reactive extrusion with epoxy-functionalized chains. Rheologica Acta. 50(7-8): 613-629. 2011.
[37] Coltelli MB, Toncelli C, Ciardelli F, Bronco S. Compatible blends of biorelated polyesters through catalytic transesterification in the melt. Polymer Degradation and Stability. 96(5): 982-990. 2011.
[38] Hwang SS, Hsu PP, Yeh JM, Chang KC, Lai YZ. The mechanical/thermal properties of microcellular injection-molded poly-lactic-acid nanocomposites. Polymer Composites. 30(11): 1625-1630.2009.
[39] Ray SS, yamada K, Okamoto M, Ogami A, Ueda K. Polylactide-Layered Silicate Nanocomposite: A Novel Biodegradable Material. Macromolecules. 35(8):3104-3110. 2002.
[40] Amar K, Mohanty M, Lawrence TD. Michigan: Taylor & Francis. Vol.1-Chapter 16. 2005.
[41] Kopinke FD, Mackenzie K. Mechanistic aspects of the thermal degradation of poly(lactic acid) and poly(β-hydroxybutyric acid). Journal of Analytical and Applied Pyrolysis. 40-41: 43-53. 1997.
[42] Fan YJ, Nishida H, Shirai Y, Tokiwa Y, Endo T. Thermal degradation behaviour of poly(lactic acid) stereocomplex. Polymer Degradation and Stability. 86 (2):197-208. 2004.

[43] Lucas N, Bienaime C, Belloy C, Queneudec M, Sylvestre F, Nava-Saucedo. Polymer biodegradation: Mechanisms and estimation techniques – A review. Chemosphere. 73(4) :429-442. 2008.
[44] Jong SJD, Arias ER, Rijkers DT, Nostrum CF, Hennink WE. New insights into the hydrolytic degradation of poly(lactic acid): participation of the alcohol terminus. Polymer. 42(7):2795-2802. 2001.
[45] Witzke DR. Doctor of philosophy, Michigan State University, Michigan1997.
[46] Ramkumar DHS, Bhattacharya M. Steady shear and dynamic properties of biodegradable polyesters. Polymer Engineering and Science. 38(9):1426-1435.1998.
[47] Harnnecker F, Derval dos Santos R, Lenz DM. Biodegradable Polyester-Based Blend Reinforced with Curauá Fiber: Thermal, Mechanical and Biodegradation Behaviour. Journal of Polymers and the Environment. 20(1):237–244. 2012.
[48] Nor Azowa I, Nazri MR, Wan Zin Wan Y, Jamaliah S. A study of poly vinyl chloride / poly (butylene adipate-co-terephthalate) blends. Journal of Polymer Research. 2011; 18 (5) : 891–896. 2011.
[49] Kanzawa T, Tokumitsu K. Mechanical properties and morphological changes of poly(lactic acid)/polycarbonate/poly(butylene adipate-*co*-terephthalate) blend through reactive processing, Journal of Applied Polymer Science. 121 (5): 2908-2918. 2011.
[50] Kijchavengkul T, Auras R, Rubino M. Measuring gel content of aromatic polyesters using FTIR spectrophotometry and DSC. Polymer Testing. 27(1): 55–60. 2008.
[51] Carrasco F, Pagès P, Gámez-Pérez J, Santana OO, Maspoch ML. Processing of poly(lactic acid): Characterization of chemical structure, thermal stability and mechanical properties. Polymer Degradation and Stability. 95(2): 116-125. 2010.
[52] Japon S, Luciani A, Nguyen QT, Leterrier Y, Manson JA. Molecular characterization and rheological properties of modified poly(ethylene terephthalate) obtained by reactive extrusion. Polymer Engineering and Science. 41(8):1299-1309. 2001.
[53] Lamnawar K, Maazouz A. Rheology and morphology of multilayer reactive polymers: effect of interfacial area in interdiffusion/reaction phenomena. Rheologica Acta. 47(4):383-397. 2008.
[54] Lamnawar K, Baudouin A, Maazouz A. Interdiffusion/reaction at the polymer/polymer interface in multilayer systems probed by linear viscoelasticity coupled to FTIR and NMR measurements. European Polymer Journal. 46(7): 1604-1622. 2010.
[55] Jianye L, Lijuan L, Wei Y, Ruogu L, Runming L, Chixing Z, Long chain branching polylactide: Structures and properties. Polymer. 51(22): 5186-5197. 2010.
[56] Munari A, Pezzin G, Pilati F, Manaresi P. Rheological characterization of highly branched poly(ethyleneterephthalate). Rheologica Acta. 28 (1): 25-29. 1989.
[57] Wood-Adams P, Costeux S. Thermorheological Behavior of Polyethylene: Effects of Microstructure and Long chain Branching. Macromolecules. 34(18): 6281-6290. 2001.
[58] Yuan H, Liu Z, Ren J. Preparation, characterization, and foaming behavior of poly(lactic acid)/poly(butylene adipate-co-butylene terephthalate) blend. Polymer Engineering and Science. 49(5): 1004-1012. 2009.
[59] Zhang N, Wang Q, Ren J, Wang L. Preparation and properties of biodegradable poly(lactic acid)/poly(butylene adipate- co -terephthalate) blend with glycidyl methacrylate as reactive processing agent. Journal of Materials Science. 44(1):250–256. 2009.
[60] Arraiza A. Lopez, Sarasua JR, Verdu J, Colin X. Rheological Behavior and Modeling of Thermal Degradation of Poly(ε-Caprolactone) and Poly(L-Lactide). International Polymer Processing XXII 5: 389-394. 2007.
[61] Li K, Peng J, Turng LS, Huang HX. Dynamic rheological behavior and morphology of polylactide/poly(butylenes adipate-co-terephthalate) blends with various composition ratios. Advances in Polymer Technology. 30 (2): 150-157. 2011.
[62] Holland BJ, Hay JN. The thermal degradation of PET and analogous polyesters measured by thermal analysis–Fourier transform infrared spectroscopy.Polymer. 43(6):1835-1847. 2002.

Chapter 3
Chain extension/branching balance of modified PLA and PBAT polymers with a multifunctional epoxide: rheological and solution properties

3

I Abstract

The poly (lactic acid) (PLA) and the poly (butylene-adipate-co-terephtalate) (PBAT) were chain extended with the help of a chain extension agent, named Joncryl ADR®-4368 and containing reactive Glycidyl methacrylate (GMA) /epoxide functions. The blends were prepared through a twin-screw reactive extrusion system. The resulted chain extension/branching balance, due to the reactive highly functionalized epoxide, has been discussed. It was assessed using rheological investigations (relaxation spectra, flow activation energy, Van Gurp Palmen plots) coupled to the solution viscosimetric properties (size-exclusion chromatography, solution viscosimetry properties, gyration and hydrodynamic radii). Based on these results, the topology of modified PLA and PBAT has been studied and analyzed. Indeed, they exhibited a typical feature of a mixture of linear and randomly branched polymers.

Keywords: Chain extension-branching- rheology- structural and solution viscosimetric properties

II Introduction

Poly (lactic acid) (PLA) and poly (butylene-adipate-co-terephthalate) (PBAT) are biodegradable aliphatic polyesters, which being semi-crystalline and thermoplastic can be processed by conventional methods [1]. The physical properties of PLA are determined by the stereoisomers L:D ratio. The amorphous commercial grade has a ratio L: D of 80:20 to 98:2 (molar ratio) and the semi-crystalline one has an L:D ratio of 98.4:1.6 to 98:2 [2] [3].

PLA is a well-known biodegradable polymer with applications ranging from the medical to the packaging field. Today, according to rising oil prices and massive consumption of fossil resources, this biodegradable aliphatic polyester is on the way to become a widely used commodity polymer. In many ways it is comparable to poly (ethylene terephthalate), with a similar rigidity and food contact ability, and it fulfills the packaging industry requirements for most rigid objects [4] [5]. Whereas, because of its lower melt strength, commercially linear PLA cannot be applied into some processes where elongational properties and melt strength are dominant, such as foaming, blow molding and film blowing [6][7][8][9]. So it is necessary to modify the physical properties of the polymer by changing in structure. Indeed, it is a daunting task to summarize all the papers dedicated to this area. According to the literature, two main routes may be considered in order to enhance the melt strength and the elasticity of linear polymer.

The first one, largely used, is the chain – extension method [10][11][12][13][14]. For polyesters, it consists in increasing the molecular weight by bridging the hydroxyl or carboxyl reactive end-groups, at high temperatures and shear, using bi or poly-functional molecules. The different reactive pairs able to react with each other are -COOH/epoxy, -OH/epoxy, -COOH/isocyanate, -COOH/amine, -OH/-COOH, -OH/pyromellitic dianhydride PMDA and -OH/triglycidyl isocyanurate TGIC. The first related chain extension experiments of PLA were performed with an isocyanate compound [10] [14] [15]. Some authors employed the hydroxylation route by sequentially reacting 1,4-butanediol (BD) with PLA before adding 1,4-butane diisocyanate (BDI) as a chain extender [16]. In the same way, other researchers have tried reacting a PLA-PCL copolymer with BD and then performed chain extension with hexamethylene diisocyanate (HDI), which resulted in a (polyester-urethane) elastomer [11]. All these bi-functional molecules have a narrow pro-

cessing window and can lead to gel formation. Moreover, the interest in using such a molecule is limited to its toxicity and its high volatility. Other chain extenders reported in the literature are DGEBA-based resins. Some studies have been focused on the conversion of PLA to a fully hydroxylated or carboxylated polyester with the help of specific reactants before reaction with DGEBA. Such a selective functionalization has been performed in order to increase the reactivity of specific chain extenders [17] [18]. Chain extension of PLA has also been performed by initiating polymerization with either tetrol or hexol. This approach led to the synthesis of four- and six-armed PLAs [19]. In a recent study, the mechanical and rheological properties of biodegradable epoxy (epoxy-methally sorbithol and epoxy-methallyl malthytol) have been studied [20]. Recently, a multifunctional styrene-acrylic-epoxy random oligomer has been proposed as chain-extension agent for PLA [21][22].

A second possibility is to modify the PLA chain architecture by the introduction of long chain branches into the polyester backbone [7][13][23][24][25]. For example, ethylene-methyl acrylate-glycidyl methacrylate copolymers have successfully been used for the branching of PET [25]. According to the literature, the important routes for PLA branching are (i) branch by adding long-random copolymers with multiple reactive sites such as multifunctional alcohol, isocyanate, phenyl phosphite and epoxies, (ii) branch during polymerization using a multifunctional initiator like branched polyols or dendrimer macroinitiators, (iii) branch after polymerization using free radical crosslinking usually with peroxides, and, (iv) Combinations of the above. As can be seen, many types of branched PLA can be prepared.

Considering the environment protection and the cost, solution reactions (ii) are not the best choice. Compared with free radical branching, (iii), the functional group reactions by using a multifunctional comonomer tend to more easily obtain long chain branching (LCB). This way make the molecular weight increases, however, it was reported that the chain extending can also occur. However, it is often more dominant than LCB since chain branching reaction requires higher activation energy and longer reaction time. But, by adjusting the multifunctional monomers reactivity, the formation of branching structures instead of chain extending can occur [13]. It is widely documented the impact of the branching degree on the polyester physical properties and polymer network. For instance, a low concentration of long chain branching in the polymer backbone influences melt rheology, mechanical behavior, and solution properties [26][27][28]. However, a high degree of branching in the polymer backbone provides enhanced solubility, lower viscosity and lower crystallinity [29].

Therefore, a fundamental understanding of branching and how it influences polymer properties is essential for tailoring a polymeric material for high performance applications.

Most of the research works have dealt with the incorporation of branching for the enhancement of the foamability of PLA. The branching has been introduced by a commercial multifunctional epoxide (Cesa Extend, which is a master batch of PLA and a multi-functional epoxide) [8][30][31][32] and by reactive molecules based on the pyromellitic dianhydride (PMDA) and the triglycidyl isocyanurate (TGIC) [13]. Moreover, an electron beam irradiation explored on PLA blended with glycidyl methacrylate (GMA) has showed an efficient branching effect [33].

The rheology of blends of linear and branched PLA architectures has been carried out [34][35][36]. The researchers reported excellent rheological properties including improved shear thinning and longer relaxation time in the terminal region for branched PLA compared to the analogous linear polymer. Moreover, the longer relaxation time manifests itself as a higher zero shear viscosity, melt elasticity, storage modulus, and melt strength. Most importantly, a strain-hardening in elongational deformation was observed.

Furthermore, the branched PLA thermal behavior has been also investigated. It was demonstrated that the branch structure lowered the glass transition temperature, the melting temperature, the crystallinity than that of its linear counterpart. The crystallization kinetics of the branched polymer is inferred to be faster than the linear counterparts [25].

In PBAT case, it was reported that the introduction of aromatic polyester into the backbone chain of aliphatic polyester not only improves the mechanical properties but also the melt strength. Oth-

er authors demonstrated that under Ultraviolet (UV) exposure associated with temperature, the degradation of PBAT could occur from chain scission and crosslinking due to the recombination of the free radicals at the aromatic structures. This photodegradation promotes a reduction of mechanical properties of the polymer [37]. Furthermore, in our previous study [12], we have demonstrated that PBAT is able to degrade under specific conditions. Its thermal degradation can be avoided by the incorporation of a multi-functional epoxide through chain-extension strategy [11][30][31][38]. Despite the interesting nature of the kind of research, no efforts have been dedicated to truly understand and quantify the PBAT chain extension/branching balance caused by the multi-functional epoxide.
Here we propose an approach to get long chain branched PLA and PBAT via functional group reactions with a higher multi-functionalized epoxide by reactive processing. The evaluation and characterization on its topological structures, rheological and solution viscosimetric properties will be also discussed.
This paper deals also with the comparison between the structural properties of linear PLA, PBAT and their branched counterparts.

III Results and discussions

Earlier studies of Corre et al. [40] and especially Al-Itry et al [12] have been dedicated to gain a fundamental understanding of the mechanisms governing both thermal degradation and chain extension reaction of poly (lactic acid) (PLA) and poly(butylene adipate-co-terephtalate) (PBAT) upon processing conditions. The reactive extrusion of polymers was performed with various amounts of chain extension agent, containing about nine Glycidyl methacrylate (GMA) functions (i.e. Joncryl ADR®). The incorporation of this multi-functional oligomer showed an improvement of the thermal stability. SEC and intrinsic viscosity measurements of the modified PLA confirmed the increase of viscosity and molecular weight. This increase becomes more pronounced as the concentration of Joncryl ADR® increases. Viscoelastic properties as the storage modulus and the dynamic viscosity were assessed and related to the molecular structure of modified polymers. Hence, the mechanisms of degradation, chain extending with GMA functions and their competition have been proposed.
The main objective of Al-Itry et al. [12] works was also dedicated to investigate how the reaction extrusion experiments progressed with changing the residence time and the chain extender amount. Furthermore, the optimal reaction times were evaluated based on the monitoring of the experimental in-situ stabilization of the torque versus time as also given in the recent works of Jianye et al. [13] and Raffa et al. [41]. In our previous works, we have also plotted the evolution of the relative storage modulus ($\eta^*(t)/\ \eta^*(t=0)$ vs time) of modified polymers at 180°C and the rheo-kinetic properties as the end reaction time are determined.
Based on the Al-Itry work [12], the epoxide groups of Joncryl ADR® can react with both hydroxyl and carboxyl groups of the PLA Chains. The work differentiating between the reaction of carboxylic acid and hydroxyls groups with epoxide, since epoxide groups are known to react differently with –COOH and –OH groups (Carboxylic acid/Epoxide and the Hydroxyl/Epoxide reactions constant are respectively 18 and 1.2) [39]. In the case of polyesters, glycidyl esterification of carboxylic acid end groups precedes hydroxyl end group etherification. This latter reaction competes with etherification of secondary hydroxyl groups and main chain transesterification. The resultant couplings involve epoxy ring-opening reactions and the creation of covalent bonds via hydroxyl side group formation.
A porposed reaction mechanism between PLA chains and multi-functionalized oxirane were also pointed out in the work of Al-Itry et al. [12].The contents of carboxylic acid are given and quanti-

fied using "Titration method" and the experimental results were corroborated by FTIR, SEC and solution viscosimetry properties.
For the sake of clarity, only the results of the modified PLA and PBAT upon the end of the reaction in the rheometer will be studied in this paper, where the viscoelastic parameters (complex viscosity and storage modulus) remain unchanged during time. The reaction stabilization times for all the used PLA (NW 4032D) polymers were studied elsewhere in the paper of Al-Itry et al [12] and we have shown that ith higher Joncryl ADR® amount (more than 0,7% wt), the reaction need longer time in the rheometer (more than 30 min) and in the twin-screw extruder (more than 10 min) to be stabilized according to the competition between the degradation and the chain/branching reaction.
Therefore, the averages residence times were determined by the way of (i) the calculation based on the twin screw speed and the used profile and, (ii) using also the colored PLA Master batch.
We should point out that prior to their blown extrusion and biaxial stretching experiments (Chapter V and VI), rheological and micro-structural studies, the compounds with 0.7 and 1% of Joncryl were regranulated and passed once again through the twin screw extruder (at lower speed rate under nitrogen) until obtaining a stable torque.

III.1 Rheological behavior of neat PLA and PBAT polymers

Figure III-1 depicts the evolution of the complex viscosity modulus for both PLA and PBAT polymers. Compared to PLA, PBAT showed a greater frequency dependence of the viscosity, which is a typical behavior of linear polymers with high polydispersity [42]. A Newtonian behavior was observed for PLA only in the lower frequency region (<10 rad/s). Beyond 10 rad/s, the shear-thinning behavior of PLA led to a much higher viscosity of this polymer as compared to PBAT [12].

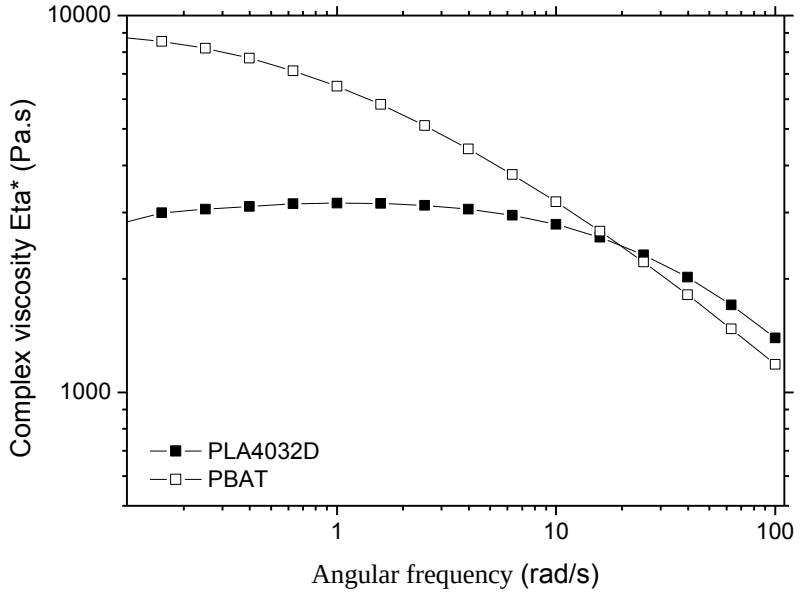

Figure III-1 Complex viscosity versus angular frequency for the neat PLA and PBAT at 180°C

The rheological investigation of the thermally stable modified PLA and PBAT with 0.25, 0.5 and 1wt % of Joncryl is discussed.
Figure III-2 shows that an increase of the multi-functional epoxide ratio enhances the onset shear thinning behavior and the complex viscosity modulus (Eta*). Many authors are aware that the enhancement in both shear-thinning and zero shear viscosity is more likely due to the significant increase in molecular weight and polydispersity for the branched chains relative to the linear ones during reactive extrusion, for instance, when passing from the linear to the four and six-armed PLAs from lactide [19][43]. Therefore, in our case, the modified samples were believed to present complex topological structures. The next section will be dedicated to this purpose.
The average molecular weight evolution versus the Joncryl ADR® amount is depicted in figure III-3. It was shown the significant dependence of the $\overline{Mw}$ with the amount of the GMA/epoxide functions and the reaction time because of the chain extension, branching and degradation reactions competition. These results are in correlation with the literature [34][44].
The drastic increase of $\overline{Mw}$ at higher amount of Joncryl pointed out the presence of longer chains or even long-chain branching in the reactive system. Moreover, Figure III-4 shows the storage modulus evolution versus the angular frequency. For both modified polymers, the G′ values increased steadily over the whole frequency range. As described in previous studies [12][19][43] an augmentation of the chain extension/branching level resulted in higher G′ (ω) values especially at low angular frequencies and the storage modulus became less shear- sensitive when the Joncryl ADR® content was increased, thus revealing a cohesive network viscosity.

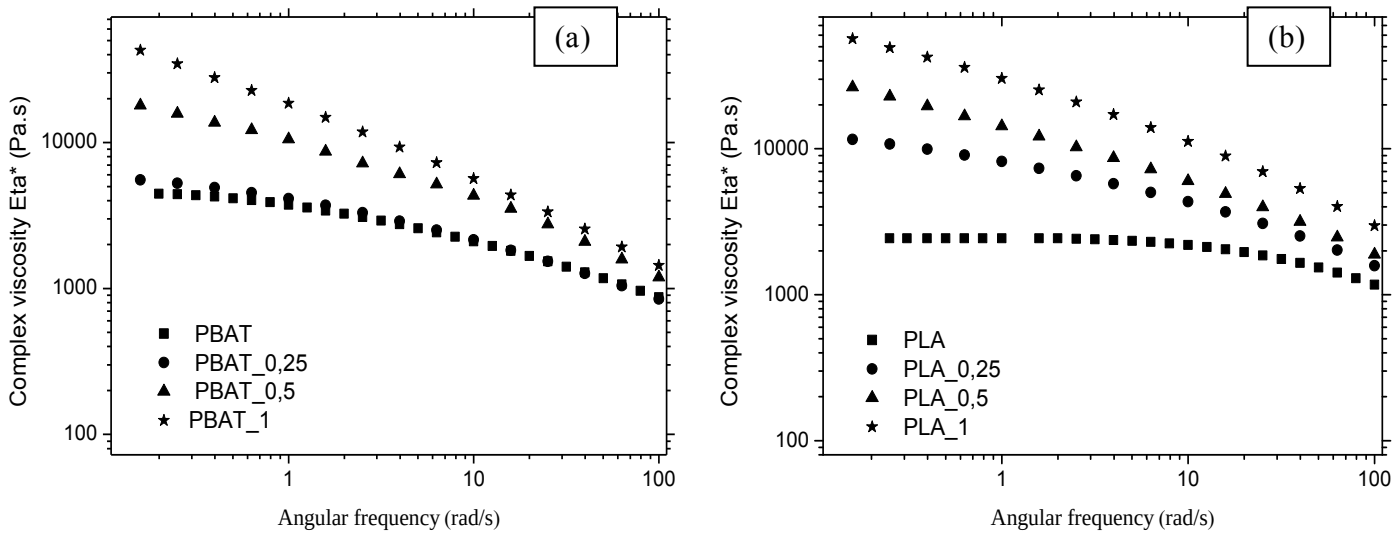

Figure III-2 The angular frequency dependence of the complex viscosity (at 180°C) for the neat and modified (a): PBAT (b): PLA with chain extender at 180°C after reaction stabilization

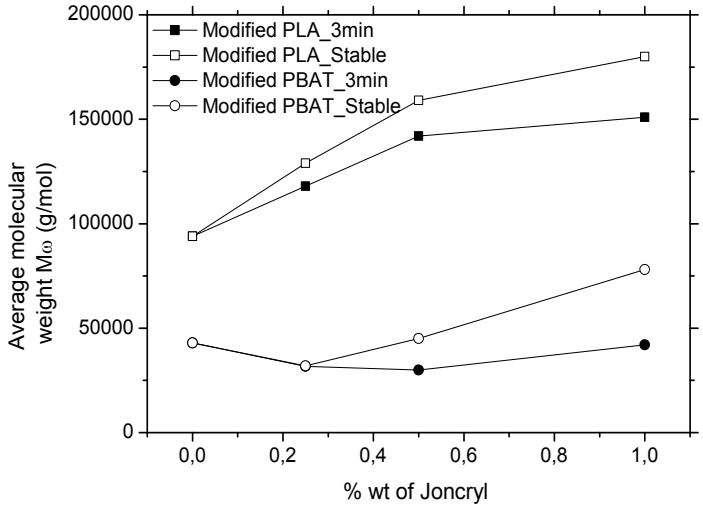

Figure III-3 Evolution of the average molecular weight modified polymers at two different reaction times in the rheometer

In other words, the larger elasticity of the modified PLA and PBAT compared to the unmodified polymers at low frequencies is attributed to more entanglements due to the presence of long-chain branches [45].
However, as the frequency increases, the number of entanglements decreases due to the more shear-thinning character of the modified polymers.

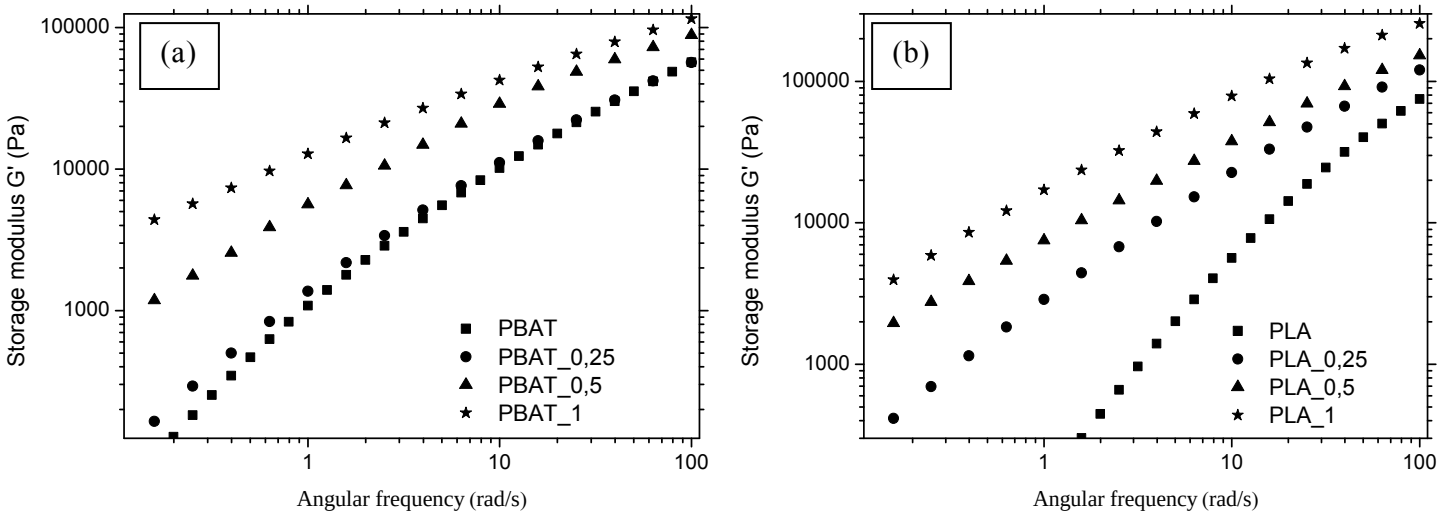

Figure III-4 The angular frequency dependence of the storage modulus for the neat and modified (a): PBAT (b): PLA with chain extender at 180°C after reaction stabilization

More interestingly, the G′ (ω) converge at the same value of plateau at higher frequency regardless the amount of Joncryl. The introduction of chain branches due to chain extension reactions could explain the improvement of the melt elasticity [46].

Furthermore, capillary measurements seemed to be complementary to the dynamic measurements described above. Figure III-5 displays the experimental capillary rheometry curves of the extended/branched PLA with three different amounts of the multi-functionalized epoxy. The validity of the Cox–Merz rule is demonstrated here.

The agreement between the two types of viscosities (dymanic and capillary experiments) is better for the linear PLA than for its modified counterparts. According to the work of Lehermeier et al [34] and Corre et al [40] the broad deviation could be linked in either to certain heterogeneity such as cross-linking/ gelation or to an increase of the branched content, respectively. In our present work, the perfect solubility of the modified PLA and PBAT polymers confirmed that no gel appeared. The same trend was detected for the PBAT polymer. Consequently, this observation could explain the presence of a long-chain-branching structure in our modified materials.

Indeed, the next section will be dedicated to the investigation of the chain extension/branching balance.

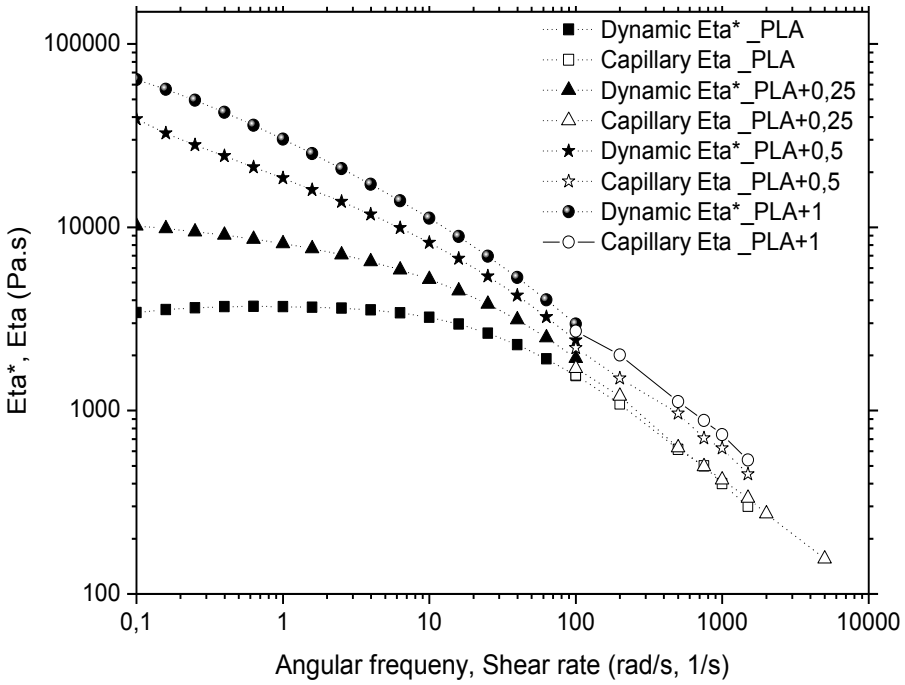

Figure III-5 Cox-Merz validity: Dynamic viscosity modulus and shear viscosity vs angular frequency, shear rate for the neat and modified PLA, carried out at 180°C (Full symbol: Dynamic rheology/ Open symbol: capillary rheology

III.3 Investigation of the chain extension/branching balance

The main focus of this part deals with the attempting of the chain extension/branching balance after reactive modification. Indeed, we have used four different methodology based on the melt and the solution rheology:

- Flow activation energy determination
- Solution viscosimetry

- Relaxation spectrum determination
- Van-Gurp-Palmen plots

III.3.1 Flow activation energy evaluation

It is common that the melt processing is governed by the flow properties of the polymer. Based on the Arrhenius equation, the main flow property, which is the flow activation energy (E_a), is conventionally determined by Eq.7. Dynamic shear experiments were performed at 5 different temperatures (180-185-190-195-200°C).

Equation 7

$$\left|\eta^*\right| = A° \exp \frac{E_a}{RT}$$

where η* is the dynamic viscosity modulus at 0,1 rad/s as reference, "A°" is the pre-exponential factor, "Ea" is the flow activation energy of the polymer, "R" is the gas constant (R=8.314 J/mol.K) and "T" is the temperature in Kelvin. The usual consequences of a chain branching process include the increase of the flow activation energy as reported by different authors mainly on polyolefins [47][48][44] investigated the influence of long-chain branching in the case of polyesters on the flow activation energy and found inconsistent results for the different polyesters. An increase in Ea was reported for a series of branched poly (butylene terephtalate) (PBT) compared to their linear analogous. However, only a slight increase in Ea was observed for branched PET [49]. Moreover, no enhancement in Ea was observed for branched PBI [50]. In this case, the activation energy is reported to be independent of molecular weight and is only dependent on the local segmental nature of the chain.

The literature attributed these discrepancies of activation energy of linear and branched polymers to whether or not the branches formed a stable entanglement network [19]. The chain structure parameters, such as M_b values (average molecular weight between branch points), branch density and length in comparison with the backbone structure, are usually presented as key factors explaining this E_a deviation. It can further arise when considering the mode by which entangled chains relax [51]. In our case, the curves of (ln η*) versus 1/T were plotted and they were linear. Therefore, the Arrhenius law is validated for the studied samples. Table III-1 lists the obtained flow activation energy values for the modified PLA and PBAT with various amounts of multi-functional-epoxide. The activation energy of the modified polymers were higher than the one of the modified ones.

One possible explanation of the increase in E_a values with multi-functional epoxide comes from the polar interactions [52] between PLA chains of different components in the blend (i.e., hydrogen bonding). These results corroborate with the SEC experiments, where the number and weight average molecular weight increased with the incorporation of reactive epoxide functions as given in figure III-3.

Table III-1 Flow activation energy parameters from Arrhenius plots of data obtained at ω=0,1 rad/ for neat and modified polymers

Samples	Ea (KJ/mol)	Fit accuracy (r^2)
PBAT_0	58	0.99
PBAT_0.25	80	0.9
PBAT_0.5	93,5	0.99
PBAT_1	182	0.999

Samples	Ea (KJ/mol)	Fit accuracy (r^2)
PLA_0	88	0.99
PLA_0.25	136	0.99
PLA_0.5	146	0.98
PLA_1	170	0.99

III.3.2 Solution viscosimetry and physico-chemical/structural properties

Figure III-6 shows one example of curve to determine the intrinsic viscosity, [η], could be calculated from the extrapolation of the reduced (ηsp/c) and inherent viscosities to zero concentration, according to (Eq.8):

Equation 8

$$\lim_{c\to 0}\left(\frac{\eta_{sp}}{C}\right)=\lim_{c\to 0}\left(\frac{\eta_{rel}-1}{C}\right)=\lim_{c\to 0}\left(\frac{\frac{t}{t_0}-1}{C}\right)$$

where $\eta_{sp}=\frac{t-t_0}{t_0}$ and $\eta_{rel}=\frac{t}{t_0}$ represent the specific viscosity and relative viscosity; and t and t_o denote the efflux time of the solution and solvent, respectively [53] [54]. The dependency of the polymer concentration on the viscosity can be expressed by the Huggins and the Kraemer equations (Eq. 3 and 4), respectively where K′ is the Huggins constant, K″ is the Kramer constant and K′+K″=0.5 for Gaussian and linear chains. For instance, the constant K' has been found to be 0.35 for a good solvent [54].

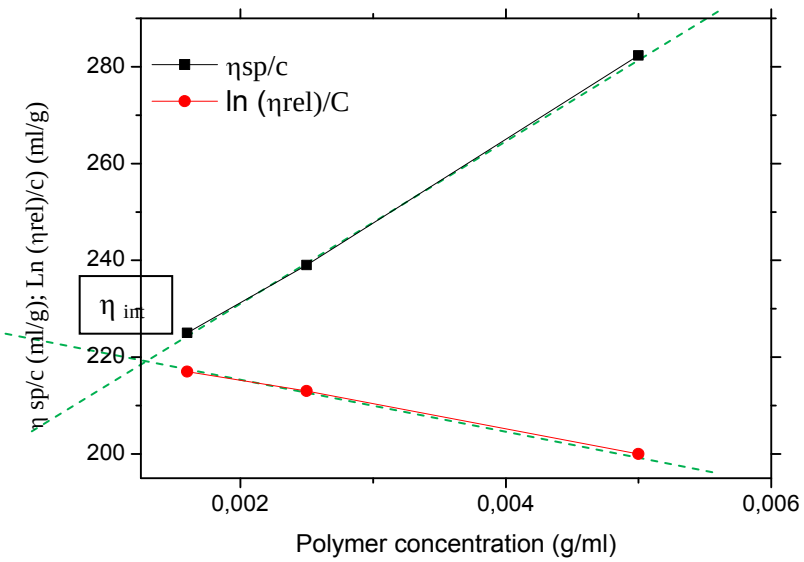

Figure III-6 Example of plots of the reduced viscosity (ηsp/c) and inherent viscosity as a function of the polymer concentration in chloroform solutions for PLA_0,5

The magnitude of the increase of K′ can be related to the width of the molecular weight distribution or branching of the solute. It seems to be a linear relationship between ηsp/c and c in the experimental range of the polymer concentration. From the slope of the extrapolated line, the intrinsic viscosity can be deduced [54] [55].

Moreover, the viscosity average molecular weight can be calculated according to the "Mark-Houwink Yasuda Sakurada" equation (Eq.9):

Equation 9 $$[\eta]_{int} = K * M_v^{a}$$

Here, "K" and the constant "a" were known only for PLA ($K=2.21*10^{-4}$ dl/g and a=0.77) [4] [55]. The viscosimetric weight (M_v) of PBAT was not determined because no "K" and "a" values are given in the literature. Therefore, the intrinsic viscosity was used to compare the molecular weights of different samples.

The intrinsic viscosities and K′ values for all the studied materials are listed in table III-2. The increase in intrinsic viscosity of the modified polymers, compared to their unmodified counterparts, could be explained by the higher molecular weight and the branching structures of the polymers. Finally, the measurements of intrinsic viscosity corroborated the results obtained from the SEC experiments and the obtained results given by rheology.

The values of the Huggins constant K′ for PLA (K′=0.3) and PBAT (K′=0.93) indicated that chloroform was a good solvent for the neat polyesters, and that the hydrodynamic volume of the polymer chain shrunk with the favorable interaction between polymer and solvent [54].

Moreover, the K′ values of PLA and PLA_1 increased from 0.3 to 0.54, and a similar trend was observed for PBAT and PBAT_1 where the K′ values increased from 0.93 to 3.42. The higher

value obtained for PBAT_1 can be related to a very high degree of branching compared to the other modified PBAT samples, as demonstrated in our previous work [12]. In addition, in PLA case, close K′ values are obtained for PLA_0,5 and PLA_1.

Table III-2 K′ and intrinsic viscosity values for neat and modified polymers

Samples	K′	Intrinsic viscosity (ml/g)	Samples	K′	Intrinsic viscosity (ml/g)
PLA_0	0,3	115	PBAT_0	0,93	79
PLA_0,25_stable	0,42	178	PBAT_0,25_stable	1,8	71
PLA_0,5_stable	0,5	220	PBAT_0,5_stable	1,44	100
PLA_1_stable	0,54	250	PBAT_1_stable	3,42	170

Furthermore, it is worth noting that the polymer-polymer interactions were stronger than those of polymer-solvent thanks to hydrophobic interactions and hydrogen bonding. The increase in K' values indicates that the solubility of both modified PLA and PBAT was lowered probably due to branching caused by the incorporation of the reactive GMA/epoxy functions [54]. Meanwhile, it is important to mention that the values of $[\eta_{intrinsic}]$, which give a measure of the effectiveness of coupling and/or branching reactions of PLA and PBAT, increased with increasing Joncryl ADR® concentration. The similar evolution is observed with increasing reaction time.
In dilute solutions, the $[\eta]_{int}$ property can be used to get an approximation of the radius of gyration "R_g" and the hydrodynamic radius "R_h" of a polymeric molecule in a solvent. The respective relations between "R_g" and "R_h" and [η] are given by the following equations (Eq.10 and Eq.11):

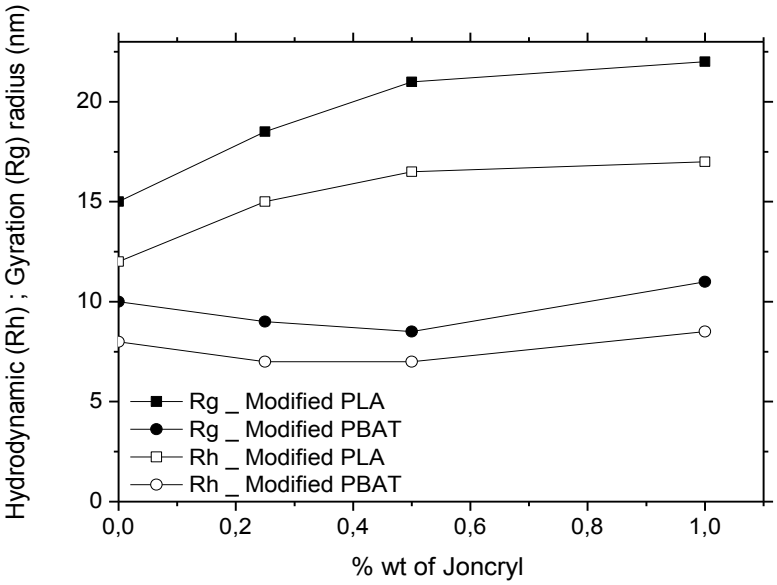

Figure III-7 Plots of the hydrodynamic and gyration radius as a function of the Joncryl concentration

Equation 10

$$R_h = \left[\frac{\left(3 \times [\eta] \times \overline{Mw}\right)}{10 \times \pi \times N_A} \right]^{1/3}$$

Equation 11

$$R_g = \left[\frac{\left([\eta] \times \overline{Mw}\right)}{\left(6^{3/2} \times \Phi\right)} \right]^{1/3}$$

where Φ is a universal constant ($2.55*10^{23}$ mol^{-1}), $\overline{Mw}$ is the average molecular weight and N_A is the Avogadro number ($6.022*10^{23}$ mol^{-1}) [56]. Figure III-7 portrays the evolution of R_g and R_h versus the weight percentage of Joncryl ADR® in each polymer. The obtained results showed an increase on the radius of gyration for both modified polymers compared to their neat counterparts.

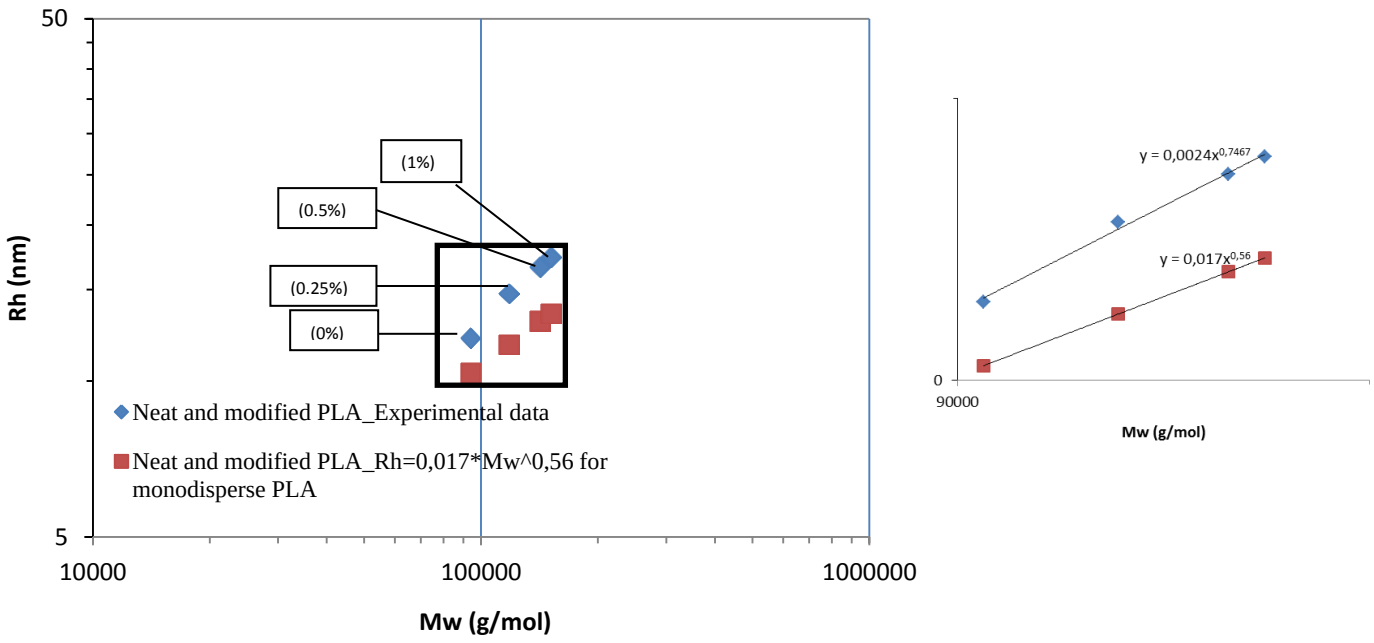

Figure III-8 The dependence of radii of hydrodynamic "Rh" on the average molecular weight "$\overline{M\omega}$ for neat and modified PLA with Joncryl: (♦) Their Experimental data and (■) The data according to Rh = 0,017*Mw0.56
(Zoom-in on the [10-20 µm] vs [90.000 – 200.000 g/mol] region of the graph)

For higher amounts of Joncryl ADR® i.e. more than 0.5 %, a slow increase of the radius gyration is noted especially for PLA chains. It is get of the nice correlation between the close evolution of K' and R_h, R_g beyond 0,5% of Joncryl, respectively. However, the latter continued to increase

with the amount of Joncryl in the PBAT matrix. These results confirmed that the reaction between PLA/Joncryl and PBAT/Joncryl led to chain extension/branching chains.

Moreover, figure III-8 shows the dependance of "R_h" on the average molecular weight $\overline{Mw}$ for the neat and modified PLA with Joncryl, compared to the scaling relation $R_h = 0.017 \times \overline{M\omega}^{0.56}$ [56] for monodisperse and linear PLA. It can be noticed that the data of the modified samples diverge from the reported results by the relation since Joncryl is added in the blend. The resultant trend line in our case is $R_h = 0.0024 \times \overline{M\omega}^{0.74}$. Lastly, the same trend was observed for PBAT.

This discrepancy between the slopes can confirm the polydispersity and the non-linearity of our studied modified PLA.

III.3.3 Relaxation Spectra analysis

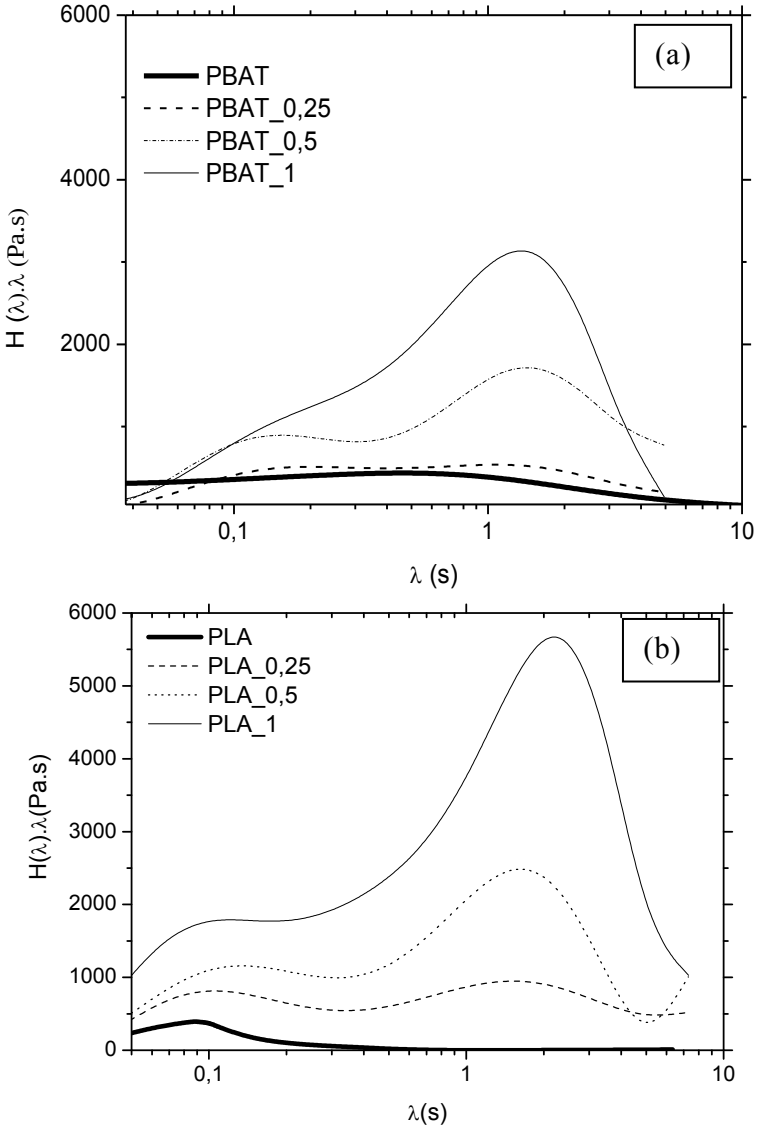

Figure III-9 Relaxation spectra of the neat and modified stable polymers
(a): PBAT (b): PLA

To compare the relaxation behavior of the unmodified and modified PLA and PBAT, the weighted relaxation spectra were evaluated. Such spectra (λH (λ)) have been determined by Honerkamp, Weese, Elster, and recently by Hansen [45] [40] and plotted according to Eq.6: The weighted relaxation spectra are presented in figure III-9. It is clear that the neat polymers presented only one relaxation time, corresponding to a single component.

However, in the case of the modified polymers, two main relaxation times can be clearly identified, which were interpreted as the simultaneous occurrence of two relaxation processes given by short and long chains [12] [40] [48]. When taking into account both the SEC results and rheological relaxation spectra, it is obvious that even with a small amount of Joncryl ADR®, and an enlargement of the relaxation spectrum was obtained. The bimodal spectra for the modified polymers could be attributed to the polydispersity of the extended / branched materials. The modification of the chain topology by chain extension/branching would change the relaxation mechanism from *reptation* to fluctuations and *stress release* [51] [40] [45]. The simple reptation, as expected for linear polymers, no longer suffices to relieve stress when there are enough branches present and slower events such as arm retraction must occur.

III.3.4 Van-Gurp-Palmen plots

Recently, Trinkle and Friedrich (2002) proposed a useful and reliable tool for characterizing polymer melts and the topology of chains based on a reduced Van-Gurp-Palmen plot (rVGP) [57]. Several authors have used this approach to analyze the topology of the branched PLA [13].
This is a plot of the loss angle δ (=tan $^{-1}$[G"/G'] versus the logarithm of the reduced modulus G_{red} defined as a magnitude of the complex modulus (G*) divided by the plateau modulus $G°_N$, obtained when δ->0, or from the viscoelastic properties according to Eq.12 and Eq. 13 [60] [61].

Equation 12
$$G_N° = \frac{2}{\pi}\int_{-\omega}^{\omega} G''(\omega)\, d\ln(\omega)$$

Equation 13
$$\tau_n = \frac{\eta_0}{G_N°}$$

The objective of such plots was proved to be a more transparent way to show the correlation between rheological data with the polymers topology (long chain, H-shaped, star shaped or comb-shaped branched structure…) whereby low levels of long chain branching can be detected and quantified by the linear viscoelastic behavior. The shape of the Van-Gurp-Palmen plot has been found to not change with the molar mass [57]. However, the polydispersity stretches the curves at low Gred along the abscissa.
As illustrated in Figure III-10, a transition exists between the neat and the modified polymers. Indeed, the obtained curves from the rheological data of PLA_0 and PBAT_0 have the classical shape of a linear polymer: From low to high G_{red}, the phase angle exhibits a relatively long flat span at δ=90° before falling at higher values of G_{red} [40] [57].
On the one hand, for the modified PLA samples, the Van-Gurp-Palmen plots are gradually shifted towards lower phase angle values up to 0.5% wt and the non-plateau at 90° can be reached as was also the case for PLA_0. This kind of flat profile is clearly characteristic of the presence of long-chain branching as has been well defined by numerous studies [47] [58] [59]. Moreover, in the modified polymers case, the number of epoxy functions reaches nine. After only the first extension reaction (with the stoichiometric ratio: 1 epoxy/1 acid or alcohol function), the excess of reactive functions allows the branching reaction between epoxy and -COOH or -OH ends of the

PLA chains. At shorter time in the rheometer (3min), the phase angle decreases with the addition of Joncryl for both polymers (cf. figure III-10a) and figure III-10b)). This result was in agreement with the study by Corre et al. where the phase angle was reduced when increasing the amount of chain extender in a less viscous PLA3051D [40].

Figures (III-10c and III-10d) depict the loss angle evolution versus the reduced modulus for the stable modified polymers. The obtained data show that the loss angle drastically decreases for modified PLA with 0.25 and 0.5%wt of Joncryl confirming their higher elasticity. Moreover, PLA_0.5 contained the largest amount of long-chain branching (LCB) out of all the samples. However, with 1%wt of Joncryl ADR®, where the reaction time in the rheometer is higher, an increase of the phase angle was observed. It indicates a decrease of the amount of LCB. A slight cross-linking phenomenon at higher reaction time could probably reduce the formation of long-chain branching.

On the other hand, for the modified PBAT samples, the incorporation of 0.25 % wt of Joncryl presented a δ value close to 90° regardless of the reaction time, which indicates that short-chain branching were occurred instead of LCB. However, when increasing the amount of reactive GMA functions above 0.25% wt, the phase angle values became reduced, highlighting the presence of LCB, which was more present to a larger extent in samples with long reaction times.

Based on the detailed study of Trinkle et al [57] concerning the classification of long-chain branched polymers by their topology, rVGP plots of different systems of varying topologies were developed. An assymetric three-armed star polymers behaved very similarly to become a linear polymer ($\delta = 90°$) owing to the fact that the side arms were too short to entangled with each other. Also, symmetric four-armed star-polymers presented a comparable behavior. As the lengths of the arms increased, a bump developed due to a shift in balance between the two different relaxation processes. However, the δ values of an H-shaped polymer indicate that it has a higher elasticity than its star-shaped counterpart. The comb-shaped polymers, on the other hand, cannot be unambiguously identified.

They can be differentiated from H-polymers by the straight line in the rVGP curves between the $G°_N$ region and their minimum at G_{red}-values below 1. In addition, the $G°_N$ –minimum of a comb-shaped polymer is located at significantly higher δ values than its linear analog. Their distinction from mixtures of linear and randomly branched polymers is hard to perform. Since modified PLA and PBAT do not present a similar trend to polymers with known topologies (symmetric star, assymetric, star-H-shaped, comb-shaped…), we can conclude that they exhibited a typical characteristic of a mixture of linear and randomly-branched polymers. They may have complex structures in which there are distributions of backbone lengths, branch lengths, branch point locations and branching complexity. A fairly good characterization of branching in randomly-branched systems is possible when the branching structure has been established by modeling of the branching reaction.

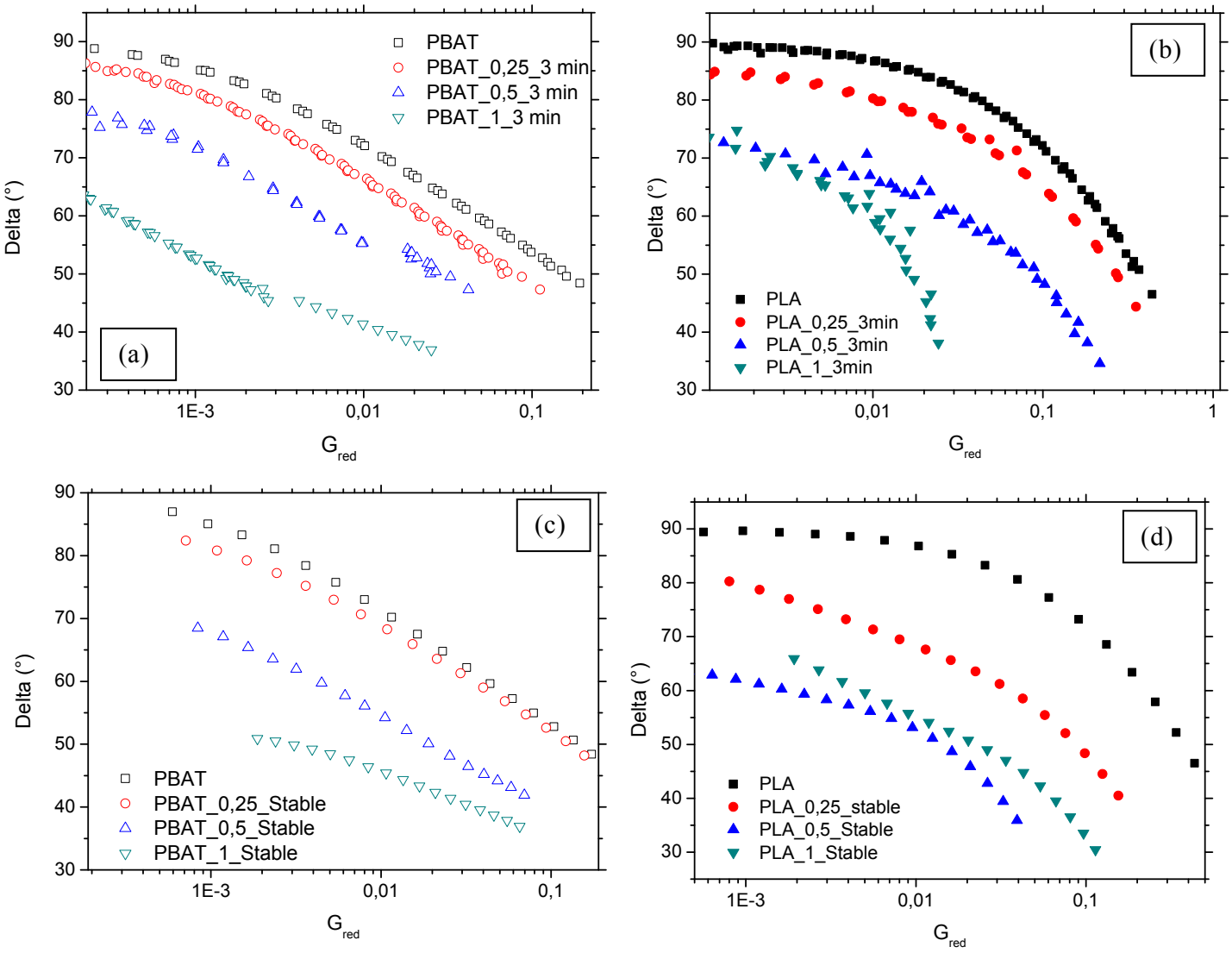

Figure III-10 Reduced Van-Gurp-Palmen plots from master curves at a reference temperature of 180°C for

(a): Neat and modified PBAT, upon processing during 3minutes@ 180°C

(b): Neat and modified PLA, upon processing during 3 minutes @ 180°C

(c): Modified stable PBAT @ 180°C

(d): Modified stable PLA @ 180°C

IV Conclusions

Throughout this work, the effect of the addition of a multi-functionalized epoxide into PLA and PBAT on the chain extension/branching balance has been investigated. It was shown that the incorporation of the multi-functional epoxide at various amounts, a drastic increase of the complex viscosity, average molecular weight and the intrinsic viscosity was noted. This enhancement indicates the presence of medium or even long-chain branching. Moreover, the number of epoxy functions reached nine after only a first extension reaction (with stoichiometric ratio: 1 epoxy/1 acid or alcohol functions). The excess of reactive functions rendered possible the branching reaction between epoxy and the -COOH or -OH ends of the PLA chains.

An improvement of the onset shear thinning behavior and storage modulus values for both modified PLA and PBAT was also observed. Once again, the introduction of chain branches and chain extending reactions could explain the improvement of the melt elasticity. For more details, the chain extension/branching balance, in modified PLA and PBAT systems, was investigated by different methods (i) the calculation of the flow activation energy, (ii) the experimental evaluation of Huggins parameters K', gyration & hydrodynamic radii values, (iii) relaxation spectra and, (iv) r-VGP plots.

Firstly, the E_a values showed an increase with the GMA/epoxide functions, which could come from both polar interactions (i.e., hydrogen bonding) between chain entities and an increase of the chain length and the degree of branching. Secondly, the K' values of PLA and PLA_1 increased from 0.3 to 0.54 respectively, and the same trend was observed for PBAT and PBAT_1. This indicates that the solubility of both modified PLA and PBAT gets lower probably due to the branching chain. In the other hand, an improvement of the gyration and hydrodynamic radii was noted. The gyration radius varied from 15 to 21 nm, when comparing PLA to PLA_1, and went from 10 to 16 nm, for PBAT and PBAT_1. We were able in this paper to show a real correlation between the slight increase of K', R_h and R_g and their effects on the phase angle.

Finally, the molecular weight of modified PLA and PBAT increased with GMA, epoxide functions and with the residence time. This increase was accompanied by a bimodal relaxation spectrum. Lastly, the reduced Van-Gurp-Palmen plots brought information about the presence of branching in modified polymers depending on the Joncryl amount and the reaction time. These plots revealed characteristic curves of long-chain branched polymers. Indeed, they exhibited a typical feature of a mixture of linear and randomly branched polymers.

References

[1] Jiang L, Wolcott MP, Zhang J. Study of biodegradable polylactide/poly(butylene adipate-co-terephthalate) blends. Biomacromolecules. 7(1):199-207. 2006.
[2] Kawahima N, Ogawa S, Obuchi S, Matsuo M, Yagi T. Polylactic acid "LACEA" Biopolymers. Wiley-VCH Verlag GmbH, Weiheim : 251-274. 2002.
[3] Ikada Y, Tsuji H. Biodegradable polyesters for medical and ecological applications. Macromololecular Rapid Communications. 21(3): 117-132. 2000.
[4] Henton DE, Gruber P, Lunt J, Randall J. Polylactic acid Technology, in: A.K. Mohanty, M.Misra, L.T. Drzal (Eds.), Natural Fibers, Biopolymers, and Biocomposites, Taylor & Francis, Boca Raton, FL, 527-577. 2005.
[5] Sungsanit K, Kao N, Bhattacharya SN, Pivsaart S. Physical and rheological properties of plasticized linear and branched PLA. Korea-Australia Rheology Journal. 22(3): 187-195. 2010.
[6] Witzke, DR, PhD thesis, Chemical Engineering, Michigan State University. 1997.
[7] Dorgan JR, Lehermeier H, Mang M. Thermal and rheological properties of commercial Grade poly (lactic acid)s . Journal of Polymer and the Environment. 8(1): 1-9. 2000.
[8] Mihai M, Huneault M, Favis BD. Rheology and extrusion foaming of chain-branched poly(lactic acid). Polymer Engineering & Science. 50(3): 629-642. 2010.
[9] Ryan CM, Nangeroni JF, Hartmann MH. Branching of Poly(Lactic Acid) to Increase Melt Strength for Extrusion Coating. TAPPI Proceedings, Polymers, Laminations, and Coatings Conference, 139-144. 1997.
[10] Li BH, Yang MC. Improvement of thermal and mechanical properties of poly(L-lactic acid) with 4,4-methylene diphenyl diisocyanate. Polymers for advanced technologies. 17(6): 439-443. 2006.
[11] Kylma J, Seppala JV. Synthesis and characterization of a biodegradable Thermoplastic poly(ester-urethane) elastomer. Macromolecules. 30(10): 2876-2882. 1997.
[12] Al-Itry R, Lamnawar K, Maazouz A. Improvement of thermal stability, rheological and mechanical properties of PLA, PBAT and their blends by reactive extrusion with functionalized epoxy. Polymer Degradation and Stability. 97(10): 1898–1914. 2012.
[13] Jianye L, Lou L, Yu W, Liao R, Li R, Zhou C. Long chain branching polylactide: Structures and properties. Polymer. 51(22): 5186-5197. 2010.
[14] Zhong W, Ge J, Gu Z, Li W, Chen X, Zang Y, Yang Y. Study on biodegradable polymer materials based on poly(lactic acid). I. Chain extending of low molecular weight poly(lactic acid) with methylenediphenyl diisocyanate. Journal of Applied Polymer Science. 74(10): 2546–2551. 1999.
[15] Hiltunen K, Seppala JV, Harkonen M. Lactic acid based poly(ester-urethane)s: The effects of different polymerization conditions on the polymer structure and properties. Journal of Applied Polymer Science. 64(5): 865-873. 1997.
[16] Di Y, Iannace S, Di Maio E, Nicolais L. Reactively Modified Poly(lactic acid): Properties and Foam Processing. Macromolecular Materials and Engineering. 290(11):1083-1090. 2005.
[17] Zhou ZF, Huang GQ, Xu WB, Ren FM. Chain extension and branching of poly(L-lactic acid) produced by reaction with a DGEBA-based epoxy resin. EXPRESS Polymer Letters. 1(11): 734–739. 2007.
[18] Lamnawar K, Baudouin A, Maazouz A. Interdiffusion/reaction at the polymer/polymer interface in multilayer systems probed by linear viscoelasticity coupled to FTIR and NMR measurements European Polymer Journal. 46(7): 1604-1622. 2010.
[19] Dorgan JR, Joshua SWJ, David NL. Melt rheology of poly(lactic acid): Entanglement and chain architecture effects. Journal of Rheology. 43(5): 1141-1155. 1999.
[20] Acierno D, Russo P, Savarese R. Proceedings of the Polymer Processing Society 24th Annual Meeting. 2008.
[21] Villalobos M, Awojulu A, Greeley T, Turco G, Deeter G. Oligomeric chain extenders for economic reprocessing and recycling of condensation plastics. Energy. 31(15): 3227-3234. 2006.

[22] Karayan V, Villalobos M. Cesa-extend a User Friendly Technology to Enhance Reprocessing and Recycling of Condensation Plastics; Processing Global Plastic Environment Conference, 52. 2004.
[23] Gotsis AD, Zeevenhoven BLF, Hogt AH. The effect of long chain branching on the processability of polypropylene in thermoforming. Polymer Engineering and Science. 44(5): 973-982. 2004.
[24] Cicero JA, Dorgan JR, Garrett J, Runt J, Lin JS. Effects of molecular architecture on two-step, melt-spun poly(lactic acid) fibers. Journal of Applied Polymer Science. 86(11): 2839-2846. 2002.
[25] Ouchi, T, Shunsuke I, Ohya Y. Synthesis of branched poly(lactide) using polyglycidol and thermal, mechanical properties of its solution-cast film. Polymer. 47(1): 429-434. 2006.
[26] McKee MG, Unal S, Wilkes GL, Long TE. Branched polyesters: recent advances in synthesis and performance. Progress in Polymer Science. 30(5): 507–539. 2005.
[27] Shroff RN, Mavridis H. Long-chain-branching index for essentially linear polyethylenes. Macromolecules. 32(25): 8454–8464. 1999.
[28] Pitsikalis M, Pispas S, Mays JW, Hadjichristidis N. Non-Linear Block Copolymer Architectures. Advances in Polymer Science. 44: 1-137. 1998.
[29] Tande BM, Wagner NJ, Mackay ME, Hawker CJ, Jenng M. Viscosimetric, Hydrodynamic, and Conformational Properties of Dendrimers and Dendrons. Macromolecules. 34(24): 8580–8583. 2011.
[30] Pilla S, Kim SG, Auer GK, Gong S, Park CB. Microcellular extrusion-foaming of polylactide with chain-extender. Polymer Engineering & Science. 49(8): 1653-1660. 2009.
[31] Pilla S, Kramschuster A, Yang L, Lee J, Gong S, Turng LS. Microcellular Injection-Molding of Polylactide with chain-extender. Materials Science and Engineering. 29(4): 1258-1265. 2009.
[32] Corre YM, Maazouz A, Duchet J, Reignier J. Batch foaming of chain extended PLA with supercritical CO(2): Influence of the rheological properties and the process parameters on the cellular structure. Journal of Supercritical Fluids. 58(1): 177-18. 2011.
[33] Shin B, Han D, Narayan R. Rheological and Thermal Properties of the PLA Modified by Electron Beam Irradiation in the Presence of Functional Monomer. Journal of Polymers and the Environment. 18(4): 558-566. 2010.
[34] Lehermeier HJ, Dorgan JR. Melt rheology of poly(lactic acid): Consequences of blending chain architectures. Polymer Engineering & Science. 41(12): 2172-2184. 2001.
[35] Drumright RE, Hartmann M, Wolf R. Copolymers of monocyclic esters and carbonates and methods for making same. International Applied WO 02/100921A1 (2002)
[36] Wang L., Jing X., Cheng H., Hu X., Yang L., Huang Y. Blends of Linear and Long-Chain Branched Poly(l-lactide)s with High Melt Strength and Fast Crystallization Rate. Industrial & Engineering Chemistry Research. 51(30): 10088–10099. 2012.
[37] Zhao L, Gan Z. Effect of copolymerized butylene terephthalate chains on polymorphism and enzymatic degradation of poly(butylene adipate). Polymer Degradation & Stability. 91(10): 2429-2436. 2006.
[38] Yuanliang W, Chunhua F, Yongxiang L, Changshun R, Yaoyao Z, Ya F. Melt synthesis and characterization of poly(L-lactic acid) chain linked by multifunctional epoxy compound. Journal of Wuhan University of Technology-Mater. Sci. Ed. 25(5): 774-779. 2010.
[39] Lamnawar K, Maazouz A. Rheology and morphology of multilayer reactive polymers: Effect of interfacial area in Interdiffusion/reaction phenomena Rheologica Acta. 47(4): 383- 397. 2008.
[40] Corre YM, Duchet J, Maazouz A, Reignier J. Melt strengthening of poly (lactic acid) through reactive extrusion with epoxy-functionalized chains. Rheologica Acta. 50(7-8): 612-629. 2011.
[41] Raffa P, Coltelli M-B, Savi S, Bianch S, Castelvetro V. Chain extension and branching of poly(ethylene terephthalate) (PET) with di- and multifunctional epoxy or isocyanate additives: An experimental and modelling study. Reactive & Functional Polymers. 72(1):50–60. 2012.

[42] Li K, Peng J, Turng LS, Huang HX. Dynamic Rheological Behavior and Morphology of Polylactide/Poly(butylenes adipate-co-terephthalate) Blends with Various Composition Ratios. Advances in Polymer Technology. 30(2): 150–157. 2011.
[43] Zhang N, Wang Q, Ren J, Wang L. Preparation and properties of biodegradable poly(lactic acid)/poly(butylene adipate-co-terephthalate) blend with glycidyl methacrylate as reactive processing agent. Journal of Materials Science. 44(1): 250–256. 2009.
[44] Munari A, Pezzin G, Pilati F, Manaresi P. (1989) Rheological characterization of highly branched poly(ethyleneterephthalate). Rheologica Acta. 28: 25–29. 1989.
[45] Seyed HT, Pierre JC, Abdellah A. Rheological properties of blends of linear and long-chain branched polypropylene. Polymer Engineering & Science. 50(1): 191–199. 2010.
[46] Wu D, Wu L, Sun Y, Zhang M. Rheological properties and crystallization behavior of multiwalled carbon nanotube/poly(ε-caprolactone) composite. Journal of Polymer Science Part B: Polymer Physics. 45(23): 3137-3147. 2007.
[47] Savvas G. (2000) Long chain branching and polydispersity effects on the rheological properties of polyethylenes. Polymer Engineering & Science. 40(11): 2279–2287. 2000.
[48] Wood-Adams P, Costeux S. Thermorheological Behavior of Polyethylene: Effects of Microstructure and Long Chain Branching. Macromolecules. 34(18): 6281–6290. 2001.
[49] Munari A, Pilati F, Pezzin G. Linear and branched poly (butyleneterephthalate): Activation energy for melt flow, Rheologica Acta. 24(5): 534-536. 1985. s
[50] Munari A, Pezzin G, Pilati F. Linear and branched poly (butyleneisophthalate): activation energy for melt flow. Rheologica Acta. 29(5): 469-474. 1990.
[51] Baker W, Scott C, Hu GH. Reactive polymer blending, Hanser Publishers: Progress in polymer processing. 2001.
[52] Wool RP. Biobased polymers and composites, Academic, Burlington: 202–255. 2005.
[53] Kraemer EO. Molecular weights of cellulose and cellulose derivates. Industrial and Engineering Chemistry. 30(10): 1200–1203. 1938.
[54] Cho J, Heuzey MC, Begin A, Carreau PJ. Viscoelastic properties of chitosan solutions: Effect of concentration and ionic strength. Journal of Food Engineering. 74(4): 500-515. 2006.
[55] Donald G. A literature review of Poly (lactic acid). Journal of Polymer and the Environment. 9(2): 63-84. 2001.
[56] Norhayani O, Jazrawi B, Mehrkhodavandi P, Hatzikiriakos S. Wall slip and melt fracture of poly(lactides). Rheologica Acta. 51(4) : 357-369. 2012.
[57] Trinkle S, Walter P, Friedrich C. Van Gurp-Palmen Plot II: classification of long chain branched polymers by their topology. Rheologica Acta. 41(1-2) : 103–113. 2002.
[58] Fleury G, Schlatter G, Muller R. Non Linear Rheology for Long Chain Branching characterization, comparison of two methodologies: Fourier Transform Rheology and Relaxation. Rheologica Acta. 44(2): 174–187. 2004.
[59] Garcıa-Franco C, Lohse DJ, Robertson CG, Georjon O. Relative quantification of long chain branching in essentially linear polyethylenes. European polymer journal, 44(2): 376–391. 2008.
[60] John D. Ferry. Viscoelastic properties of polymers. John Wiley & sons. 641 pages. 1980.
[61] Dealy JM, Larson RG. Structure and Rheology of Molten Polymers: From Structure To Flow Behavior and Back Again. Hanser Gardner publication. 499 pages. 2006.

Chapter 4
Rheological investigation and interfacial tension properties of PLA/PBAT/ multifunctional epoxide blends

4

I Abstract

The focus of this paper has been to gain a true understanding of the impact of a multi-functional epoxide on the interfacial properties of biodegradable of poly (lactic acid) (PLA) and poly (butylene-adipate-co-terephthalate) (PBAT) blends. Various amounts of a chain extension agent, named Joncryl ADR®-4368, containing reactive Glycidyl Methacrylate (GMA)/epoxy functions have been incorporated into PLA/PBAT blends through mixing in a laboratory-scale twin-screw extruder. Their effects on the rheological and morphological behavior of PLA/PBAT blends were investigated systematically. Furthermore, the role of the epoxy-functionalized chains as a compatibilizer was assessed and confirmed by the decrease of the interfacial tension values; Different sandwich model systems were studied in order to probe and quantify the role of the functionalized chains on the interfacial forces. According to the obtained results, it was possible to achieve a clear understanding of the compatibilization effect during *in-situ* interfacial reactions between epoxide functions and the PLA, PBAT phases. Hence, for compatibilized blends, the obtained data were discussed based on the mechanisms of coalescence and the Marangoni theory. Meanwhile, the decrease of the interfacial tension values with the addition of multi-functional epoxide highlighted the larger degree of compatibilization which is confirmed in turn by TEM observations. For uncompatibilized PLA/PBAT blends, the obtained values of interfacial tension given by the Palierne model corroborated data obtained from the deformed drop retraction method (DDRM). The failure of the rheological methods using palierne model was also discussed in the case of PLA/PBAT/multifunctionalized epoxy. The co-existence of chain extension/branching of PLA and PBAT blends coupled to the PLA-joncryl-PBAT creation during the in-situ compatibilization have to be taken into-account in this complex system.

Keywords Biodegradable blends - Reactive extrusion - Interfacial tension - *in-situ* Compatibilization.

II Introduction

One of the most interesting biomaterials in the field of alternative biodegradable polymers is the poly (lactic acid) which has many properties in term of stiffness, tensile strength and gas permeability comparable to polyolefins and polystyrene. However, its major weakness, its brittleness, has hindered its wide spread usages. Blending PLA with other polymers is the one the several methods for improving this drawback. The literature is very rich on investigations of blends of PLA and other biopolymers like thermoplastic starch, PCL, PBAT, chitosan, etc. [1][2][3][4]. The poly (butylene adipate-co- terephtalate) (PBAT), an aliphatic-aromatic copolymer, is highly flexible material. It is considered as a good candidate for toughening PLA. However, the incompatibility due to the differences in the hydrophilicity of these two polymers leads to poor mechanical properties of the blend. Even not miscible, PLA/PBAT blend should be compatibilized in order to strengthen the interface between phases.
Compatibilizers are usually copolymers which could be added as the premade copolymer, to blend or generated in-situ at the interface due to chemical reaction between phases during blending. In

this latter case, interfacial reaction must occur during typical short processing time thus coupling reaction should be fast.
Certain approaches aimed at trying to enhance the mechanical properties of such PLA/PBAT blends are presented in the literature. Numerous ways to compatibilize this blend have been described by several authors. The trans-esterification reaction, in the molten state, at the interface between PLA and PBAT has been studied [5][6]. Other researchers have used a chain extender of neat polymers to compatibilize the blend [7]. The incorporation of glycidyl methacrylate (GMA) functions into PLA/PBAT to investigate the mechanical properties of the blend was discussed [3]. A surprisingly low elongation at break value of 3% was obtained of PLA/PBAT/GMA blends. This is lower than those of PLA (4.5%) and PBAT (500%) alone. A better understanding of the rheological and morphological properties is required to explain this strange result. Other studies highlight the improvement of interfacial tension of ternary blends of PLA/PBAT/TPS by using MDI (methylenediphenyl diisocyanate) as a compatibilizer [8]. SEM observations and mechanical properties have enabled the authors to confirm that the presence of MDI promoted the interfacial interaction. No quantifying study of the interfacial tension for the blends has been performed however.
In this context, a real understanding of the effect of the coupling agent with high reactivity on the compatibilization of PLA/PBAT blends is necessary. The study of the chain extension/branching of polymer chains (see the previous chapter) coupling to the compatibilization effects will be the great interest. Therefore, much effort has been devoted to understand the relationship between viscoelastic properties and the morphology of polymer blends. Immiscible polymers, when subjected to shear, show a high elasticity presented as a plateau in the modulus curve at low frequency region due to shape relaxation of droplets. An additional relaxation plateau interpreted as the interface relaxation has been observed in compatibilized blends (especially the physical compatibilization using copolymers). Several studies have been dedicated to quantify the interfacial tension of uncompatibilized and compatibilized commodity blends as well as PS/PP, PE/PA, PDMS/PTMDSE, PS/HDPE, etc. using rheology, an indirect method from elongation measurements [9] and optical observations of droplet morphologies. The rheological method (RM) takes into account certain theoretical models (Palierne, Bousmina [10], Gramespacher and Meissner [11], Coran [12], Choi and Schowalter [13]) that have been developed to study the linear viscoelastic behavior of polymer blends in the molten state. Thanks to these models, it is possible to infer the interfacial tension from the dynamic behavior of the blend once its morphology is characterized. By calculating the interfacial tension with the theoretical model, we studied the effect of the molecular weight and composition dependence of the polymer-polymer interaction parameter in a theoretical model, which might lead to significant theoretical errors. The effects of geometrical confinements and physical compatibilization on the steady-state behavior of single droplets of PDMS have been also studied by using Minale Model [14]. For unconfined droplets, it was shown that the effects of compatibilization can efficiently be implied in the equilibrium capillary number, taking into account the reduction in interfacial tension. However, for confined droplets, it was shown that the confinement induces an increase in droplet deformation and enhances orientation towards the flow direction, independent of confinement ratio.
Many other attempts have recently been made to develop accurate and convenient techniques to measure the interfacial tension for polymers by optical observations. Some of them are equilibrium methods (pendant drop, sessile drop and spinning drop) that are used for low viscosity materials. Additionally, thermal degradation can occur for highly viscous polymeric materials. However, dynamic methods (breaking thread (BT), imbedded fiber retraction (IFR), deformed drop retraction (DDR)) can overcome such limitations. In these methods, the interfacial tension is obtained by observing the shape evolution of the interface svia Rayleigh instability [10]. A significant coalescence inhibition corresponding to important interface coverage was observed for relatively highly compatibilized blends.
Finally, more details about the (RM) and (DDR) methods, used in the present study, will be given in the corresponding following sections.

To the best of our knowledge, no efforts have been dedicated to determine the interfacial tension of compatibilized PLA/PBAT blends. The challenge of our study is thus to assess the effect of the coupling agent, which plays a role of chain extender/branching agent, on the interfacial properties of PLA/PBAT blends.
The main focus of the present paper is to quantify, using rheological and dynamic methods, the interfacial tension of PLA/PBAT blends and to probe the effect of multifunctionalized epoxy on the rheological, morphological and interfacial properties. We will try to gain a discussion of the interfacial tension measurements depending on (i) the viscoelastic properties of the PLA, PBAT chains and (ii) the interfacial reaction in the blend with the creation of PLA-Joncryl-PBAT copolymer. To achieve our objective, various model systems were prepared and studied by the way of (DDRM). The failure of the rheological methods using palierne model was also discussed in the case of PLA/PBAT/multifunctionalized epoxy.

III Experimental section

III.1 Interfacial tension measurements

The effect of the multi-functional epoxide on the interfacial tension of the PLA/PBAT (80/20) blends was determined using two different techniques: a rheological approach (RM) and the deformed drop retraction method (DDRM).

III.1.1 Rheological method (RM)

The interfacial rheological properties of the PLA/PBAT blends were investigated using the Palierne Model in the linear viscoelastic domain. The main focus of this work was to obtain the interfacial tension especially for the unmodified systems. For the sake of clarity, more details will be given in the Results and Discussion section.

III.1.2 Retraction of deformed drop method (DDRM)

Melt blends of PBAT and PLA were observed, in the quiescent state or during shear, using a Leitz Orthoplan microscope lens with a 20x and 32x lens coupled with a LINKAM CSS-450 high-temperature stage. The sample was positioned in the gap between the two quartz plates and was sheared by rotating the bottom plate by a precision stepping motor, while the top plate remained stationary. Indeed, to ensure a complete cohesion between the polymer films and completely imbedded droplets, the gap between the plates was modified with a stepping motor to a value smaller than the thickness of the two films. In order to obtain well defined spherical droplets, the dispersed particles were subjected to a shear treatment during few seconds (30 s; steady shear ranging from 0.1 to 5 s^{-1} for various model systems in the Newtonian rheological zone) under 180°C. The sheared droplets were observed through two holes made in the heating plates. These holes had a diameter of 5 mm and rendered it possible to observe the sample thickness by light transmission. The center of the observation area was located 7.5 mm from the center of the glass. A video camera, linked to the software LINKSYS, was used to take pictures every second during the experiments. This enabled us to almost continuously follow the dimensional evolution of the droplets.

IV Results and discussions

IV.1 Rheology of unmodified and reactively modified PLA/PBAT blends

IV.1.1 Linear viscoelastic properties

Figures II-15 and II-17 compare the evolution of the normalized viscosity as a function of time for non–reactive and reactive blends of PLA/PBAT. The stabilization of the viscosity of PLA/PBAT blends with Joncryl ADR® over time is typical for a relatively interfacial chemical reaction [15]. Small amplitude oscillatory measurements are useful to probe the droplet-matrix morphology. Figure IV-I shows the shear rate dependence of the complex viscosity modulus for the unmodified and thermally stable modified PLA/PBAT blends. The interpretation of the results for such reactive systems is not straightforward due to the complexity of the reaction products and lack of specific information such as their location in the blend microstructure. However, the information that is available clearly demonstrates that there are significant rheological differences between modified and unmodified blends at low frequencies. This indicates that the some part of the epoxide functions can be consumed to make reaction at the interface [16]. Furthermore, it is clear that the PLA/PBAT blends showed a more significant shear-thinning behavior at all frequencies compared with the PLA melt. This phenomenon has been also observed by Corre et al [17].

Meanwhile, the evolution of the storage modulus (G′) can provide more information about the different qualitative behaviors of the PLA/PBAT blends depending on the amount of added Joncryl ADR®. As can be seen from Figure IV-1, at low frequencies, an increase of the storage modulus of the blends with the incorporation of Joncryl ADR® can be noticed.

Moreover, no clear plateau at low frequencies is observed, indicating that both the droplet relaxation and the interfacial relaxation times are very long, where the rheometer could not detect them. This highlights the pronounced increase of the elasticity of the material and chain entanglements due to either branching or the presence of a higher molecular weight.

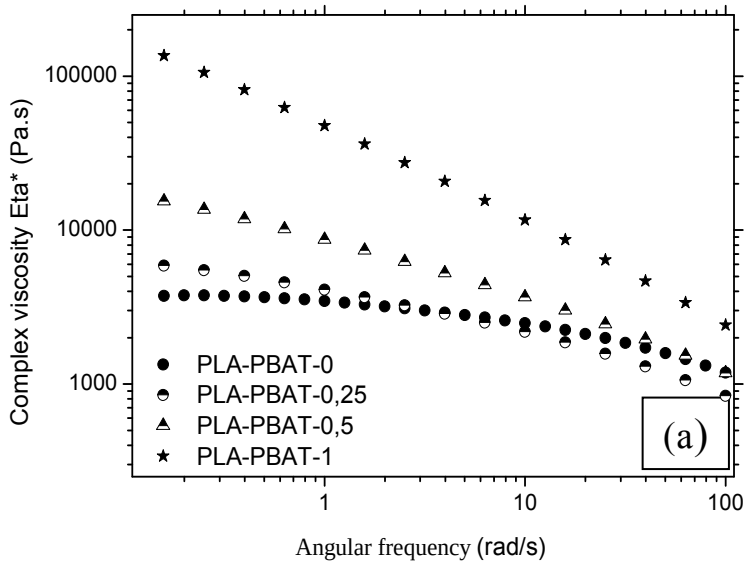

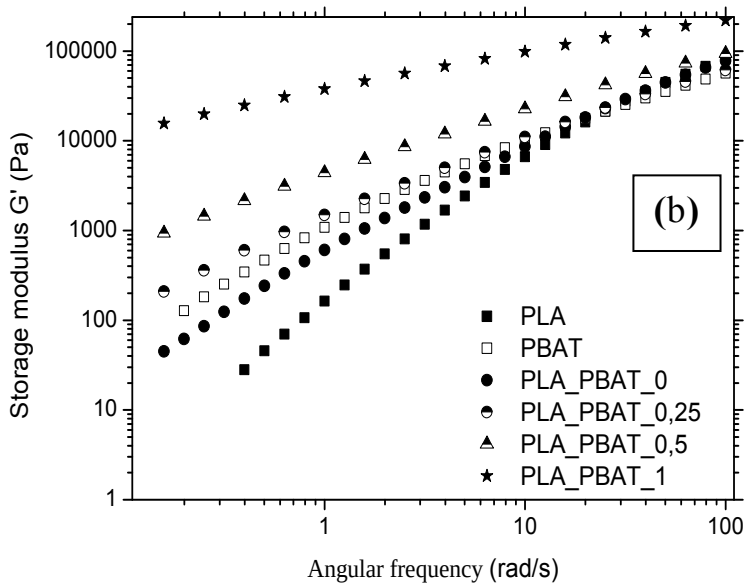

Figure IV-1 The angular frequency dependence of a) the complex viscosity and b) the storage modulus (G') versus angular frequency at 180°C for unmodified and modified PLA/PBAT (80/20) blends

IV.1.1.1 Cole-Cole plots

On the other hand, a better tool for comparing the differences in viscoelastic behavior resulted from variations in the umodified and modified structure of polymers is the Cole-Cole plots.

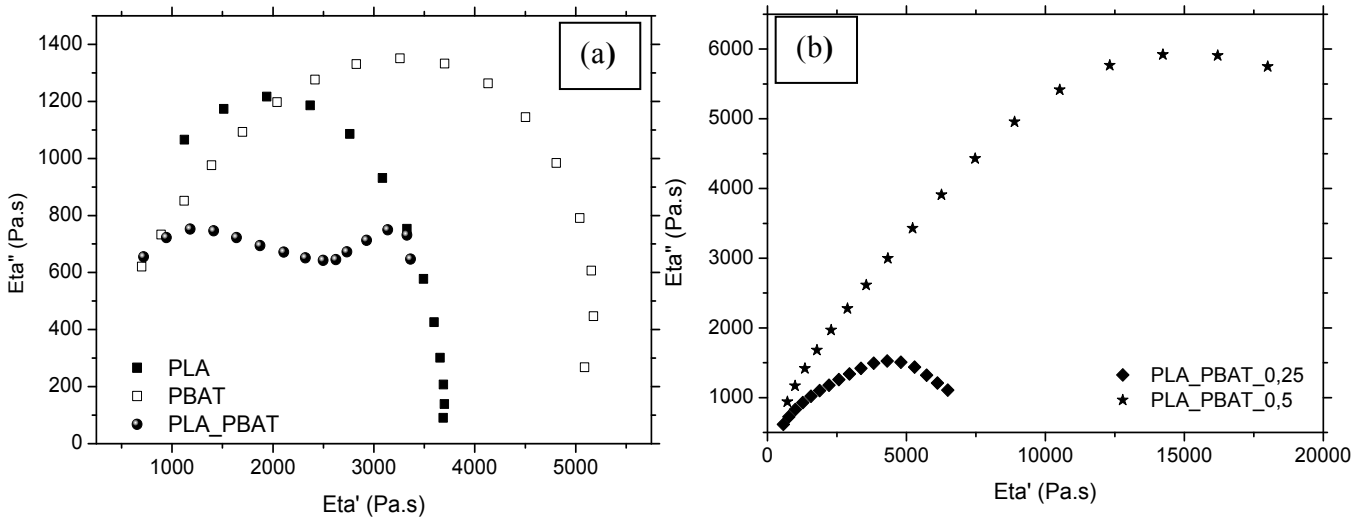

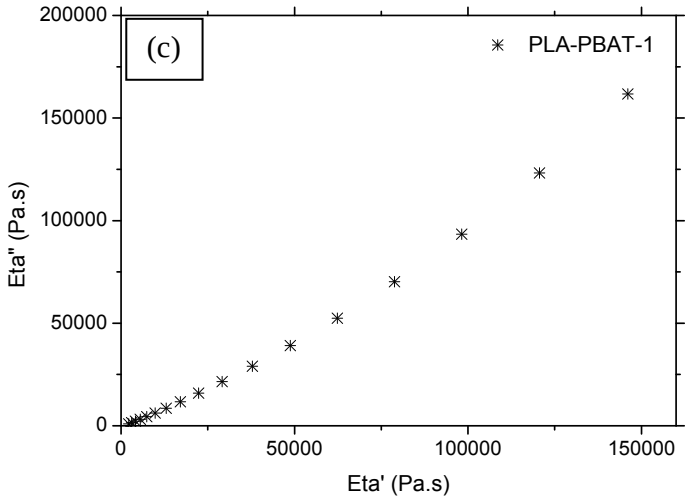

Figure IV-2 Cole-Cole plots at 180°C of a) PLA, PBAT and their unmodified blend b) PLA_PBAT blends modified with 0,25 and 0,5 %wt of Joncryl and, c) PLA_PBAT blend modified with 1%wt of Joncryl

Such graphs were obtained by plotting the imaginary versus the real parts of the complex viscosity [18]. This technique can give some important viscoelastic polymer properties like the weight-average relaxation time λ_0 and the zero-shear viscosity η_0. Figures.IV-2a), IV-2b) and IV-2c) portray the Cole-Cole plots for PLA/PBAT blends. The characteristic relaxation time λ_0, given at the maximum of η'' ($\omega\lambda=1$), is related to the frequency. The single arc obtained for PLA and PBAT suggests that they were linear with monomodal molecular weight distributions [19].
However, and more interestingly, for the PLA/PBAT blends, the obtained Cole-Cole plots showed the contributions from the two coexisting phases of the blend, the dispersed droplets and the matrix. Consequently, two relaxation arcs could be observed and interpreted by the simultaneous occurrence of two relaxation mechanisms with largely different relaxation times, as reported in the literature [19][20]. A remarkable shift to the high viscosity region when increasing the Joncryl ADR® loadings indicates that chain branching and extension retards the overall relaxation of the PLA/PBAT blend systems and leads to the formation of branched structures of PLA and PBAT in the blend. When the loading reached 1%wt, the local relaxation arc nearly disappeared, indicating a long-term relaxation time for the PLA and/or PBAT chains. The respective calculated average relaxation times for PLA and PBAT are about 0.019 and 0.25 sec. However, the times increase with the incorporation of Joncryl. It varies from 0.04 and 0.2 sec (for unmodified blends), 1.6 sec (PLA/PBAT/0.25), 6.3 sec (PLA/PBAT/0.5) to more than 6.3 sec for PLA/PBAT/1.
Cole-Cole plots cannot provide additional information on the relaxation time for the PLA/PBAT/1 system due to the relaxation arc which is not fully appearing in the experimental ranges of the frequency.

IV.1.1.2 Relaxation behavior

To quantify the characteristic relaxation time of different modified and unmodified blends, the relaxation spectra were calculated from the dynamic moduli. Such spectra ($\lambda H(\lambda)$) have been determined by Honerkamp, Weese, Elster, and recently by Hansen [17] [21] and plotted according to Eq.6. Figure IV-3b portrays the weighted relaxation spectra λ. H (λ) versus λ for the modified and unmodified PLA/PBAT blends.

For the unmodified blend, two relaxation peaks are clearly observed at about 0.08 and 3 s. The first peak (0.08 s) corresponds to the relaxation of PLA matrix, probably influenced by the presence of PBAT chains. A second one could correspond to the shape relaxation of the dispersed PBAT phase. It could be also originated from to the superposition of the shape droplet and the PLA-PBAT interface relaxations. The presence of the interface relaxation time in the blend without epoxy can be proved the presence of reactions between two condensation polymers.

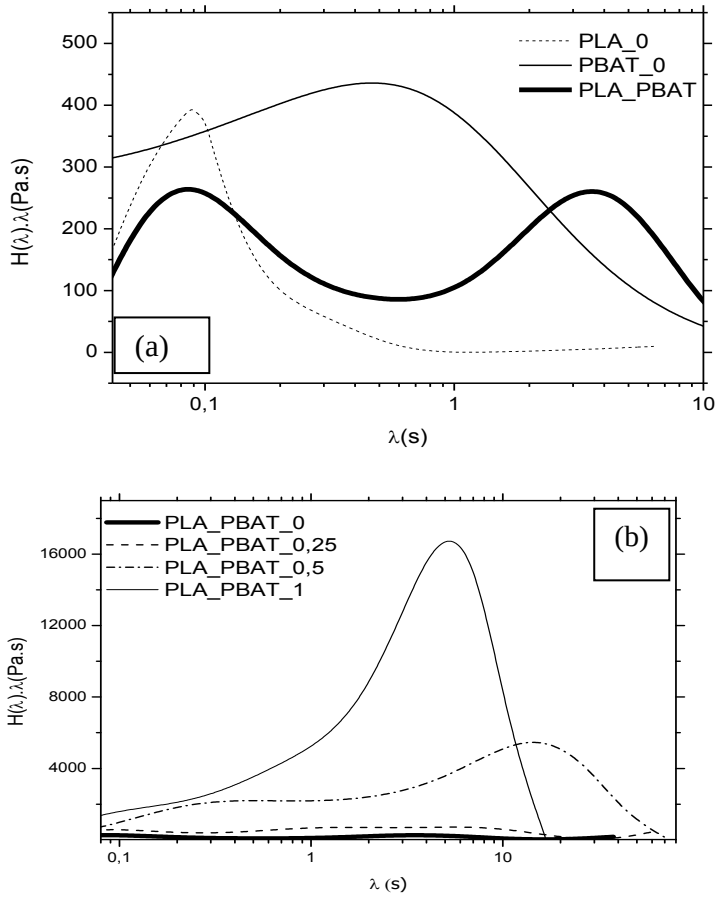

Figure IV-3 Weighted relaxation spectra of the a) neat PLA, PBAT, their unmodified blend, and, b) unmodified and modified PLA/PBAT blends at 180°C and under 5% strain

In the case of modified PLA/PBAT, the second relaxation time accorded to shape droplet phase is shifted to higher values for an amount of Joncryl up to 0.5 %wt. This evolution can be related to the longer time taken by the interface of the dispersed droplet to relax. The degree of compatibility of the blends increased, as also reported in the literature [22].
Nevertheless, HuoY et al. [49] noted that two characteristic relaxation times, τ_s and τ_β, can clearly be seen in the curves of compatibilized PP/PS blends, except for the blend with 5wt% compatibilizer. In comparison with that of the uncompatibilized blend, the shape relaxation time of the compatibilized blends, τ_s, slightly shifts to lower values. The extra relaxation time, τ_β, decreases substantially with increasing amount of compatibilizer. The same trends were also observed in the physically compatibilized blend systems [50]. When increasing the amount of the compatibilizer further to 5wt%, the two relaxation times merge, as was also reported for the physically compatibilized system [polyisoprene/poly(dimethyl siloxane), PI/PDMS] when the block copolymer concentration is more than 1% [48].

We remind here that both of PLA chains in the matrix and PBAT chains in the dispersed phase are modified during reactive extrusion with the formation of extended and the branched chains allowing also to explain the longer obtained times. Nevertheless, no additional extra relaxation times accorded to the PLA-joncryl-PBAT copolymer at the interface are clearly identified for the modified PLA/PBAT blends. At 1% of Joncryl, the two peaks are merged into one, indicating that due to the high concentration of the reactive epoxy, the matrix and the dispersed droplets could relax at the same time.

IV.2 Morphological properties of PLA/PBAT blends

Recently, much attention has been focused on the reactive blending process in order to understand how the phase morphology develops in a blend. The morphology generation during melt-mixing of immiscible blends involves processes such as fluid drops becoming stretched into threads, break-up of the threads into smaller droplets and coalescence of the droplets into larger ones. The balance of these competing processes determines the final particle size which results upon cooling of the blend. The viscosities of the major and minor phase, the viscosity ratio, the interfacial tension between the components, the mobility of the interface as well as the shear stress and shear rate conditions were controlling these processes. Furthermore, different types of morphologies of the dispersed phase can be obtained such nodular, laminar or fibrillar ones.

A minimum of five micrographs were obtained for each sample, and approximately 200 particles were considered in order to determine the droplet diameter of the dispersed phase using image analysis software (Scion image). The number ($\overline{D_n}$) and and the volume average diameter ($\overline{D_v}$) were calculated based on the real particle size distribution using the following equations (14a, b), respectively:

The number average diameter: $$D_n = \frac{\sum_i n_i D_i}{\sum_i n_i} \quad (14a)$$

The weight-average diameter: $$D_v = \frac{\sum_i n_i \overline{D_i^4}}{\sum_i n_i \overline{D_i^2}} \quad (14b)$$

In which ni and Di are respectively the number and the particle diameter. The polydispersity (d) was characterized by means of the ratio $d = \frac{D_v}{D_n}$

.

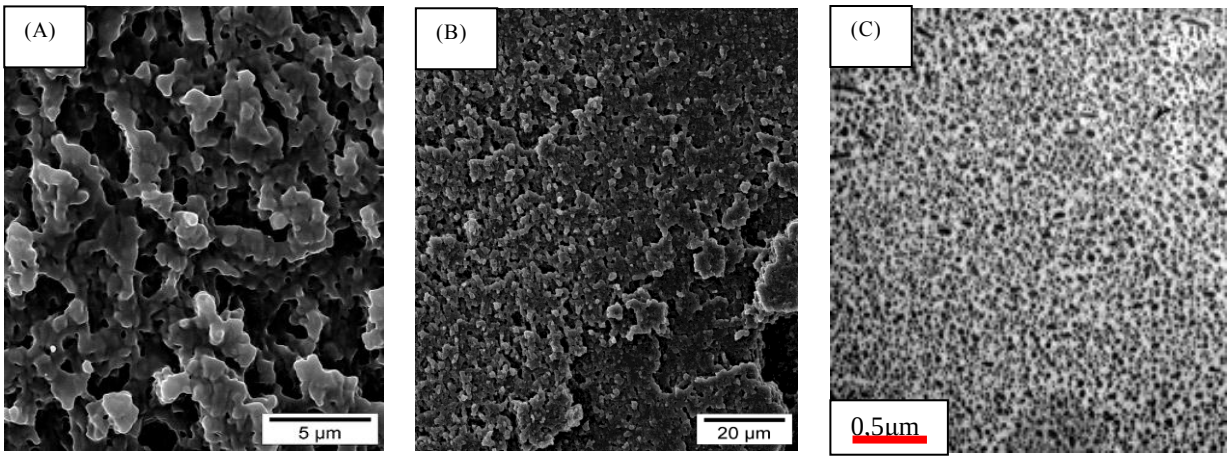

Figure IV-4
A): SEM micrographs of PLA/PBAT blends;
B): SEM micrographs of PLA/PBAT blends;
C) : TEM micrographs of PLA/PBAT/Joncryl (80/20/0.5)

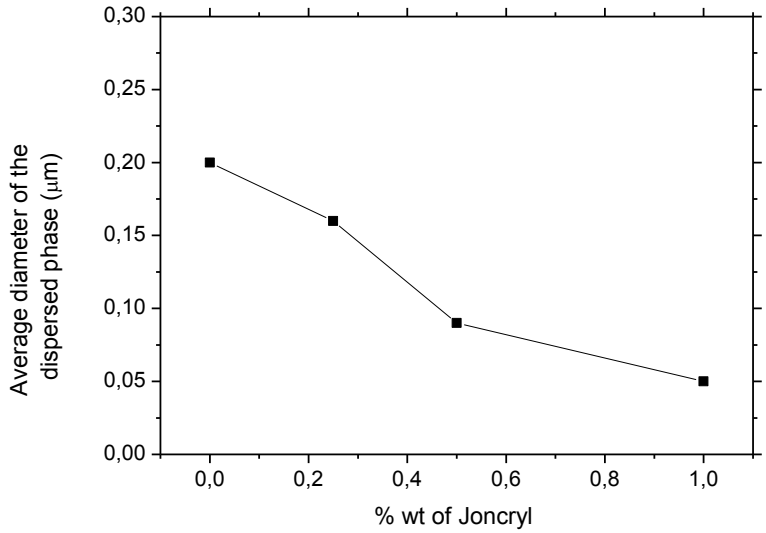

Figure IV-5 Evolution of the volume average diameter of the dispersed phase as a function of the amount of Joncryl from Image Analysis, the polydispersity "d" range from 1.15 to 1.27 for all the studied systems. (TEM observations).

Figure IV-4 showed that the binary PLA/PBAT blends exhibited the typical morphological features of incompatible systems.

The larger particles in the size distribution of dispersed phase were due to two main reasons [23]; (i) a viscosity ratio between the matrix and the dispersed phase far from 1 and (ii) a coalescence phenomenon due to the poor interfacial adhesion between the matrix and the dispersed phases. For the compatibilized systems, the chemical reaction between PLA, PBAT and Joncryl ADR® on the interface led to (i) a reduction of the average size of the dispersed phase due to the suppression of coalescence and the decrease of the interfacial tension, even at very short mixing times (3 minutes); the ultimate size of the PBAT particles in the reactive PLA/PBAT/Joncryl system was much smaller (0.05 µm) than in the non-reactive blend (0.2 µm) (Figure IV-5), (ii) an increase in

the break-up of the largest particles in the size distribution of the dispersed phase, (iii) a substantial narrowing of the size distribution of the dispersed phase, and (iv) a decrease of the mobility of the interface which slowed down the coalescence rate, related to the formation of the copolymer at the interface. These hypotheses will be developed in details and discussed in the next section.

IV.3 Effect of multifunctionalized epoxy on the interfacial tension properties in PLA/PBAT blends the interfacial tension in PLA/PBAT blends

Basically, there are three distinct strategies to compatibilize the immiscible polymers; (i) a non-reactive compatibilization by adding a non–reactive block or graft copolymer that is miscible with both phases or a copolymer with one of its parts miscible with one of the blend's components and the second part miscible with the second blend component, (ii) a specific compatibilization by attaching groups with non-bonding specific interactions to the polymer chains and finally, (iii) a reactive compatibilization by introducing reactive molecules capable of forming the desired block and/or graft copolymers *in-situ*, directly during blending.
Accordingly, the rheological behavior of PLA/PBAT/GMA reactive functions as well as the relaxation spectrum and Cole-Cole diagram coupled to the TEM and SEM morphology confirmed that Joncryl ADR® played the role of a compatibilizer. The challenge of the following paragraph was to understand, probe and quantify the effect of GMA/epoxy functions on the interfacial forces in the blends. As mentioned earlier, past research has shown that rheological properties can serve as a convenient probe of morphological evolution in droplet/matrix blends. According to the literature, several methods developped for light fluids, to determine the equilibrium interfacial tension, are in principle applicable to polymer liquids and melts. However, only few methods are practical. In general, the different techniques include three dynamic methods (the breaking thread method "BTM", the imbedded fiber retraction method "IFRM" and the retraction of deformed drop method "DDRM") and three equilibrium methods include the "pendant drop", " the sessile drop" and "the spinning drop" approaches [10]. The dynamic methods are based on the balance between the *interfacial forces* and *viscous forces* whereas the equilibrium methods are based on the balance between the interfacial forces and gravitational forces. One most used technique is the rheological method that is based on dynamic shear measurements in linear viscoelasticity. One emulsion model, the Palierne model, has generally been used to extract the interfacial tension from the experimental dynamic moduli, G' and G''. According to the model, the increase of the elasticity at very low frequency for immiscible molten polymers is related to the deformation and relaxation of the dispersed drops caused by interfacial tension. As mentioned before, we propose in this section to offer the first study on the interfacial tension of PLA/PBAT blends based on rheological methods.

Deformed Drop retraction method

Droplets inside an incompatible matrix tend to stay or become spherical due to the natural tendencies of the drop to try to maintain the lowest possible surface-to-volume ratio. However, a flow field within the mixer applies a stress on the droplets, pushing them to deform. If this stress is high enough, it can eventually cause a dispersion of the drops. A capillary number calculation can help understanding the balance between the interfacial and the viscous forces. The droplets will disperse when the surface tension can no longer maintain their shape in the flow field and the filaments break into smaller droplets. These dispersion and distribution phenomena continue until the flow field stresses can no longer overcome the surface tension of the new formed droplets. The break-up of droplets occurs when a critical capillary number is reached. Because of the continuously decreasing thread radius, the critical capillary number is reached at some specific point in time. Due to the competing stresses and interfacial forces, the cylindrical shape becomes unstable and small disturbances at the surface lead to a growth of capillary waves. These waves are

commonly referred to as Rayleigh disturbances with various wavelength forms on the cylinder/fibrillar surface. The interfacial chemical reaction thus has several effects, which influence the morphology evolution and the final blend morphology. The formation of a copolymer at the interface reduces the interfacial tension. This is expected to increase the capillary number, resulting in easier domain break-up and smaller domain sizes. The rate of particle-particle coalescence is reduced due to the steric hindrance caused by the copolymer at the interface [23].
In this paper, the retraction of deformed drop method was chosen for the PLA/PBAT/Joncryl systems. This method consists of deforming a given spherical drop and then recording, the output as a function of time. It thus requires the equilibration and deformation of the drop by a shear strain step in order for it to become an *axisymmetric* ellipsoid before it retracts into a spherical shape [26][27]. The greatest advantage of this method is the short time required to complete the experiments, thus avoiding thermal degradation of the polymers. Nonetheless, there are limitations of DDRM, e.g. issues related to transparency, droplet size, viscosity ratio and cross-linked drops.
The deformation of a melt polymer droplet suspended in another polymer has been considered by many authors from both theoretical and experimental points of view based on the pioneering work of Taylor and Grace [28]. The drop deformation, its aspect ratio and its eventual breakup are controlled by two dimensionless parameters, namely the viscosity ratio of the dispersed phase and the matrix (Eq.15)

Equation 15
$$p = \frac{\eta_d}{\eta_m}$$

In two-phase blends in the Newtonian region, the structural evolution is a competition, during flow, between the hydrodynamic deforming stresses ($\sigma = \eta_m \times \dot{\gamma}$) that tend to deform the drops and interfacial forces (α/R) that resist the stress or deformation and tend to recover the initial shape of the drop. The deformation can be determined by the capillary number as follows:

Equation 16
$$Ca = \frac{\sigma \times R}{\alpha_{12}}$$

where σ (Pa) is the stress and α is the interfacial tension.
The critical value of C_a can be calculated by the following expression as a function of the viscosity ratio using De Bruijin equation [29][30].

Equation 17
$$Log(Ca_{crit}) = -0,506 - 0,0994\log(p) + 0,124(\log(p))^2 - \frac{0,115}{\log(p) - 0,6107}$$

The master curve for single drop break-up is usually referred to as Grace's curve. According to this curve, the droplet can be deformed only with "p" less than 4 in shear deformation.
The relaxation kinetics are based on a theoretical equation describing the evolution of the shape of an ellipsoidal liquid drop in an infinite fluid domain. The expression used for the deformation "D" upon cessation of the flow, is given by the **Taylor method**:

Equation 18

$$D = D^{\circ}\exp-\left\{\frac{40(p+1)}{(2p+3)(19p+16)}\frac{\alpha_{12}}{\eta_m R^{\circ}}t\right\} = D^{\circ}\exp\left\{-\frac{t}{\tau_d}\right\} = \frac{L-B}{L+B}$$

Here, "D" is the drop deformation parameter defined as D = (L-B) / (L+B), "L" and "B" are the major and minor axes of the ellipsoid drop, respectively. "D°" is the initial deformation parameter, "p" is the viscosity ratio of the dispersed to the matrix phase, "α" is the interfacial tension, "η_m" is the viscosity of the matrix phase and "R°" is the radius of the drop at the equilibrium. Plotting ln (D) vs t renders possible an estimation of the interfacial tension «α» from the plot's slope. In light of Eq.19, an interfacial relaxation time (τ_d) for deformed droplet retraction can be defined as:

Equation 19

$$\tau_d = \frac{\eta_{eq} \times R^{\circ}}{\alpha_{12}}$$

where the equivalent viscosity η_{eq} is calculated from the following equation

Equation 20

$$\eta_{eq} = \frac{(2p+3)(19p+16)\eta_m}{40(p+1)}$$

For a given viscosity ratio, the drop breaks up when the capillary number, Ca, exceeds a certain critical capillary number, Ca_{crit}. The variation of Ca_{crit} with the viscosity ratio was determined experimentally by Grace [28] for a single Newtonian drop suspended in a Newtonian medium in both shear and elongational flows [28][29]. Various authors have studied the mechanism of deformation and breakup [31][32][33]. Based on what is well-known in the literature, the drop will be able to deform or break depending on the ratio Ca/Ca_{crit}.

In this way, we attempted to measure the effect of the reactive multi-functional epoxide (Joncryl ADR®-4368) on the interfacial tension of PLA and PBAT (80/20) blends by using the drop retraction method. Two model systems (Model A and Model B) were prepared as shown in Figure IV-6. The retraction process of PBAT particles is shown in Figure IV-7. Figure IV-8 portrays the plausible role of the Joncryl in the system as well Model B for example.

Model A

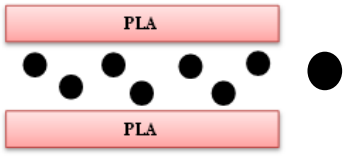

PBAT droplets

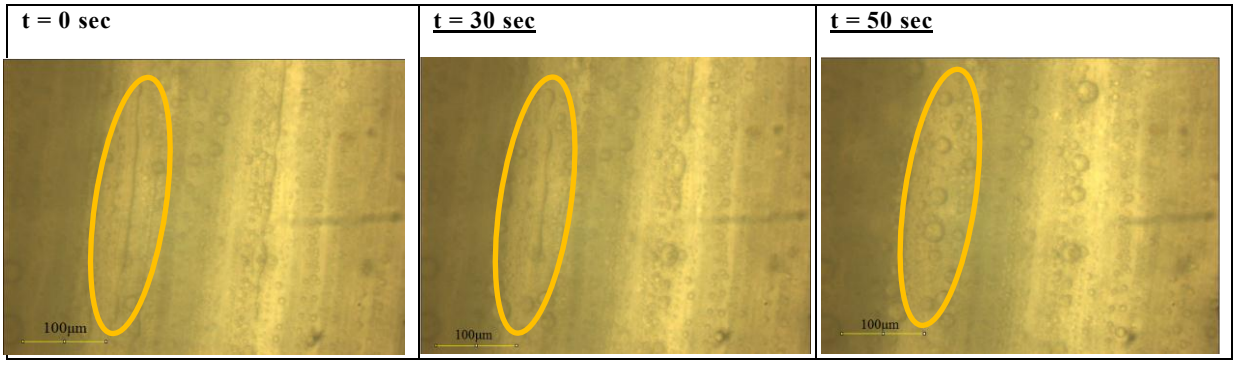

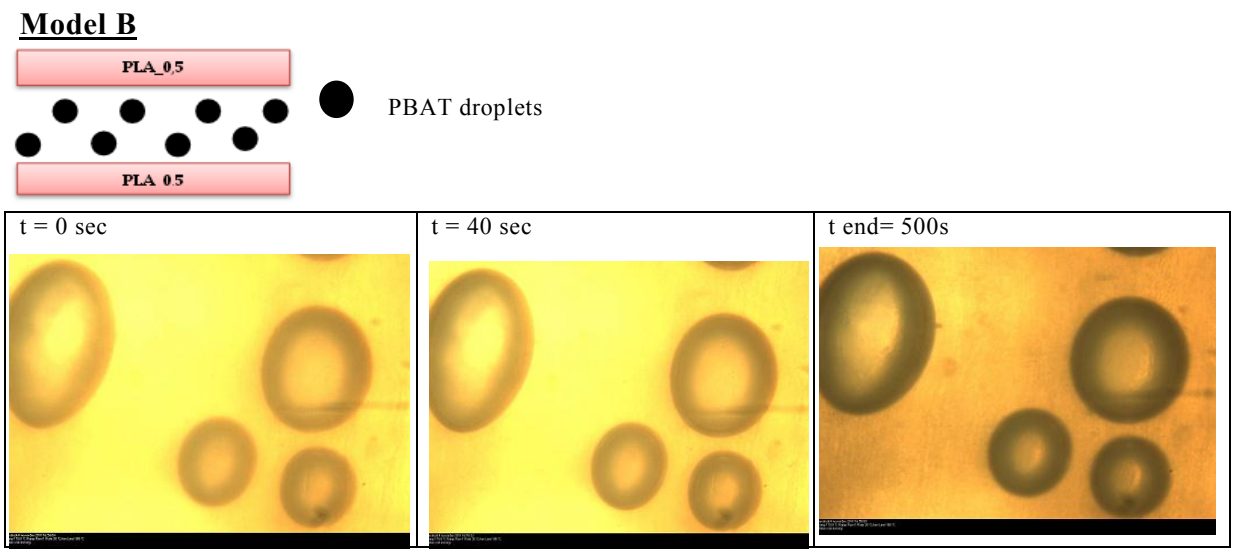

Figure IV-6 Examples of illustrations of the ellipsoid drop retraction, immersed in a fluid matrix at 180°C of Model A (where PBAT droplets are dispersed into PLA matrix) and Model B (where PBAT droplets are dispersed into PLA_0,5 matrix).The measurement time (in second) is noted on each micrographs

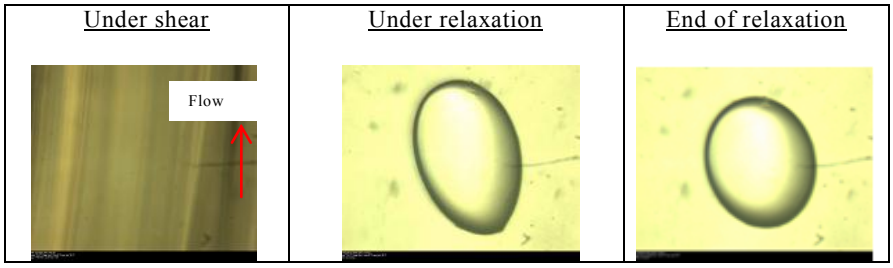

Figure IV-7 Examples of droplets shapes under shear, under relaxation and at the end of relaxation for PLA_PBAT_1. Other illustrations are given in the next section

Referring to Taylor's theory, Ln (D) was plotted versus time at 180°C and the plot displays a linear evolution with a slope, from which "σ" is estimated. From the appropriate curves and the corresponding linear fits, interfacial values of the studied systems were calculated. Table IV-1 summarizes the values of the different parameters used in this study.

Table IV-1 Viscosity ratio p, droplet relaxation time, equivalent viscosity, capillary number and critical capillary number values for Model A and Model B

Samples (Drop/Matrix)	P	Relaxation time (τ) (sec)	η^{eq} (Pa.s)	C_a	C_a critique
Model A	1.1	47	4800	5.84	0.49
Model B	0.32	555	11031	35.29	0.476

The observation of the drop deformation from a vertical view enables the determination of both axes of the sheared droplet in the flow direction, L, as well as in the gradient direction, B. From these magnitudes, the droplet deformation parameter, D, was measured as a function of the experimental time at a shear-rate value for the corresponding system. It was found that both L and D changed until reaching closed values, indicating the retraction of fibrils into droplets ($Ca >>> Ca_{crit}$). According to the literature, when $Ca/Ca_{crit} >>> 1$, the drop deforms first into a long fibril and then breaks up into a large number of droplets through Rayleigh capillary instabilities. In other words, once the drop shape can be well represented by a slightly deformed ellipsoid, the deformation parameter decreases exponentially with time. And so, the drop retracts under the influence of two driving forces, i.e., viscous forces and Laplace pressure originating from the interfacial tension. The C_a values obtained for the studied samples were far above the critical value, and the droplets actually turned into filaments as predicted by Jansen et al when $Ca > 2*Ca_{crit}$ [34].
The calculated values of interfacial tension for these two samples are shown on Figure IV-9. The uncompatibilized PLA/PBAT blend (Model A) become deformed into ellipsoids or even fibrils as reported in earlier studies [35] and severe drop break-up phenomena occurred. The interfacial tension value in this case was found to be 7,34 mN/m, which explains the lack of compatibility between the two polymers. However, by changing the PLA matrix (Model A) into an extended/branched PLA with Joncryl ADR® (Model B), the mechanisms of deformation and breakup become altered and some droplets showed a particular shape.
The presence of such a chain extension/branching agent, decreased the interfacial tension from 7.34 to1.68 mN/m, which resulted in an increase in the capillary number and consequently in a change in drop deformation [12][26][27][36][37][38].

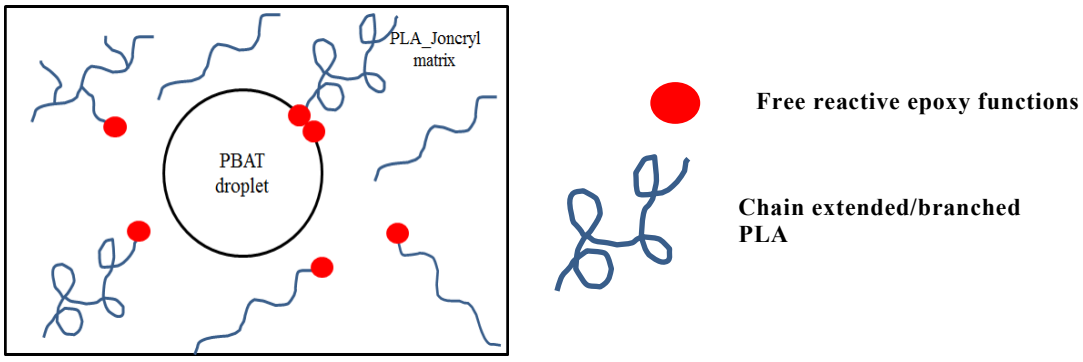

Figure IV-8 Illustration of the interfacial reaction between extended/branched PLA and PBAT droplets

Based on these results, a decrease of the interfacial tension confirmed the compatibilization effect in addition to that of chain extension and branching of PLA by using reactive GMA/Epoxy functions.

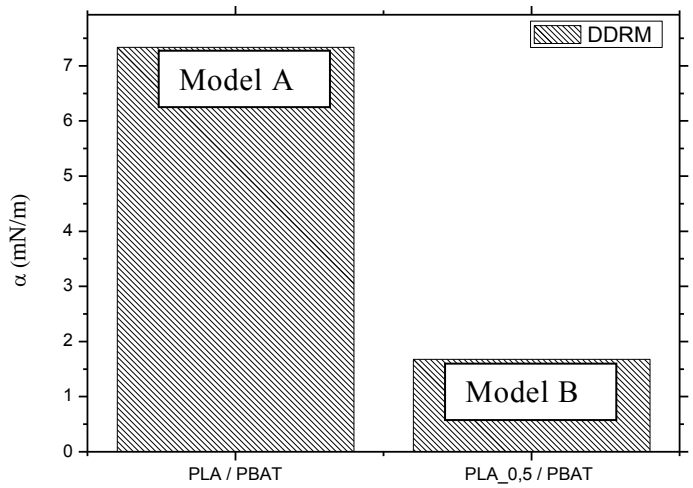

Figure IV-9 Interfacial tension values for Model A and Model B calculated according to DDRM (The samples notations are written according to Matrix/droplets form)

The decrease in droplet morphology observed by TEM corroborates the obtained results. The increase in elastic modulus also confirmed this purpose. The objective of these model experiments was to assess and understand the compatibilization/branching and chain extension balance. In this case, by increasing the viscous forces of the PLA matrix as comparing to model "A" experiments, the interfacial forces were significantly decreased as a result of a lower interfacial tension. Beyond chain extension / branching of the PLA matrix, the physical interactions between the modified PLA/PBAT chains increased (Figure IV-9).
In addition, deformed droplets relaxation time was much higher for the second case where the matrix phase was viscoelastic and formed by the extended/branched PLA.
Consequently, the stabilization of the interface retarded the relaxation of the deformed interface, and thus the retraction of PBAT particles was much longer than that for the blank blend as we can see in Figures IV-10 and IV-16. However, what can be said about the real mechanism responsible

for the reduction of the interfacial tension (α)? Is it due to the contribution of the viscoelastic properties of the PLA, PBAT chains during reactive extrusion or to the interfacial reaction in the blend with the creation of PLA-Joncryl-PBAT copolymer?
In order to compare the evolution of the interfacial tension depending on the reaction between Joncryl ADR® and each polymer, one more experiment was performed (Model C). The idea was to create a sandwich where the dispersed phase was formed by PLA, and the matrix phase was a chain extended/branched PBAT (Figure IV-11). As we can see in Figure IV-12 and table IV-2, the closer values of the interfacial tension obtained for both Model B (1.68mN/m) and Model C (1.43 mN/m) confirmed that even when increasing the viscous forces of PLA or PBAT, the physical interactions between the PLA/PBAT chains increased, leading to a reduction of the interfacial tension.

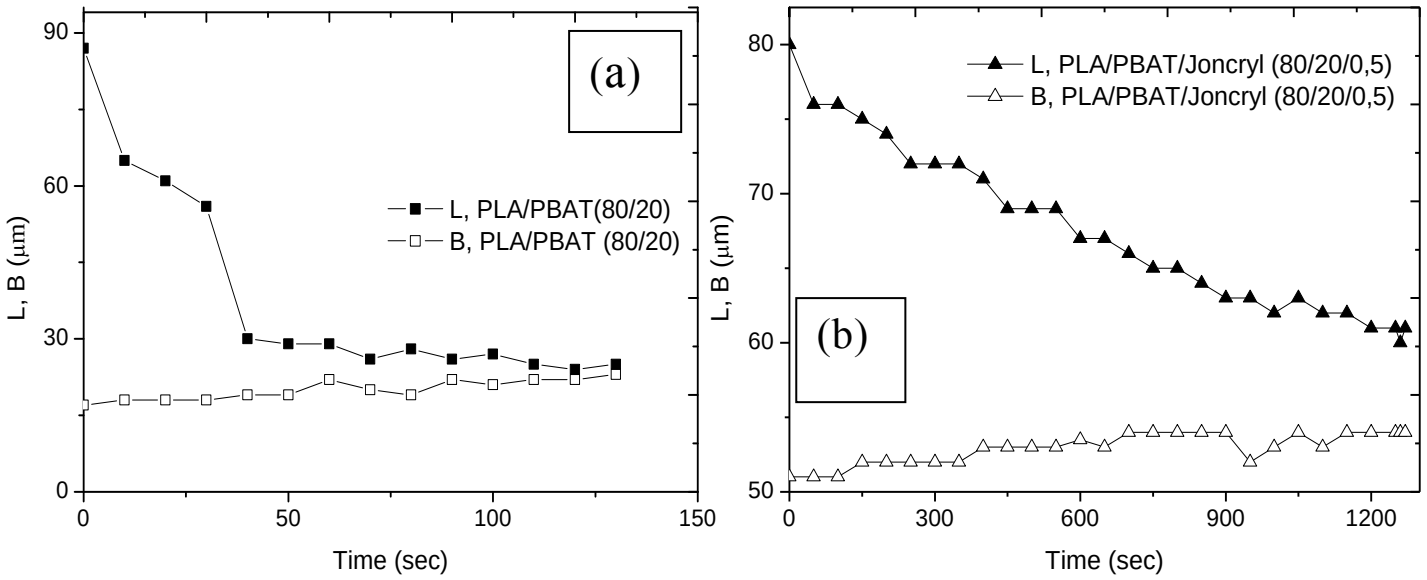

Figure IV-10 Major and minor droplet radius evolution with time for (a) incompatible PLA/PBAT blends and (b) compatible PLA/PBAT/Joncryl blends

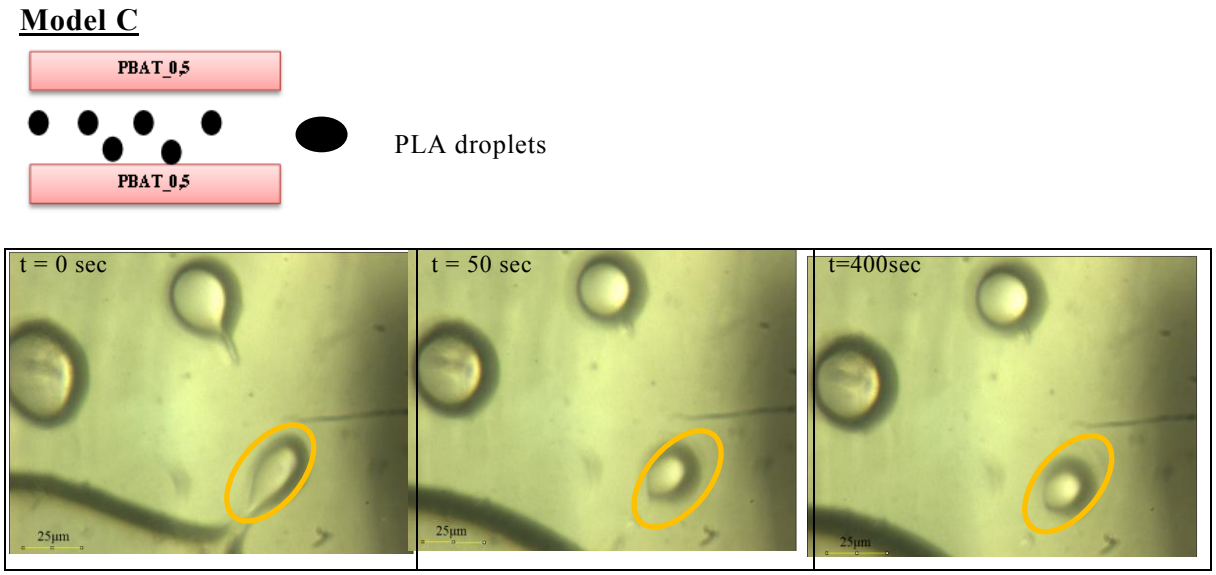

Figure IV-11 Retraction of an ellipsoid drop immersed in a fluid matrix at 180°C

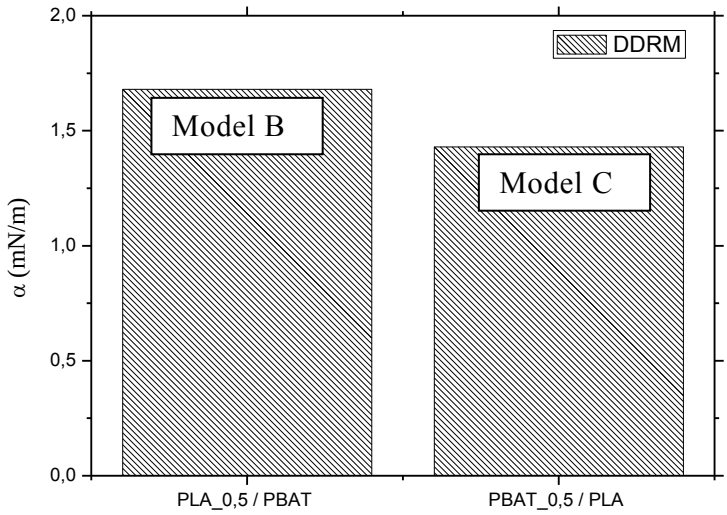

Figure IV-12 Interfacial tension values for Model B and Model C according to DDRM (The samples notations are written according to Matrix/droplets form)

Table IV-2 Viscosity ratio p, droplets relaxation time, equivalent viscosity, capillary number and critical capillary number values for Model B and Model C

Samples (Drop/Matrix)	P	Relaxation time (τ) (sec)	η_{eq} (Pa.s)	Ca	Ca critique*
Model B	0.32	555	11031	35.29	0.476
Model C	0.45	270	8584	26.2	0.46

To provide more information about the major role of Joncryl ADR® on the morphology of PLA/PBAT blends, another experimental model was carried out. Here, 0.5 % wt. of the reactive epoxy functions was incorporated into both dispersed and matrix phases (Model D) (Figure IV-13).

Model D

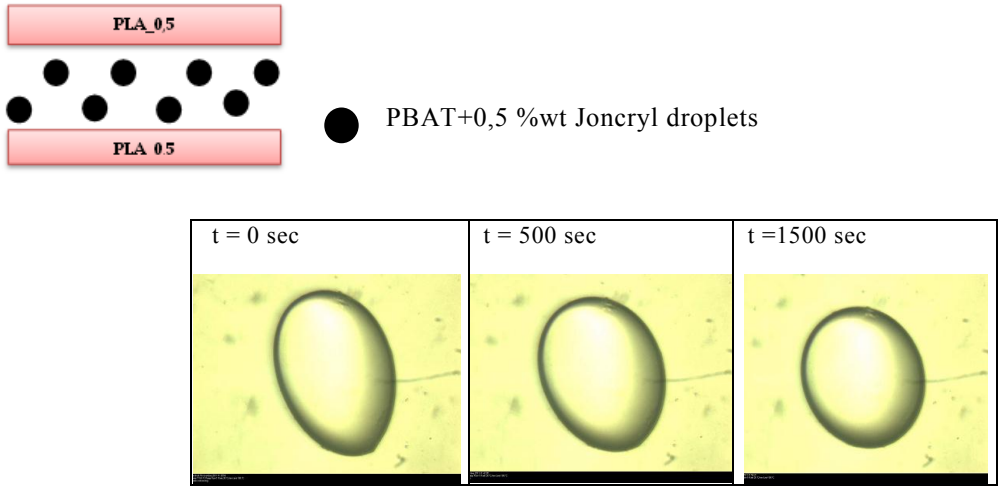

Figure IV-13 Retraction of an ellipsoid drop immersed in a fluid matrix at 180°C

A further decrease of the "α" value was observed from 1.68 (Model B) to 0.36 mN/m (Model D). Indeed, the effect of Joncryl ADR® on the interfacial tension was more efficient when it reacted with both of the neat polymers.The Model D represents probably the more complex system with thr rheological changes of PLA, PBAT structures with Joncryl. The epoxide functions have a role of physical compatibilizer rendering it possible to relate Rayleigh instabilities and obtain a fiber break–up with a smaller droplet morphology and to inhibit the particle coalescence by the formation of PLA_Joncryl_PBAT at the interface.
Figure IV-14 summarizes the effect of Joncryl in ln (D) evolution of experimental models A, B,C and D

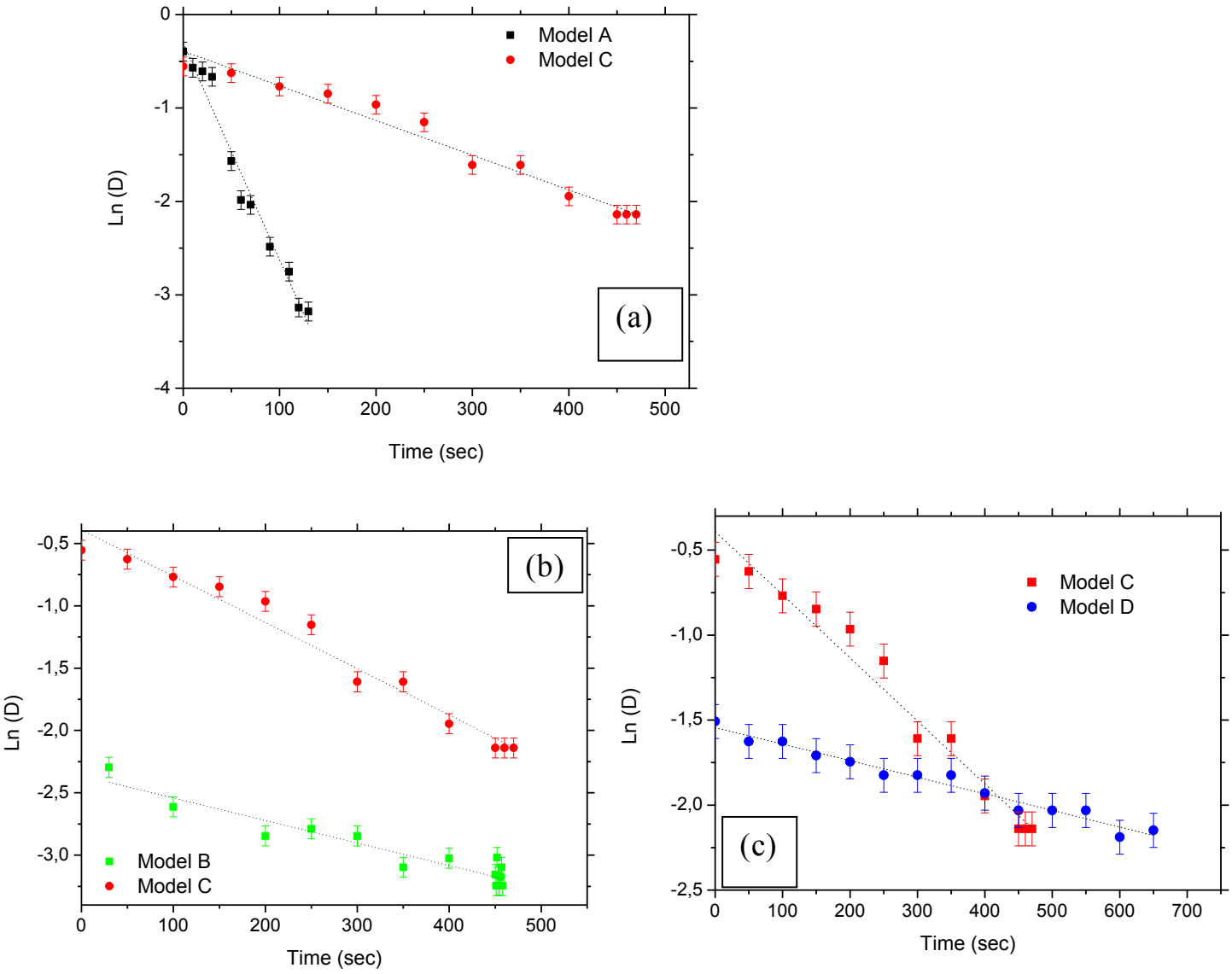

Figure IV-14 Example of the given results of Ln (D) evolution as a function of time for (a) Model A vs Model C and (b) Model B vs Model C and, (c) Model C vs Model D

Figure IV-15 and table IV-3 summarize the respective values of interfacial tension for the different studied samples.

Table IV-3 Viscosity ratio p, relaxation time, equivalent viscosity, capillary number and critical capillary number values for the four studied models

Samples (Drop/Matrix)	P	τ (sec)	η_{eq} (Pa.s)	Ca	Ca critique*	Interfacial tension (mN/m)
Model A	1.1	47	4800	5.84	0.49	7.34
Model B	0.32	555	11031	35.29	0.476	1.68
Model C	0.45	270	8584	26.2	0.46	1.43
Model D	0.7	1000	12015	91	0.459	0.36

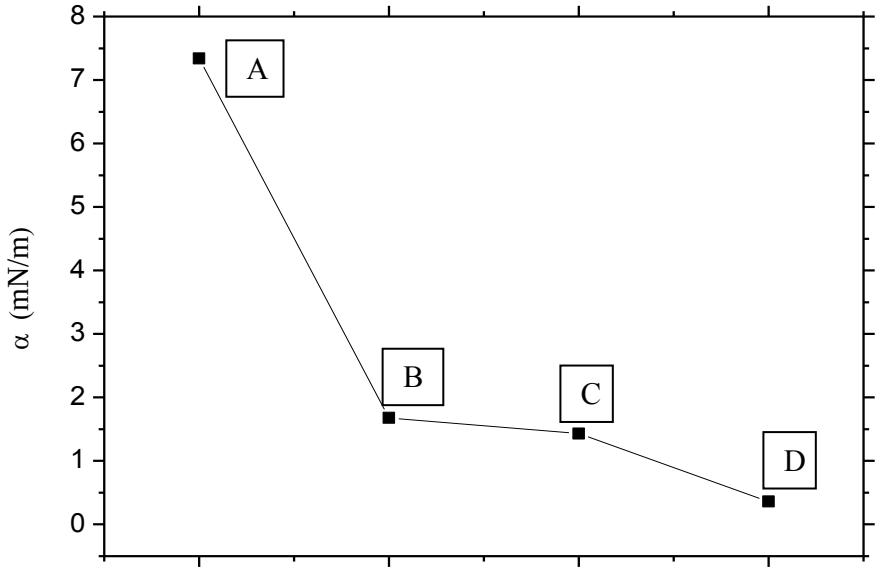

Figure IV-15 Interfacial tension values for Model A, Model B, Model C and Model D according to DDRM (The samples notations are written according to Matrix/droplets form)

Several experiments have shown that the addition of a compatibilizer causes a drastic decrease in the rate of coalescence leading to a stable morphology. This effect is generally termed coalescence suppression, and it has been hypothesized that a compatibilizer promotes morphological refinement more by suppressing coalescence during processing than by promoting the breakup of droplets. At least, in this context, two explanations have been elucidated. Some authors assumed that when two droplets approach one another, a squeeze of the flow in the intermediate matrix fluid, leads to a concentration gradient of compatibilizer along the interface. The Marangoni stresses (tangential stresses caused by the resulting gradient in interfacial tension) immobilize the interface, thereby suppressing coalescence (Figure IV-16a). The magnitude of these Marangoni stresses strongly depends on the surface coverage [39][40].

Based on all the models, it can firstly be shown that the critical capillary number for break-up decreased with the amount of Joncryl ADR® in the blend and the steady shear capillary number was

found to increase strongly with the addition of GMA functions, supporting the effect of Marangoni stresses described by Li and Pozrikidis [43][44]. Moreover, the added Joncryl ADR® affected on the one hand, the deformation and break-up by reducing the interfacial tension. On the other hand, it hindered a coalescence phenomenon between droplets due to the formation of a rigid particle layer when the interface was immobile at p<<1.
Another explanation has been suggested by Sundararaj and Macosko [41][42]. They assumed that the resistance against coalescence arises mainly from the steric repulsive force between the droplets, chain extended/branched droplets in our study, as a result of the compression of the compatibilizer block extending into the matrix phase when two droplets approach. This phenomenon reduces the number of possible conformations that the compatibilizer can achieve (Figure IV-16b) and it happens only when the compatibilizer is present at the interface. Marangoni stresses remain the most likely explanation for the observed droplet behavior.

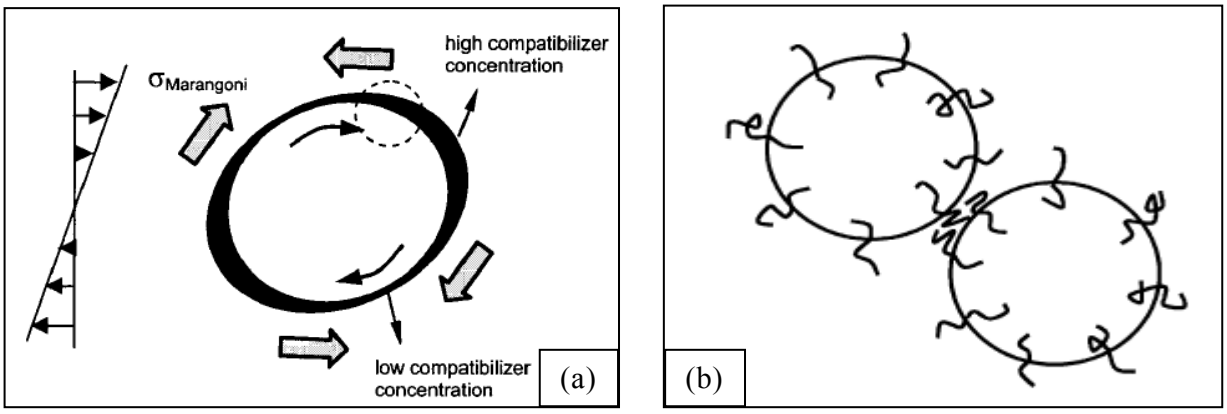

Figure IV-16 Schematic representation of the theoretical approaches to explain the coalescence suppression in compatibilized PLA/PBAT blends.
(a)Two drolets, squeezing flow in the intermediate matrix fluid leads to a concentration gradient of compatibilizer along the interface (Marangoni stress), (b) the resistance against coalescence arises mainly from the steric repulsive force between droplets

From the above results, it was well accepted that the presence of Joncryl ADR® in PLA/PBAT blends emulsified the phase interface and consequently reduced the interfacial tension. More discussion will be given at the end of the chapter.

Palierne model:
The most important advantage of the Palierne model is that it takes into account the viscoelastic behavior of the incompressible fluids under a small-amplitude oscillatory flow, and the data is representative of the total interfacial area. It has been found that the model provides useful information for describing the microscopic state of a blend. In this model, the viscoelasticity of the two phases, the hydrodynamic interactions, the droplet size and drop nature polydispersity, as well as the interfacial tension (shear and dilatation of the interface) are indeed included. The morphology development in the melt state is controlled by the interaction of domain deformation, break-up and coalescence. The flow field deforms the domains and, if sufficiently strong, breaks them into smaller domains.
For non–compatibilized blend, which interaction between phases is low, β″ (interfacial shear modulus) could be set to zero. Assuming that the particle size distribution is narrow (Rv / Rn < 2) and the interfacial tension is independent of the shear, Graebling simplified the Palierne model to Eq.21 [10][24]

Equation 21

$$G_b^*(\omega) = G^*_m(\omega)\frac{1+3\phi H(\omega)}{1-2\phi H(\omega)}$$

where ∅ = volume fractions of the dispersed phase corresponding to the particles with the voulume average radius of the droplets R_v. R_v has been determined from SEM micrographs by using an image analyzer and H(ω) is determined according to Eq.22

Equation 22

$$H(\omega) = \frac{4(\frac{\alpha}{Rv})\left[2G_m^*(\omega)+5G_d^*(\omega)\right]+\left[G_d^*(\omega)-G_m^*(\omega)\right]\left[16G_m^*(\omega)+19G_d^*(\omega)\right]}{40(\frac{\alpha}{Rv})\left[G_m^*(\omega)+G_d^*(\omega)\right]+\left[2G_d^*(\omega)+3G_m^*(\omega)\right]\left[16G_m^*(\omega)+19G_d^*(\omega)\right]}$$

where "α" is the interfacial tension between the two polymer blends components, G^*_m, G^*_d, G*b, the complex shear moduli of respectively the matrix, the dispersed phase and the blend at angular frequency (ω).

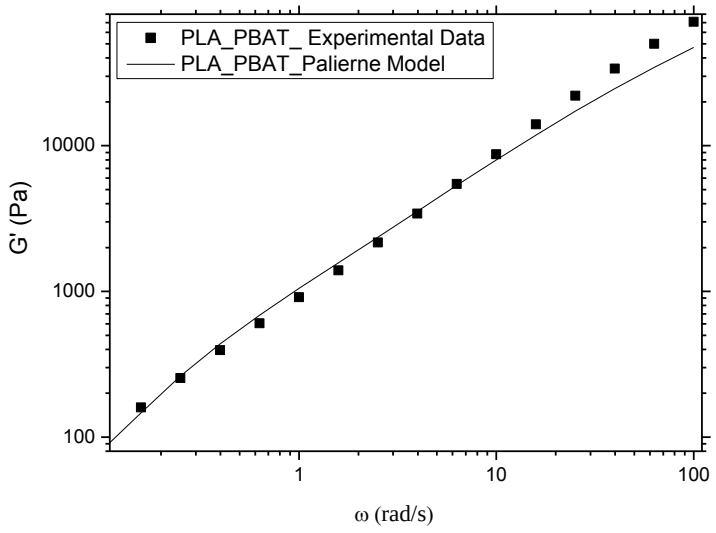

Figure IV-17 Example of experimental data and comparisons with predictions from the Palierne model for the PLA/PBAT blend (80/20)

Figure IV-17 shows the best predictions on the experimental data using Palierne model. The obtained values of effective interfacial tension α/ R_v and the calculated value of the interfacial tension α is listed in table IV-4. The interfacial tension of PLA and PBAT blends has been calculated and found to be 6,15mN/m. This higher value confirms the larger degree of incompatibility between PLA and PBAT. This value corroborates the calculated value by DDRM. The differences in the obtained values of interfacial tension from the two approaches were attributed to the theories on which they are based. The small deviation might also depend on the polymer-polymer contact time during measurements [45].

Bousmina [24] accounted for some experimental difficulties with this rheological method. The technique is limited for systems with a very high viscosity where the relaxation time may be very long and the terminal zone is shifted to very low frequencies. Such systems may not be accessible experimentally due to the limitation of the frequencies available on the rheometer and the thermal instability. Moreover, another limitation involves the estimation of the particle size which directly

affects the determination of the interfacial tension. Finally, some errors can also originate from the fitting procedure.

Table IV-4 Interfacial tension values for PLA/PBAT blends

Samples	α/R (Pa)	R (nm)	α (mN/m)
PLA80_PBAT20	5000	1230	6.15

* MEB observations have been used for uncompatibilized PLA/PBAT blends

Furthermore, Palierne emulsion model has been widely used to quantitatively describe the linear viscoelastic properties of polymer blends and to derive the interfacial tension from them [25-19]. The situation could be even more complicated with compatibilized polymer blends for which even experimental results themselves have been subject of controversy in the literature [50] [51] [52]. For example, unlike Riemann et al. and Jacobs et al., Velankar et al. [37] did not observe the expected slow interfacial relaxation process in the PDMS/PIB blends they investigated. Reasons for those discrepancies could be of different types. In most blends, the material responses did not cover the form relaxation region or the form relaxation processes were too slow to be within the experimental frequency or time range [53].

Basically, there are three distinct strategies to compatibilize the immiscible polymers; (i) a non-reactive compatibilization by adding a non–reactive block or graft copolymer that is miscible with both phases or a copolymer with one of its parts miscible with one of the blend's components and the second part miscible with the second blend component, (ii) a specific compatibilization by attaching groups with non-bonding specific interactions to the polymer chains and finally, (iii) a reactive compatibilization by introducing reactive molecules capable of forming the desired block and/or graft copolymers *in-situ*, directly during blending.
The third strategy seems to be the more complex as well in our system where the multifunctionalized epoxy plays a role of compatiblizer as demonstrated by the reduction of interfacial tension by DDRM. PLA/PBAT/Joncryl systems are complex and this paragraph deals with the discussion of the validity of the rheological methods. As reported in the literature, the Palierne model can be used if one simply ignores interfacial viscoelasticity. The rationale is that, since there is only one shoulder in G', there is no compelling reason to include interfacial viscoelasticity in the analysis. It can be used still ignoring interfacial viscoelasticity, but including a variable volume fraction of the dispersed phase as an additional fitting parameter. Moreover, there are some drops with relaxation times that are very far from the mean and they do not contribute to the shoulder in G'. In the recent work of Taheri et al [54], the interfacial tension of the compatibilized SAN/ EPDM blend was determined from the morphological studies and the relaxation time using the simple models of simple Palierne model compared to Choi-Schowalter one. The results of interfacial tension were consistent with the results obtained from the rheological and morphological studies with 20% of SAN-g-EPDM compatibilizer. The caluclated values were in good agreement eventough they observed three relaxations characteristics times according respectively to the matrix, the dispersed phase and the SAN, EPDM copolymer.

Based on the previous disccussion, it is seen that the use of Palierne model gives better prediction on the blank blend than the compatibilized one (figure IV-18).

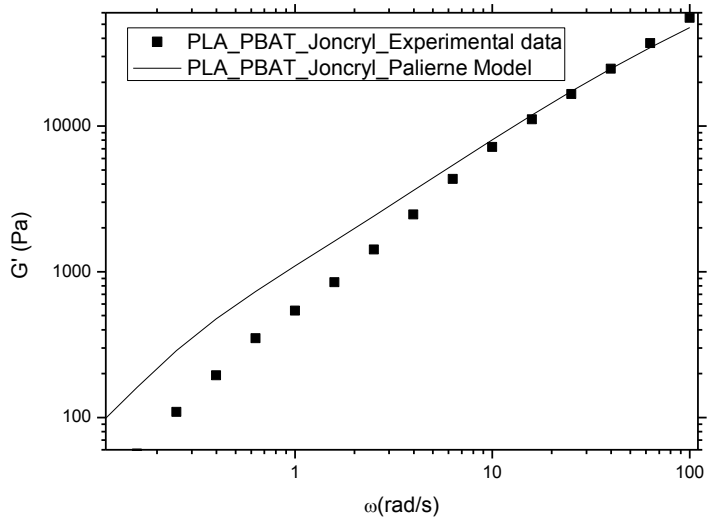

Figure IV-18 Example of experimental data and comparisons with predictions from the Palierne Model for the PLA/PBAT/Joncryl blend (80/20/0.5)

To sum up, for uncompatiblized PLA/PBAT blends, this model relates the complex moduli of blends to those of the components, the volume fraction of the dispersed phase, and the parameter α/R. Thus the mean relaxation time of the blend can be obtained by fitting the Palierne Model to the complex moduli of the blend using the quantity α/R as a fitting parameter. However, for compatibilized blends, the 'complete' Palierne model predicts more complex behavior due to the interfacial viscoelasticity caused by the presence of the compatibilizer. In the case of modified PLA/PBAT with joncryl, we remind that both of PLA chains in the matrix and PBAT chains in the dispersed phase are modified during reactive extrusion with the formation of extended and the branched chains allowing also to explain the longer obtained times in figure IV-3. Nevertheless, no additional extra relaxation times accorded to the PLA-joncryl-PBAT copolymer at the interface are clearly identified for modified PLA/PBAT blends.
In this manner, two frequency-independent parameters are necessary to fit the storage moduli of the blend, i.e., α/R_v and β''/ R_v. Here, β'' is the interfacial shear modulus [20], [27] [46] [48]. It will be the base of our future works but it is very important to note that the physical phenomenon is completely complex.
The multifunctionalized epoxy is not only a classical compatibilizer as demonstrated by DDRM but some coupled chain extension, branching reaction during the in-situ compatibilization have to be taken into account. Also, as prospects of this work, it will be very interesting to compare the obtained DDRM datas to other relaxation models as well the minale-Mafetone model [47].

V Conclusions

Throughout this work, we have demonstrated the complexity of the compatibilization phenomenon during *in-situ* interfacial reaction between GMA/epoxide functions and PLA, PBAT phases.
In one hand, the rheological investigations of the unmodified and modified PLA/PBAT blends have been performed. It was shown that the viscosity evolution during time presented different qualitative behaviors depending on the amount of reactive GMA/epoxide functions. Indeed, at a given oscillatory angular frequency, the complex viscosity and the elastic modulus of PLA_PBAT_Joncryl was higher than for the uncompatibilized PLA_PBAT_0.
On the other hand, to assess the effect of the compatibilization on the interfacial tension in PLA/PBAT blends, two different techniques were used. They include (i) a rheological method (RM) for the unmodified blend based on Palierne model and (ii) a dynamic approach (deformed drop retraction method) based on the balance between the interfacial and viscous forces.
To probe and quantify the role of the functionalized chains on the interfacial forces, different sandwich model systems (droplet/matrix) were studied. The latters are named as follows; Model A (neat PBAT/neat PLA), Model B (neat PBAT/modified PLA), Model C (neat PLA/modified PBAT) and Model D (modified PBAT/modified PLA).

The interfacial tension value given by the DDR method for Model A was about 7.34 mN/m, which explains the lack of compatibility between PLA and PBAT. This value decreased to 1.68 mN/m for Model B. The chain extension/branching of only PLA chains with the multi-functional epoxide resulted in an enhancement of the interfacial adhesion. Moreover, the chain extension/branching of PBAT (Model C) also led to a reduced interfacial tension value (1.43mN/m). The similarities of the interfacial tension values between Model B and Model C confirmed that even when increasing the viscous forces of either PLA or PBAT, the physical interactions between the PLA/PBAT chains increased. This reduction is mainly related to the interfacial reaction of the blend. Finally, a further reduction of the interfacial tension value (0.34 mN/m) was observed with the incorporation of Joncryl ADR® into both PLA and PBAT (Model D). The obtained data was then analyzed and discussed based on the mechanisms of coalescence and Marangoni's theory for compatibilized blends. For uncompatibilized PLA/PBAT blends, the obtained values of interfacial tension given by the Palierne model corroborated those obtained from the deformed drop retraction method. Such a reduction would facilitate the break-up of the dispersed phase into much finer droplets, thus improving the final properties of the blends. The failure of the rheological methods using palierne model was also discussed in the case of PLA/PBAT/multifunationalized epoxy. Meanwhile, the decrease of the interfacial tension values with the addition of multi-functional epoxide highlighted the larger degree of compatibilization which it is confirmed in turn by TEM and SEM observations. The co-existence of chain extension/branching of PLA and PBAT blends coupled to the PLA-Joncryl-PBAT creation during the in-situ compatibilization have to be taken into-account in this complex system.

References

[1] Huneault MA, Hongbo L. Morphology and properties of compatibilized polylactide/thermoplastic starch blends. Polymer 48(1): 270-280. 2007.
[2] Sarazin P, Li G, Orts W.J, Davis B.D. Binary and ternary blends blends of polylactide, polycaprolactone and thermoplastic starch. Polymer. 49(2):599-609. 2007.
[3] Kumar M, Mohanty S, Nayak SK, Parvaiz MR. Effect of glycidyl methacrylate (GMA) on the thermal, mechanical and morphological property of biodegradable PLA/PBAT blend and its nanocomposites. Bioresources Technology. 101(21): 8406-8415. 2010.
[4] Correlo VM, Boesel LF, Bhattacharya M, Mano JF, Neves NM, Reis RL. Properties of melt processed chitosan and aliphatic polyester blends. Material Science and Engineering: A 403(1-2):57-68. 2005.
[5] Coltelli M-B, Toncelli C, Ciardelli F, Bronco S. Compatible blends of biorelated polyesters through catalytic transesterification in the melt. Polymer Degradation and Stability. 96 (5): 982–990. 2011.
[6] Lee S, Lee Y, Lee JW. Effect of Ultrasound on the Properties of Biodegradable Polymer Blends of Poly(lactic acid) with Poly(butylene adipate-co-terephthalate). Macromolecular research. 15 (1): 44-50. 2007.
[7] Frenz V, Scherzer D, Villalobos M, Awojulu AA, Edison M, van der Meer R. Society of Plastics Engineers Annual Technical Conference. 2008
[8] Phetwarotai W, Aht-Ong D. Reactive Compatibilization of Polylactide, Thermoplastic Starch and Poly(butylene adipate-co-terephthalate) Biodegradable Ternary Blend Films. Materials Science Forum 695: 178-181. 2011.
[9] Levitt L, Macosko CWJ. Extensional rheometry of polymer multilayer: A sensitive probe of interfaces, Journal of Rheology. 41 (3): 671-685. 1997.
[10] Xing P, Bousmina M, Rodrigue D. Critical Experimental Comparison between Five Techniques for the Determination of Interfacial Tension in Polymer Blends: Model System of Polystyrene/Polyamide-6. Macromolecules. 33(21): 8020-8034. 2000.
[11] Yang HS, Nam JG, Kim HS, Lee JW. Interrelationship between Interfacial Tension and Rheological Properties of LDPE/PS Blends. Journal of the Society of Rheology, Japan. 30(4): 187-193. 2002.
[12] Jafari SH, Yavari A, Asadinezhad A, Khonakdar HA, Bohme F. Correlation of morphology and rheological response of interfacially modified PTT/m-LLDPE blends with varying extent of modification. Polymer 46(14): 5082–5093. 2005.
[13] Sung YT, Han MS, Hyun JC, Kim WN, Lee HS. Rheological properties and interfacial tension of polypropylene-poly(styrene-co-acrylonitrile) blend containing compatibilizer. Polymer. 44(5):1681–1687. 2003.
[14] Vananroye A, Van Puyvelde P, Moldanaers P. Deformation and orientation of single droplets during shear flow: combined effects of confinement and compatibilization. Rheologica Acta. 50(3): 231-242. 2011.
[15] Al-Itry R, Lamnawar K, Maazouz A. Improvement of thermal stability, rheological and mechanical properties of PLA, PBAT and their blends by reactive extrusion with functionalized epoxy. Polymer Degradation and Stability. 97(10): 1898–1914. 2012.
[16] Lamnawar K, Maazouz A. Rheology and morphology of multilayer reactive polymers: effect of interfacial area in interdiffusion/reaction phenomena. Rheologica Acta. 47(4):383-397. 2008.
[17] Corre YM, Duchet J, Maazouz A, Reignier J. Melt strengthening of poly (lactic acid) through reactive extrusion with epoxy-functionalized chains. Rheologica Acta. 50 (7-8): 612-629. 2011.
[18] Dealy MJ, Larson RG. Structure and Rheology of molten polymers, from structure to flow behavior and back again, Hanser Verlag Publishers, 2006 (516 pages).
[19] Wu D, Wu L, Sun Y, Zhang M. Rheological properties and crystallization behavior of multiwalled carbon nanotube /poly(ε -caprolactone) composites. Journal of Polymer Science: Part B. Polymer physics 45: 3137-3147. 2007.

[20] Palierne J. F. Linear rheology of viscoelastic emulsions with interfacial tension. Rheologica Acta 29(3): 204–214. 1990.
[21] Seyed HT, Pierre JC, Abdellah A. Rheological properties of blends of linear and long-chain branched polypropylene. Polymer Engineering and Science. 50(1): 191–199. 2010.
[22] Hansen S. Estimation of the relaxation spectrum from dynamic experiments using Bayesian analysis and a new regularization constraint. Rheologica Acta. 47(2):169–178. 2008.
[23] Baker W, Scott C, Hu G-H. Reactive polymer blending, Hanser Publishers: Progress in polymer processing. 2001.
[24] Bousmina M. Effect of interfacial tension on linear viscoelastic behavior of immiscible polymer blends. Rheologica Acta. 38(3): 251-254. 1999.
[25] Dean S, Guo-Hua H, Zhuo K, Li RKY, Jinghua Y. Relaxation behavior of polymer blends with complex morphologies : Palieme emulsion model for uncompatibilized and compatibilized PP/PA6 blends. Polymer. 47 (13): 4659–4666. 2006.
[26] Velankar S, Zhou H, Jeon HK, Macosko WC. CFD evaluation of drop retraction methods for the measurement of interfacial tension of surfactant-laden drops. Journal of Colloid and Interface Science. 272(1):172–185. 2004.
[27] Velankar S, Van Puyvelde P, Mewis J, Moldenaers P. Steady-shear rheological properties of model compatibilized blends. Journal of Rheoloy. 48(4):725–44. 2004.
[28] Grace HP. Dispersion phenomena in high viscosity immiscible fluid systems and application of static mixers as dispersion devices in such systems. Chemical Engineering Commununications. 14(3-6): 225–77. 1982.
[29] Abbassi-Sourki F, Huneault M, Bousmina M. Effect of compatibilization on the deformation and breakup of drops in step-wise increasing shear flow. Polymer. 50(2): 645–653. 2009.
[30] Filippone G, Netti P.A, Acierno D. Microstructural evolutions of LDPE/PA6 blends by rheological and rheo-optical analyses: Influence of flow and compatibilizer on break-up and coalescence processes. Polymer. 48(2): 564-573. 2007.
[31] Stone HA. Dynamics of drop deformation and breakup in viscous fluids. Annual Reviews, Fluid Mechanics. 26(1):65–102. 1994.
[32] Son Y, Yoon JT. Comparative Measurement of Interfacial Tension by Transient Dynamic Methods. Polymer. 42(16):7209-7213. 2001.
[33] Okamoto K, Takahashi M, Yamane H, Kashihara H, Watanabe H, Masuda T. Shape recovery of a dispersed droplet phase and stress relaxation after application of step shear strains in a polystyrene/polycarbonate blend melt. Journal of Rheology. 43(4): 951–966. 1999.
[34] Janssen JMH, Meijer HEH. Droplet breakup mechanisms: Stepwise equilibrium versus transient dispersion. Journal of Rheology. 37(4): 597-608. 1993.
[35] Van Puyvelde P, Velankar S, Moldenaers P. Rheology and morphology of compatibilized polymer blends. Current Opinion in Colloid and Interface Science. 6(5-6):457–463. 2001.
[36] Hu YT, Pin DJ, Leal LG. Drop deformation, breakup, and coalescence with compatibilizer. Physics of Fluids 12(3):484–489. 2000.
[37] Velankar S, Van Puyvelde P, Mewis J, Moldenaers P. Effect of compatibilization on the breakup of polymeric drops in shear flow. Journal of Rheology. 45(4):1007–1019. 2001.
[38] Van Puyvelde P, Velankar S, Mewis J, Moldenaers P. Effect of Marangoni stresses on the deformation and coalescence in compatibilized immiscible polymer blends, Polymer Engineering and Science. 42(10):1956–64. 2002.
[39] Cristini V, Blawzdziewicz J, Loewenberg M. Near-contact motion of surfactant-covered spherical drops. Journal of Fluid Mechanicas. 366:259-287. 1998.
[40] Blawzdziewicz J, Cristini V, Loewenberg M. Near-Contact Motion of Surfactant-Covered Spherical Drops: Ionic Surfactant. Journal of Colloid and Interface Science. 211(2): 355-366. 1999.
[41] Sundararaj U, Macosko CW. Drop Breakup and Coalescence in Polymer Blends: The Effects of Concentration and Compatibilization. Macromolecules. 28(8): 2647-2657. 1995.

[42] Macosko CW, Guegan P, Khandpur A, Nakayama A, Marechal P, Inoue T. Compatibilizers for Melt Blending: Premade Block Copolymers. Macromolecules. 29(17): 5590-5596. 1996.
[43] Li X, Pozrikidis C. The effect of surfactants on drop deformation and on the rheology of dilute emulsions in Stokes flow. Journal of Fluid Mechanics. 341:165-194. 1997.
[44] Li K, Peng J, Turng L-S, Huang HX. Dynamic Rheological Behavior and Morphology of Polylactide/Poly(butylenes adipate-co-terephthalate) blends with Various Composition Ratios. Advances in Polymer Technology. 30 (2):150–157. 2011.
[45] Mo H, Zhou C, Yu W. A new method to determine interfacial tension from the retraction of ellipsoidal drops. Journal of Non-Newtonian Fluid Mechanics 91(2-3):221–232. 2009.
[46]Shi D, Hu G-H, Ke Z, Li RKY, Yin J. Relaxation behavior of polymer blends with complex morphologies: Palierne emulsion model for uncompatibilized and compatibilized PP/PA6 blends. Polymer. 47(13). 4659-4666. 2006.
[47]Cardinales R, Moldanaers P. Droplet relaxation in blends with one viscoelastic component: bulk and confined conditions. Rheologica Acta. 49(9): 941-951. 2010.
[48]Van Hemelrijick E, Van Puyvelde P. Velankar S, Macosko CW, Moldanaers P. Interfacial elasticity and coalescence suppression in compatibilized polymer blends. Journal of Rheology. 48(1): 143-158. 2004.
[49] Huo Y, Groninckx G, Moldenaers P. Rheology and morphology of polystyrene/polypropylene blends with in situ compatibilization. 46(4): 507-520. 2007
[50] Riemann RE, Cantow HJ, Friedrich C. Rheological investigation of form relaxation and interface relaxation processes in polymer blends. Polymer Bulletin. 36(5):637–43. 1996.
[51] Hu GH, Li H, Feng LF. A theoretical model for quiescent coarsening in immiscible polymer blends. AIChE Journal. 48(11):2620–2628. 2002.
[52] Jacobs U, Fahrländer M, Winterhalter J, Friedrich C. Analysis of Palierne's emulsion model in the case of viscoelastic interfacial properties. Journal of Rheology. 43(6):1495‐1509. 1999.
[53] Germain Y, Ernst B, Genelot O, Dhamani L. Rheological and morphological analysis of compatibilized polypropylene/polyamide blends. Journal of Rheology. 38(3):681. 1994.
[54] Taheri M, Morshedian J, Khonakdar H. A. Effect of compatibilizer on interfacial tension of SAN/ EPDM blend as measured via relaxation spectrums calculated from Palierne and Choi–Schowalter models. Polymer Bulletin. 66(3):363-376. 2011.

Chapter 5
Blowing Extrusion of poly (lactic acid) and its blends: Improvement of the processing stability

5

I Abstract

This work deals with the study of the blowing extrusion process of Poly (lactic acid) and its blends, which mainly present a poor shear and elongation viscosities. In order to enhance their processability, two main routes were selected: (i) the modification of its structure, rheological and thermo-mechanical properties by adding a multi-functional epoxide molecules (Joncryl ADR® - 4368) acting as a chain extension/branching agent and (ii) blending it with other ductile thermoplastic biopolymer such as the poly (butylene adipate-co-terephtalate) (PBAT). The effect of the improved rheological properties on the stability map of their blends has been also investigated. Based on the obtained results, a great enhancement of the blowing processing windows of modified PLA with Joncryl was demonstrated. The extension chain/ branching balance and the nucleating effects of the multifunctional epoxide have been analyzed. Higher Blow Up Ratio (BUR) and Take Up Ratio (TUR) values were obtained. Besides, the incorporation of PBAT into PLA matrix leads to an enlargement of the stability domain according to the improvement of their shear and elongation properties especially for the compatibilized blends. Indeed, the adding of Joncryl into PLA_PBAT matrix, the instability defects zone were reduced. Finally, the crystalline structure and the thermo-mechanical properties of blown films were characterized thanks respectively to the Differential Scanning Calorimeter (DSC) and the dynamic mechanical thermal analysis (DMTA).

Keywords: Blowing extrusion – rheological properties – processing stability-crystallization – thermomechanical properties

II Introduction

In packaging applications, the blown film extrusion represents an efficient way to make films with thin thickness and the polymer needs to possess relatively high melt strength [1][2][3].

Unfortunately, compared to polyolefins, PLA is typically a linear polymer with a rather low molecular weight distribution [4]. Consequently, it has a processing instability as it is highly vulnerable to thermal, oxidative and hydrolytic degradation [5][6][7][8]. These degenerative effects lead, during processing, to the cleavage of the polymer manifested by a loss of the molecular weight and deterioration of rheological properties when robust shear and extensional rheological properties are required in film extrusion blowing [9]. Therefore, PLA should be melt strengthened due to its weak melt strength under processing [10][11][12][13].
Moreover, its limited processability is related to its poor mechanical properties.

The route aiming, in one hand, to increase the PLA met strength through chain entanglements involves either increasing the molecular weight or degree of branching degradation [4][14][15][16]. In polyethylene case, branched material is accordingly characterized by greater shear and elongation melt properties than the linear counterparts [27]. A higher entanglement level was thus assumed to hinder the chain orientation during mechanical stretching [26].

The use of chain extenders into PLA polymer is thus required [17][14][18][19] [20][21]. One commercially available coupling agent for PLA is made-up of a copolymer of styrene, methyl methacrylate and a glycidyl methacrylate (Joncryl). Some other interesting papers have been dedicated to the reactive extrusion of PLA with DGEBA [22]. Sodergard et al. [23] has disclosed a method to stabilize PLA and enhance its melt strength by adding 0.01 to 3% by weight of an organic peroxy compound during melt processing.
Moreover, some experiments have been conducted by Mihai et al. [14] on linear and branched PLA reacted with various amounts of a multifunctional epoxide during reactive extrusions. It was obvious that the zero-shear viscosity and also the elasticity increase, the shear-thinning behavior is accentuated and relaxation time is increased.
The improvement of shear and rheological properties is shown to be related to the chemical chain-extension which consists in increasing the molecular weight by bridging the carboxyl and/or hydroxyl reactive end groups of the polyesters using poly-functional molecules. Other observations can be derived a broader relaxation time spectra. Moreover, a relevant strain hardening appeared, in extensional flows, for the branched PLA due to the presence of long chain branches [28][29][30].
The subtle changes in molecular architecture are readily detected in the processing performance of PLA and more readily visible in extensional deformations, important key for film blowing extrusion. For instance, Ghijsels and Ente [24] used the melt strength as an identifier, in blown film extrusion, to assess the bubble stability for polyolefins and polyesterswhere high melt strength is identified with good bubble stability [25].

On the other hand, blending PLA with other biopolymers such as the poly (butylene adipate-co-terephtalate) (PBAT) presents a suitable tool to improve its mechanical properties. In our previous work [6], we have demonstrated that the incorporation of Joncryl overcome the thermal and hydrolytic degradation and leads to an increase of the melt strength and elasticity of both PLA and PBAT in the molten state.

Compared to polyethylene [31][32][33][34], few papers have been dedicated to the effect of PLA modification on the stability blown effect. Moreover, no research efforts have been carried out to investigate the blowing extrusion process of neat and chain extended PLA, PBAT and their blends. Despite the interesting nature of the literature, it is no help when attempting to understand either the effect of chain extension, branching coupled to the compatibilization phenomenon, as decribed previously (as demonstrated in chapter 3 and 4), on the stability blowing extrusion.

The ultimate objective of the present work is to optimize the film blowing process for PLA and its blends. It deals also with the better understanding of chain extension, branching and compatibilization phenomenon generated by Joncryl on the stability flow during blow extrusion process for PLA and PLA/PBAT (80/20 % by weight) blends. We will try to give a clear correlation between the induced shear and elongation properties on the blown extrusion stability process.
The structural and thermo-mechanical properties of the obtained blown films will be also investigated.

III Experimental section

III.1 Materials and experimental methods

More details about the used polymers and the multi-functional epoxide are given in Table I-1, in chapter 1. Meanwhile, we remind that the Polylactic acid, PLA4032D was purchased from Natureworks and the Poly (butylene-adipate-co-terephtalate), PBAT, wassupplied by BASF. Commercial available multifunctional epoxide, Joncryl ADR®-4368 is used to prepare both modified PLA, PBAT and their compatibilized blends.

Table V-1 summarizes the composition and the notations of the main prepared blends in the present study.

Table V-1 The composition and the notations of the main blends

Notations	Composition
PLA_0	100 % wt PLA
PLA_0,5	PLA+0.5 % wt Joncryl
PLA_0,7	PLA+0.7 % wt Joncryl
PLA80_PBAT20	80 % wt PLA+20 % wt PBAT
PLA80_PBAT20_0,7	79.44 % wt PLA+19.86 % wt PBAT+0.7 wt% Joncryl

III.1.1 Blow extrusion process

A PRISM TTW co-rotating twin-screw extruder with a screw diameter of 16mm (Thermo Electron Polylab System Rhecord RC400P) was used in this study [6]. More details about the twin-screw extruder profile are given in chapter I. Before compounding, both PLA and PBAT pellets were dried to remove moisture under vacuum at 80°C for 12 hours. Then, the extrusion was carried out, under nitrogen, at a screw speed of 40 rpm, during 3 minutes. The profile temperature was about 140-190-190-190-180- 180 °C. The optimal reaction time was evaluated based on the monitoring of the experimental in-situ stabilization of the torque versus time;
In our previous works, we have also plotted the evolution of the relative storage modulus ($\eta^*(t)/\eta^*(t=0)$ vs time) of modified polymers at 180°C and the rheo-kinetic properties as the end reaction time are determined.
For the sake of clarity, only the results of the modified PLA and PBAT and their blends, where their viscoelastic parameters (complex viscosity and storage modulus) remain unchanged during time. The reaction stabilization times for all the used PLA were studied elsewhere in the paper of Al-Itry et al [6] and we have showed that for modified PLA with less than 0.7% of multi-functionalized epoxy, 3 min are quite sufficient at 190°C as melt temperatures in the twin-screw

extruder to obtain a total conversion. However, with higher Joncryl amount, wa have showed that the reaction need more longer time in the extruder (higher than 10min) to be stabilized according to the competition between the former phenomenon and the chain/branching reaction especially.
Therfore, prior to their blowing extrusion and biaxial stretching experiments, the compounds with 0.7 % of Joncryl were regranulated and passed once again through the twin screw extruder (at lower speed rate under nitrogen) until obtaining a stable torque and reproductible viscoelastic properties.
A schematic diagram of tubular film blowing extrusion is shown in figure V-1. A thin film is produced by means of the extrusion of a polymer through an annular die:
Concerning the blowing extrusion set-up, the molten polymer, in the form of a tube, exiting from the die is drawn upward by a take-up device. When the process starts up, the air is introduced at the bottom of the die to inflate the tube and form a bubble. The size of the bubble is maintained at a certain internal pressure. The tube is then flattened in the nip rolls and taken up by the winder. An air ring is also used to rapidly cool the hot bubble and solidify it at some distance above the die exit. This distance is usually called Frost Line Height (FLH).

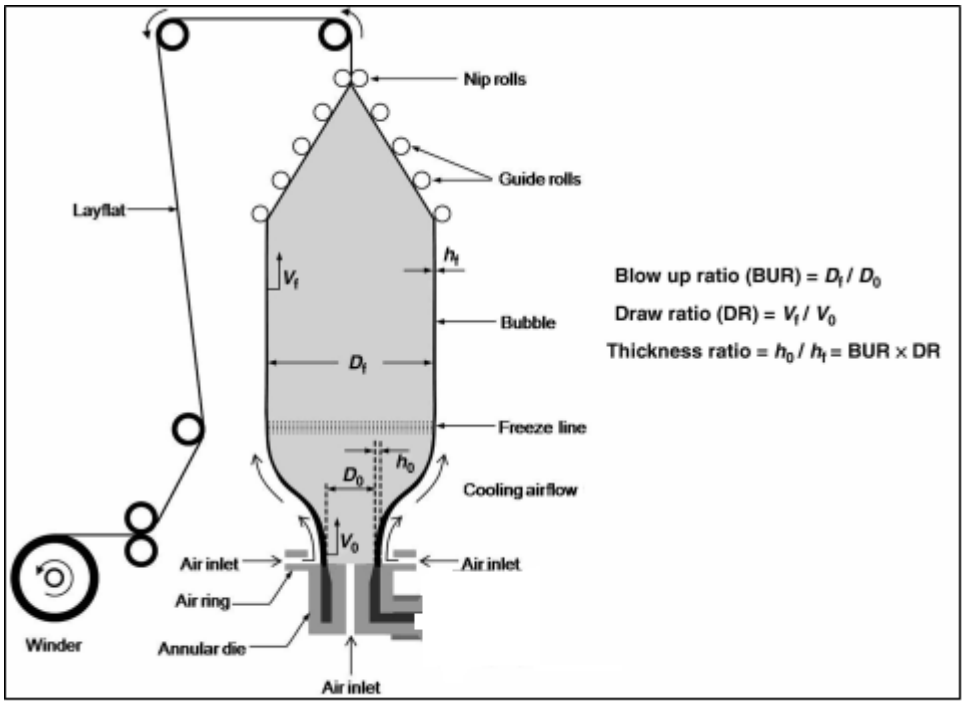

Figure V-1 Schematic diagram of the film blowing experimental set-up.

The inflated and solidified bubble is then flattened as it passes through the nip rolls. The nip rolls is driven by a variable-speed motor which provided the axial tension needed to pull the film upward. They form also an airtight seal to keep a constant pressure inside the bubble. The pressure is controlled by the air supply to the bottom of the die.
As the polymer film moves towards the nip rolls, it is drawn longitudinally by the nip rolls and stretched transversely by the internal pressure. The transition of the melt polymer to a solid film is accelerated and localized by a jet of cold air directed onto the outer surface of the film from an annular ring just above the die. The amount of air and the nip roller speed are adjustable parameters which are important from the bubble stability point of view.
During the film blowing process, the molten polymer is subjected to different stress fields that develop at various stages of the process. First, as the melt flows through the annular die, it is subjected to shearing stresses, resulting in a partial molecular orientation in the machine direction

(MD). Upon leaving the die, where the melt is suddenly free of the constrains imposed by the contact with the die wall, this orientation may be partially relaxed but further orientation of the macromolecules will occur as a result of biaxial stretching [35][36][37][38].
The film dimensions are determined by the blow-up ratio (BUR) and the take-up ratio (TUR) (Cf. figure V-1). These parameters are very important because they provide the stability of the process.

1°- Blow-up ratio (BUR) is the ratio of bubble diameter (D_f) to die diameter (D_0). It indicates the increase in the bubble diameter over the die diameter. The die gap divided by the BUR indicates the theoretical thickness of the melt after reduction by blowing.

2°- Take-up ratio (TUR) is the ratio of film velocity (V_f) to melt velocity (V_0). The melt velocity is the molten polymer flow through the die head and film velocity is done by tuning nip speed. It thus indicates the degree of stretching of the molten polymer in the main direction.

By varying the BUR, screw speed, air pressure, and winder speed, films of different thicknesses (10–150 μm) and degree of orientation can be achieved.

In blown film extrusion, the optimized shear and elongation rheological properties are important because they allow high blow-up ratios, excellent bubble stability, and enhanced optical properties at low thicknesses. As a result, the film processability depends on the molecular parameters, namely, molecular weight and its distribution, and the degree of long chain branching. What makes the matter more complicated is that, whereas the rheological behavior of a polymer is a direct response to molecular parameters, it also depends on many other factors, which including: 1) the types of flow field, 2) the intensity of the rate of deformation and 3) the deformation and thermal histories.
The main objective of this work is to gain a clear understanding of the role of (i) experimental processing parameters (ii) structural properties on the flow stability during blow extrusion. Beyond the investigation of blown properties of the blends, it is very important to study the behavior of neat and modified polyesters.

IV Results and discussions

IV.1 Linear viscoelastic and capillary flow properties of neat/modified PLA, PBAT and their blends

Linear viscoelastic properties of the two neat polymers PLA and PBAT have been firstly compared in terms of dynamic viscosity modulus versus angular frequency at 180°C as shown in figure V-2. At low frequencies (< 10rad/s), the PBAT has the highest viscosity and the PLA, the lowest. The PBAT is more shear-thinning and does not depict a pronounced Newtonian plateau in the low-angular frequency region. Meanwhile, at high angular frequencies, the viscosities of the PLA and the PBAT are close [6][39].
In our previous study [6], we remind that we have demonstrated that the rheological behavior of PLA and PBAT is highly affected by the incorporation of a multi-functional epoxide, Joncryl® ADR-4368 through chain extension and branching. This reveals firstly an enhancement of its melt strength, elastic modulus (G'), viscous modulus (G''), complex viscosity modulus (η*) and its shear-thinning behavior, depending on the shear rate and the amount of the multi-functional epoxide was reported. The longer and heavy chains are, the more they created entanglement and the higher viscosity is. A shift of the chains relaxation time for both PLA and PBAT to higher values

following the incorporation of Joncryl was also highlighted. These results corroborated with the higher average molecular weight and the broader distribution obtained from SEC measurements.

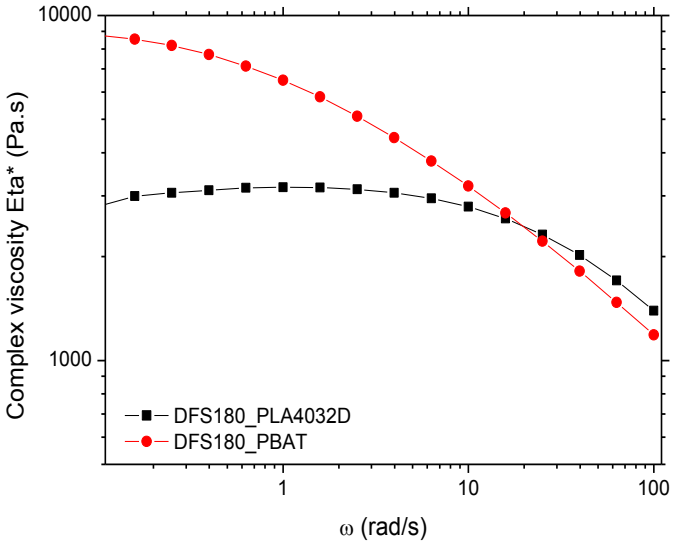

Figure V-2 Complex viscosity versus angular frequency for the neat PLA and PBAT

Moreover, according to figure V-3, the Cox-Merz rule works fairly well with neat polymers into the shear thinning region but still shows slightly deviation for the modified PLA and PBAT materials. This can be related to the heterogeneity of the prepared blends and the increase of their polydispersity [13][40]. It is important to note that the increase of the modified PLA's viscosity is more pronounced compared to the modified PBAT's viscosity.

To sum up, the occurred structural modification (High chain lengths, branching, high Mω…) highlights the enhancement of the elastic properties and the melt strength resistance under shear. By this way, the elongation properties during processing can be affected.

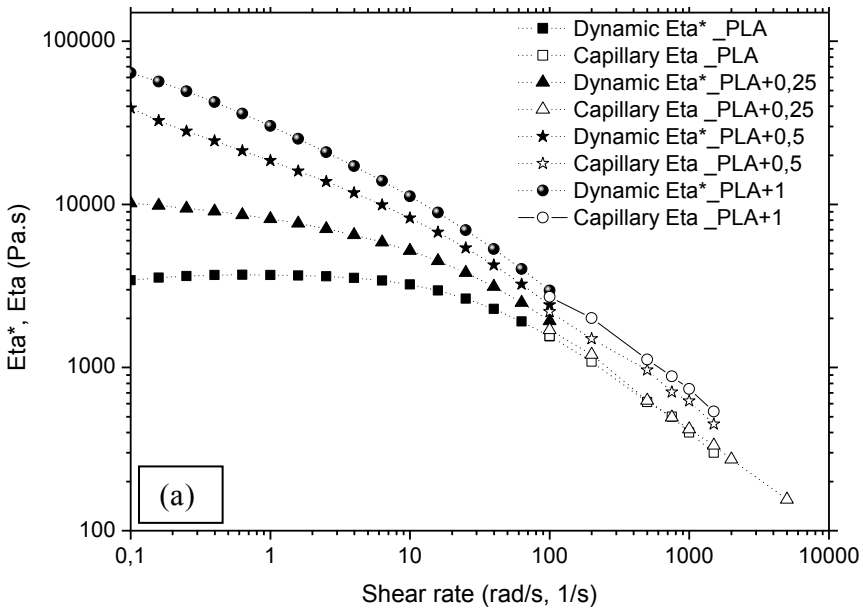

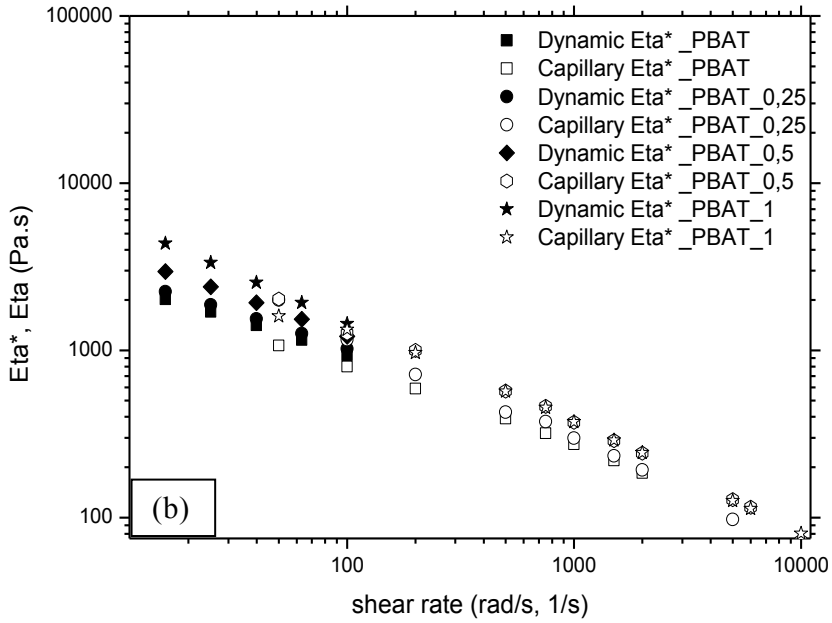

Figure V-3 Cox-Merz Validity: Dynamic viscosity modulus and shear viscosity vs angular frequency, shear rate respectively for (a) neat and modified PLA and (b) neat and modified PBAT performed at 180°C

(Full symbol: Dynamic rheology/ Open symbol: capillary rheology)

It is well known that the melt elastic behavior of polymer under shear is linked to the elastic behavior during processing by indirect Cogswell method [41][42]. It is a simple rheological technique based on the entrance pressure drop method and based on the relationship between the elongation viscosity and the pressure at the die during capillary experiments which is governed by the melt elasticity.

The method is used to quantify the elastic properties and the elongation viscosity, which is difficult to measure, especially at high strain rate as in blowing extrusion process. However, because of the numerous assumptions of the theory and of some surprising results in the literature, the method has been widely discussed and some contradictions still remain.

Figure V-4 depicts an example of the evolution of the elongation viscosity "η_E" after Bagley Correction, for the modified PLA with three different amounts of Joncryl (up to 1% by weight) at a fixed elongation rate ($30s^{-1}$). It can be noticed that the elongation viscosity is increasing with the amount of Joncryl®. The enhancement of melt strengthening of modified PLA was confirmed by the drastic increase of the elongation viscosity. In the Corre et al's study [13], the elongation viscosity evolution versusu time shows that compared to linear PLA, a strain-hardening, characteristic of chain extended/branched polymer, was observed.

The linear PLA, where the polymer chains are free from any branch points, maintains a linear response over time. The chains are not prevented from slipping over each other. In chain-branched polymers, the slipping of the chain is perturbed by the presence of branches, which are entangled with the main chains therefore causing strain hardening. Therefore, the stretching force or stress reaches a pseudo-steady-state and then rises again due to the resistance caused by the branches intermingled with the main chains of the polymer. A critical strain for the onset strain hardening is shifted to a lower value when the amount of the chain extender increased. The aforementioned increase in relaxation time response could explain this earlier strain hardening, as observed for bimodal LDPE [30].

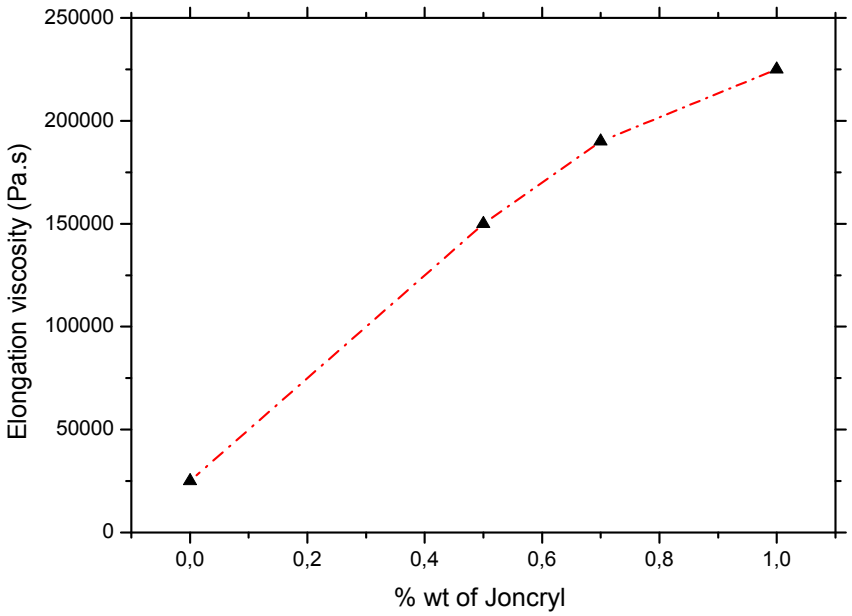

Figure V-4 Example of the evolution of the elongation viscosity versus the Joncryl® amount of the modified PLA

For the clarity purpose of this paper, and in order to compare the rheological properties of all the studied materials in the real experimental conditions at higher shear and strain deformation presented in the extrusion process, the elongation viscosity calculated by cogswell method will be only presented.

While the incorporation of the multifunctionalized epoxy affects the rheological properties of neat PLA and PBAT polymers, it is believed their blends rheological properties can be also affected.

The study of the rheological properties of modified and unmodified PLA/PBAT blends was detailed in our previous paper [6]. We have demonstrated the impact of the multifunctional epoxide on the enhancement the interfacial adhesion between these two neat polymers. The best blend's properties were achieved for an optimum amount of Joncryl between 0,5 and 0,7%wt.

As the modified PLA, the cox-Merz rule is invalid in this case. The polydispersity and heterogeneity caused by the chain extension/branching/compatibilisation agent explain this deviation from the rule (cf. figure V-5a). It can be also pointed out, from figure V-5b for example, an increased slope indicating that the elongation viscosity is increasing with the amount of Joncryl according the reaction between PLA, PBAT chains and the multifunctional epoxide.

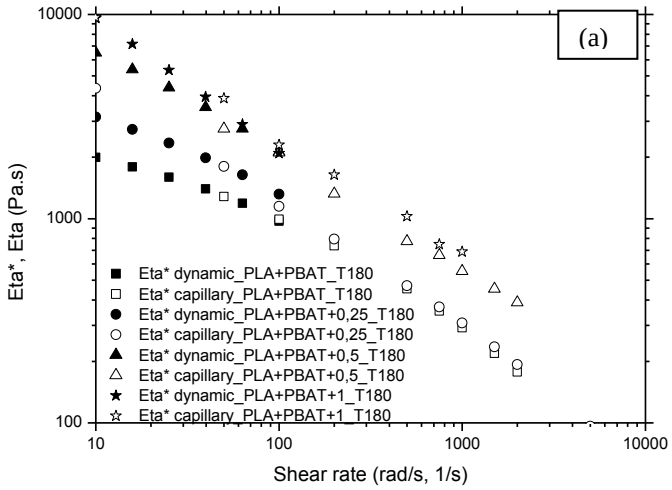

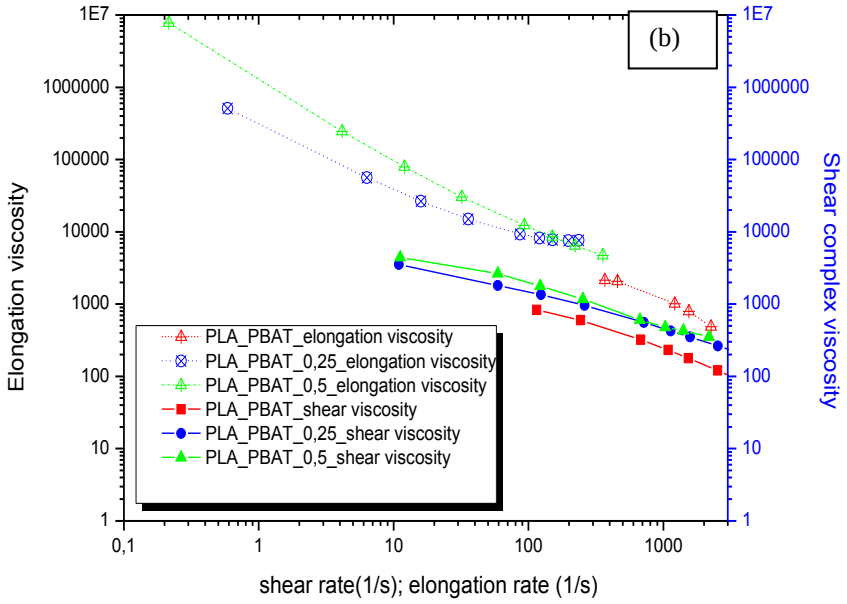

Figure V-5 (a) Cox-Merz Validity: Dynamic viscosity modulus and shear viscosity vs angular frequency, shear rate respectively for unmodified and modified PLA_PBAT blends, performed at 180°C (Full symbol: Dynamic rheology/ Open symbol: capillary rheology) (b) Elongation viscosity versus elongation rate for unmodified and modified PLA_PBAT blends

IV.2 Stability processing investigation of neat/modified polymers and their blends

Depending on the processing parameters and the rheological properties of materials, different instabilities can appeared. Thus, the instability in blown film was firstly reported by Han and coworkers [43][44]. They observed that lowering the extrusion temperature stabilized the blown bubble for high density polyethylene (PEHD) and low density polyethylene (PELD). Moreover, some other authors have more extensively discussed the instabilities during blown film processing [45][46][47][48][49]. Three main instabilities were observed during processing. They are (i) the axisymmetric periodic variation of the bubble diameter, (ii) the helical motions of the bubble and (iii) the variation in the position of the solidification line. We call the first two forms of these instabilities, after previous authors [43][44][45][50], bubble instability and helical instability, respectively.

Furthermore, the study of the stability of the process of PLA was conducted by establishing maps of stability. Thereby, the two main parameters (BUR and TUR) of blown films were changes and bubble stability or un-stability was observed.
In our case, the BUR values have changed according to air flow inflated into the die. The TUR (s) have changed based on the variation of the chill roll velocity and the melt flow was kept constant. The process was considered as stable since no defect appeared for a given BUR-TUR pair during at least 10 minutes.

We should point out therefore that at die temperature about 180°C, less stable blown PLA films were observed. PBAT has no ability to be processed by blowing extrusion eventhough the changing of the experimental conditions.

The following figure V-6 shows the various instabilities encountered in extrusion blown film process using PLA for an example.
It is a clear demonstration of the unstable behavior of PLA during its blown extrusion processing. They include (i) draw resonance, (ii) helical instability, (iii) frost line oscillation, (iv) breathing, (v) dancing and, (vi) bubble sag.

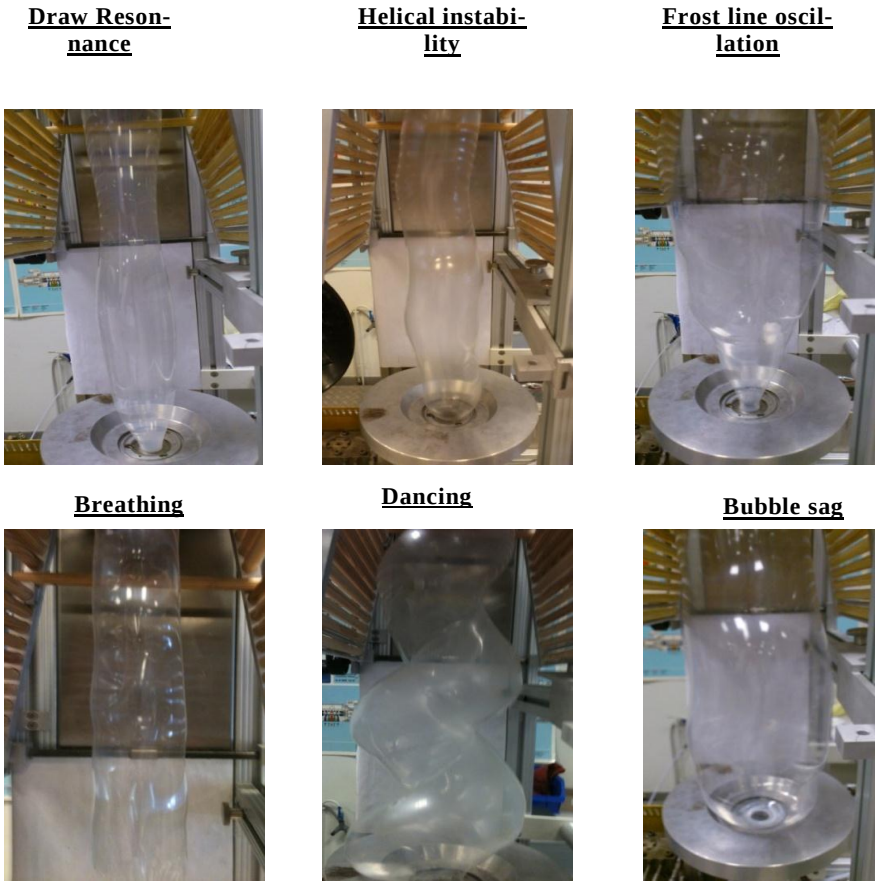

Figure V-6 Diagram of various instabilities obtained in this study for the neat used PLA

Moreover, table V-2 summarizes the description of each obtained defects and their main processing origins in our experiments

Table V-2 Descriptions, mains origins of the apparent instabilities during the materials processing

Bubble instability	Description	Main origins
Draw resonance or '"periodic diameter oscillation"	Regular and periodic variations in the film thickness	1- Pressure fluctuatations inside the bubble 2- High TUR
Helical instability or "snacking"	Helical motion developed between the die and the nip rolls at high BUR	1- Air rotation inside the air ring 2- Freeze line to low
Frost line oscillation	Periodic oscillations of the freeze line height	1-flow of surrounding air, or relatively slow changes in ambient temperature 2- High internal pressure in the bubble 3- Changes of the bubble temperature.

Based on these observations mentioned above, the stability-unstability maps were plotted in figure V-7. It is worth notice that the PLA show a limited blowing ability. No stable blown film can be obtained at higher BUR-TUR values. PBAT has no ability to be blown and no stable point is observed.

Our challenge is thus to make this process stable at 180°C in order to obtain stable films at higher BUR-TUR couples. As a result, blending PLA with ductile PBAT or with a multifunctional epoxide is a suitable tool to achieve these objectives.

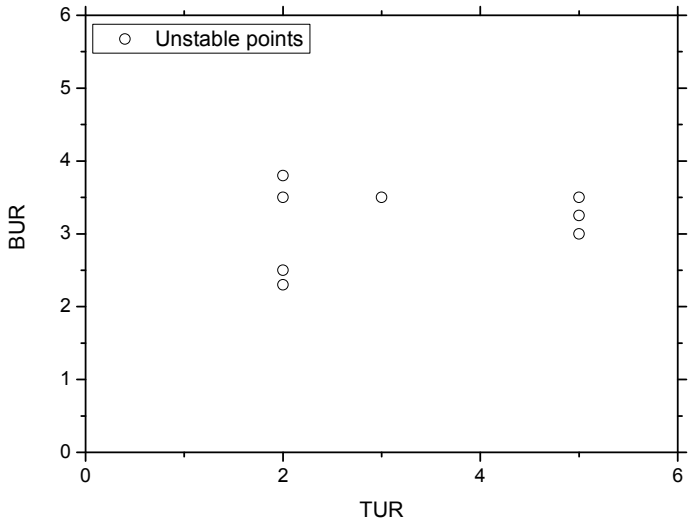

Figure V-7 Stability maps of neat PLA with die temperature about 180°C where "o" are the unstable points

The improvement of the shear and elongation rheological properties of PLA by the incorporation of Joncryl ensures the stability, as also confirmed in figure V-8.

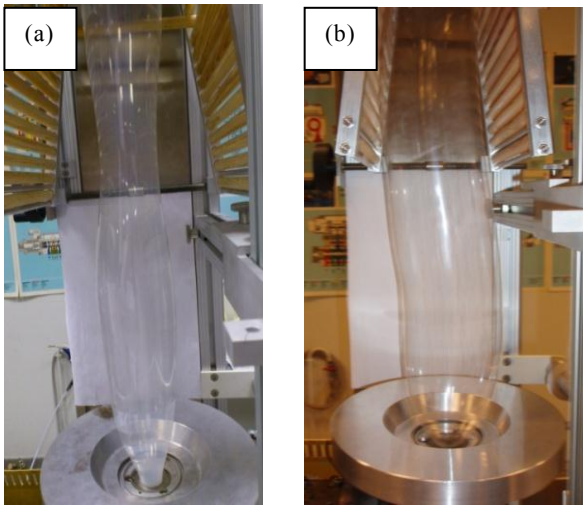

Figure V-8 Comparison of the bubble shape between a) PLA and b) PLA_0,7 during blowing extrusion at 180°C

The stability map, reported in figure V-9, showed that the Blow Up Ratio (BUR) values rose from 2.5 to 7 and the occurred instabilities are less chaotic compared to pure PLA. Some authors reported, in the case of PE, that the long chain branched polymer is suitable in the blown film process due its better melt strength for bubble stability and is responsible for the significant increase of the BUR at high TUR values [9][32][46][52][53].

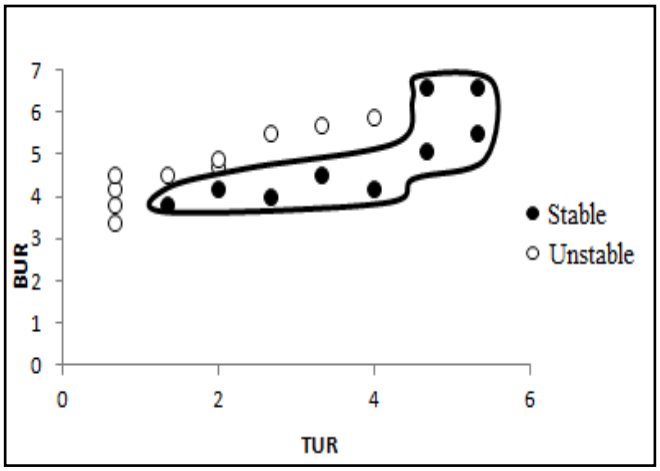

Figure V-9 Stability maps of modified PLA with 0.7%wt of Joncryl at die temperature of 180°C

Figure V-10 summarizes the obtained stability maps in which we compare the blowing extrusion properties of uncompatibilized and compatbilized blends with 0,7%wt of Joncryl.

For PLA/PBAT (80/20) (w/w) blends, three types of defects have been detected which are breathing, draw resonance and dancing. But, breathing instability remains the majority. We remind that breathing instability occurred when fluctuations in bubble width and machine direction film thickness were observed. The breathing cycles can be shorter or longer, which depends on the amount of variation or speed of the cycle [54][55]. It is important to note that the PLA/PBAT blends present a more stable region compared to the neat PLA and PBAT polymers.

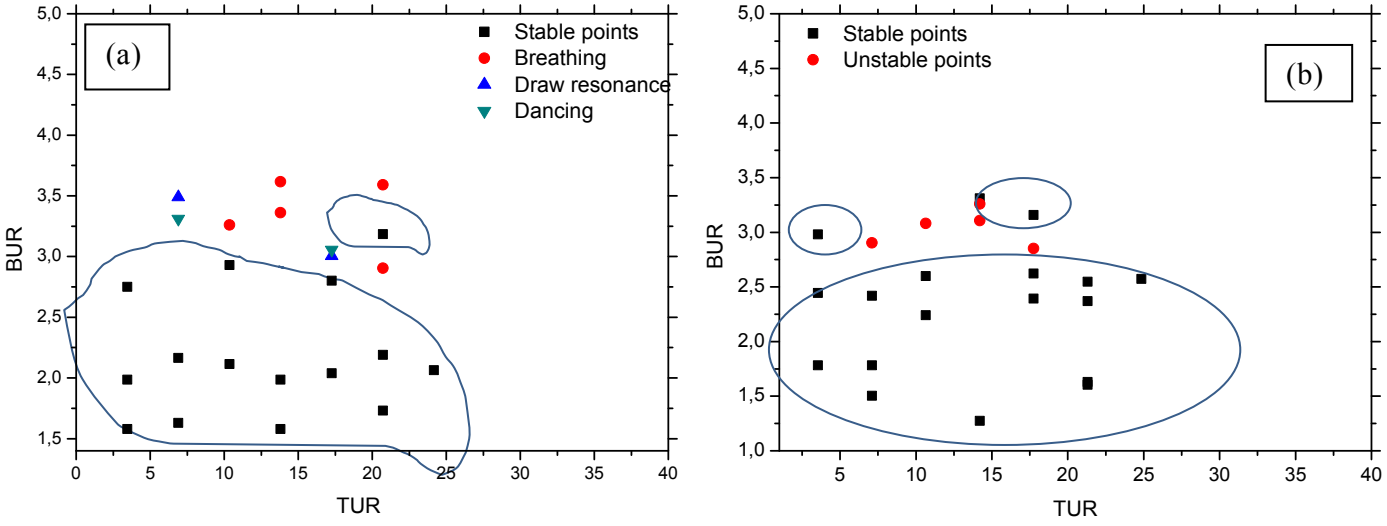

Figure V-10 Stability maps of (a) unmodified PLA-PBAT blends and (b) modified PLA-PBAT blends with 0,7%wt of Joncryl (die temperature is 180°C)

Moreover, the incorporation of PBAT into PLA matrix leads to an enlargement of the stability domain, as seen in Figures V-11 and V-10a). The elasticity of this blend allows a development of larger size bubbles (BUR rises to 3,5, instead 2).

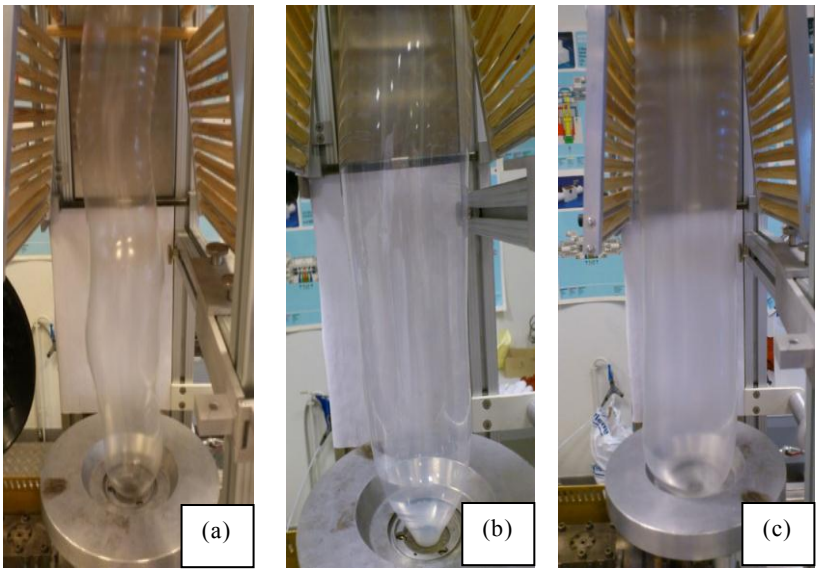

Figure V-11 Comparison of the bubble shape between a) PLA, b) PLA_PBAT and c) PLA_PBAT_0,7

Furthermore, with the incorporation of Joncryl ADR® into PLA_PBAT matrix, the breathing instability zone is reduced (Cf.figure V-10b)) and the draw resonance instability is eliminated. We can conclude that Joncryl helps process stabilization at lower and higher TUR which ensure an achievement of high BUR values. This is the main difference with the uncompatibilized systems. Moreover, a new zone of stable bubble can be obtained with higher TUR values and BUR reaching 3,5.

This phenomenon can be explained by the impact of the chain extension/branching agent on the extensional properties of the blends. The compatibilization effects of the Joncryl play a real role to eliminate dancing and draw resonance defects which are accorded to the lower elasticity.
The influence of the phase structure on these properties for compatibilized PLA blends has not been addressed in the literature but some results, for instance, for polyolefin, suggested that miscible polypropylene blends exhibit strain hardening. Similar enhancements in strain hardening have been reported before for PE blends [24][57], as well as linear/branched PP blends [53][56]. Assuming that a strain-hardening can occurred for compatibilized PLA/PBAT blends, we can link the improved stabilized zone to the presence of branched chains.

IV.3 Solid- state viscoelastic and crystalline properties of the blown films

IV.3.1 Crystalline properties of the blown films

Figure V-12 depicted the DSC thermograms of PLA pellets and blown films; upon the second heating. It is worthy concluded that the film blowing extrusion altered hardly the crystalline properties of PLA due to the alignment of polymer chains. Therefore, an exothermic cold crystallization peak "T_{cc}" about 110°-120°C was observed, contrarily to the PLA pellets.

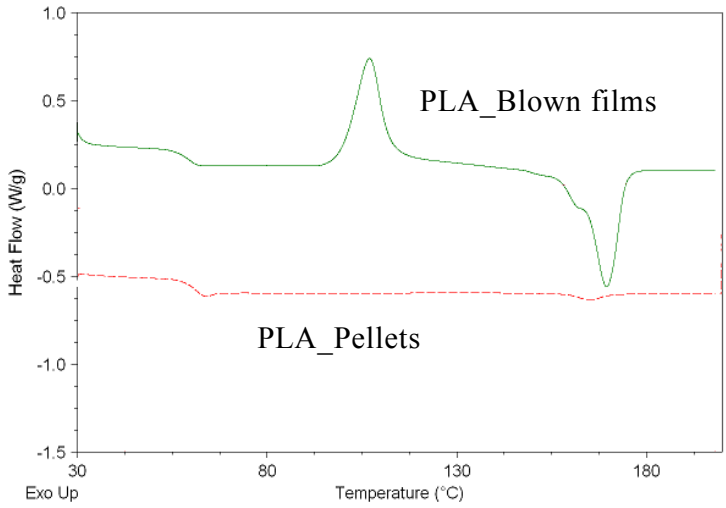

Figure V-12 DSC thermograms of PLA (pellets (X_c=1.7%) and blown film (X_c=6.4%))

Moreover, table V-3 lists a comparison of thermal parameters between neat and modified PLA blown upon extrusion. In particular, the multi-functional chain extender causes a significant depression of the crystallization temperature, T_{cc}. Compared to PLA, the low degree of branching of the chain extended PLA can promote the crystallization by increasing the chain mobility (due to the less efficient packing) while not hindering the formation of smaller crystallites [54][55]. We should point out that the glass transition temperature, occurring within the 60-65°C range, is nearly unaffected by the structural changes induced upon reaction with the chain extender.

Table V-3 Thermal parameters and crystallinity values for PLA and modified PLA with 0.7 %wt of Joncryl after blowing compared in the same BUR and TUR experimental conditions

Films	T_{cc} (°C)	ΔH_{cc} (J/g)	T_m (°C)	ΔH_m (J/g)	X_c (%)
PLA	110	27	170	33	6.4
PLA_0.7	98	28	170	40	13

Furthermore, the investigation of the crystalline behavior of the uncompatibilized PLA/PBAT blown film was carried out. We were able to compare the cold crystallization temperature, melting temperature and their respective enthalpies upon the second heating. It is worth notice a cold crystallization drop with the addition of PBAT.

The thermal study of the uncompatbilized and compatibilized PLA/PBAT blown film showed a slight shift of the cold crystallization temperature to lower temperature. A reduction of the crystallinity, as reported in table V-4, level could affect the FLH. These thermal modifications could be related to the presence of branched chains which hinder the orientation of the macromolecular chains of both PLA and PBAT and therefore decrease the crystallinity level.

Table V-4 Thermal parameters and crystallinity values for blown PLA and for PLA in the blends films compared in the same BUR and TUR conditions

Films	T_{cc} (°C)	ΔH_{cc} (J/g)	T_m (°C)	ΔH_m (J/g)	X_c (%)
PLA	110	27	170	33	6.4
PLA80-PBAT20	103	11	171	29	24
PLA80-PBAT20-0,7	95	13	169	19	8

IV.3.2 Solid State viscoelastic properties of the blown films

Representative curves of DMTA recording tan δ and log E' for the blown PLA film are shown in Figure V-13. The solid-state rheological properties of PLA typically show in its glassy state, a storage modulus (E') of about $3*10^9$ Pa below the α-relaxation temperature (T_α) or transition temperature. As the sample is heated above T_α, a sharp drop in modulus occurs between 55° and 75°C and E' decreases to $5*10^6$ Pa by softening of the film. This region is accompanied by a maximum peak of tan δ of about 65°C, which corresponds to the α-relaxation of PLA. The obtained data regarding the relaxation α of PLA and modified PLA corroborate those in the literature [58][59].

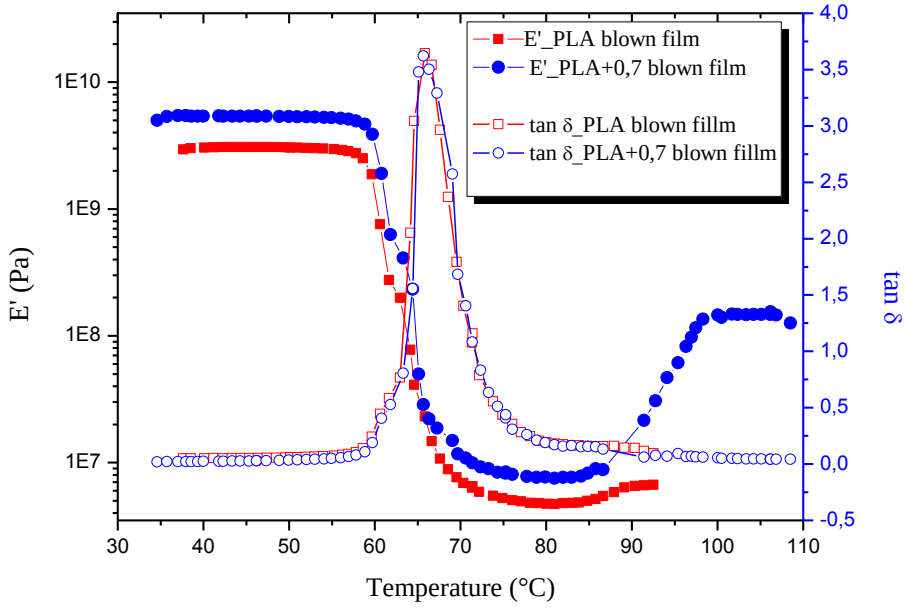

Figure V-13 Storage modulus and loss factor evolution versus temperature for PLA and PLA_0,7 blown films obtained in for the same BUR and TUR values

The β-transition of PLA, which was attributed to a very restricted degree of molecular mobility, is very small and is scarcely detectable by DMTA. The T_g determined from tan δ of DMTA relaxa-

tion spectra at a frequency of 1 Hz is in good agreement with the one determined by DSC. The storage modulus then increases at a temperature around 83-85°C. This recovery is attributed to the cold crystallization of the PLA chains, being higher with increasing the crystallinity of PLA when comparing with DSC thermograms.

From Figure V-13, we can conlude that the curve of PLA_0,7% almost has the same shape as the neat PLA below the melting temperature. An increase of the storage modulus (E') below the α-relaxation is observed. A strain-induced crystallization may had occurred upon biaxial blowing below T_α, where Joncryl acts as precursor of new nucleation sites, enhancing the growth of the crystalline phase, thus the increasing the rigidity of PLA upon drawing (which is related to the FLH value)
Moreover, the tan δ curves is nearly unaffected by the structural changes induced upon reaction with the chain extender indicating that the Joncryl ADR® did not act as a plasticizer agent.

Moreover, the thermo-mecahnical behavior of the modified and unmodified PLA/PBAT blends is presented in figure V-14. The high storage modulus observed for PLA/PBAT (80/20) compared to PLA/PBAT/Joncryl (80/20/0.7) is probably to the high obtained crystallinity upon blowing as we have shown in table V-4). In both cases, an increase of the storage modulus is also observed at around 80°C, highlighting the cold crystallization behavior of PLA. Such evolution indicates that the prepared blown films are semi-crystalline, as also confirmed by DSC data. The development of crystalline structure in compatibilized PLA/PBAT blends is effectively hindered. This can be related to the higher branching density, as demonstrated for PET [54], despite they exhibit a slightly increase of the cold crystallization compared to the uncompatibilized one.

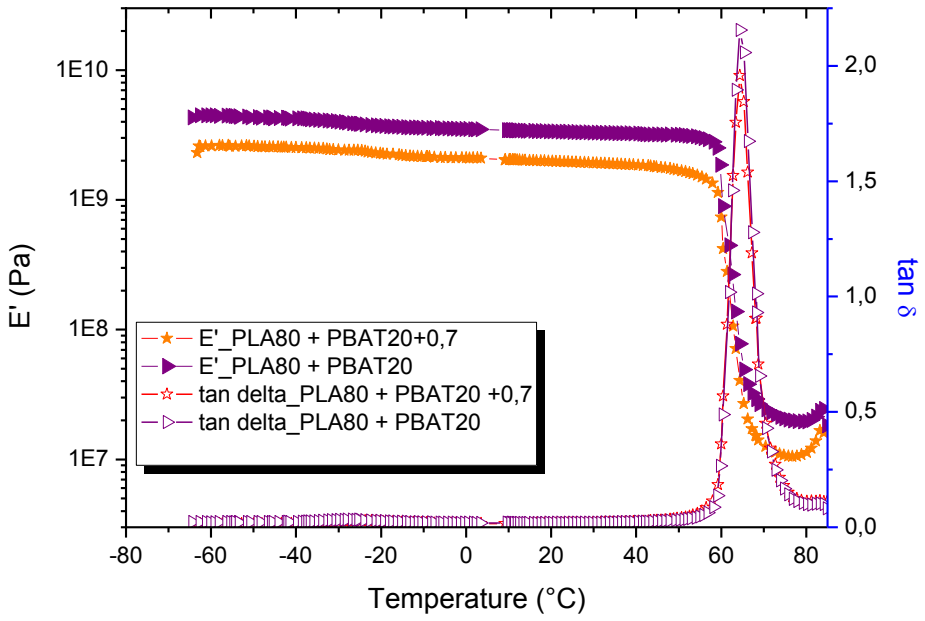

Figure V-14 Storage modulus and loss factor evolution versus temperature for PLA/PBAT blown filmsin the same conditions

The glass transition temperature (T_g) of PLA/PBAT blends is observed at about the same temperature (65°C) where the main relaxation (α) of PLA is located. At low temperature relaxation (-27°C) and for low contents of PBAT (~20% by weight), the PBAT α-relaxation is not clearly visible. Moreover, the chain extender/branching/compatibilizer molecules did not affect the tan δ of

PLA/PBAT blends. Moreover, the loss factor peak of blends (tan δ=2.2) showed a decreased magnitude of tan δ in comparison to virgin PLA (tan δ=3.7). This behavior is mainly due to the rubbery phase of PBAT which is well dispersed in PLA matrix.

V Conclusions

Through this work, we have shown that PLA and the PBAT are not able to blowing extrusion. The improvement of both processing stability and microstructural properties of the blown materials based on the PLA was investigated by using two different routes. The obtained results were analyzed and discussed based on the shear and elongation properties ofneach modified material.
We have demonstrated that the incorporation of 0.5% and 0.7% by weight of Joncryl lead to an enhancement of the blowing processing windows of PLA. Higher BUR and TUR values were obtained. This enhancement is probably due to the chain extension/branching phenomenon accompanied with the nucleating effect of this multifunctional epoxide.
Besides, blending PLA with other ductile thermoplastic polymer, which is the poly (butylene adipate-co-terephtalate) (PBAT) induces an enlargement of the stability domain. However, with the addition of 0.7%wt of Joncryl into PLA_PBAT matrix, the instability zone was reduced. Various defects are removed.
The draw resonance and the dancing defects are totally eliminated for compatibilized blends based on PLA, PBAT and the multifunctionalized epoxy. Higher values of BUR have been reached at higher TUR and a new zone of stability is obtained. Moreover, it was demonstrated that the blowing extrusion process lead to obtain semi-crystalline films. The T_α relaxation is not affected and the loss factor peak value decreased due to the ductility of PBATand the elastic behavior according to the chain extension and branching reactions.

Appendix

I- Bagley Correction:

During the flow of polymer in the capillary rheometer, it passes from a reservoir having a large-diameter to a die with a smaller diameter. This transition is abrupt and entry effects occurred: the flow lines are oriented as if the die was extended. This phenomenon is important with higher velocity gradient.

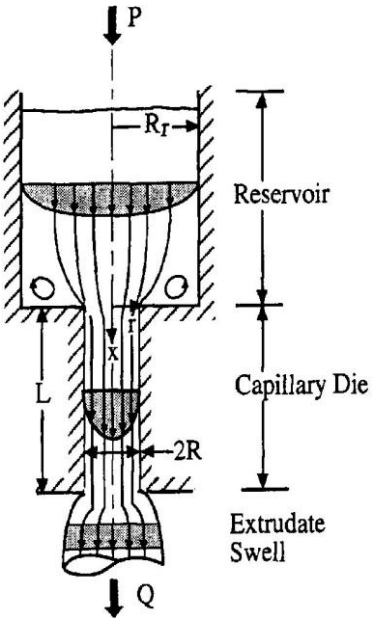

Bagley proposed a method of determination of the pressure drop at the entrance of the die (PE). Conventionally the entrance pressure drop is evaluated experimentally from the measurement data of at least two, preferably three, capillaries of same diameter but different length. This is accomplished by plotting the pressure drop (P0) at constant shear rate versus capillary L/D and fitting a linear fit on the data. The linear Bagley plot is then extrapolated to zero and the point at which the line intersects with y axis is the "e", length values added to the real dimension of the capillary in order to calculate the true pressure drop. It is also possible to calculate the true shear as:

$$\tau = \frac{(P_0 - P_E)R_C}{2L_C} = \frac{P_0}{2(\frac{L_C}{R_C} + e)} \qquad \text{(Eq.i)}$$

Where, the L/R represents the capillary length to radius ratio. However, sometimes the points do not fall in the linear fit but tend to curve either upwards or downwards. If the Bagley plot shows a curvature upwards it is probably due to pressure effects.

I- Rabinovitch Correction

A second correction is necessary in order to most closely match the actual behavior of the polymer. Indeed, the calculations above consider a Newtonian material. It is known that PLA has a shear-thinning behavior. Rabinovitch has therefore established a method to take into account this non- Newtonian behavior of polymers, by applying the following law to the apparent shear rate $\dot{\gamma}_A$:

$$\dot{\gamma}_{true} = \frac{3n+1}{4n}\dot{\gamma}_A \qquad \text{(Eq.ii)}$$

$$\dot{\gamma}_A = \frac{4Q}{\Pi R^3}; \qquad n = \frac{\partial \log \tau}{\partial \log \dot{\gamma}_A} \qquad \text{(Eq.iii)}$$

where n is determined by plotting log(τ) versus log $\dot{\gamma}$ A. This formula applies only in the case of a cylindrical flow.

II- "Cogswell" method:

The indirect method of determination of the elongation viscosity which is the most widely used, because it can deal with the largest variety of fluids, is isothermal melt spinning. Cogswell developed an analytical analysis to determine the "elongation viscosity" from the capillary rheometer data. He considered that the pressure drop at the entry of the die is due to shear and elongation contributions.
Cogswell has found a way to evaluate it with capillary rheometer. For the author, the presence of vortexes enables us to treat the flow in a similar way to what takes place in a slightly converging pipe. Assuming that the viscosity under simple shear can be described by a power-law relationship over a limited stress range and that the elongation viscosity is independent of stress, he solved these equations for an infinite set of very short tapes and obtained analytical expressions for the elongation viscosity and stress:
This approximation ensures to calculate the elongation variables as given at the foot of this paragraph.

$$\eta_e = \frac{9(n+1)^2(\Delta P_{ent})^2}{32\eta\dot{\gamma}^2};\ \dot{\gamma} = \frac{4Q}{\Pi R^3} \quad \text{(Eq.iv)}$$

$$\dot{\varepsilon} = \frac{4\eta\dot{\gamma}}{3(n+1)\Delta P_{ent}} \quad \text{(Eq.v)}$$

Where $\dot{\varepsilon}$ is the elongation rate (s^{-1}), $\dot{\gamma}$ the shear rate ($rad.s^{-1}$), ΔP_{ent} the capillary drop pressure (Pa), n the pseudoplastic coefficient, η the shear viscosity obtained after Bagley correction. The advantage of this method is that it gives an indication about the elongation viscosity data which is difficult to measure by plotting the elongation viscosity versus the elongation rate.

This method provides data at significantly higher strain rates (100 s-l) than do the previous ones. However, because of the numerous assumptions of the theory and of some surprising results in the literature, the method has been widely discussed and some contradictions still remain. For instance, in 1971, Cogswel compared results obtained from a steady-state experiment with a melt tensile rheometer and from convergent flow analysis (CFA). Although the assumptions made by Cogswell in his theory might be questionable, inconsistencies between the authors can also find their origin in unreliable experimental values of elongation viscosity. For example, the experimental values obtained from isothermal fiber-spinning are questionable, the elongation rates are not constant along the threadline, and the steady state is seldom achieved. On the other hand, with an elongation viscosimeter, the values are much more reliable but, unfortunately, the level of strain rates reached is much smaller than the one obtained with convergent flows and the results are not easily comparable.
Although Cogswell's theory has been established for 180° die entry angles. In his original study, Cogswell considered a power-law equation for the viscosity, which means that the power law index n is assumed to be constant whatever the shear rate is. As regards the shear

flow curves, n obviously changes with the shear rate. The power law index has therefore been taken as a variable in the calculations.

III- Cox-Merz Rule

For highly elastic fluids and polymer melts, it is very difficult to measure steady viscosity at high shear rates using a rotational device. in this case, the shear viscosity can be estimated fiom the Cox-Merz relation. This empiricism seems to work well for homogeneous polymer solutions and melts.

The so-called Cox-Merz "rule" is empirical relationship which has been found to be of great use in rheology. It was observed by Cox and Merz that for many polymeric systems correspondence occurred between the steady state shear viscosity, η, plotted against shear rate, and the magnitude of the complex viscosity, |η*|, plotted against angular frequency, ω. The complex viscosity is defined by: η* = G* / iω
It is based on an assumption that the dynamic viscosities are quite similar, especially at low shear rates. For $\dot{\gamma} = \omega$, the Rule is described as follow:

$$|\eta^*(\omega)| = \sqrt{\eta'^2(\omega) + \eta''^2(\omega)} = \eta(\dot{\gamma}) \qquad \text{(Eq.vi)}$$

IV- Cole-Cole Diagram

There are several approaches helping us to determine the relaxation time. Among them, the Cole-Cole diagram. It is represented by the plot of η" versus η', having typical shape of arc of a circle. This representation defined the following three parameters:

a) The zero shear viscosity of "η_0", the point of intersection of the semi-circle and abscissa axes.
b) λ_0, the relaxation time corresponding to the frequency where η" is maximum ($\lambda 0 = 1 / \omega$).
c) The coefficient "β", the angle between the diameter and the straight line passing through the origin of the circle. β=hπ / 2 where "h" characterizes the width of distribution of relaxation times. Therefore η * is defined as the following equation:

$$\eta^* = \frac{\eta_0}{1 + (i\omega\lambda_0)^{1-\beta}} \qquad \text{(Eq.vii)}$$

References

[1] Kanai T, Campbell G, (1999) Film Processing, Hanser, Munich 1-10
[2] Lim LT, Auras R, Rubino M. Processing technologies for poly(lactic acid). Progress in Polymer Science. 33(8): 8820–852. 2008.
[3] Jung HW, Hyun JC. Instabilities in extensional deformation polymer processing. Rheology Reviews. 131 - 164. 2006.
[4] Ryan CM, Nangeroni JF, Hartmann MH. Branching of poly(lactic acid) to increase melt strength for extrusion coating. Polymers, Laminations, & coatings conference / 139. 1997.
[5] Arraiza A. Lopez, Sarasua JR, Verdu J, Colin X. Rheological Behavior and Modeling of Thermal Degradation of Poly(ε-Caprolactone) and Poly(L-Lactide). International Polymer Processing XXII 5: 389-394. 2007.
[6] Al-Itry R, Lamnawar K, Maazouz A. Improvement of thermal stability, rheological and mechanical properties of PLA, PBAT and their blends by reactive extrusion with functionalized epoxy. Polymer Degradation & Stability. 97(10): 1898-1914. 2012.
[7] Rankumar DHS, Bhattacharya M. Steady shear and dynamic properties of biodegradable polyesters. Polymer Engineering & Science. 38(9): 1426-1435. 1998.
[8] Sodergard A, Nasman JH. Melt stability study of various types of poly(l-lactide). Industrial and Engineering Chemistry Research. 35(3): 732-735. 1996.
[9] Baird DJ. The role of extensional rheology in polymer processing. Korea-Australia Rheology Journal. 11(4): 305-311. 1999.
[10] Xu Y, You M, Qu J. Melt rheology of poly (lactic acid) plasticized by epoxidized soybean oil. Wuhan University Journal of Natural Sciences. 14(4): 349-354. 2009.
[11] Zhong W, Ge J, Gu Z, Li W; Chen X, Yi Z, Yang Y. Study on biodegradable polymer materials based on poly(lactic acid). I. Chain extending of low molecular weight poly(lactic acid) with methylenediphenyl diisocyanate, Journal of Applied Polymer Science. 74(10): 2546-2551. 1999.
[12] Yingwei D, Di Maio E, Luigi N. Reactively modified poly (lactic acid): Properties and foam processing. Macromolecular materials and engineering. 290(11): 1083-1090. 2005.
[13] Corre YM, Duchet J, Maazouz A, Reignier J. Melt strengthening of poly (lactic acid) through reactive extrusion with epoxy-functionalized chains. Rheologica Acta 50(7-8), 612-629. 2011.
[14] Mihai M, Huneault M, Favis BD. Rheology and extrusion foaming of chain-branched poly(lactic acid). Polymer Engineering & Science. 50(3): 629-642. 2010.
[15] Japon S, Luciani A, Nguyen QT, Leterrier Y, Manson JAE. Molecular characterization and rheological properties of modified poly(ethylene terephthalate) obtained by reactive extrusion. Polymer Engineering and Science. 41(8): 1299-1309. 2001.
[16] Xanthos M, Young MW, Karayanndis GP, Bikiaris DN. Polymer Engineering and Science. 41(4): 643-655. 2001.
[17] Grimes E, Keely S. Foaming of PLA - the use of melt strength enhancers to achieve lower density foams produced by chemical blowing agents. Rubber World 243(1): 1-28. 2010.
[18] Dean KM, Petinakis E, Meure S, Yu L, Chryss A. Melt Strength and Rheological Properties of Biodegradable Poly(Lactic Aacid) Modified via Alkyl Radical-Based Reactive Extrusion Processes. Journal of Polymers and the Environment. DOI: 10.1007/s10924-012-0461-2. 2012.
[19] Yuanliang W, Chunhua F, Yongxiang L, Changshun R, Yaoyao Z, Ya F. Melt synthesis and characterization of poly(L-lactic acid) chain linked by multifunctional epoxy compound. Journal of Wuhan University of Technology-Mater. Sci. Ed. 25(5):774-779. 2010.
[20] Najafi N, Heuzey MC, Carreau PJ, Wood-Adams PM. Control of thermal degradation of polylactide (PLA)-clay nanocomposites using chain extenders. Polymer Degradation and Stability. 97(4): 554–565. 2010.
[21] Villalobos M, Awojulu A, Greeley T, Turco G, Deeter G. Oligomeric chain extenders for economic reprocessing and recycling of condensation plastics. Energy. 31(15):3227-3234. 2006.

[22] Zhou ZF, Huang GQ, Xu WB, Ren FM. Chain extension and branching of poly (L-lactic acid) produced by reaction with a DGEBA-based epoxy resin, Express Polymer Letters. 1(11): 734–739. 2007.
[23] Sodergard A, Näsman JH (1994) Stabilization of poly(Image -lactide) in the melt Polymer Degradation and Stability. 46(1), 25-30. 1994.
[24] Ghijsels A, Ente JJSM, Raadsen J. Melt Strength Behavior of Polyethylene Blends, International Polymer Processing VII 7(1): 44-50. 1992.
[25] McCallum TJ, Kontopoulou M, Park CB, Muliawan EB, Hatzikiriakos SG. The Rheological and Physical Properties of Linear and Branched Polypropylene Blends. Polymer engineering and science. 47(7): 1133-1140. 2007.
[26] Cicero John A, Dorgan John R, Garrett J, Runt J, Lin JS. Effects of molecular architecture on two-step, melt-spun poly(lactic acid) fibers, Journal of Applied Polymer Science. 86 (11): 2839–2846. 2002.
[27] La Mantia FP, Scaffaro R, Carianni G, Mariani P. Rheological Properties of Different Film Blowing Polyethylene Samples Under Shear and Elongational Flow. Macromolecular Materials and Engineering 290(3):159–164. 2005.
[28] Corre YM, Maazouz A, Duchet J, Reignier J. Batch foaming of chain extended PLA with supercritical CO_2: Influence of the rheological properties and the process parameters on the cellular structure. Journal of Supercritical Fluids. 58(1): 177-188. 2011.
[29] Wagner MH, Bastian H, Hachmann P, Meissner J, Kurzbeck S, Münstedt H, Langouche F. The strain-hardening behaviour of linear and long-chain-branched polyolefin melts in extensional flows. Rheologica Acta. 39(2): 97-109. 2000.
[30] Stadler FJ, Kaschta J, Münstedt H, Becker F, Buback M. Influence of molar mass distribution and long-chain branching on strain hardening of low density polyethylene. Rheologica Acta. 48(5): 479-490. 2009.
[31] Kim YM, Park JK. Effect of short chain branching on the blown film properties of linear low density polyethylene. Journal of Applied Polymer Science. 61(13): 2315–2324. 1996.
[32] Majumder KK, Hobbs G, Bhattacharya SN. Molecular, rheological, and crystalline properties of low-density polyethylene in blown film extrusion. Polymer Engineering & Science. 47(12): 1983–1991. 2007.
[33] Godshall DL. Investigations of structure-propertu relationships in semi-crystalline thermocrystalline thermoplastic polymers: Blown polyethylene films and polyacrylonitrile copolymers, Dissertation submitted to the faculty of the Virginia Polytechnic Institute and State University. 2002.
[34] Yunli F, Sadeghi F, Fleuret G, Carreau PJ (2008) Properties of blends of linear and branched polypropylenes in film blowing. The Canadian Journal of Chemical Engineering. 86(1): 6–14. 2008.
[35] Ghaneh-Fard A. Study of the Film Blowing Process and On-line Measurements of Birefringence, Ph.D Dissertation Departement Chemical Engineering, École Polytechnique de Montréal. 1997.
[36] Maddams WF, Preddy JE. X-Ray Diffraction Orientation Studies on Blow Polyethylene Films. II. Measurements on Films from a Commercial Blowing Unit. Journal of Applied Polymer Science. 22(10): 2739-2749. 1978.
[37] Middleman S. Fundamental Studies of Polymer Processing, McGraw-Hill, New York. 1977.
[38] Freissner M. Elongational flow of HDPE samples and bubble instability in film blowing, International Polymer Processing. 2(3-4) ; 229-233. 1988.
[39] Li K, Peng J, Turng LS, Huang HX. Dynamic Rheological Behavior and Morphology of Polylactide/Poly(butylenes adipate-co-terephthalate) Blends with Various Composition Ratios. Advances in Polymer Technology. 30(2), 150–157. 2011.
[40] Lehermeier HJ, Dorgan JR. Melt rheology of poly (lactic acid): Consequences of blending chain architectures. Polymer Engineering & Science. 41(12), 2172-2184. 2001.

[41] Cogswell FN. Converging flow of polymer melts in extrusion dies. Polymer engineering and Science. 12(1):64-73. 1972.
[42] Kanev D, Takacs E, Vlachopoulos J. Rheological Evaluation and Observations of Extrusion Instabilities of Biodegradable Polyesters. International Polymer processing. 22(5): 395-401. 2007.
[43] Han CD, Park JY. Studies on blown film extrusion. III. Bubble instability. Journal of Applied Polymer Science. 19(12): 3291–3297. 1975.
[44] Han CD, Shetty R. Flow Instability in Tubular Film Blowing. 1. Experimental Study, Industrial & Engineering chemistry Fundamentals. 16 (1): 49–56. 1977.
[45] Kanai T, White JL. Kinematics, Dynamics and stability of tubular film extrusion of various polyethylenes. Polymer Engineering & Science. 24(15): 1185-1201. 1984.
[46] Minoshima W, White JL. Instability phenomena in tubular film and melt spinning of rheological characterized high density, low density and linear low density polyethylenes. Journal of Non-Newtonian Fluid Mechanics. 19(3): 275-302. 1986.
[47] White JL, Yamane H. A collaborative study of the stability of Extrusion, Melt spinning and tubular film Extrusion of Three high Density, Two Low Density and a Linear Density Polyethylene Samples. Pure and Applied Chemistry. 59(2): 193-216. 1987.
[48] Barq P, Haudin JM, Agassant JF. Instability phenomena in film casting process, International Polymer Processing. 5(4): 264-271. 1990.
[49] Andrianarahinjaka H. Etude des instabilités lors de la fabrication des films thermoplastiques biétirés par le procédé de soufflage de gaine, Thèse de doctorat, Université de Lille. 1992.
[50] Ghaneh-Fard A, Carreau PJ, Lafleur PG. Study of Instabilities in Film Blowing. AIChE Journal. 42(5): 1388-1386. 1996.
[51] Ren J. Biodegradable poly(Lactic Acid): Synthesis, Modification, Processing and Applications, TSINGHUA University Press, Springer. 2010.
[52] Mekhilef N, Hedhli L, Moyses S. Effect of Rheological Strain Hardening on Extrusion Blown Film of Polyvinylidene Fluoride. Journal of Plastic Film and Sheeting. 23(3): 203-219. 2007.
[53] Stange J, Uhl C, Münstedt H. Rheological behavior of blends from a linear and a long-chain branched polypropylene. Journal of Rheology. 49(5): 1059-1080. 2005.
[54] Raffa P, Coltelli M-B, Savi S, Bianch S, Castelvetro V. Chain extension and branching of poly(ethylene terephthalate) (PET) with di- and multifunctional epoxy or isocyanate additives: An experimental and modelling study. Reactive & Functional Polymers. 72(1):50–60. 2012.
[55] Guang L, Shenglin Y, Jianming J, Junhong J, Chengxun W. The complicated influence of branching on crystallization behavior of poly(ethylene terephthalate). Journal of Applied Polymer Science. 110 (3): 1649–1655. 2008.
[56] Spitael P, Macosko CW. Strain hardening in polypropylenes and its role in extrusion foaming. Polymer Engineering and Science. 44(11): 2090-2100. 2004.
[57] Cho K, Lee BH, Hwang KM, Lee H, Choe S. Rheological and mechanical properties in polyethylene blends. Polymer Engineering and Science. 38(12): 1969-1975. 1998.
[58] Henton DE, Gruber P, Lunt J, Randall J. Polylactic acid Technology in: A.K. Mohanty, M.Misra, L.T. Drzal (Eds.), Natural Fibers, Biopolymers, and Biocomposites, Taylor & Francis, Boca Raton, FL, 527-577. 2005.
[59] Huda MS, Yasui M, Mohri N, Fujimura T, Kimura Y. Dynamic mechanical properties of solution-cast poly(L-lactide) films. Materials Science and Engineering. A : 333(1-2), 98-105. 2002.

Chapter 6
Biaxial orientation of materials based on Poly (lactic acid): Structure and properties

Part A- Neat and modified PLA, PBAT and their blends with multi-functional epoxide

6-A

I Abstract

This works deals with the study of the strain-induced structural changes for biodegradable polymers, namely Poly (lactic acid) (PLA) and poly (butylene adipate-co-terephtalate) (PBAT) chain extended/branched with 0,5 and 0,7 % by weight of multi-functional styrene-acrylic oligomers (Joncryl ADR®-4368) and their blends. The films were prepared using a cast extrusion in the same experimental conditions. Bi-axially simultaneous stretching at 75°C, above the glassy transition temperature, was performed and leads to semi-crystalline films with in-plane isotropy. Their structural, morphological and thermo-mechanical properties are studied using various techniques as dynamic mechanical thermal analysis (DMTA), differential scanning calorimetry (DSC), wide-angle X-ray diffraction (WAXS), scanning electron microscopy (SEM), and tensile tests. The thermal kinetics investigations confirm that no induced thermal crystallization could be developed during the time scale of the experiments. The appeared strain-induced crystals of PLA includes mesophase and α' crystals. Besides, for stretched PBAT, it is interesting to find that the induced mixed-crystal structure of BT and BA units undergoes PBT-like crystal form. Significant thermal and structural changes are occurred with the incorporation of Joncryl into PLA matrix. An increase of the stress at break and a shift of the optimum draw ratio at lower values are obtained. The same trend was observed for compatibilized PLA_PBAT blends. The effect of annealing on the mechanical behavior of films was also studied. It was shown that it leads to an earlier strain hardening accompanied with a higher stress at break. We should point out that an obvious strain-hardening behavior is observed for modified samples with the increase of strain rate.

Keywords: biodegradable polymers-simultaneous biaxial stretching-strain induced crystallization-mesophase-annealing

II Introduction

Driven by environmental concerns, packaging film made of bio-degradable and renewable raw materials is getting more attractive [1][2][3]. One of the most prominent polymers among these polymers is Poly (lactic acid) (PLA). There is a growing interest in it for many applications including packaging, electronic housing, automobile interiors [4][5][6][7][8]. Unfortunately, some shortcomings like its poor ductility, poor melt properties and low kinetic of crystallization regard to PET, have restricted its use in packaging applications. Recent attempts such as blending PLA with other flexible and biodegradable polymers (Polyε-caprolcatone) (PCL) [9], Poly(butylene adipate-co-terephtalate) (PBAT) [10], Polyhydroxyalkanoate (PHA) [11] has proven to be very effective in enhancement the stiffness of poly(lactic acid). Besides, in our previous work, we have demonstrated that the PLA/PBAT blends can be a suitable solution to upcoming the physical and mechanical drawbacks of each neat polymer, where PBAT, it is a promising aliphatic-aromatic copolyester, due to the balance of biodegradability and physical properties [12]. Moreover, the incorporation of a chain extender/branching agent leads in one hand to the improvement of the melt strength of each polymer and plays in other hand the role of a compatibilization agent in their blends by modifying the interfacial adhesion [12].

Furthermore, the low kinetic of crystallization of PLA presents a major drawback to overcome [13][14][15]. It is well common that the thermal crystallization of PLA, occurred during non-isothermal conditions, is not compatible with an industrial process as extrusion and injection molding processes. It is hard to achieve high PLA crystallinity in a short time during the processes [16][17][18][19]. Therefore, the gas barrier properties of PLA can not be enhanced. Thus, the question of how to enhance crystallization behavior and increase crystallinity has been widely discussed in literature. It has been reported that the high crystallinity can be achieved by several methods as isothermal annealing [20][21], polymer blending [22][23], adding nucleating agents [24][25], strain-induced crystallization [26][27][28] and foaming process [16][29]. These approaches achieve performance requirements by bring up the polymer intrinsic properties. We should notice that three different types of crystallization have been discussed in the literature; they are (i) the crystallization from the melt (melt crystallization), (ii) the crystallization from the glassy state to the melt (cold crystallization), and (iii) the strain or shear induced crystallization (SIC).

The strain-induced crystallization represents a suitable way to enhance the crystallinity development in polymers such as PP and PET. The contribution of biaxial orientation in improving the mechanical properties of PLA films is therefore quite evident and this route represents an important approach for manufacturing biodegradable PLA films with good properties for several practical applications [19][30][31].
But, few studies have addressed the question of strain-induced crystallization during stretching of PBAT and their blends, compared to the neat PLA.

According to previous works [27][28], crystal structure could be formed in amorphous PLA films in uniaxial and biaxial stretching. It is interesting to note that, due to the polymorphism behaviour of PLA, it is able to crystallize in four forms under shear effect (α, α', β, γ and stereo-complex), where the regularity of PLA chains is affected by the ratio of L component over "D" component depending on the synthesis conditions [32][33][34]. It is reported that an amorphous commercial grade of PLA has a ratio L: D of 80:20 to 98:2 (molar ratio) and a semi-crystalline commercial grade a L:D ratio of 98.4:1.6 to 98:2 [35][36].

Under uniaxial drawing, the initial amorphous sheet would develop strain-induced nanoscale crystals α-form and a high degree of spatial arrangements for the integrated assembly of amorphous and crystalline phases [37]. Furthermore, the crystals transition α - β forms of PLA depends on the synergistic effects of stretching temperature and strain rate. At high drawing temperature, a higher orientation for semi-crystalline PLLA is observed. However, at a low stretch ratio and moderate deformation temperature (85°C), molecular orientation in the crystalline regions was found to progress more slowly than in the amorphous zones. In addition, it was revealed that the plastic deformation transformed the amorphous blend into a crystalline fibrillar texture oriented in the flow direction [38].

Concerning P(BA-co-BT) or PBAT, its crystalline structure and thermal properties during uniaxial stretching have been reported by several research groups [39][40]. Based on their analysis on molecular mobility of the aliphatic methylene group in PBAT by using solid state ^{13}C-NMR, their opinions diverge from each other on whether its crystal structure is formed by pure BT unit [39] or by both BT and BA units [40]. Some other authors found that the aliphatic methylene group is not suitable to be used to assign crystalline component in aliphatic/aromatic copolymers, because with the presence of bulky and rigid benzene ring, as in the case of PBT, the mobility of soft methylene group is promoted. Thus, no difference in molecular mobility of soft methylene group whether they are in crystalline or amorphous region [41]. Therefore, Marchessault and co-workers [40], suggested the co-crystallization of the P(BA-co-BT) copolymer and proposed a cocrystallization model in which the adipate units fit into the crystal lattice of PBT. Mixed crystallization

enabled PBAT to have well-developed PBT-like crystal structure despite of its ideal randomness and (1:1) composition. The introduction of soft BA unit into BT crystal lattice led to the significant lower melting temperature compared with that of PBT. DSC results displayed a single diffuse "T_m" endotherm at 125°C, which is explained as being due to co-crystallization because the *T*m for PBT is 230°C.

In the same way, it was revealed that the crystallinity and dimensional stability of bioriented PLA films are most sensitive to the stretching and annealing temperatures [42]. Biaxial oriented PLA film with high crystallinity ensures dimensional stability at temperatures above 100 C. The structural evolution during simultaneous and sequential rubbery state biaxial stretching of PLA films have been also studied [31]. Simultaneous biaxial stretching always leads to films with in-plane isotropy and poor crystalline order. Otherwise, during sequential biaxial stretching oriented crystallization gradually developed. Application of transverse stretching destroys the crystalline structure oriented in machine direction. Oriented films of PLA showed an improvement in gas O_2, N_2, CO_2 and CH_4 barrier properties [43]. It is explained, in one hand by the crystallization of PLA during stretching and in another hand, by the orientation of macromolecular chains. It has been reported that the crystallization and orientation of polymers during stretching is correlated to the relaxation time of chains (related to the stretching temperature and the molecular weight). For instance, the high shear rate makes the chains orient along the shear flow, while at low shear rates, the oriented chains have sufficient time to relax, and stable nuclei cannot be formed. When the draw rate ($1/\tau_{sollicitation}$) is slower than the rate of chain reptation ($1/\tau_{rept}$), no oriented crystallization is observed in PLA polymers [38][44].
As the literature is poor regarding the uniaxial and biaxial stretching properties of PLA blends, we can underline Chapeleau et al study [27] For PLA/TPS blends, at the lowest temperature of the processability range (70 °C), the tensile modulus and tensile strength increased as a function of biaxial draw ratio and the elongation at break only increased significantly for the blends having low TPS contents [27].

Furthermore, as far as we know, no efforts have been dedicated to understand the crystalline microstructure of PBAT under biaxial stretching. It is therefore of great interest to be able to afford an accurate characterization of molecular orientation and structure in oriented PBAT samples. Moreover, the fundamental knowledge of the relationship between microstructure and toughness of films based on PLA is still not complete, especially for (i) the blends based on PLA and PBAT (ii) the chain extended/branched PLA and PBAT in which shear and elongation properties for modified PLA were extensively investigated in the literature [45][46].

The key feature of our study is to shed further light on the relationship between both mechanical and microstructural properties for films based on compatibilized and non-compatibilized PLA and PBAT blends. The studied films with controlled thickness will be obtained. The microstructure of the materials (i.e. degree of crystallinity and conformation of molecular chain segments during drawing) will be studied by means of several complementary methods including differential scanning calorimetry (DSC), dynamic thermal mechanical analysis (DMTA) and wide-angle X-ray scattering (WAXS). The information thus gathered made it possible to study the influence of stretching parameters on the induced crystallization of the modified and unmodified PLA and PBAT polymers and their blends.

III Experimental Section

III.1 Materials

The PLA Grade 4032D purchased from Natureworks with a D-isomer content of approximately 2%, exhibits a weight- average molecular weight of 100.000 g/mol (SEC analysis), a glass transition and melting temperatures of approximately 60°C and 170°C (DSC analysis), respectively. PBAT copolymer was supplied by BASF, (Grade Ecoflex FBX 7011). The molar fraction of BT and BA units are 44% and 56%, respectively. It exhibits a weight- average molecular weight of 40.000 g/mol (SEC analysis) a glass transition temperature and melting point of -30°C and 110-120°C (DSC analysis), respectively. Both polymers are supplied in pellets form. Commercial available Joncryl (BASF, Joncryl ADR®-4368) has been used as Chain Extension molecules for polyesters. It is an epoxy functional oligomeric acrylic with the following physical characteristics: $T°_g$ = 54°C, EEW (epoxy equivalent weight) = 285 g/mol, Mw = 6800 g/mol, obtained in flake form. Table VI-1 summarizes the composition of the various samples used in our study.

Table VI-1 Composition of different studied samples

Composition	Notations
100wt% PLA	PLA
99,5wt% PLA + 0,5wt% Joncryl	PLA_0,5
99,3wt% PLA + 0,7wt% Joncryl	PLA_0,7
100wt%PBAT	PBAT
99,5wt% PBAT + 0,5wt% Joncryl	PBAT_0,5
99,3wt% PBAT + 0,7wt% Joncryl	PBAT_0,7
80wt% PLA + 20wt% PBAT	80 PLA_20PBAT
79,6wt% PLA + 19,9wt% PBAT + 0,5wt% Joncryl	80 PLA_20PBAT_0,5
79,44wt% PLA + 19,86wt% PBAT + 0,7wt% Joncryl	80 PLA_20PBAT_0,7
20wt% PLA + 80wt% PBAT	20 PLA_80PBAT
19,9wt% PLA + 79,6wt% PBAT + 0,5wt% Joncryl	20 PLA_80PBAT_0,5
19,86wt% PLA + 79,44wt% PBAT + 0,7wt% Joncryl	20 PLA_80PBAT_0,7

III.2 Preparation of the Cast films

The films were extruded in two steps; Firstly, the modified and non modified PLA and PBAT with Joncryl ADR® as well as their blends were blended by means of a co-rotating twin screw extruder (Thermo Electron PolyLab System Rheocord RC400P, screw diameter = 16 mm). Before

processing, PLA and PBAT pellets were dried under a vacuum oven at 80°C for 12h. As we have demonstrated previously, we remindthat a residence time about 3 minutes is sufficient to stabilize the torque. Theprocessing conditions are listed Chapter 1-processing and blend preparation section. More details about their rheological, thermal, mechanical, morphological properties are presented in our previous work [12]. We should point out that the incorporation of Joncryl makes the processability more stable.
The granulated samples are also dried before cast-film extrusion. Cast-films were prepared with a 30 mm single-screw extruder and quenched with a 30°C chill roll. The chilled roll was kept as close as possible to the die and two air fans were used as an air knife throughout the experiment. The temperature profile is reported in table VI-2.

Table VI-2 Processing parameters for films, prepared through a single screw extruder

Single screw extruder						
Zone 1	**Zone 2**	**Zone 3**	**Zone 4**	**Zone 4**	**T° die**	**Screw speed (rpm)**
177	200	200	190	200	190°C	90

Under these conditions, cast films of about 500 µm of thickness are prepared. Morphologies of the cryogenically fractured surfaces were examined by scanning electron microscopy (SEM). The film surface was coated with gold prior to the SEM examination.

III.3 Biaxial film stretching

The extrusion-cast films were stretched by a biaxial test machine, named ETIFI. Care was taken to cut the square test specimens from the central region of the extruded films, as showed in Figure VI-1. The uniformity of specimen's thickness was checked and validated. Heating steps are achieved by blowing heated air to the surface of the specimen.

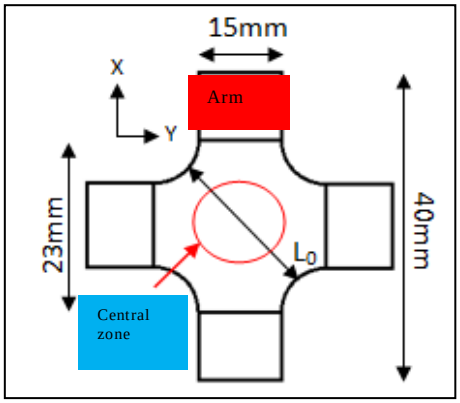

Figure VI-1 Cross-shaped specimen used in the biaxial experiments

The force to stretch the sample is recorded against displacement on each axis by two force transducers (500 and 5000N) mounted on the central grip of each axis. This force and displacement data are then converted to nominal stress-nominal strain data, according to Eq.23 and Eq.24, useful datas to plot the stress-strain curves. In this case, the specimens are assumed to be incompressible,

so the nominal stress "σ" can be calculated from the measured force F ($\sigma = \frac{F}{S}$ (Pa)). Moreover, the biaxial draw ratio (λTD × λMD = LTD/L°TD × LMD/L°MD) is associated to the changes in length (L) from the initial value (L°) along two principal stretch directions.

Equation 23
$$\sigma(t) = \frac{\sqrt{2} \times F(t)}{e_0 \times L_0 \times e^{-\varepsilon}}$$

Equation 24
$$\varepsilon_{x,y}(t) = \ln(\lambda) = \ln(\frac{l(t)}{l_0})$$

Where, **L°** and **L** are the local sample length before and after stretching, respectively. $\boldsymbol{\lambda_{MD}}$ is the stretch ratio in machine direction and $\boldsymbol{\lambda_{TD}}$ is the stretch ratio in the transverse direction.

III.3.1 Biaxial properties

In this study, the biaxial testing experiments were conducted at 75°C. This temperature was chosen in the rubbery plateau of both PLA and PBAT polymers. The cross-shaped specimens were heated for 5 min to allow a homogeneous temperature distribution. The stretching rates were thus chosen to be 0.1, 1 and 10 mm/s, which correspond to 0.004, 0.04 and $0.4s^{-1}$ respectively.
For the sake of clarity, only the obtained results with 0.1 mm/s (or $0.4s^{-1}$) were presented in this paper.
The constitutive behavior of the different films was investigated for simultaneous equi-biaxial mode, where the square specimen is simultaneously stretched at a constant nominal strain rate in both the x and y axis to a specific draw ratio. Only the central testing zone of the specimen (a 23 mm side square) is heated and deformed which prevents the polymer from shrinking and slipping in the grips while the arms are under uniaxial stress. This gives an equal biaxial dimension of the final sample. Thus, to differentiate the microstructural changes induced during the stretching from the ones that appeared during the relaxation under stress, a quenching step to the room temperature was used in order to freeze the orientation due to drawing.
We should note that the stresses in both machine and transverse directions are similar, which is representative of the initial isotropy of the cast sheets, as highlighted in figure VI-2. The same trend of stress-strain for the four arms of the specimen is a good indication of near symmetric stretching.

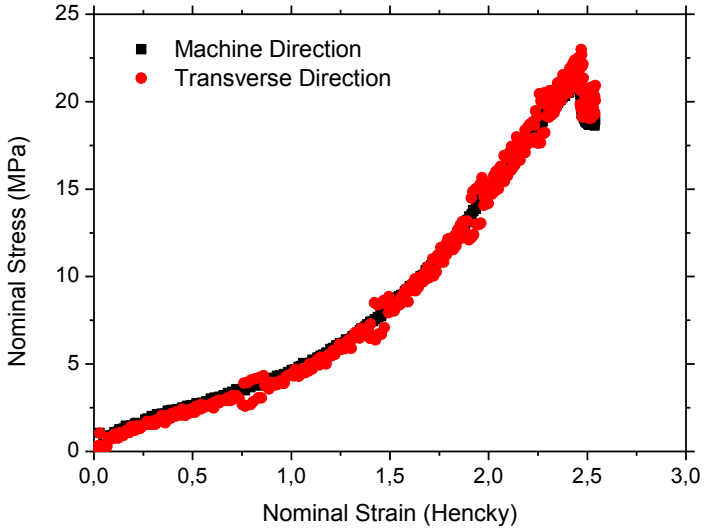

Figure VI-2 Stress-Strain curves for PLA samples in both Machine and Transverse Directions

III.3.2 Microstructural properties of the stretched films

III.3.2.1 Debye-Scherrer method

X-ray measurements were carried out using an X-ray goniometer. The generator was set up at 20 KV and 15 mA and the monochromatized Cu Kα radiation, with wavelength λ=1.54178 Å, was selected. The sample-to-detector distance (EO) was about 50mm, as presented in figure VI-3.

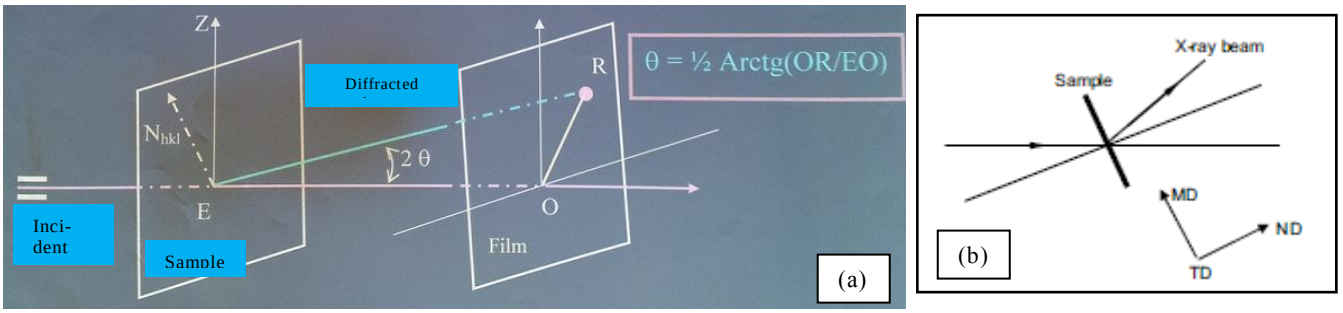

Figure VI-3 a) Schematic representation of Debye-Scherrer method and b) Sample orientation in the sample holder

The obtained Debye-Scherrer patterns are used to determine both chain orientation and crystallite morphology. The d-spacing (The interplanar spacing) (d_{hkl}) of the successive atomic, an *(hkl)* plane was determined using Bragg's law (Eq.25):

Equation 25
$$n\lambda = 2d_{hkl}\sin\theta_{hkl}$$

Where "*n"* is a small integer indicating the order of diffraction; "λ" is the wavelength of the characteristic line x-rays from the x-ray tube, *"d"* is the distance between a set of parallel lattice planes, and *"θ"* is the angel between the incident collimated x-ray beam and an atomic lattice plane in the crystal, calculated as follow:

Equation 26

$$2\theta = Arctg(\frac{OR}{EO})$$

III.3.2.2 Wide Angel X-ray Diffraction (WAXD)

More careful determination of the development of chain conformation in crystalline phase was also enabled by wide angle X-ray diffraction (WAXD) by using a diffractometric 2θ scans (XPERT-PRO) with a θ/2θ reflection mode. This technique allows a quantitative study of the crystal lamellar morphology through 2θ integration. During scanning, MD (machine direction) of the samples was oriented horizontally in the sample holder. The voltage and current were set to be 150KV and 40 mA. It is based on the diffraction of a monochromatic X-ray beam by the crystallographic planes *(hkl)* of the polymer crystalline phase. The intensity of the diffracted radiation for a given *hkl* plane is measured as the sample is rotated through all possible spherical angles with respect to the beam. This allows the determination of the probability distribution of the orientation of the normal to *hkl* plane with respect the directions of the sample. Finally, the X-ray beam was mono-chromatized.

III.3.3 Estimation of Crystallinity in stretched films

III.3.3.1 Hermans and Weidinger method

The evolution of the crystallinity is estimated by using "Hermans and Weidinger" method. The principle of this method is the recording with monochromatic radiation of diffractograms of several samples. X-ray is thus obtained directly from the diffractogram after subtraction of the amorphous halo. Integrated intensities, which may be assumed to be proportional to either amorphous or crystalline fraction, were selected and measured. The "Hermans and Weidinger" expression is as follow:

Equation 27

$$X_c = \frac{1}{1 + \frac{p}{q}\frac{S_a}{S_c}}$$

Where "$\frac{p}{q}$" a constant equal to 1.297, "S_a" the area of the amorphous halo, "S_c" the sum of the area of all crystalline reflections and "$\frac{S_a}{S_c}$" the ratio of the area under the resolved Gaussian crystalline peaks to the amorphous area.

III.3.3.2 Dynamic Scanning Calorimetry (DSC)

Thermal analysis were carried out using a TA instrument DSC Q10 in -80°C to 200°C range with 10°C/min heating rate under nitrogen atmosphere. The samples were crimped into Aluminum

pans to a total weight of 5-10 mg. The crystalline weight fraction, X_c (%), was computed from the enthalpy of the melting endotherm according to the following equation (Eq.28):

$$X_c(\%) = \frac{\Delta H_m - \Delta H_{cc}}{\Delta H_{m\infty}} \times 100 \qquad \textit{Equation 28}$$

Where ΔHm is the melt enthalpy; ΔHcc is the cold crystallization enthalpy; $\Delta Hm\infty$ was taken as 93 J/g and 114 J/g for PLA and PBAT respectively. It represents the specific enthalpy of fusion of the perfect crystal.
We should note that the X-ray diffraction and thermal analysis were conducted on both "Arm" and "Central zone" of the specimens (figure VI-1). It is assumed that the Central part underwent both thermal and mechanical treatment. However, the arms undergo only a thermal one.

III.3.4 Thermo-mechanical properties

The thermo-mechanical properties was conducted through dynamic mechanical thermal analysis (DMTA) performed on a RSA II (TA instruments). Oscillating tensile-compressions tests under a strain of 0.01% at a frequency of 1Hz were performed during temperature sweeps from -80°C up to 110°C at a rate of 3°C/min.

IV Results and discussions

IV.1 Biaxial stretching properties of the neat PLA and PBAT

IV.1.1 Thermal properties of neat polymers cast-films

Prior to investigate the biaxial drawing behavior of our studied samples and the strain-induced structural changes, a thermal analysis was performed. Figure VI-4 depicted the DSC thermograms of pristine and processed PLA cast-film; upon heating, PLA pellets went through a glass transition temperature of about 62°C followed by a small single melting peak "T_m" at about 168°C.

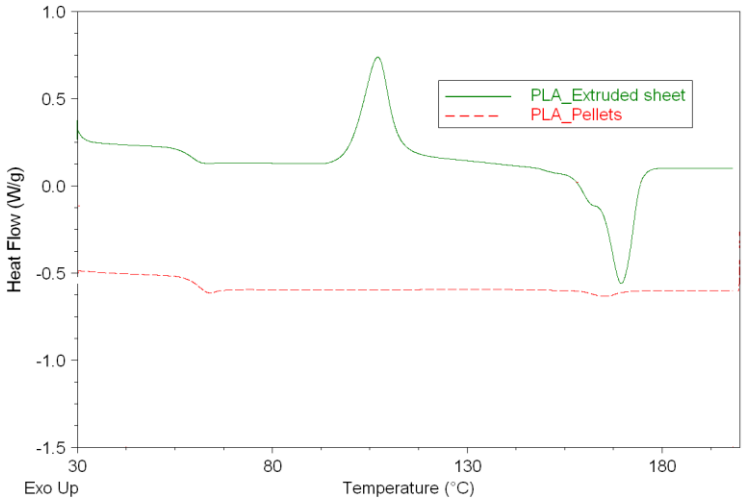

Figure VI-4 DSC thermograms of PLA pellets and PLA extruded sheet during the first heating

The crystallinity of the as-received polymer pellet is about 1.7%. No exothermic peak related to the cold crystallization is observed according to its lower crystallization kinetic. Otherwise, it is clear that the DSC thermogram of PLA sheet is very different from that of PLA pellets. The difference is highlighted by the appearance of an exothermic cold crystallization peak "T_{cc}" close to 110°-112°C. The degradation of PLA chains, during process, can be evocated to explain this phenomenon since a slight decrease in the average molecular weight from 100.000g/mol (Pristine PLA) to 94,000g/mol (Extruded PLA) was detected [12]. The by-products of the degradation (*i.e.* PLA oligomers and lactic acid) would then act as nucleating agent [47]. Some authors reported that the generated cold crystals at 110-120°C have α-form [19]. Moreover, the small melting peak close to the main one corresponds to the co-existence different morphologies or structures of crystalline phase [19][32].
The area under the cold crystallization peak (32 J/g) for the cast film is slightly smaller than that under the melting peak (36 J/g) indicating that the cast PLA film is slightly crystalline (4%) and it can further crystallized by drawing. For PBAT polymer, it cannot crystallize to a significant amount due to the random structure of the copolymer. In our case, a crystallization amount close to 23% is achieved. Therefore, the well-developed crystal structure in PBAT is an extremely rare phenomenon as reported by some authors [48]. It is worthy concluded that the extrusion process and the thermal history of PLA altered hardly the crystallization behavior of the polymer due to the alignment of polymer chains.

IV.1.2 Impact of biaxial stretching on the thermal and mechanical behavior of neat polymers

For biaxial drawing, the determination of processing conditions, notably the deformation temperature is essential. Generally, in PLA case, it is bounded by a glass transition and cold crystallisation. This range is estimated thanks to DMTA measurements, represented in figure VI-5, and can be determined between the α-relaxation temperature (peak of the loss factor = 65°C) and the onset cold crystallization temperature (85°C).
Ultimately, the biaxial drawing temperature was set at 75°C, in the rubbery plateau of both PLA and PBAT, as shown in figures VI-5a and VI-5b.

Moreover, as shown in figure VI-10, the study of thermal kinetics of PLA and PBAT at 75°C confirms that no induced thermal crystallization could be developed during the stretching experiments carried out here since the time scale of the test (preheating + stretching) is about 10min.

The constitutive behavior of PLA and PBAT is shown in figure VI-6 by the stress-strain (S-S) curves obtained under simultaneous biaxial stretching mode at 75°C (~T_g+15°C). The extensional behavior of PLAs was studied extensively by several authors [49][50]. The load-extension curve of PLA follows the typical ductile deformation behavior without yielding region. It is worth notice that PLA undergoes a plastic deformation above "T_g" [38]. Some authors reported that the deformation of an amorphous PLA films increases the tg't population, thereby facilitating strain-induced crystallization. The notation tg't refers to a trans-planar ester C-O, gauche O-Cα, and trans Cα-C torsions [51].

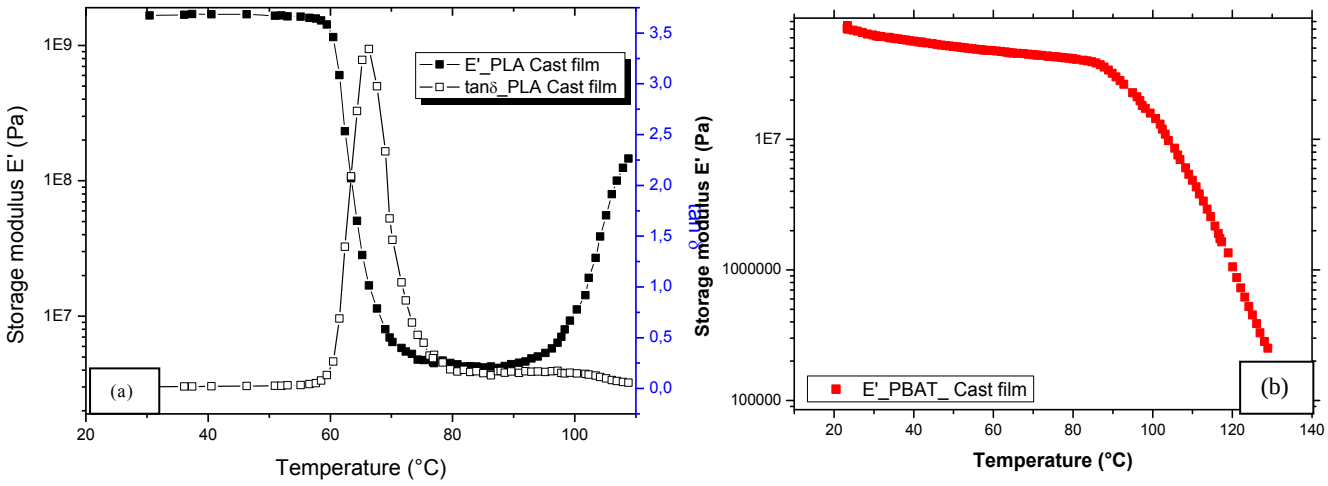

Figure VI-5 Dynamic mechanical analysis of a) PLA film and b) PBAT film at 1Hz and 0.01%

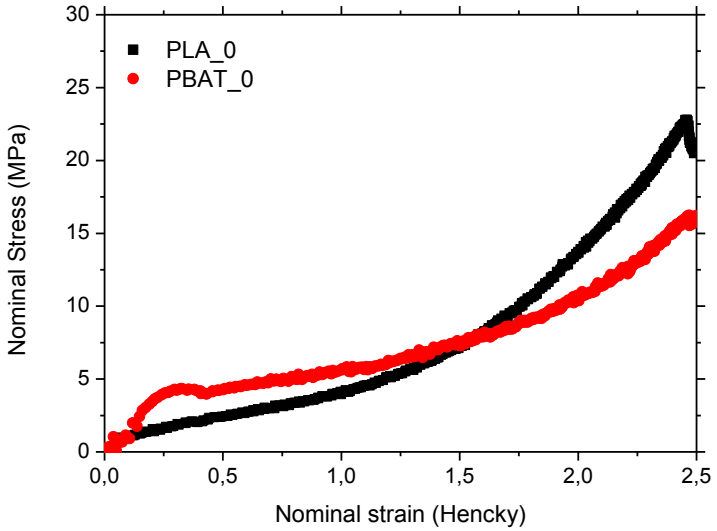

Figure VI-6 Nominal stress vs Nominal biaxial strain curves for PLA and PBAT samples

After the strain softening region, PLA begins to strain harden at about 1.7 Hencky, when the stress steadily increases ultimately. This strain threshold is determined from the intersection point of the line tangent to the plateau region and upswing region in the stress-strain curve. The strain-hardening is thus related to a molecular ordering due to the dynamics of molecular relaxation, particularly when the longest relaxation time exceeds the characteristic time for deformation as previously reported and explaining the visible intensive whitening in the neck areas in deformed PLA films at the end of stretching [19][32][50]. Consequently, the formation of crystals or the orientation of amorphous chains (mesomorphic phase or mesophase) during the stretching process restricts elongation of polymer chains. This phenomenon is accurately developed in several studies [52]. We should note that the mesophase can exist in the earlier stages of crystallization, acting as precursor and disappearing to form an imperfect crystal or mesophase which develops by becoming more and more ordered [32][53]. Indeed, a similar mechanical behavior was observed in PET stretched above the glass transition temperature [54][31][[55].

Yet the stress-strain curves of PBAT at 75°C did not exhibit any yield point but a quasi-rubber-like deformation behavior. After stretching, PBAT shows a lower amount of induced crystallization under strain compared to PLA according to Table VI-4. It was reported that theoretically according to Bernoullian statistics the average block length in such kind of copolymer is close to 2, generally too short to form regular crystalline packing, or at least the crystallinity will be quite low even if it manages to crystalline. This observation was confirmed by several studies on uniaxial drawing of PBAT [56][57][58][59].

The next step is thus to study the effect of such a biaxial stretching on the crystalline structure evolution of both PLA and PBAT. We firstly compared the thermal and crystalline properties of the arm and the central parts of the stretched specimens. These properties were thus compared to those of the un-stretched films. Figure VI-7 displays DSC thermograms of cast and stretched PLA and PBAT films. For the bi-axially stretched PLA film, two features are noted. Firstly, an increase of glass transition temperature (T_g) of a stretched PLA film, from 60° to 69°C, was observed. This increase suggests limited polymer chain motion in the stretched film because of the packing of molecules in the matrix. Surprisingly, the determined T_g after biaxial drawing is largely higher, of about 10°C, than the Tg of the cast film. The presence of of a slight endothermic peak, when passed the glass temperature at around 70°C isrelated to the PLA physical aging and can falsify the determination of the T_g value more accurately. Moreover, the second endothermic peak, near 80°C can be probably due to either a thermal relaxation enthalpy or melting of formed mesophase upon biaxial stretching. More details about the mesomorphic phase are given in the next section.
Secondly, the cold crystallization peak disappeared after stretching. A possible mechanism is explained by the increased of oriented amorphous chains and the formation of a semi-crystalline film after biaxial stretching [34][60][37]. Hence a 41% is obtained as a crystallization amount.
The presence of an exothermic peak in DSC curve of the undrawn cat film confirms the assumption that it is crystallizable during heating.

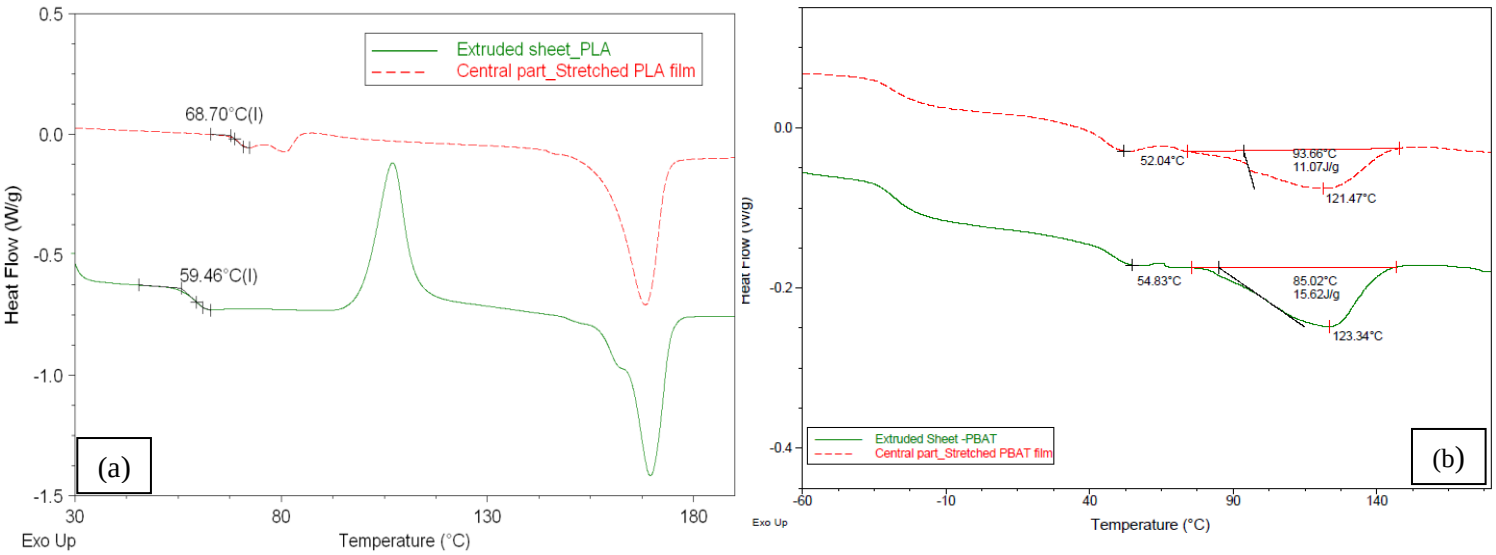

Figure VI-7 DSC thermograms of a) extruded and stretched (central zone) PLA films and b) extruded and stretched (central zone) PBAT films during the first heating

Hence, extruded and drawn PBAT films present a multiple melting behavior, a unique characteristic for semi-crystalline polymers [48][61]. Therefore, the existence of different crystal structures for PBAT can interprets this mechanism. One of the crystal structures is more likely formed by mixed-crystallization of BT and BA units, corresponding to a melting temperature about 123°C. It was demonstrated in the literature that the crystallized BT and BA units share a common crystal

lattice, since soft BA unit was introduced into BT crystal lattice [40]. The other one, in smaller amount, contains mainly BA units, corresponding to a melting temperature around 53°C. Further verification will be given below.
Besides, for both PLA and PBAT and with respect to the cast film, the stretching had a great influence on the crystallinity as estimated by Hermans and Weidinger method. Table VI-3 summarizes the evolution of the estimated crystallinity before and after drawing.
Moreover, more details about the formed crystalline structures will be given in the next section. Typical WAXD flat film patterns of unstretched and stretched cast PLA films are depicted in figure VI-14 (page 143). A diffuse and slightly halo appeared for unstretched PLA. However, the sharp diffraction arc of stretched PLA revealed a strain-induced crystallization with well oriented crystals having their (hkl) planes parallel to the draw axis. This means that PLA is able to build-up crystalline order as observed in the case of quiescent extruded PLA sheet. The amorphous PLA chains are gradually oriented in the film plane after biaxial drawing to 2.4 Hencky (final fixed biaxial strain). The WAXS patterns with the X-ray beam taken along MD exhibit two very sharp meridional peaks superposed over the amorphous halo. This type of pattern in the absence of other higher order peaks represents nematic-like order in the material indicating that in this mode the three-dimensional order crystalline order is not established even well into the strain hardening range. The formation of the mesomorphic phase was also confirmed by the endothermic peak close to T_g, which can be attributed to its melting [62].

Table VI-3 Thermal properties and the crystallinity evolution of extruded and stretched PLA and PBAT films

Sample	"Tg" PLA (°C)	"Tg" PBAT (°C)	Cold crystallization temperature "Tcc" (°C)	Cold crystallization Enthalpy (J/g)	Melt temperature "Tm" (°C)	Melt Enthalpy (J/g)
PLA_Cast	60	---	107	32	170	36
PLA_Stretched	69	---	---	---	168	38.5
PBAT_Cast	---	-29	---	---	122	24
PBAT_Stretched		-29	---	---	121	30

Sample	Calculated Crystallinity (%)	Estimated Crystallinity by "Hermans and Weidinger" method
PLA_Cast	4.3	1.09
PLA_Stretched	41	30
PBAT_Cast	23	3.23
PBAT_Stretched	26	11

However, for PBAT film, there is no indication about the crystal planes according to WAXD patterns. Moreover, there is a need to undertake more experiments (WAXS analysis for instance) in

order to get deeper understanding of PLA and PBAT crystallization under strain. Therefore, figure VI-8 depicted the X-ray diffraction on two different zones (Central and Arm zones) of each stretched sample and compared to the un-stretched films.
In PLA and PBAT case, regarding to the arm of the specimen, the intensity profile is quite similar to the one of the undrawn samples, confirming that absolutely minor thermal crystallization can occur during biaxial stretching. For PLA, the evolution of the diffraction peak at around 2θ =32° is subjected to a solid-state extrusion [38][44]. The stretched central zone of PLA is crystalline and highly oriented according to in –situ 2D-WAXS patterns. An important peak at 2θ =15.5°, calculated from the Bragg relation and corresponding to (110) and (200) plans was observed. It is ascribed to the α-form of PLLA as reported by other authors [30][63]. By using Bragg's law, interplanar spacing between its different crystalline planes was evaluated to be 2.5Å and 2.9Å. The appearance of 2θ =15.5° and the improvement of the peak intensity indicates the increase in the number and size of perfect crystalline structure and higher crystallinity [37]. Meanwhile, for PBAT samples, several characteristic crystallographic reflections in WAXD pattern are observed in un-stretched and summarized in table VI-4.

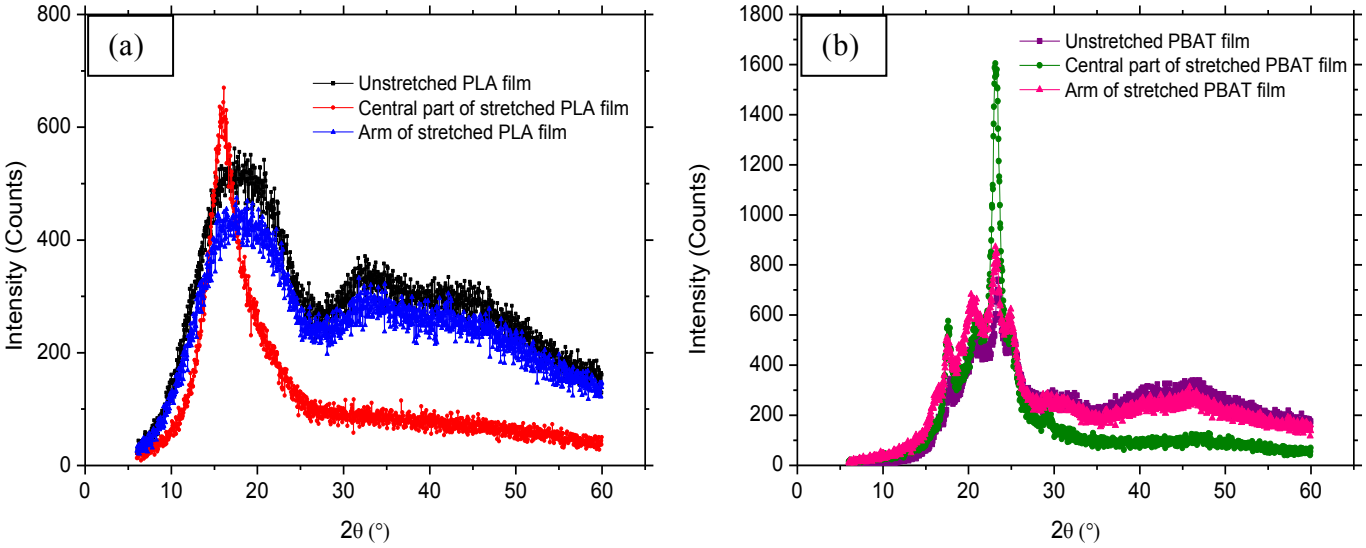

Figure VI-8 Integrated intensity profiles of the 2D-patterns of unstretched, Central part/Arm parts for stretched films for a) PLA and b) PBAT

The presence of such peaks confirmed the coexistence of α- and β-forms of PBT [64] [49].

Table VI-4 The *(hkl)* crystalline plans observed in extruded PBAT film

2θ (°)	*hkl* crystalline plans	2θ (°)	*hkl* crystalline plans
16.06	$(0\bar{1}1)$	25.3	$(1\bar{1}1)$
17.9	(010)	29.3	$(\bar{1}04)$
20.74	$(\bar{1}01)$	31.5	$(\bar{1}04)$
23.38	(100)	43	$(\bar{1}04)$

Therefore, for stretched PBAT film, the appeared crystalline peaks are at 2θ = 17.9 (010), 20.74 ($\bar{1}$01), 23.38 (100), 25.3 (1$\bar{1}$1), 28.9° ($\bar{1}$04). The last peak is the most representative peak of β-forms of PBT [57]. Based on the analysis, the crystal structure of PBAT was characterized to be formed by mixed-crystallization of BT and BA units, where BA units were incorporated into the BT lattice. This mixed-crystal structure was found to undergo PBT-like reversible crystal modification. Table VI-6 summarizes the four interplanar spacing of PBAT determined according to Bragg's law, which were evaluated to be 1.7, 1.9, 2 and 2.9Å. Unlike PLA, PBAT shrinks due to its elastomeric property during the transition from stretching to relaxation. This is related to the coexistence of soft (BA units) and hard segments (BT units), hence the need of "thermo-setting" at the end of the biaxial drawing experiments.

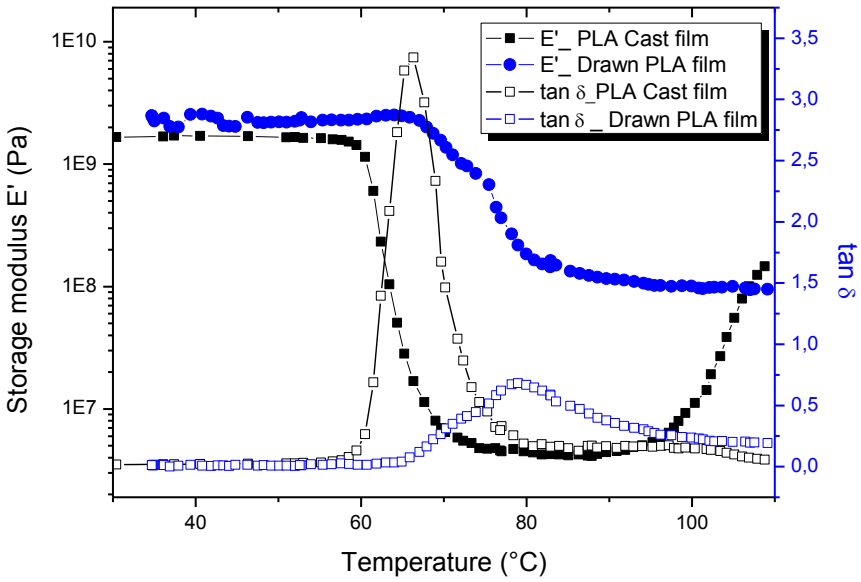

Figure VI-9 Plots of storage modulus (E') and loss factor (tan δ) versus temperature for extruded and drawn PLA films

Figure VI-9 shows the influence of temperature on storage modulus, E' and loss factor, tan δ as measured by dynamic viscoelastic analysis for both Cast and drawn PLA films. With respect to the glass transition peak, the initial cast PLA exhibit sharp tan δ peak at 65°, whereas samples in which orientation-induced crystallization occurs exhibit weak broad peak around 79°C for PLA. The increase in E' in the drawn PLA samples between 80 and 100°C is probably due to the occurred crystallization during stretching measurements. Furthermore, the T_g values obtained by DMTA are not exactly the same as those given by DSC. Such discrepancies have been reported and discussed by many authors for various polymeric systems [65][66]. They are ascribed to the heating rate and loading frequency used in both experiments. T_α is defined as the temperature mechanical transition accorded to the glass transition temperature T_g.

Summarizing the above, it is interesting to find that mixed-crystal structure of BT and BA units also undergoes PBT-like crystal form. The diffraction patterns of modified drawn PLA samples demonstrate arcs that are sharp and concentrated in center, indicating large crystalline orientation compared to undrawn film. However, the intensity of the arcs is decreased for modified drawn PBAT sample; the generation of numerous small crystals can be concluded. Finally, the experi-

ment undertaken in our conditions leads to crystallization occurring during the deformation, which could confirm the lock-in of the chains conformation of neat PLA and PBAT [67].

IV.2 Biaxial stretching of long chain randomly branched PLA and PBAT

In our previous study, we have demonstrated that PLA and PBAT can be chain extended by reactive extrusion with a multifunctional epoxide, named Joncryl ADR®-4368. We have also shown that the final modified polymers are obtained from the balance chain extension reaction and branching [12].
The effect of Joncryl on the non-isothermal crystallization of both PLA and PBAT was firstly investigated. The DSC thermograms represented in figure VI-10a), obtained from the second heating at 10°C/min with various compositions of chain extension/branching agent. It reveals some interesting changes in the crystallization behavior when going from neat to modified polymer. Regarding the cold crystallization of the modified PLA, it can be noticed that the related exothermic peak is shifted to lower temperatures from the neat suggesting a nucleating effect of the multifunctionalized epoxide, which is also confirmed by the isothermal crystallization represented in figure VI-10b. The same trend is observed for the melting peaks for both PLA and PBAT.
As can be seen in Figure VI-10b), the crystallization process at the drawing temperature (75°C) is faster for the chain extended/branched PLA with an amount of Joncryl close to 0,7%. Numerous thermal crystals are generated during the time scale of the experiment compared to neat and modified PLA with 0,5%wt of Joncryl where a minor thermal crystallization is induced. This can be understood by the fact that Joncryl promotes the kinetic of crystallization [47]. Therefore, no thermal crystallization is observed for modified PBAT regardless the amount of Joncryl, indicating that no induced thermal crystallization during biaxial drawing could be developed.

Furthermore, the stress-strain curves obtained under our processing conditions are shown in figures VI-11a) and VI-11b) for linear and extended/branched PLA, PBAT films, respectively. In the strain hardening region and with the incorporation of Joncryl ADR®, a slight earlier strain hardening accompanied with an increase of the stress before break was occurred. Such accelerated strain hardening might be related to the nucleating effect of Joncryl ADR®and the reduced PLA volume fraction because of the depression of chain contraction. Besides, Menary et al. [68] related this occurred phenomenon in one hand to the fact that a sufficient level of orientation for strain hardening can occur during deformation process at a lower strain for the samples having higher intrinsic viscosity. In the other hand, the increasing number of entanglements per chain leads to an increase in resistance to entanglement slippage, which in turn promotes an earlier strain hardening.

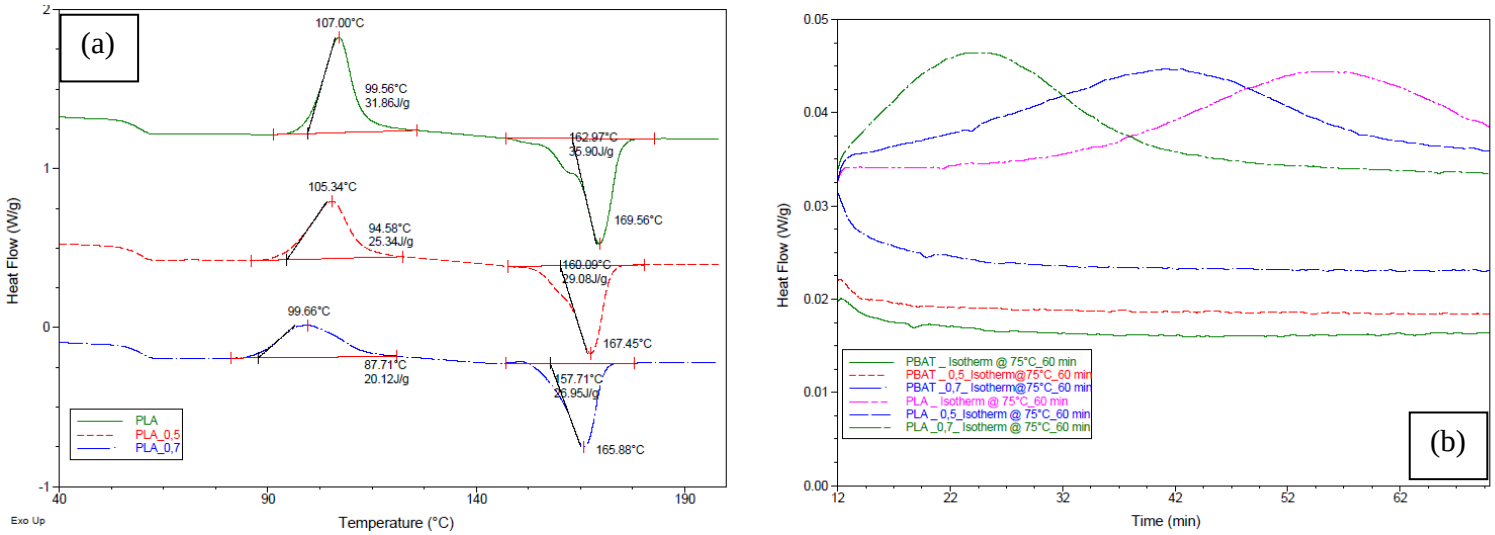

Figure VI-10 DSC thermograms for a) non-isothermal crystallization for neat and chain extended/branched PLA and b) isothermal crystallization at 75°C for neat and modified PLA and PBAT polymers

Unlike PLA, the incorporation of Joncryl ADR® into PBAT matrix did not show any structural changes, as shown in figure VI-11b.

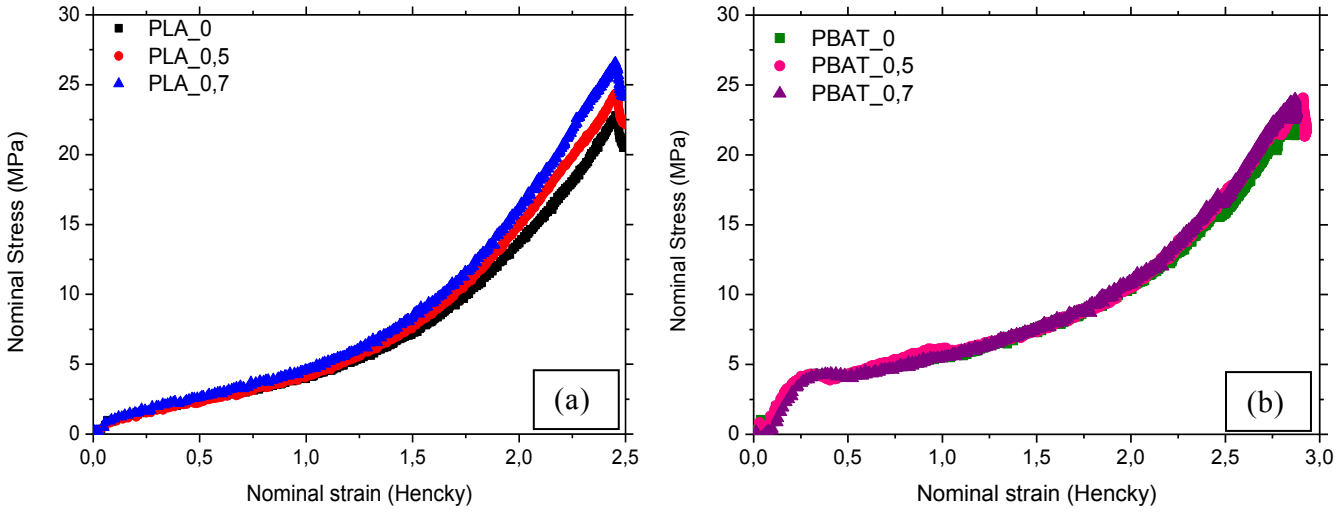

Figure VI-11 Nominal stress vs. Nominal biaxial strain curves for neat and chain extended/branched a) PLA and b) PBAT samples

The DMTA measurements of cast modified PLA films with Joncryl ADR® are presented in figure VI-12a). A reduction of the rubbery zone of PLA was observed. The tan δ peak amplitude is not affected by the presence of long and branched chains in PLA matrix. The increase in E' in the drawn modified PLA samples, as shown in figure VI-12b) between 80 and 100°C is certainly due to the occurred crystallization during stretching measurements.
When the studied films are oriented, significant changes in their thermal and crystallization properties were detected. These properties are presented in figures VI-13a and VI-13b. It was shown that the cold crystallization of modified and unmodified PLA films disappeared. The related

mechanism can be explained by the reduced entropy of the polymer chains due to an increased orientation in the amorphous regions as the deformation proceeds. On the other hand, the increase in crystalline domains in the system restricts the molecular mobility in the amorphous domains, which become aligned in the stretching directions and as a result the increase of "T_g". Besides, the glass transition is immediately followed by two distinct endotherms, more pronounced for drawn modified PLA. The presence of the first slight endothermic peak, when passed the glass temperature at around 70°C isrelated to the PLA physical aging and can falsify the determination of the T_g value more accurately. Moreover, the second endothermic peak, near 80°C can be probably due to either a thermal relaxation enthalpy or melting of formed mesophase upon biaxial stretching. The presence of the mesomorphic phase was demonstrated by Stoclet et al. [69]. They showed that this mesophase is almost as much cohesive as the crystalline form in spite of its imperfect ordering and it can be formed for a slightly semi-crystalline PLA (X=5%) at 75°C. All these observations were confirmed by other different studies [70][71][72].

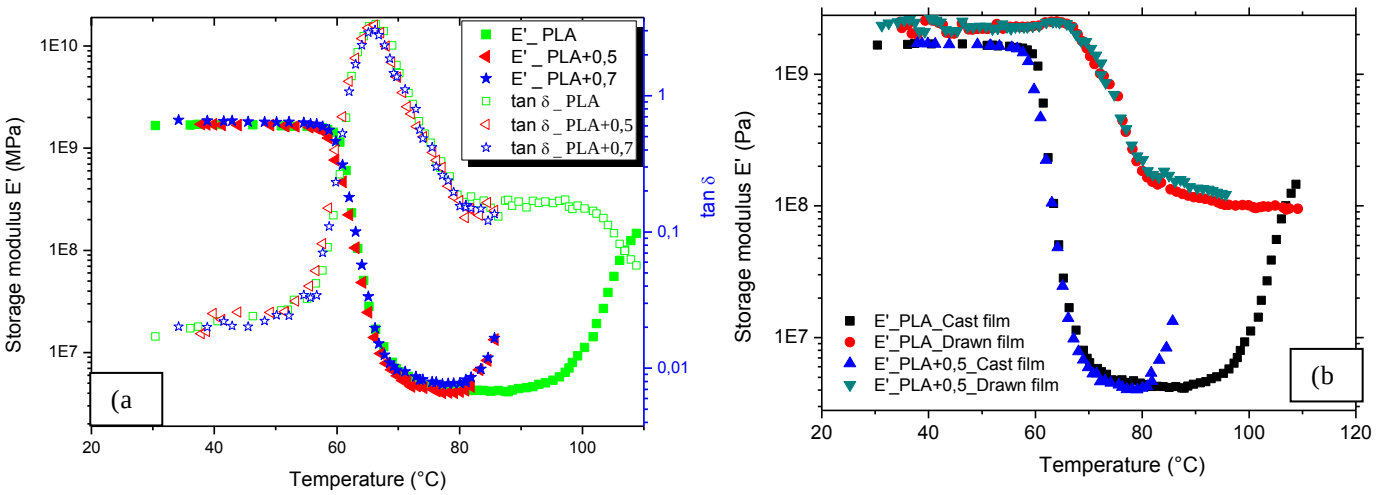

Figure VI-12 a) Plots of storage modulus (E') and loss factor (tan δ) versus temperature for cast neat and modified PLA, b) Plots of storage modulus (E') versus temperature for cast and drawn neat and modified PLA

It is worth notice that the stretched modified PLA and PBAT are semi-crystalline films. The crystallization level is shown to be increased greatly due to the stretching, as confirmed by in –situ 2D-2-WAXS, WAXD, patterns and the estimated value following Hermans and Weidinger method presented in figure VI-14, VI-16 and table VI-5 respectively. Figure VI-14 shows 2D-WAXS patterns for different studied samples recorded for the drawing at 75°C. The cast neat and modified PLA films look amorphous.

Moreover, drawing modified PLA with 0,5 and 0,7 %wt (Figure VI-14, parts d and f) gradually promotes the growth of crystalline phase with a strong fiber texture. A partially well-developed three-dimensionally ordered crystalline phase (α' crystal form) is observed in parallel with the mesomorphic form ((200 & 110)). Different crystalline peaks were thus detected and correspond to (203 & 113), (206 & 116) and (0 0 10) as shown in figure VI-15 [10]. The interplanar spacing values between these plans were summarized in Table VI-6.

The remaining amorphous phase still displays a rather low chain orientation, as revealed by the nearly uniform intensity of the amorphous halo.

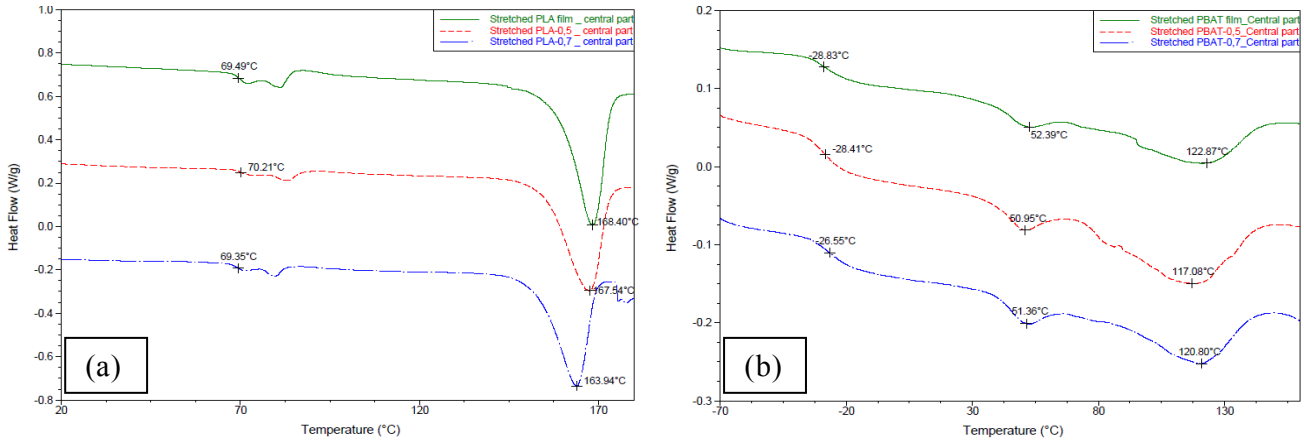

Figure VI-13 DSC thermograms of a) neat and modified PLA and b) neat and modified PBAT with 0,5 and 0,7%wt of Joncryl during the first heating at 10°C/min

However, as shown in figure VI-14 - parts g to l, for PBAT samples, the absence of the X-ray diffraction clear line is probably due to the smaller size of crystallites compared to the wavelength of the characteristic line x-rays from the x-ray tube.

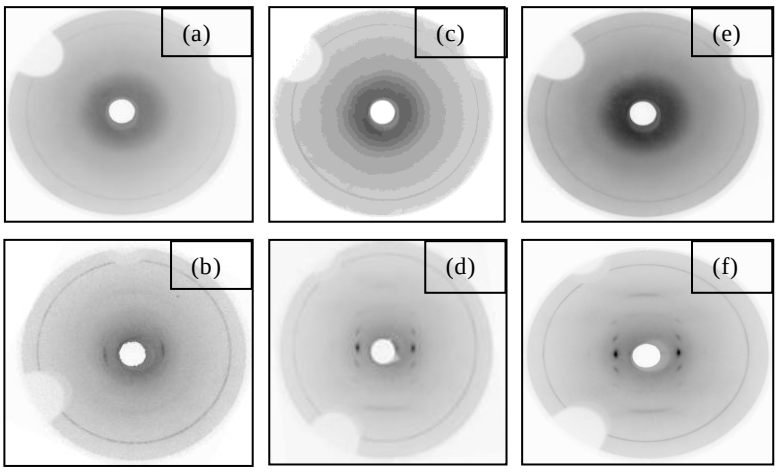

(a) Unstretched PLA, (b) Stretched_PLA_Central part, (c) Unstretched_PLA_0,5, (d) Stretched_PLA_0,5_Central part, (e) Unstretched_PLA_0,7, (f) Stretched_PLA_0,7_Central part

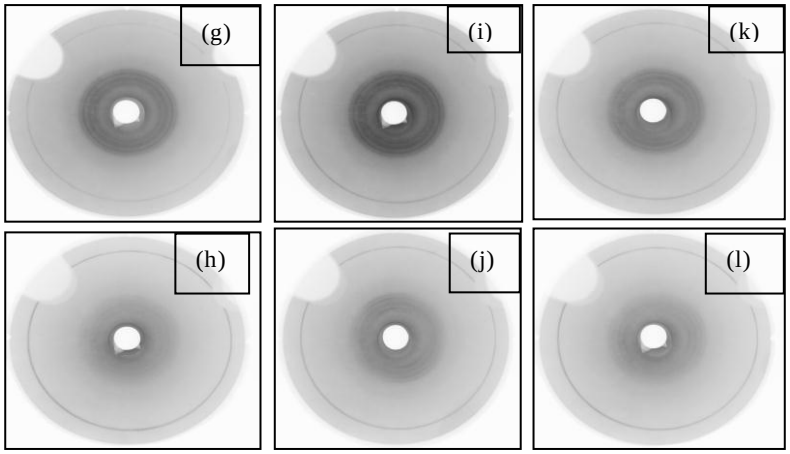

(g) Unstretched_PBAT, (h) Stretched_ PBAT _Central part , (i) Unstretched_ PBAT _0,5 , (j) Stretched_ PBAT _0,5_Central part , (k) Unstretched_ PBAT _0,7, (l) Stretched_ PBAT _0,7_Central part

Figure VI-14 2-WAXS patterns of specimens taken from the central part of the samples

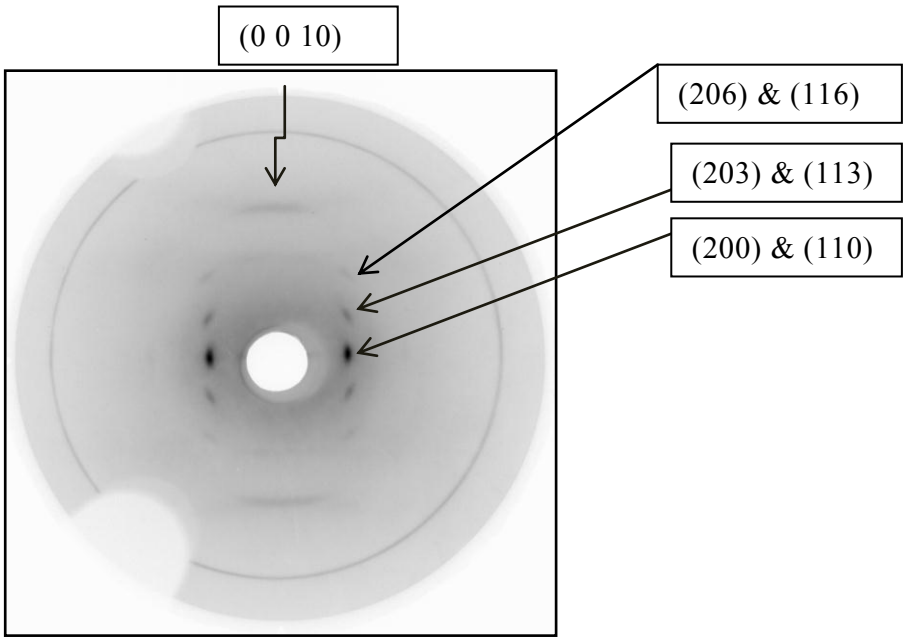

Figure VI-15 Illustration of crystal planes of drawn modified PLA films

According to WAXS experiments (Cf. figure VI-16), the crystalline structure of the cast film of chain extended/branched PBAT is very similar to the neat PBA. Besides, the same crystalline structure is observed for drawn neat and modified PBAT.

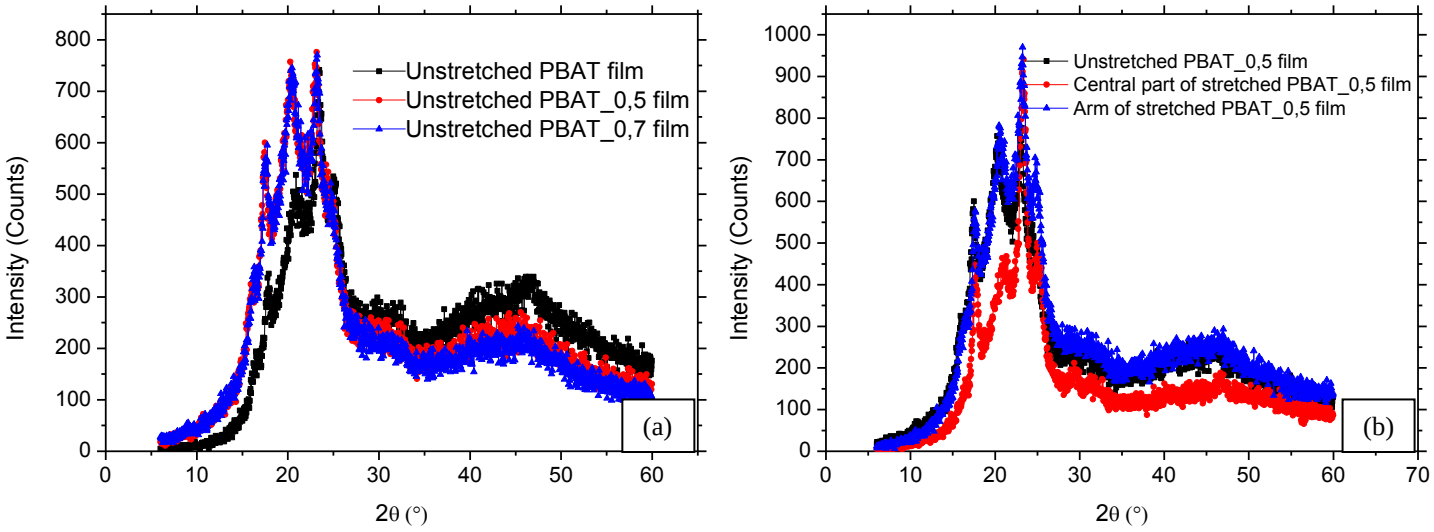

Figure VI-16 Integrated intensity profiles of the 2D-patterns of a) unstretched neat and modified PBAT and b) comparison between the extruded-film and Arm/ Central part of the stretched one

The Hermans and Weidinger method whose values are reported in Table VI-5 highlights the strain-induced crystallization occurred for neat and modified PBAT films. A significant increase of the estimated crystallinity was shown after stretching.

Table VI-5 Thermal properties and the crystallinity evolution of a) cast film of neat and modified PLA and PBAT films and b) neat and modified stretched PLA and PBAT films

a) Sample	"Tg" PLA (°C)	"Tg" PBAT (°C)	Cold crystallization temperature "Tcc" (°C)	Cold crystallization Enthalpy (J/g)	Melt temperature "Tm" (°C)	Melt Enthalpy (J/g)
PLA_0	60	---	107	32	170	36
PLA_0,5	60	---	105	25	167	29
PLA_0,7	60	---	100	20	165	27
PBAT	---	-29	---	---	122	24
PBAT_0,5	---	-29	---	---	120	23
PBAT_0,7	---	-30	---	---	120	22

Sample	Crystallinity (%)	Estimated Crystallinity by "Hermans and Weidinger"method
PLA_0	4.3	1,09
PLA_0,5	4.3	1,07
PLA_0,7	7.5	2,2
PBAT	23	3,23
PBAT_0,5	20	5,66
PBAT_0,7	21	5,06

b) Sample	"Tg" PLA (°C)	"Tg" PBAT (°C)	Melt temperature "Tm" (°C)	Melt Enthalpy (J/g)	Estimated Crystallinity by "Hermans and Weidinger"method
PLA_0	69	---	168	38.5	29,7
PLA_0,5	70	---	167	35.5	35,5
PLA_0,7	69	---	164	30	-----
PBAT	---	-29	51-121	30	11,07
PBAT_0,5	---	-28	51-117	27	7,11
PBAT_0,7	---	-26	51-121	25	8,09

Table VI-6 The optimum strain hardening parameter and the interplanar spacing between the different crystalline planes for biaxial drawn neat and modified PLA and PBAT and their blends

Samples	Strain-hardening parameter (SHP) or strain threshold [73] (Hencky)	d_{hkl} (Å)
PLA_0	1.67	2.5-2.9
PLA_0.5	1.6	1.5-1.8-2.4-2.6-2.8
PLA_0.7	1.51	1.5-1.9-2.3-2.5-2.7
80PLA_20PBAT_0	1.6	2.9
80PLA_20PBAT_0.5	1.5	1.5-1.8-3-2.85
80PLA_20PBAT_0.7	1.5	1.4-1.85-2.4-2.85-2.2

Samples	Strain-hardening parameter (SHP) or strain threshold [73] (Hencky)	d_{hkl} (Å)
PBAT_0	2	1.7-1.9-2-2.9
PBAT _0.5	2	1.8-2-2.3-2.85
PBAT _0.7	2	1.7-1.8-2.3-2.85
20PLA_80PBAT_0	2	1.8-2.6-2.8-2-1.9
20PLA_80PBAT_0.5	2	2-2.2-2.5-3
20PLA_80PBAT_0.7	1.5	2-2.2-2.5-3

IV.3 Biaxial stretching properties of PLA/PBAT blends

Polylactic acid (PLA)/ Poly (butylene adipate-co-terephtalate) (PBAT) blends are also prepared and their properties were compared to those of neat, modified PLA and PBAT [12]. In our best of knowledge, no effort has been dedicated to study the microstructural evolution of such blends under uniaxial deformation. In the following section, the study of the orientation induced crystallization of PLA/PBAT/Joncryl films has been carried out. All studied films were presented in table VI-1.

On one hand, we demonstrated that the incorporation of PBAT into PLA matrix decreased the cold crystallization temperature indicating an enhanced crystalline ability of PLA. Therefore, adding PBAT did not increase significantly the final crystallinity of the PLA in the blend. We should point out that we demonstrated in our previous work that the chain extension/branching agent acts as a compatibilization agent in blends of polyesters.

The TEM observations related to the compatibilized and uncompatibilized PLA/PBAT blends prepared in this present study are shown in figure VI-17. A finer dispersion, related to a decrease of the interfacial tension, of PBAT into PLA matrix and of PLA into PBAT matrix was highlighted.

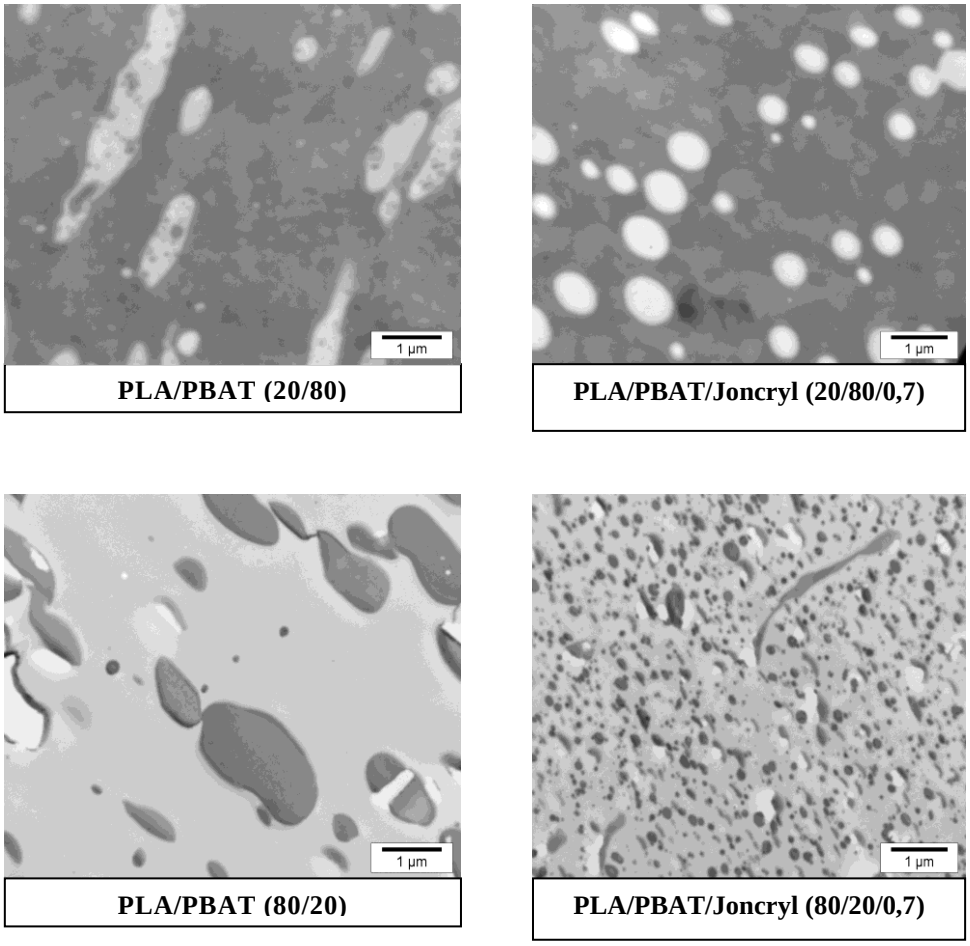

Figure VI-17 TEM observations of modified and unmodified cast PLA/PBAT films

Figure VI-18 shows the plotted nominal stress versus nominal strain for simultaneously stretched blends prepared with and without compatibilizer.

Each blend was stretched up to a final biaxial draw ratio close to 2.4 Hencky. It was observed that the stretchability of PLA/PBAT films was improved at 75°C for higheramounts of PBAT, according to the values of strain threshold reported in table VI-6.

Moreover, the presence of a compatibilizer agent in PLA/PBAT blends caused thus a slightly earlier strain-hardening phenomenon while increasing the maximum stress before breaking. This increase is more pronounced for compatibilized PLA/PBAT (20/80) (w/w) with 0,7%wt of Joncryl. We should point out that the strain hardening is shifting to lower values due to the highly entanglements density that prevented chain relaxation as reported in the literature [37].

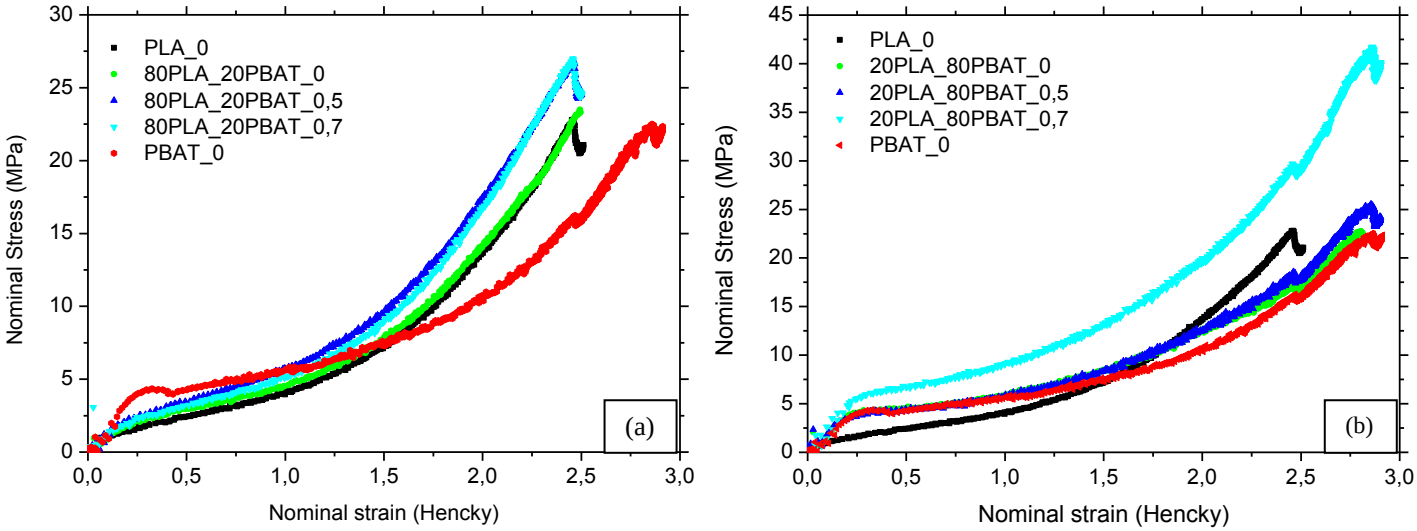

Figure VI-18 Nominal stress vs. Nominal biaxial strain curves for uncompatibilized and compatibilized a) PLA_PBAT (80/20) and b) PLA_PBAT (20/80)

In the other hand, for biaxial stretching PLA/PBAT films having higher contents of PLA, we observed in figure VI-19 an endothermic peak (stain induced enthalpy relaxation) close to "T_g" of PLA which is attributes once time again to either the melting of the formed mesophase or the PLA physical aging. Also, the cold crystallization disappeared after stretching. A possible explanation is related to the increase of fraction of oriented amorphous chains [34].
The increase of the crystallization amount after biaxial drawing was also demonstrated by DSC method. Table VI-7 summarizes the different values of the thermal and crystallization properties of unmodified and modified PLA/PBAT blends.

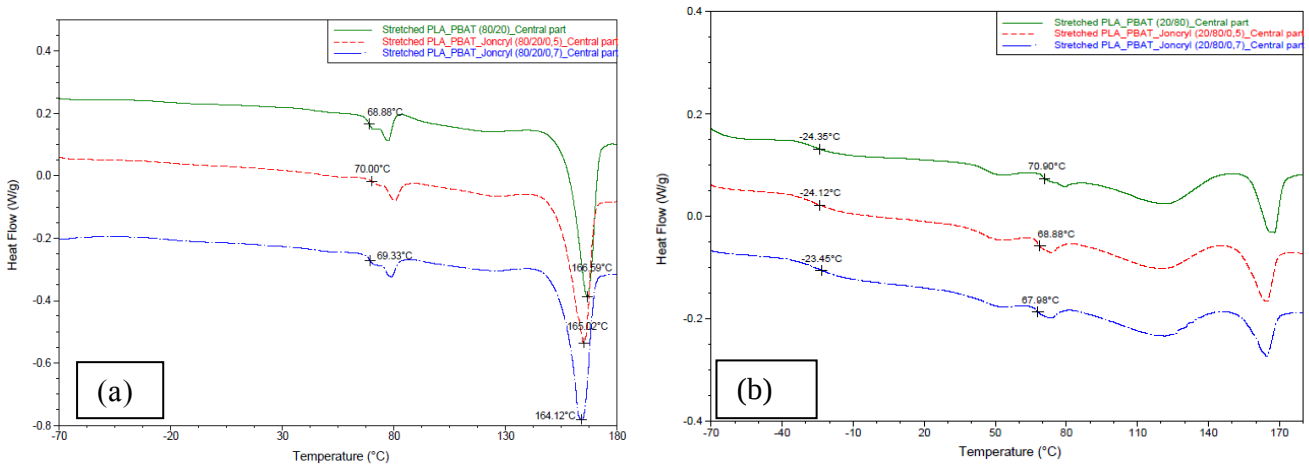

Figure VI-19 DSC thermograms of a) uncompatibilized and compatibilized PLA_PBAT (80/20) and b) uncompatibilized and compatibilized PLA_PBAT (20/80) during the first heating at 10°C/min

Table VI-7 Thermal properties and the crystallinity of a) modified and unmodified PLA/PBAT blends_Cast films and b) modified and unmodified PLA/PBAT blends_Drawn films

a) Sample	"T_g" PLA (°C)	"T_g" PBAT (°C)	Cold crystallization temperature "T_{cc}" (°C)	Cold crystallization Enthalpy (J/g)	Melt temperature "T_m" (°C)	Melt Enthalpy (J/g)	Crystallinity (%)
PLA_PBAT_Joncryl (80/20/0)	59	-32	102	23	168.5	27	5.3
PLA_PBAT_Joncryl (80/20/0,5)	59	-27	101.5	16	166	19.5	4,7
PLA_PBAT_Joncryl (80/20/0,7)	59	-27	105	18	167	20	2,6
PLA_PBAT_Joncryl (20/80/0)	60	-28	103	2,7	168	12	12.5
PLA_PBAT_Joncryl (20/80/0,5)	60	-28	105	6	167	12	8
PLA_PBAT_Joncryl (20/80/0,7)	60	-29	107	1	166	7.5	8

b) Sample	"T_g" PLA (°C)	"T_g" PBAT (°C)	Melt temperature "T_m" (°C)	Melt Enthalpy (J/g)	Crystallinity (%)
PLA_PBAT_Joncryl (80/20/0)	68.5	-23	166.5	29	39
PLA_PBAT_Joncryl (80/20/0,5)	70	-22	165	28	38
PLA_PBAT_Joncryl (80/20/0,7)	69	-24	164	30	40
PLA_PBAT_Joncryl (20/80/0)	70	-24	168	22	24
PLA_PBAT_Joncryl (20/80/0,5)	69	-24	165	19	21
PLA_PBAT_Joncryl (20/80/0,7)	67	-23	165	17	19

IV.4 Effect of the strain rate on the mechanical properties of PLA/PBAT blends

The effect of the strain rate on the mechanical properties of PLA/PBAT blends was studied. Figure VI-20 shows that the Strain –Stress curves for drawn pure PLA and PBAT and their unmodified blends are independent of the strain rate, in particular when going from 0,004 s-1 (0,1mm/s) to 0,4 s-1 (10mm/s). However, the biaxial stretching of the modified PLA, PBAT and their blends with Joncryl is greatly dependent of the strain rate.

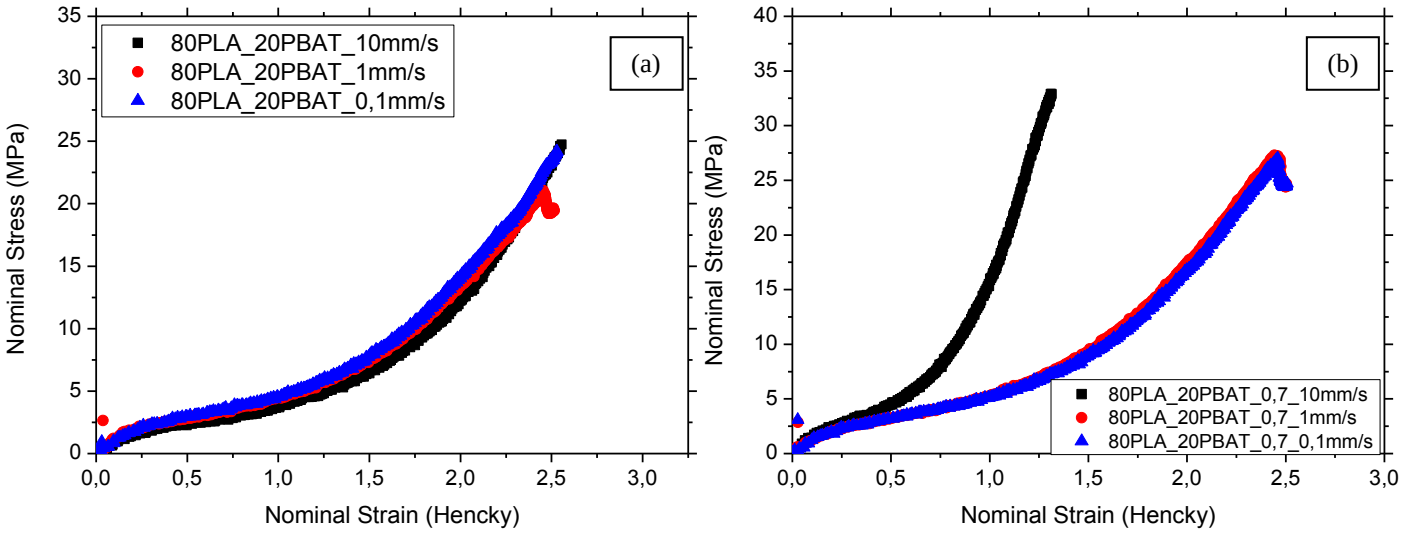

Figure VI-20 Nominal stress vs. Nominal biaxial strain curves for a) uncompatibilized PLA/PBAT blends and b) compatibilized PLA/PBAT blends at different strain rates

An earlier strain hardening was observed at 0,4 s-1 (10mm/s). In this case, the solicitation time is lower than the reptation time of polymer chains which means that the orientation along stretching direction increases faster than chains relaxation. However, the deformed chains at low extension rate have sufficient time to relax, resulting in the low chain orientation. Similar mechanical behavior was observed in PET stretched above the glass transition temperature [54].

IV.5 Effect of annealing on the mechanical properties on modified and unmodified PLA, PBAT and their blends

The effect of annealing on the stretching films properties was also investigated. It was observed that the samples turned opaque when annealed at 100°C during 1 hour. Figure VI-21 shows the reduction of the ability of polymer to be stretched during annealing for all the studied films based on PLA. Different hypothesis can explain this phenomenon, as reported in the literature: [31][34]

- The formation of isolated small crystals randomly distributed in the polymer sheet. The presence of crystallites result in the formation of defects in the polymer film which hindered the elongation of polymer during stretching process and resulted in un-uniform film
- The imperfect and small crystals are melted and re-crystallized into larger and more perfect crystalline state. Thus, the chain segments spanning the amorphous phase become less mobile
- The retraction of the chain helix

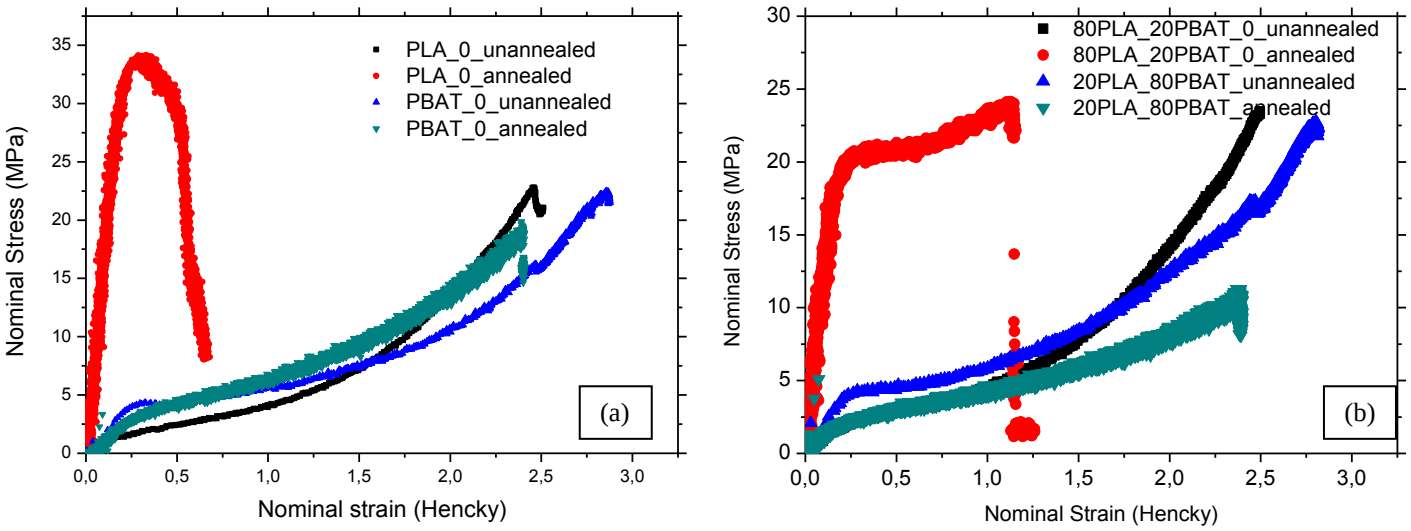

Figure VI-21 Nominal stress vs. Nominal biaxial strain curves for a) annealed and unannealed pure polymers and b) annealed and unannealed PLA/PBAT blends

The initial crystallinity, caused by annealing, was confirmed by the increase of the storage modulus E' at room temperature up to 100°C, regardless the PLA/PBAT ratio as shown in figure VI-22. It provides a physical crosslinking and prevents the chain relaxation and thus promotes an early orientation of the strained chains. Besides, the significant increase of the stress is related to the high strength and toughness caused by the annealing.

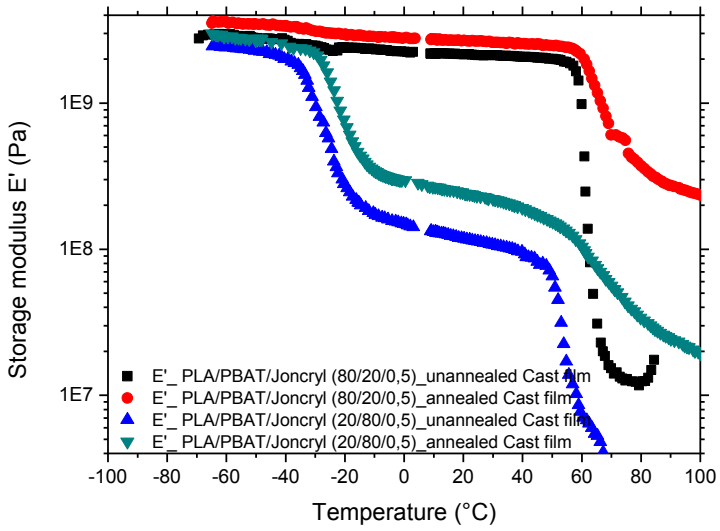

Figure VI-22 Plots of storage modulus (E') versus temperature for compatibilized annealed and unannealed PLA/PBAT films

Conclusions

On the basis of the thermal/thermomechanical characterizations, X-ray diffraction and mechanical behavior studies of the specimens, we may draw several conclusions. Firstly, the isothermal crystallization help us understanding that Joncryl promotes the kinetic of crystallization with big crystals domains for modified PLA. Regarding to the arm of the specimen, the intensity profile is quite similar to the one of the undrawn sample, confirming that absolutely minor thermal crystallization can occur during biaxial stretching during the time scale of our experiments. Secondly, the load-extension curves of PLA and PBAT at 75°C follow the typical rubber –like ductile deformation behavior.

The stretched central zone of PLA is crystalline and highly oriented according to in –situ 2D-WAXS patterns where two very sharp meridional peaks superposed over the amorphous halo. Besides, it is interesting to find that mixed-crystal structure of BT and BA units also undergoes PBT-like crystal form. Thirdly, some differences are observed in the strain hardening region for modified PLA with a chain extension/branching agent. In comparison with linear PLA, the onset of strain-hardening of modified PLA with Joncryl appears slightly before and is accompanied with a reduced optimum draw ratio. Different crystalline planes were detected in parallel with the mesomorphic phase. Unlike PLA, the incorporation of Joncryl into PBAT matrix did not show any structural changes regardless the incorporated amount.

Fourthly, it was observed that the stretchability of PLA/PBAT films was improved at 75°C for high amounts of PBAT. Moreover, the presence of chain extension/branching/compatibilization agent in PLA/PBAT blends caused thus an earlier strain-hardening phenomenon while increasing the maximum stress before breaking. Furthermore, the increase of strain rate leads also to an earlier strain-hardening for modified polymers and their respective modified blends. Finally, a significant increase of the stress at break related to the high strength and a significant reduction of the stretching ability are caused by the annealing.

References

[1] Gross RA, Kalra B. Biodegradable polymers for the environment. Science. 297 (5582): 803–807. 2002.
[2] Schut H. What's ahead for green plastics. Plastics Technology. 54(2): 64–89. 2008.
[3] Stevens ES. Green plastics: an introduction to the new science of biodegradable plastics. Princeton University Press, NJ (2002) 238 clothISBN: 0-691-04967-X
[4] Lunt J. Large-scale production, properties and commercial applications of polylactic acid polymers. Polymer Degradation and Stability. 59(1-3):145–152.1998.
[5] Lim LT, Auras R, Rubino M. Processing technologies for poly(lactic acid). Progress in Polymer Science. 33(8): 820–852. 2008
[6] Auras R, Harte B, Selke S. An overview of polylactides as packaging materials. Macromolecular Bioscience. 4(9): 835–864. 2004.
[7] Hashitani T, Yano E, Ando Y. Biodegradable packing materials for LSIs. Science and Technology Journal. 38 (1): 112–118. 2002.
[8] Harris AM, Lee EC. Heat and humidity performance of injection molded PLA for durable applications, Journal of Applied polymer Science. 115(3): 1380–1389. 2010.
[9] Takayama T, Todo M. Improvement of impact fracture properties of PLA/PCL polymer blend due to LTI addition. Journal of Materials Science. 41(15): 4989-4992. 2006.
[10] Ou X, Cakmak M. Influence of biaxial stretching mode on the crystalline texture in polylactic acid films. Polymer. 49(24): 5344-5352. 2008.
[11] Parelukar YS. Modified biobased materials from polyhydroxyalkanoates for packaging and engineering applications. Ph.D., Michigan State University. 284 pages. 2007.
[12] AL-Itry R, Lamnawar K, Maazouz A, Improvement of thermal stability, rheological and mechanical properties of PLA, PBAT and their blends by reactive extrusion with functionalized epoxy. Polymer Degradation and Stability. 97(10): 1898–1914. 2012.
[13] Li H, Huneault M. Effect of nucleation and plasticization on the crystallization of poly(lactic acid). Polymer. 48(23):6855-6866. 2007.
[14] Kawamoto N, Sakai A, Horikoshi T, Urushihara T, Tobita E. Nucleating agent for poly(l-lactic acid) – an optimization of chemical structure of hydrazide compound for advanced nucleation ability. Journal of Applied Polymer Science. 103(1):198-203. 2007.
[15] Byrne F, Ward PG, Hughes D, Cullen J, Dowling DP, Comparative study of the processing conditions required for PLA and PET polymers. Proceedings of the IMF Conference, Waterford Institute of Technology. 2007.
[16] Wentao Z, Yoorim K, Wenli Z, Anson W, Chul B P. A Study of the Crystallization, Melting, and Foaming Behaviors of Polylactic Acid in Compressed CO2. International Journal of Molecular Sciences. 10(12), 5381-5397. 2009.
[17] Gupta B, Revagade N, Hilborn J. Poly(lactic acid) fiber: An overview. Progress in Polymer Science. 32(4): 455-482. 2007.
[18] Auras R, Harte B, Selke S. An overview of polylactides as packaging materials. Macromolecular Bioscience. 4(9): 835-864. 2004.
[19] Stoclet G, Seguela R, Vanmansart C, Rochas C, Lefebvre JM. WAXS study of the structural reorganization of semi-crystalline polylactide under tensile drawing. Polymer. 53(2): 519-528. 2012.
[20] Yasuniwa M, Tsubakihara S, Iura K, Ono Y, Dan Y, Takahashi K. Crystallization behaviour of poly(L-lactic acid). Polymer. 47(21): 7554–7563. 2006.
[21] Tsuji H, Takai H, Saha SK. Isothermal and non-isothermal crystallization behavior of poly(L-lactic acid): Effect of stereocomplex as nucleating agent. Polymer. 47(21): 3826–3837. 2006.
[22] Yu L, Dean K, Li L. Polymer blends and composites from renewable resources. Progress in Polymer Science. 31(6), 576–602. 2006.

[23] Yeh JT, Wu CJ, Tsou CH, Chai WL, Chow JD, Huang CY, Chen KN, Wu CS. Study on the crystallization, miscibility, morphology, properties of poly(lactic acid)/poly(ε-caprolactone) blends. Polymer Plasics Technology and Engineering. 48(6), 571–578. 2009.
[24] Pan P, Zhu B, Kai W, Dong T, Inoue Y. Effect of crystallization temperature on crystal modifications and crystallization kinetics of poly(l-lactide). Journal of Applied Polymer Science. 107 (1): 54–62. 2008.
[25] Magon A, Pyda M. Study of crystalline and amorphous phases of biodegradable poly(lactic acid) by advanced thermal analysis. Polymer. 50(16): 3967–3973. 2009.
[26] Hoogsteen W, Postema AR, Pennings AJ, Brinke GT. Crystal Structure, Conformation, and Morphology of Solution-Spun Poly(L-lactide) Fibers. Macromolecules. 23(2): 634-642. 1990.
[27] Chapleau N, Huneault MA, Li H. Biaxial orientation of polylactide/thermoplastic starch blends. International Polymer Processing. 22(5): 402–409. 2007.
[28] Kokturk G, Serhatkulu TF, Cakmak M, Piskin E. Evolution of phase behavior and orientation in uniaxially deformed polylactic acid films. Polymer Engineering and Science. 42(8), 1619–1628. 2002.
[29] Mihai M, Huneault MA, Favis BD. Rheology and extrusion foaming of chain-branched poly(lactic acid). Polymer Engineering and Science. 50(3):629-642. 2010.
[30] Tabatabaei S, Ajji A. Crystal structure and orientation of uniaxially and biaxially oriented PLA and PP nanoclay composites films. Journal of applied polymer science. 124(6): 4854-4863. 2001.
[31] Ou X, Calmak M. Comparative study on development of structural hierarchy in constrained annealed simultaneous and sequeltial biaxially stretched polylactic acid films. Polymer. 51(3): 783-792. 2010.
[32] Stoclet G, Seguela R, Lefebvre JM, Elkoun S, Vanmasart C. Strain-induced molecular Ordering in polylactide upon uniaxial stretching. Macromolecules 43(3): 1488-1498. 2010.
[33] An YK. Crystallization behavior of polylactide on highly oriented polyethylene thin films. Chinese Journal of polymer Science. 29(4): 513-519. 2011.
[34] Yu L, Liu H, Xie F, Chen L, Li X. Effect of annealing and orientation on microstructures and mechanical properties of polylactic acid. Polymer Engineering and Science. 48(4): 634-641. 2008.
[35] Kawahima N, Ogawa S, Obuchi S, Matsuo M, Yagi T. Polylactic acid "LACEA", Biopolymers. Polyesters III. Applications and Commercial Products, 1st edition, Y. Doi, A. Steinbuchel, Eds., Wiley-VCH Verlag GmbH, Weiheim, 251-274, 2002.
[36] Ikada Y, Tsuji H. Biodegradable polyesters for medical and ecological applications. Macromolecular Rapid Communications. 21(3): 117-132. 2000.
[37] Rao Y, Greener J, Avila-Orta AC, Hsiao BS, Blanton TN. The relationship between microstructure and toughness of biaxially orientend semi-crystalline polyester films. Polymer. 49(10): 2507-2514. 2008.
[38] Pluta M, Galeski A. Plastic deformation of amorphous poly(L/DL-lactide):Structure Evolution and physical properties. Biomacromolecules. 8(6):1836-1843. 2007.
[39] Kuwabara K, Gan Z, Nakamura T, Abe H, Doi Y. Crystalline/amorphous phase structure and molecular mobility of biodegradable poly(butylene adipate-co-butylene terephthalate) and related polyesters. Biomacromolecules. 3(2):390-396. 2002.
[40] Cranston E, Kawada J, Raymond S, Morin FG, Marchessault RH. Cocrystallization model for synthetic biodegradable poly(butylene adipate-co-butylene terephthalate). Biomacromolecules. 4(4): 995-999. 2003.
[41] Gomez MA, Cozine MH, Tonelli AE. High-resolution solid-state carbon-13 NMR study of the .alpha. and .beta. crystalline forms of poly(butylene terephthalate). Macromolecules. 21(2): 388-392. 1988.
[42] Tsai C-C, Wu R-J, Cheng H-Y, Li S-C, Siao Y-Y, Kong D-C, Jang G-W. Crystallinity and dimensional stability of biaxial oriented poly(lactic acid) films. Polymer Degradation and Stability. 95(8): 1292–1298. 2010.

[43] Lehermeier HJ, Dorgan JR, Way JD. Gas permeation properties of poly(lactic acid). Journal of Membrane Science. 190(2): 243–251. 2001.
[44] Lee SC, Han J, Jeong YG, Kwon M. Strain-induced Enthalpy Relaxation in Poly(lactic acid). Macromolecules. 43(1): 25-28. 2010.
[45] Di Y, Iannace S, Maio ED, Nicolais L. Reactively Modified Poly(lactic acid): Properties and Foam Processing. Macromolecular Materials and Engineering. 290(11): 1083–1090. 2005.
[46] Liu J, Lou L, Yu W, Liao R, Li R, Zhou C. Long chain branching polylactide: Structures and properties. Polymer 51(22): 5186-5197. 2010.
[47] Corre YM, Duchet J, Reignier J, Maazouz A. Melt strengthening of poly (lactic acid) through reactive extrusion with epoxy-functionalized chains. Rheologica Acta. 50(7-8): 613-629. 2011.
[48] Kang HJ, park SS. Characterization and biodegradability of poly(butylene adipate-co-succinate)/poly(butylene terephthalate) copolyester. Journal of Applied Polymer Science. 72(4): 593-608. 1999.
[49] Palade L-I, Lehermeier H-J, Dorgan JR. Melt Rheology of High L-Content Poly(lactic acid). Macromolecules. 34(5): 1384-1390. 2001.
[50] Norhayani O, Jazrawi B, Mehrkhodavandi P, Hatzikiriakos S. Wall slip and melt fracture of poly(lactides). Rheologica Acta. 51(4): 357-369. 2011.
[51] Aou K, Kang S, Hsu SL. Morphological study on thermal shrinkage and dimensional stability associated with oriented poly(lactic acid). Macromolecules. 38(18): 7730-7735. 2005.
[52] Tsai C-C, Wu R-J, Cheng H-Y, Li S-C, Siao Y-Y, Kong D-C, Jang G-W. Crystallinity and dimensional stability of biaxial oriented poly(lactic acid) films. Polymer degradation and Stability. 95(8): 1292-1298. 2010.
[53] Gorlier E, Haudin JM, Billon N. Strain-induced crystallisation in bulk amorphous PET under uni-axial loading. Polymer. 42(23): 9541-9549. 2001.
[54] Kawakami D, Burger C, Ran S, Avila-Orta C, Sics I, Chu B, Shu-Min C., Hsiao BS, Takeshi K. New Insights into Lamellar Structure Development and SAXS/WAXD Sequence Appearance during Uniaxial Stretching of Amorphous Poly(ethylene terephthalate) above Glass Transition Temperature. Macromolecules. 41(8):2859-2867. 2008.
[55] Zhang X, Schneider K, Liu G, Chen J, Karsten B, Wang D, Manfred S. Structure variation of tensile-deformed amorphous poly(L-lactic acid): Effects of deformation rate and strain. Polymer. 52(18): 4141-4149. 2011.
[56] Bovey FA, Tiers GVD. Polymer NSR spectroscopy. II. The high resolution spectra of methyl methacrylate polymers prepared with free radical and anionic initiators. Journal of Polymer Science. 44(143): 173-182.1960.
[57] Shi XQ, Ito H, Kikutani T. Characterization on mixed-crystal structure and properties of poly (butylene adipate – co- terephthalate) biodegradable fibers. Polymer. 46 (25):11442-11450. 2005.
[58] Dupaix RB, Boyce MC. Finite strain behaviour of polyethylene terephthalate (PET) and poly(ethylene terephthalate)-glycol (PETG). Polymer. 46 (13): 4827-4838. 2005.
[59] Capt L, Kamal MR, Münstedt H, Stopperka K, Sänze J. Morphology Development during Biaxial Stretching of Polypropylene Films. 17th Polymer Processing Society Annual Meeting. 2001.
[60] Song K, White JL. Formation and Characterization of Cast and Biaxially Stretched Poly(6utylene Terephthalate) Film. Polymer Engineering and Science. 38(3): 505-515. 1998.
[61] Zhang J, Li F-X, Yu J-Y. Multiple Melting behavior of biodegradable poly(butylene succinate-co-terephtalate) (PBST) copolyester. Journal of Thermal Analysis and Calorimetry. 2012. DOI: 10.1007/s10973-012-2229-2
[62] Stoclet G, Seguela R, Lefebvre JM, Rochas C. New Insights on the Strain-Induced Mesophase of Poly(d,l-lactide): *In Situ* WAXS and DSC Study of the Thermo-Mechanical Stability. Macromolecules. 43 (17): 7228–7237. 2010.
[63] Li X-J, Zhong G-J, Li Z-M. Non-isothermal crystallization of poly(L-lactide) (PLLA) under quiescent and steady shear conditions. Chinese Journal of polymer Science. 28(3): 357-366. 2010.

[64] Li F, Luo S, Ma C, Yu J, Cao A. The crystallization and morphology of biodegradable poly(butylene succinat-co-terephtalate) copolyesters with high content of BT Units. Journal of Applied Polymer Science. 118(2): 623-630. 2010.
[65] Rezgui F, Swistek M, Hiver JM, G'Sell C, Sadoun T. Deformation and damage upon stretching of degradable polymers (PLA and PCL). Polymer. 46(18): 7370–7385. 2005.
[66] Averous L, Moro L, Dole P, Fringant C. Properties of thermoplastic blends: starch–polycaprolactone. Polymer. 41(11):4157–67. 2000.
[67] Marco Y, Chevalier L. Microstructure Changes in Poly(ethylene terephthalate) in Thick Specimens Under Complex Biaxial Loading. Polymer Engineering and Science. 48(3): 530-542. 2008.
[68] Menary GH, Tan CW, Harkin-Jones EMA, Armstrong CG, Martin PJ. Biaxial deformation and experimental study of PET at conditions applicable to stretch blow molding. Polymer Engineering and Science. 52(3): 671-688. 2012.
[69] Stoclet. G, PhD defense : Etude de la structuration différents niveaux d'échelle et du comportement thermomécanique d'un polymère issu de ressources renouvelables: l'acide poly lactique. Université de Lille. 2009.
[70] Bicakci S, Cakmak M. Development of structural hierarchy during uniaxial drawing of PEEK/PEI blends from amorphous precursors. Polymer. 43(1): 149-157. 2002.
[71] Lu XF, Hay JN. Crystallization Orientation and Relaxation in Uniaxially Drawn Poly (ethylene terephtalate). Polymer. 42(19): 8055–8067. 2001.
[72] Kattan M, Dargent E, Grenet J. Three Phase Model in Drawn Thermoplastic Polyesters: Comparaison of Differential Scanning Calorimetry and Thermally Stimulated Depolarisation Current Experiments. Polymer. 43(4): 1399–1405. 2002.
[73] Gohil RM. Properties and strain-hardening character of polyethylene terephtalate containing isosorbide. Polymer Engineering and Science. 49(3): 544-553. 2009.

Chapter 6
Biaxial orientation of materials based on Poly (lactic acid): Structure and properties

Part B- PLA, PBAT and thermoplastic cereal flour blends: An example of an industrial formulation

6-B

I Abstract

The paper investigates the biaxial stretchability of polylactic acid (PLA)/thermoplastic cereal flour (TCF or TPS)/poly (butylene adipate co-terephtalate) (PBAT) ternary blends with PLA/PBAT ratio close to 60/40 and at a constant TCF content. A twin-screw extrusion process was used to gelatinize the starch, devolatilize the water to obtain a water-free TCF and then to blend it into the compatibilized or uncompatibilized PLA/PBAT matrix, introduced at the molten state. These blends were subsequently cast into sheets and biaxially drawn using a laboratory biaxial stretcher. The obtained results showed that the prepared ternary blends showed a typical ductile behaviour. Besides, the addition of thermoplastic cereal flour did not affect significantly the biaxial stretchability of PLA/PBAT blends while lowering the maximum stress before break. The modification of interfacial tension between PLA and PBAT with Joncryl before mixing with TCF does not affect the draw-ability of the PLA/PBAT/TCF film but slightly increases the maximum of nominal stress before failure. SEM micrograph highlights the poor adhesion in PLA/PBAT/TCF blends where two different phases are observed.

Key-words Polylactic acid-Thermoplastic cereal flour/starch- PLA/PBAT blends- Biaxial deformation

II Introduction

It is well known that the most key requirement for sheet or films is the mechanical properties, which may be enhanced by uniaxial or biaxial deformation processing. The development of molecular orientation enables to produce materials with enhanced optical or barrier properties. In the packaging industry including double bubble film blowing, thermoforming, biaxial orientation is preferred and can provide different or equivalent mechanical properties in machine (MD) and transverse (TD) directions [1]. In general, both sequential and simultaneous biaxial stretching modes are widely used. More details about these two modes of stretching were given by Ou et al [2]. It is believed that the deformation behavior of polymers is the result of the synergic effects of stretching temperature and strain rate. Extensive efforts have been devoted to understand the molecular structure and morphology of different polymer systems and their relationship to mechanical properties during biaxial orientation. Among these polymers, polypropylene, poly (ethylene terephthalate) and polystyrene, which are widely used in the packaging applications [3][4][5].
Recently, poly (lactic acid) (PLA) has received a lot of attention. PLA is a biodegradable and biocompatible polymer. Its mechanical properties depend strongly on the crystallinity, crystal orientation and its morphology. But, PLA is very brittle, more expensive than conventional plastics and highly vulnerable to thermal and oxidative degradation during processing [6]
Its processing instability results in polymer chain cleavage, leading to a reduction of molecular weight and deterioration of rheological properties. This limitation can be improved by the use of a polymeric chain extender whose functional groups are reactive with hydroxyl and carboxyl groups of PLA. To date, multi-functional chain extenders have become attractive in the conventional plastics industry due to their increasing importance in polymeric extension.
Another limitation of PLA is its high cost. A common used strategy to reduce its cost is to blend it with thermoplastic starch (TPS). Native starch is a natural polymer that can be found in the plant

world. It is composed of a mixture of two polysaccharides: Amylose and Amylopectine and it is semi-crystalline (crystalline content = 15-45%) [7]. Starch can participate to the formation of blend with PLA when it is gelatinized by applying shear and heat in presence of plasticizers like water and glycerol [8][9]. Otherwise, the starch in its dry native state acts as filler involving an increase of brittleness of resulting materials. Literature is rich enough in blending TPS with other biodegradable polyesters, especially with poly(caprolactone) (PCL) [10], polyesteramide (PEA) [11], poly(butylene adipate-co-terephtalate) (PBAT) and poly(butylene succinate adipate) (PBSA).

In the case of PLA/TPS blends, Martin et al. [12] have shown a reduction of the mechanical properties (Elastic modulus, elongation at break, yield stress and the impact strength) following the addition of a small amount of starch in PLA matrix. This significant decrease is justified by the poor interfacial affinity between these two polymers. Recently, however some authors have shown that the elongation at break can be enhanced by either adding compatibilizers such as maleic anhydride (MA), dioctyl maleate or by incorporation of third flexible biodegradable polymer like PCL. Huneault et al. have shown an improved ductility by the functionalization of PLA, under the action of peroxide, with maleic anhydride before mixing with TPS [13]. The obtained blend is homogeneous with a deformation at break about 100 to 200%. In addition, it appears that the addition do 10 wt% of PCL into PLA/TPS multiplies the impact strength and the ductility by "3" compared to pure PLA as reported by Sarazin et al. [14]. So blending PLA/TPS binary blend with another flexible polymer could be a useful way to obtain a new kind of materials with excellent performances. Poly (butylene adipate-co-terephtalate) (PBAT) is a flexible copolyester which can fully degrade within a few weeks. It could be considered as a good candidate for the toughening of rigid polymers such as TPS/PLA binary blend.

Newly, Chapleau et al [1] have studied the effect of the molecular bi-orientation on the improvement of mechanical in PLA/TPS blends. They have shown an increase in tensile strength, elastic modulus and elongation at break with the deformation ratio. In this work, we will try to replace the TPS by the thermoplactic cereal flour in order to study the effect of the flour on the mechanical properties of PLA/PBAT blends under biaxial simultaneous equi-biaxial deformation. We should note that the studied blends were prepared by Ulice, industrial project partener. A laboratory biaxial stretcher was used to perform the tests. The influence of the draw ratio at fixed temperature on the maximum of stretching was also developed. Moreover, the impact of the interfacial adhesion between PLA and PBAT polymers on the mechanical behavior of ternary PLA/PBAT/TCF blends will be also investigated.

III Experimental Section

III.1 Blend compounding

The pellets (PLA/PBAT/TCF) have been received from Ulice_Limagrain. They were prepared by a twin-screw extruder as follow: The first half of the extruder was used to prepare the thermoplastic cereal flour (TCF). The initial starch content was 24 wt% and the glycerol content was 9 wt%. The water was removed by vacuum just before mid-extruder to obtain TCF with minimum residual water. The blends PLA/PBAT were incorporated in the molten state (at 190°C) at mid-extruder through a single screw extruder side-feed. For interface modification, 0,5 and 0,9 wt.% of Joncryl ADR®-4368 was added to PLA and PBAT blends before being mixed with TCF. It is believed that the residual epoxy groups initially present in Joncryl ADR®-4368 are able to react with the hydroxyl groups from TCF and glycerol.

III.2 Sheet Casting and biaxial stretching

The pellets are prepared as described above. Once received, they were dried under a vacuum oven at 80°C for 12h before processing. Cast-films were extruded with a 30 mm single-screw extruder and quenched at 40°C (chill-roll temperature). The melt temperature was set at 180°C and the residence time was maintained at 3 minutes. The amorphous obtained films have a final thickness about 500µm.

The square test specimens were cut from the uniform central region of the extruded films. The uniformity of the cross-shaped specimen thickness was checked and validated. The description of the simultaneous biaxial stretching method was presented in our previous chapter (Cf. Chapter VI-A). In this study, the biaxial testing experiments were conducted at 75°C. The stretching rates were chosen to be 0.2 and $0.4s^{-1}$, which corresponds to 4 and 10 mm/s respectively. Much thinner films (~ 50µm) were obtained.

Table VII-1 includes the different studied samples. The studied blends have different PLA/PBAT ratios and a constant TCF content It should be pointed out that the addition of Joncryl ADR® increased the consistency of film quality and make the film extrusion process more stable. Without Joncryl ADR®, fractures and defects were formed and the film broke easily.

Table VII-1 Composition of different samples with different PLA/PBAT ratios for the preliminary study

a) Samples	% wt Joncryl in the blend	%wt TCF in the blend	PLA/PBAT ratio in the blend
TPS+PLA/PBAT (0/100)	0	33%	0/100
TPS+PLA/PBAT (20/80)	0	33%	20/80
TPS+PLA/PBAT (40/60)	0	33%	40/60
TPS+PLA/PBAT (60/40)	0	33%	60/40
TPS+PLA/PBAT (80/20)	0	33%	80/20
TPS+PLA/PBAT (100/0)	0	33%	100/0

b) Samples	% wt Joncryl in the blend	%wt TCF in the blend	PLA/PBAT ratio in the blend
TPS+PLA/PBAT (20/80)	0.5	33%	20/80
TPS+PLA/PBAT (40/60)	0.5	33%	40/60
TPS+PLA/PBAT (60/40)	0.5	33%	60/40
TPS+PLA/PBAT (80/20)	0.5	33%	80/20

IV Results and discussions

IV.1 Preliminary study

The main objective of this preliminary study is to characterize the mechanical behavior of different ternary PLA/PBAT/TCF blends upon uniaxial deformation. The obtained results will help us later choosing the optimal PLA/PBAT ratio for the biaxial stretching experiments. The elastic modulus, the yield stress and the elongation at break were determined. They are summarized in table VII-2 and plotted in figure VII-1.

Table VII-2 Elastic Modulus, Yield Stress and Elongation at break values for different prepared samples

PLA/PBAT ratio intoPLA/PBAT/TCF blends	Elastic modulus (MPa)	Yield stress (MPa)	Elongation at break (%)
0/100	96.5±6.8	7.4±1.1	14.5±4
20/80	184±24	8±1	9±2
40/60	452±52.4	11.5±0.75	5.7±1.2
60/40	1029±47	19±1.35	2.4±0.4
80/20	1508±97.5	25±3.8	1.8±0.25
100/0	2103±79	29±3	1.2± 0.2

We have demonstrated in our previous chapter (Chapter 2) that the elastic modulus of PLA is about 1.35 GPa. The tensile properties of PLA/TCF blend showed a decrease of the PLA elastic modulus with the addition of TCF. It varies from 1.35 GPa to 2103 MPa. This is to be expected when a soft component is added.

Concerning PLA/PBAT/TCF blends, high elastic modulus and high yield stress were obtained with adding PLA. Therefore, the results suggested that PLA could impart strength and rigidity to the bends due to its relatively high yield stress (75MPa) and its high elastic modulus of neat PLA, as reported in the literature for PLA/TPS blends [16]. However, it should be pointed out that the incorporation of PBAT into PLA/TCF matrix allows the transition from a brittle to a ductile behavior which is highlighted by the increase of the elongation at break.

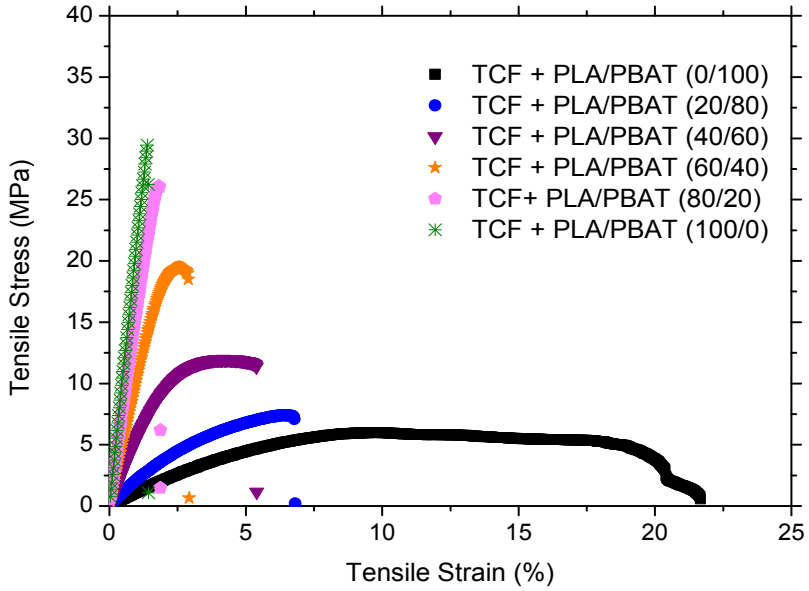

Figure VII-1 Typical tensile stress-strain curves for cast PLA/PBAT/TCF sheets with a constant "TCF" Content

With the addition of 0,5 %wt of Joncryl (which acts as a compatibilizer agent for PLA/PBAT blends, as demonstrated in our chapter IV) into PLA/PBAT before mixing with TCF, the elastic modulus of ternary blends in nearly unaffected by the interfacial modification, as shown in figure VII-2. This is not surprising considering the PLA/PBAT/Joncryl is reacted for a few seconds with TCF. It means that the Joncryl has no sufficient time to react with the hydroxyl groups of the TCF. However, the effect of the good interfacial adhesion of PLA/PBAT into PLA/PBAT/TCF blends was more significant when measuring the elongation at break. It is shown to be enhanced for a ratio PLA/PBAT about 20/80; 40/60 and 60/40.

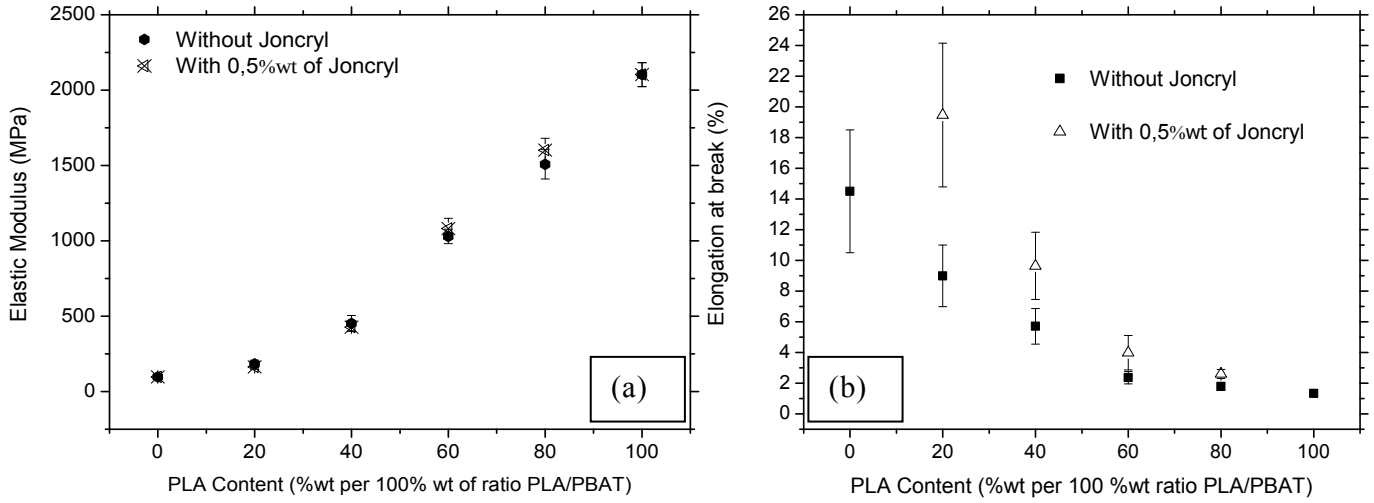

Figure VII-2 (a) Elastic modulus and (b) elongation at break evolution for different PLA/PBAT/TCF blends with and without Joncryl

We should note that Joncryl plays a role of a processing aid. In order to choose the biaxial stretching temperature, a thermo-mechanical study should be carried out. Plots of storage modulus (E') of TCF/polyesters blends versus temperature are showed in Figure VII-3.

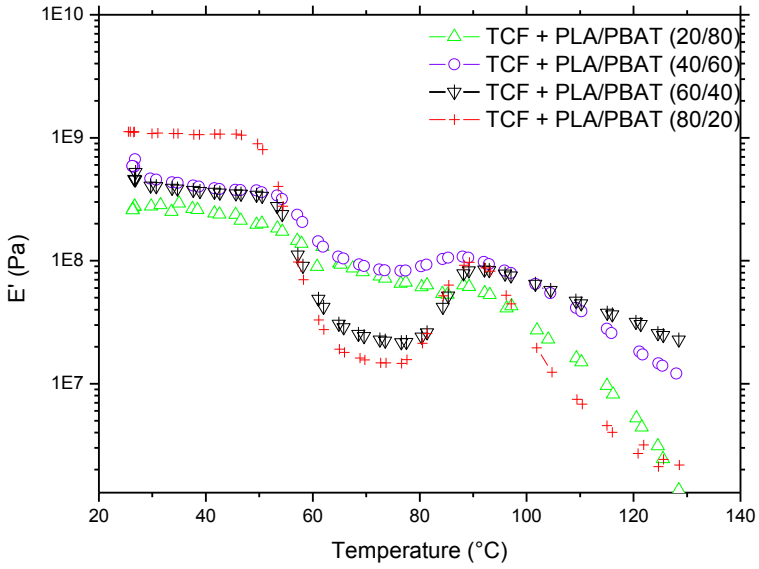

Figure VII-3 Plots of storage modulus (E') of different TCF/polyesters blends versus temperature

DMTA studies revealed that all blends had a decreasing of E' over the glass transition temperature of PLA from 50 to 65°C. The decrease in E' suggested that the material was becoming less elastic. The addition of Joncryl did not affect significantly the principal relaxation α of PLA, demonstrating that Joncryl had no plasticization effect on the films. As PBAT content increased and PLA content decreased, the value of E' decreased, which indicates that the blends with less PBAT content were more elastic. These results corroborated with uniaxial tensile strength results. The processing biaxial experiments temperature is estimated thanks to DMTA measurements. It can be determined between the α-relaxation temperature and the onset cold crystallization temperature, representative of PLA. According to the obtained curves, a temperature about 75°C was chosen for the biaxial orientation experiments.

Based on the obtained results and, we decided therefore to prepare, using the preparation method mentioned above (Cf. blend compounding), ternary samples with PLA/PBAT ratio equal to 60/40 for the biaxial orientation experiments; they are included in table VII-3. Cast PLA/PBAT/TCF films wete prepared with both 0.5% of Joncryl and 0.9% by weight (an excess of Joncryl) to expect a possible reaction between the three components, leading thus to an enhancement of the films deformation.

Table VII-3 Composition of different samples used for biaxial stretching experiments

Samples	Composition
PLA	100%wt PLA
PBAT	100%wt PBAT
TCF+PLA/PBAT (60/40)	33%wt TCF in the blend + PLA/PBAT (60/40)
TCF+PLA/PBAT/Joncryl (60/40/0,5)	33%wt TCF in the blend + PLA/PBAT (60/40)+ 0,5%wt Joncryl
TCF+PLA/PBAT/Joncryl (60/40/0,9)	33%wt TCF in the blend + PLA/PBAT (60/40) + 0,9%wt Joncryl

Moreover, as shown in Figure VII-4, the study of the isothermal behavior of the studied blends at 75°C confirms that no induced thermal crystallization could develop in the tests carried out here since the time scale of the test (preheating + stretching) is about 10min even though the starch could play the role of the nucleating agent for PLA in PLA/PBAT/TPS [15].

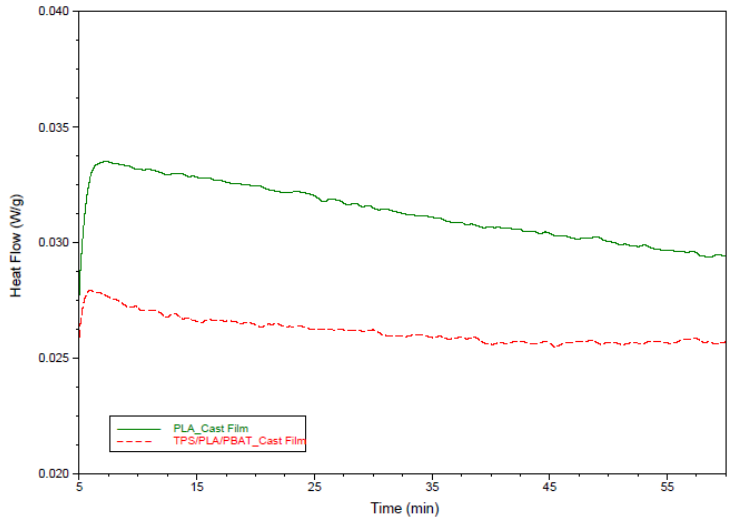

Figure VII-4 Isothermal crystallization for PLA and PLA/PBAT/TCF (PLA/PBAT=60/40) ternary blends at 75°C during 60 minutes

IV.2 Properties of bi-axially stretched films

The nominal stress vs. nominal strain curves at 75°C and for two different strain rate (0,2 and 0,4 s^{-1}) are shown in Figures VII- 6 and VII-7. We should point out that the stresses in both machine and transverse directions are similar, which is representative of the initial isotropy of the cast sheets, as can be seen in figure VII-5. For further analysis, only the data for the machine direction will be shown in the graphs.

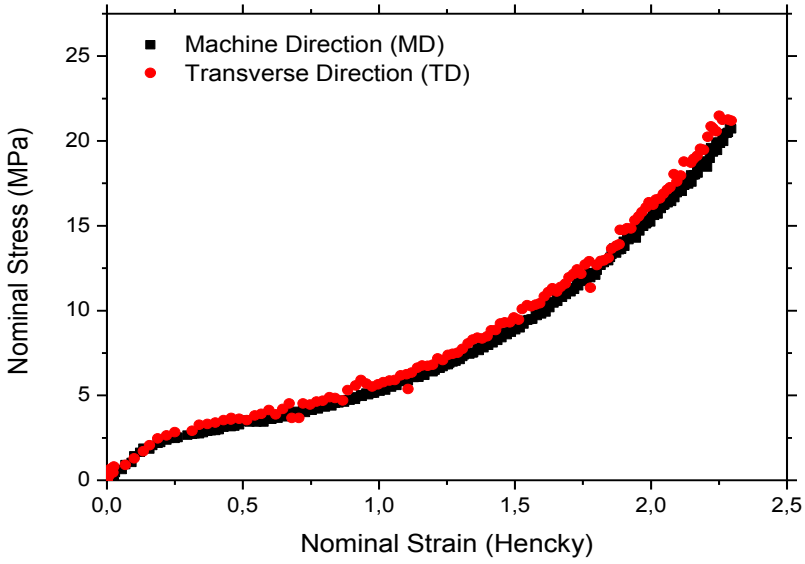

Figure VII-5 The stress-Strain curves of ternary PLA/PBAT/TCF blends in both machine and transverse directions

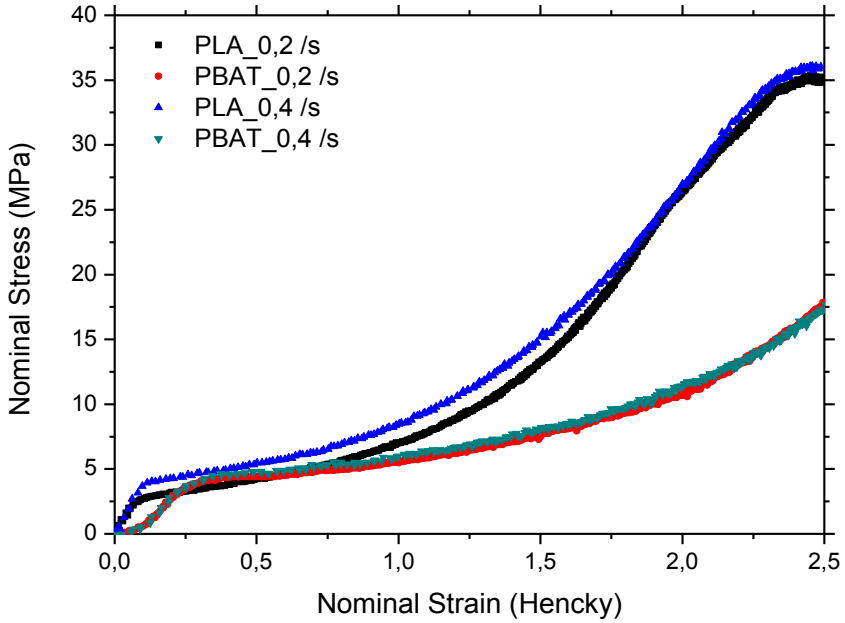

Figure VII-6 The stress-Strain curves in machine directions for PLA and PBAT at two different strain rate (0,2 and 0,4 s^{-1})

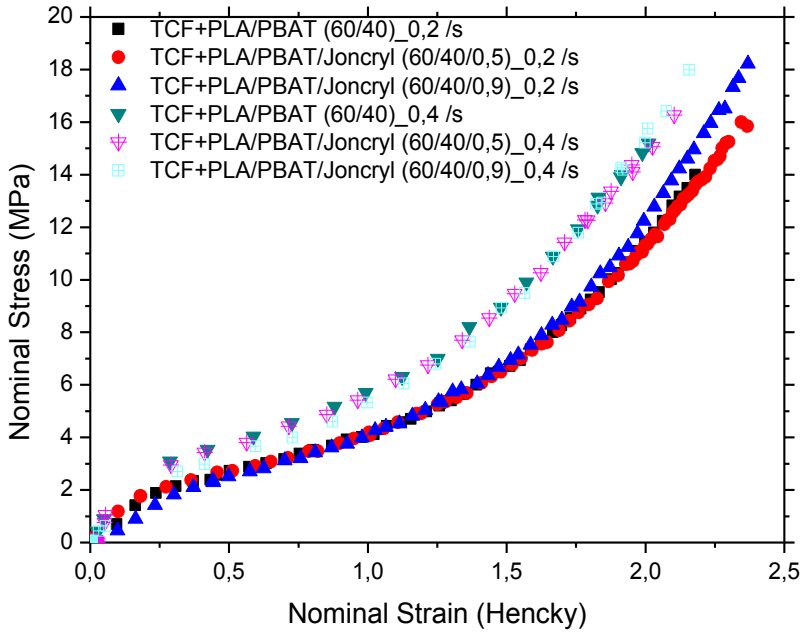

Figure VII-7 The stress-Strain curves in machine directions for PLA/PBAT/TCF at two different strain rate (0,2 and 0,4 s^{-1})

Table VII-4 summarizes the obtained results of strain hardening parameter (SHP) (or optimum draw ratio) for studied samples. It was shown that PLA and PBAT can be axially stretched reaching a maximum before failure close to 1,5 and 2,25 Hencky at 75°C respectively regardless the strain rate. The mechanical properties upon biaxial simultaneous drawing for PLA/PBAT blends were discussed in our previous work. It was observed, in one hand, that the stretchability of these blends depends on the PLA/PBAT ratio; it was improved for high amounts of PBAT.

Table VII-4 Maximum stress before break and strain hardening parameter values for the prepared samples for biaxial stretching experiments

Samples ($\dot{\gamma}$ =0,2s^{-1})	Maximum of stress before break (MPa)	Strain-hardening parameter (SHP) (Hencky)	Samples ($\dot{\gamma}$ =0,4s^{-1})	Maximum of stress before break (MPa)	Strain-hardening parameter (SHP) (Hencky)
PLA	35	1,5	PLA	35	1,7
PBAT	18	2,25	PBAT	18	2,25
TCF + PLA/PBAT(60/40)	14	1,7	TCF + PLA/PBAT(60/40)	15	1,4
TCF + PLA/PBAT/Joncryl (60/40/0,5)	16	1,75	TCF + PLA/PBAT/Joncryl (60/40/0,5)	17	1,4
TCF + PLA/PBAT/Joncryl (60/40/0,9)	19	1,65	TCF + PLA/PBAT/Joncryl (60/40/0,9)	19	1,4

The interfacial modification of the blends by the incorporation of a compatibilizer agent, Joncryl ADR®, leads to an earlier strain-hardening. This phenomenon is related to the fact that Joncryl reacts also as a nucleating agent for PLA allowing by this way the increase of the crystallization kinetic; the physical crosslinking of the macromolecular network by the crystallites prevented thus the chain relaxation.

For the unmodified PLA/PBAT/TCF, typical ductile characteristic of plastics was showed. It was observed that the addition of TCF does not affect significantly the stretchability of PLA/PBAT while lowering the maximum stress before break from ~25 MPa for PLA/PBAT blends to ~15 MPa. Since TCF has a greater affinity with PBAT compared to PLA (based on a previous project's study) we can conclude that upon drawing, the PLA matrix exhibits elongated voids around the granular PBAT/TCF particles. Clearly PLA debonded during drawing, leaving a cavitated structure at both hencky strains, 0.2 and $0.4s^{-1}$.

The incorporation of Joncryl ADR® into PLA/PBAT blends before the mixing with TCF does not affect the stretchability of the PLA/PBAT/TCF film but slightly increases the maximum of stress before failure probably related to the improvement of the interfacial adhesion between PLA and PBAT. SEM micrograph highlights the poor adhesion in PLA/PBAT/TCF blends where two different phases related to both PLA and PBAT/TCF phases are observed, as shown in Figure VII-8.

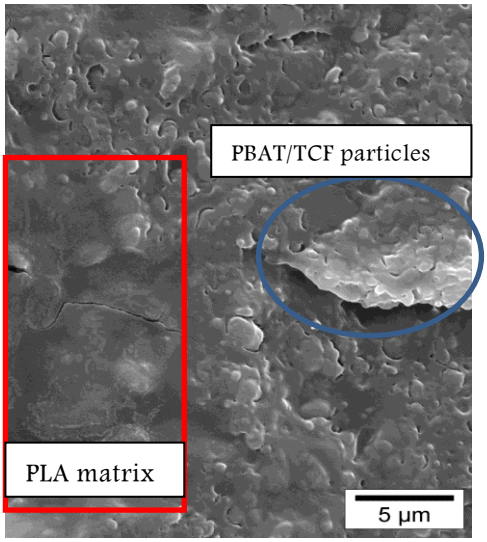

Figure VII-8 SEM Micrograph for PLA/PBAT/TCF with 0,9%wt of Joncryl.

V Conclusions

The properties and processability of TCF/polyesters were investigated. It is shown that the elastic modulus of PLA decreases with the addition of TCF. For PLA/PBAT/TCF blends, the results suggested that PLA could impart strength and rigidity to the bends. It should be pointed out also that the incorporation of PBAT into PLA/TCF matrix allows the transition from a brittle to a ductile behavior. Besides, with the addition of 0,5 %wt of Joncryl into PLA/PBAT/TCF blends, the elastic modulus is nearly unaffected by the interfacial modification but was more significant when measuring the elongation at break; it is also shown to be enhanced for a ratio PLA/PBAT about 20/80; 40/60 and 60/40.

For biaxial stretching experiments at 75°C for the unmodified PLA/PBAT/TCF, typical ductile characteristic of plastics was shown. It was observed that the addition of TPS does not affect significantly the stretchability of PLA/PBAT while lowering the maximum stress before break. The incorporation of Joncryl into PLA/PBAT blends before the mixing with TPS does not affect the stretchability of the PLA/PBAT/TCF film but increases slightly the maximum of stress before failure. SEM micrograph highlights the poor adhesion in PLA/PBAT/TCF blends where two different phases are observed.
While Joncryl is a compatibilizer for PLA/PBAT blends, it is important to give a better understanding of the TCF role and the effect of its plasticization degree on the final properties. A nanostructured morphology has to be tailored to improve the final mechanical properties.

References

[1] Chapleau N, Huneault M, Li H. Properties of biaxially oriented polylactide/Thermoplastic starch blends. Invited papers. International Polymer Processing XXII. 8 pages. 2007.
[2] Ou X, Cakmak M. Comparative study on development of structural hierarchy in constrained annealed simultaneous and sequential biaxially stretched polylactic acid films. Polymer. 51(3): 783-792. 2010.
[3] Capt L, Kamal MR, Munstedt H, Stopperka K, Sanze J. Morphology Development during Biaxial Stretching of Polypropylene Films, 17th Polymer Processing Society Annual Meeting. 2001.
[4] Hegemann B, Kech A, Goschel U, Belina K, Eyerer P. Biaxial Deformation Behavior of PET Dependent on Temperature and Strain Rate. Journal of Macromolecular Science-Part B: physics. 41(4-6), 647–656. 2002.
[5] Kanai T, Stretchability and Properties of Biaxially Oriented Polypropylene Films, International Polymer Processing, 21, 449–456. 2006.
[6] Zhang Y, Yuan X, Liu Q, Hrymak A. The effect of polymeric chain extenders on physical properties of thermoplastic starch and polylactic acid blends. Journal of Polymers and the environment. 20(2):315-325. 2012.
[7] Williams JM. Starch and its Derivatives. Ed. Radley J.A., Chapman and Hall. 1968.
[8] Tomka I. A thermoplastically processable starch and a process for making it. Patent WO9005161. 1990.
[9] Lin Y, Huff HE, Parsons MH, Iannotti E, Hsieh F. Mechanical properties of extruded high amylase starch for loose-fill packaging material. Food Science and Technology. 28(2): 163-168. 1995.
[10] Averous L, Fringant C. Association between plasticized starch and polyesters: Processing and performances of injected biodegradable systems. Polymer Engineering and Science. 41(5): 727-734. 2001.
[11] Averous L, Fauconnier N, Moro L, Fringant C. Blends of Thermoplastic Starch and Polyesteramide: Processing and Properties. Journal of Applied Polymer Science. 76(7), 1117-1128. 2000.
[12] Martin O, Averous L. Poly(lactic acid): plasticization and properties of biodegradable multiphase systems. Polymer. 42(14): 6209-6219. 2001.
[13] Huneault MA, Li H. Morphology and properties of compatibilized polylactide/thermoplastic starch blends. Polymer. 48(1): 270-280. 2007.
[14] Sarazin P, Li G, Orts WJ, Davis BD. Binary and ternary blends of poly-lactide, polycaprolactone and thermoplastic starch. Polymer, 49(2):599-609. 2007.
[15] Ke T, Sun X. Melting behavior and crystallization kinetics of starch and poly(lactic acid) composites. Journal of Applied Polymer Science. 89(5):1203–1210. 2003.
[16] Donald G. A literature review of Poly (lactic acid). Journal of Polymer and the Environment. 9(2): 63-84. 2001.

General Conclusion & Outlooks

I GENERAL CONCLUSION

In the present manuscript, we studied the structure/ processing/ properties relationships of the neat PLA, PBAT and their blends obtained by reactive extrusion, using a multi-functional epoxide (Joncryl ADR®).

In the first part, we tried to understand the mechanisms and the conditions governing the thermal degradation of both PLA and PBAT polymers upon processing conditions by means of rheological properties coupled to physico-chemical characterizations. The decrease of both intrinsic viscosity and average molecular weight with increasing temperatures highlights the thermal degradation causing chains cleavage via degradation mechanisms (hydrolysis, random main-scission chain, β-scission…). Further thermal and rheological investigations confirmed their thermal degradation phenomenon. Indeed, the complex viscosity modulus was reduced with residence time.

The incorporation of different amounts of Joncryl ADR® (0.25- 0.5 and 1% by weight), as a chain extension agent, into neat polymers matrix showed an enhancement of their thermal stability. The occurred structural modification was detected via the improvement of the melt rheological properties (storage modulus, complex viscosity modulus, shear-thinning behavior) and the melt strength resistance under shear, which in turn affects the elongation properties. These results corroborated with the higher average molecular weight obtained from SEC measurements.

Due to its high functionality, we have demonstrated that Joncryl ADR® plays a double role once incorporated into PLA and PBAT matrix; it reacts as both chain extension and branching agent. The chain extension/branching balance was successfully confirmed by the increase of the activation energy, hydrodynamic/gyration radii coupled to the bimodal relaxation spectra. The reduced Van-Gurp-Palmen plots revealed characteristic curves of long-chain branched polymers. Indeed, they exhibited a typical feature of a mixture of linear and randomly branched polymers. The mechanisms of degradation, chain extension and branching and their competition have been also discussed in the manuscript.

And now, what about the impact of Joncryl ADR® on the properties of PLA/PBAT blends? Following the addition of the chain extension/branching agent, an enhancement of mechanical properties accompanied with a finer morphology was observed. A deeper understanding of the interfacial adhesion of the blends was assessed by quantifying the interfacial tension (α) values of modified and unmodified blends. Two different rheological approaches were used; the first one was based on Palierne Model and the second one on the deformed drop retraction method. In the latter case, different sandwich model systems were studied in order to probe and quantify the role of the functionalized epoxy chains on the interfacial forces.
This study examines the changes of the interfacial tension value depending on the chain extender amount to determine its compatibilizer role and then relate these findings to the morphology. The experimental results showed, regardless the used method, a reduction of the interfacial tension values following the addition of Joncryl ADR®. Such a reduction would facilitate the break-up of the dispersed phase into much finer droplets, thus improving the final properties of the blends. The obtained data were then analyzed and discussed based on the mechanisms of coalescence and Marangoni's theories. The larger degree of compatibilization induced by Joncryl ADR® was confirmed by the transmission electron microscopy where the average diameter of the dispersed PBAT was drastically reduced with the addition of the multifunctional epoxide.

After a fundamental understanding of the effect of the multifunctional epoxide on the properties of PLA / PBAT blends, a particular attention was drawn to study the ability of modified polymers and their blends to be processed by blowing extrusion and biaxial stretching:
It was shown that PLA is not able to be blown due to its poor shear and elongation properties and exhibits some processing defects. For the modified materials, the improvement of the rheological properties ensures their blown extrusion ability.
Indeed, we have demonstrated that the incorporation of 0.5% and 0.7% by weight of Joncryl ADR® into PLA polymer leads to an enhancement of its blowing processing windows. Higher BUR and TUR values were obtained. Moreover, the PBAT elasticity induces an enlargement of the stability domain of the blends. This elasticity allows a development of larger size bubbles despite the lack of the compatibility between the two polymers. However, with the addition of 0.7%wt of Joncryl into PLA_PBAT matrix, the instability zone was reduced.

On the basis of the mechanical/thermo-mechanical behaviors of the stretched films and X-ray diffraction experiments, we have demonstrated that they exhibited a strain-induced crystallization. The load-extension curves of PLA and PBAT at 75°C follow the typical rubber –like ductile deformation behavior. The stretched PLA becomes crystalline

and highly oriented according to *in –situ* 2D-WAXS patterns where two very sharp meridional peaks superposed over the amorphous halo, highlighting the formation of a mesomorphic phase. Moreover, it was interesting to find that mixed-crystal structure of BT and BA, segment units of PBAT, undergoes PBT-like crystal form. Furthermore, some differences are observed in the strain hardening region of the modified PLA where its onset strain-hardening appears slightly earlier and it is accompanied by a reduced optimum draw ratio. Consequently, different crystalline planes were detected in parallel with the mesomorphic phase. Unlike PLA, the incorporation of Joncryl ADR® into PBAT matrix did not show any structural changes regardless the incorporated amount of the multifunctional epoxide. For PLA/PBAT films, it was observed that their stretchability was improved at higher amounts of PBAT (at about 80% wt). In this case, the presence of Joncryl ADR® caused an earlier strain-hardening while increasing the maximum stress before breaking. Moreover, through annealing, a significant increase of the stress at break and a significant reduction of the stretching ability were demonstrated.

II OULOOKS

The obtained results, through this research study, are quite conclusive. But, many investigations are still required to more deeply understand some other critical aspects of such PLA/PBAT blends. Consequently, the future issues that should be considered are presented in this section.

- ✓ The demonstration of the degradation of neat PLA and PBAT through several rheological, thermal and analytical techniques keeps this field open to further follow the kinetics of chain scissions depending on the processing conditions; analytical methods more reliable should be used, RMN ^{1}H, for instance.

- ✓ Moreover, an experimental and modeling study leading to quantify, more accurately, the branching amount into the different materials should support our scientific approach.

- ✓ Deeper understanding of the influence of various process parameters for good optimization conditions of blowing extrusion processing is important. Others additives, such as nucleant agents, in addition to Joncryl ADR® , should be tested in order to check their impact on the crystallization and thermo-mechanical properties of films.

- ✓ An accurate determination of the elongational viscosity, in uniaxial and biaxial directions, should be carried out by using an elongational rheomoter.

- ✓ Furthermore, processing of multilayer (bi or tri-layers) systems by co-extrusion can be considered. This step can be preceded by a theoretical analysis of the flow instability to predict the defects growth. By this way, films with sufficient barrier properties for industrial packaging applications could be prepared.

- ✓ Finally, it is interesting to complete this study by biodegradation and eco-toxicity measurements at short and long term for all the developed materials. A life cycle study (ACV) should be made. It would then be possible to fully demonstrate the ecological interest of our study.

PUBLICATIONS & COMMUNICATIONS

This work has already resulted in:

A- Publication in international journal

Racha AL-ITRY, Khalid LAMNAWAR, Abderrahim MAAZOUZ,"***Improvement of thermal stability, rheological and mechanical properties of PLA, PBAT and their blends by reactive extrusion with functionalized epoxy***", *Polymer Degradation and Stability*, 97(10): 1898–1914.

B- 2 submitted publications in « Rheologica acta »

Racha AL-ITRY, Khalid LAMNAWAR, Abderrahim MAAZOUZ, "***Chain extension/branching balance of modified PLA and PBAT polymers with a multifunctional epoxide: rheological and solution properties***", August 2012

Racha AL-ITRY, Khalid LAMNAWAR, Abderrahim MAAZOUZ, "***Interfacial tension investigations of compatilibized PLA/PBAT blends***", August 2012

C- 2 Publications in Progress

Racha AL-ITRY, Khalid LAMNAWAR, Abderrahim MAAZOUZ, Noelle BILLON, ***"Bi-axial orientation of materials based on Poly (lactic acid): Structure and properties relationship"***.

Racha AL-ITRY, Khalid LAMNAWAR, Abderrahim MAAZOUZ, ***"Extrusion Blown film of poly (lactic acid) and its blends: Improvement of processing stability"***

D- National and International Communications

Racha AL-ITRY, Khalid LAMNAWAR, Abderrahim MAAZOUZ, Oral communication, ***"Blends based on Poly (lactic acid): Structure/rheology/processing relationship"***. JEPO40. September/October 2012, Anduze, France

Racha AL-ITRY, Khalid LAMNAWAR, Abderrahim MAAZOUZ, ***"Improvement in melt strengthening of PLA through reactive blending with PBAT and Epoxy-functionalized chains"***. BIOPOL, August 2011, ECPM_Strasbourg (Ecole de Chimie, Polymères, Matériaux de Strasbourg), France

Racha AL-ITRY, Khalid LAMNAWAR, Abderrahim MAAZOUZ, Oral communication, ***"Compatibilization of PLA and PBAT blends for food packaging applications"***. Polymer Processing Society PPS-27, May 2011, Marrakech, Maroc

Racha AL-ITRY, Khalid LAMNAWAR, Abderrahim MAAZOUZ, ***"Formulation et caractérisation de matériaux biodégradables à base de PLA"***. Journée des Polymèristes Lyonnais, September 2010, Campus de la Doua, France

Racha AL-ITRY, Khalid LAMNAWAR, Abderrahim MAAZOUZ, ***"Formulation et caractérisation de matériaux biodégradables à base de PLA"***. 22ème Entretiens, du centre Jacques Cartier Rhône-Alpes, Matériaux Innovants, procédés innovants et développement durable, GRPP & CREPEC, November/Décember 2009, Campus Lyontech - Doua, Rotonde des humanités, France

APPENDIX

Racha Al-Itry, Khalid Lamnawar, Abderrahim Maazouz. Improvement of thermal stability, rheological and mechanical properties of PLA, PBAT and their blends by reactive extrusion with functionalized epoxy. Polymer Degradation and Stability, 2012, Vol. 97, p. 1898-1914.

Appendix B : EPOXYDES

Les époxydes- Nature chimique et réactivité

Les époxydes sont des composés contenant un hétérocycle oxygéné à trois chaînons comme le montre la figure B-1, connu communément sous le nom du cycle « Oxirane ».

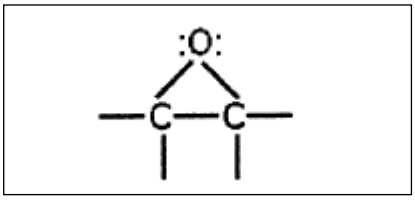

Figure B-1 : Fonction époxy ou cycle « Oxirane »

Ils doivent leur importance à leur forte réactivité qui est due à la facilité de l'ouverture du cycle contenant des liaisons C-O polaires ; Les angles de liaison du cycle, en moyenne de 60°, sont considérablement inférieurs à l'angle de carbone tétraédrique normale 109,5° ou l'angle d'oxygène divalent de 110° pour les éthers à chaîne ouverte (Morrison and Boyd, 1987). Etant donné que les atomes ne peuvent pas être situés de façon à assurer le maximum de recouvrement des orbitaux, les liaisons sont plus faibles par rapport à un éther ordinaire rendant le cycle moins stable et sensible à la réaction. Ainsi, suite à l'ouverture du cycle de l'époxyde, les systèmes acquièrent des angles tétraédriques, non soumis à des contraintes. Il en résulte, une énergie barrière plus faible pour rompre la liaison C-O d'un époxyde par rapport aux autres éthers et une cinétique de rupture plus rapide.
Les époxydes subissent une ouverture de cycle par catalyse acide ou catalyse basique (Morrison and Boyd, 1987). Sous des conditions basiques, les produits formés résultant de l'attaque du nucléophile sur l'atome de carbone le moins substitué. En revanche, sous des conditions acides (où l'oxygène de l'époxyde est protoné), la régiosélectivité de la réaction est différente. Dans ce cas, les produits résultent de l'attaque du nucléophile sur l'atome de carbone le plus substitué.
Ces systèmes époxydes peuvent subir des réactions de réticulations ou durcissement grâce au cycle oxirane avec une grande variété de composés contenant un hydrogène actif. Parmi ces composés, nous pouvons citer les amines aliphatiques et aromatiques, les acides anhydrides, phénols, acides carboxyliques, acides et bases inorganiques. La section suivante montre des exemples de réactions entre des résines époxy avec des fonctions acide carboxylique/alcool.
De la réaction entre un cycle époxyde et un acide carboxylique résultent des polyesters (Figure 3.10 (Dowd, 1968)). Chaque époxyde possède le potentiel d'être converti en deux liaisons esters. Ainsi, une réaction inter-moléculaire entre un groupe époxyde avec un groupe hydroxyle secondaire peut être favorisée. Cette réaction est connue sous le nom d'une réaction « d'éthérification ». Cela peut aboutir à des matériaux ayant des masses moléculaires élevées. En revanche, une gélification prématurée dans les polyesters résultants peut être initiée. Le mécanisme de réaction entre l'allongeur et les groupes fonctionnels d'un polyester prouve alors qu'il y a formation de branchements entre les chaînes du polymère. Des branchements des chaînes peuvent former un gel insoluble dans des solvants habituels du PLA, tels que le chloroforme et le THF, pour des quantités en allongeur de chaînes, une température et un temps de séjour importants. La formation d'un gel peut détériorer les procédés par un phénomène de prise en masse.

Appendix C : TENSION INTERFACIALE

La tension interfaciale dans les mélanges

L'évolution cinétique et les propriétés finales des matériaux sont étroitement liées à la morphologie générée au cours de leur mise en œuvre. Depuis les travaux avant-gardistes de Taylor en 1932-1934 [1][2], le mode de déformation et de rupture de gouttes isolées dans une matrice sous écoulement a fait l'objet d'une attention singulière aussi bien sur le plan théorique que sur le plan expérimental.
Nous allons donc rappeler dans cette partie quelques concepts de physico-chimie des interfaces qui seront utiles pour la compréhension de la détermination de la tension interfaciale des mélanges PLA_PBAT.

I Développement de la morphologie- Aspects généraux

L'histoire du développement des mélanges de polymères a été documentée par Utracki. D'un point de vue thermodynamique et de par leur masses molaires généralement élevées, la plupart des mélanges de polymères utilisés dans des applications industrielles sont incompatibles. En général, la morphologie de ces mélanges multiphasés dépend fortement de leur composition, des conditions du mélange, de la tension interfaciale entre les phases et des propriétés viscoélastiques de chaque constituant. Selon les conditions de mélangeage des mélanges, formés de matrice et de phase dispersée, la phase dispersée peut prendre une forme sphérique, ellipsoïdale ou fibrillaire.

L'interface qui existe entre deux matériaux immiscibles résulte d'un équilibre entre deux forces qui s'opposent : l'enthalpie de mélange tend à séparer les constituants des mélanges alors que l'entropie tend à les mélanger pour maximiser le nombre de configurations possibles du système. L'interface est donc une zone de transition entre les deux matériaux constituant le mélange qui permet de maximiser l'énergie libre du système.

Pour stabiliser la morphologie d'un mélange, et donc en quelque sorte garantir ses propriétés spécifiques, il faut agir à l'interface et créer des interactions pour augmenter l'adhésion entre les phases. La compatibilisation d'un mélange binaire peut se faire par différentes méthodes. Les deux stratégies les plus fréquemment utilisées sont :

- Ajout d'un composant, généralement un copolymère préformé, à l'interface. Ce composant est susceptible d'interagir avec les deux phases et augmentera ainsi leur adhésion.
- Formation in-situ d'un copolymère par réaction chimique à l'interface entre les phases. Ceci peut se faire par extrusion réactive ou encore en induisant des réactions de trans-estérification entre les polymères.

Le développement de la morphologie à l'état fondu est largement traité dans la littérature. Notre but dans cette partie bibliographique n'est pas de dresser une liste exhaustive de tous les travaux, mais plutôt de faire le point sur les modèles ainsi que les résultats les plus per-

tinents dans ce domaine d'étude. Ainsi, de nombreux travaux étudient le processus de déformation d'une goutte newtonienne suspendue dans une matrice newtonienne en cisaillement simple à faibles déformations. Ces travaux s'inspirent dans leur majorité du développement théorique de Taylor, étendue des travaux d'Einstein sur des suspensions diluées des sphères solides dans un fluide visqueux. Les deux revues les plus intéressantes dans ce domaine sont celles d'Acrivos [4] et Rallison [5]. Un résumé a été présenté plus tard par Stone [6] dans lequel de nouveaux problèmes concernant la rupture de la goutte, les agents actifs d'interface et l'écoulement complexe ont été pris en considération. De plus, une récente revue a été publiée par Tucker et Moldenaers où la relation entre microstructure, écoulement et rhéologie des systèmes non compatibles a été décrite. En revenant aux précieux travaux de Taylor, il a été montré que la déformabilité de la phase dispersée est gouvernée par deux paramètres adimensionnels : le rapport de viscosité « p » (Eq.1) et le nombre capillaire « Ca » (Eq.2)

Équation 1 $$p = \frac{\eta_d}{\eta_m}$$

η_d et η_m représentent respectivement les viscosités Newtoniennes de la phase dispersée et de la matrice en Pa.s.

Équation 2 $$Ca = \frac{\sigma \bullet R}{\alpha_{12}} = \frac{\eta_m \dot{\gamma} R}{\alpha_{12}}$$

« $\dot{\gamma}$ » correspond à la vitesse de cisaillement dans l'écoulement en s^{-1}, « R » représente le rayon de la gouttelette de fluide en m et « α » la tension interfaciale du mélange en $N.m^{-1}$.

Le nombre capillaire représente en fait un rapport des contraintes visqueuses ($\eta_m \dot{\gamma}$) que la matrice applique sur la phase dispersée pour la déformer et les contraintes interfaciales (α/R) qui tendent à résister à cette déformation et à maintenir la forme sphérique des particules.

Pour les fluides viscoélastiques, certains auteurs ont proposé d'observer le rapport d'élasticité K' [3]

Équation 3 $$K' = \frac{\lambda_D}{\lambda_M}$$

Où λ_D et λ_M représentent respectivement le temps de relaxation de la phase dispersée et de la matrice.

Par la suite, en 1982, Grace [7] compléta cette théorie en l'élargissant aux écoulements élongationnels tout en définissant une valeur critique de nombre capillaire Ca_{cr} (Cf .figure C-1). Son étude expérimentale menée pour relier la variation du nombre capillaire critique au rapport de viscosité p pour un cisaillement simple et un écoulement élongationnel hyperbolique montrent que les gouttes se brisent facilement en écoulement élongationnel qu'en cisaillement simple.

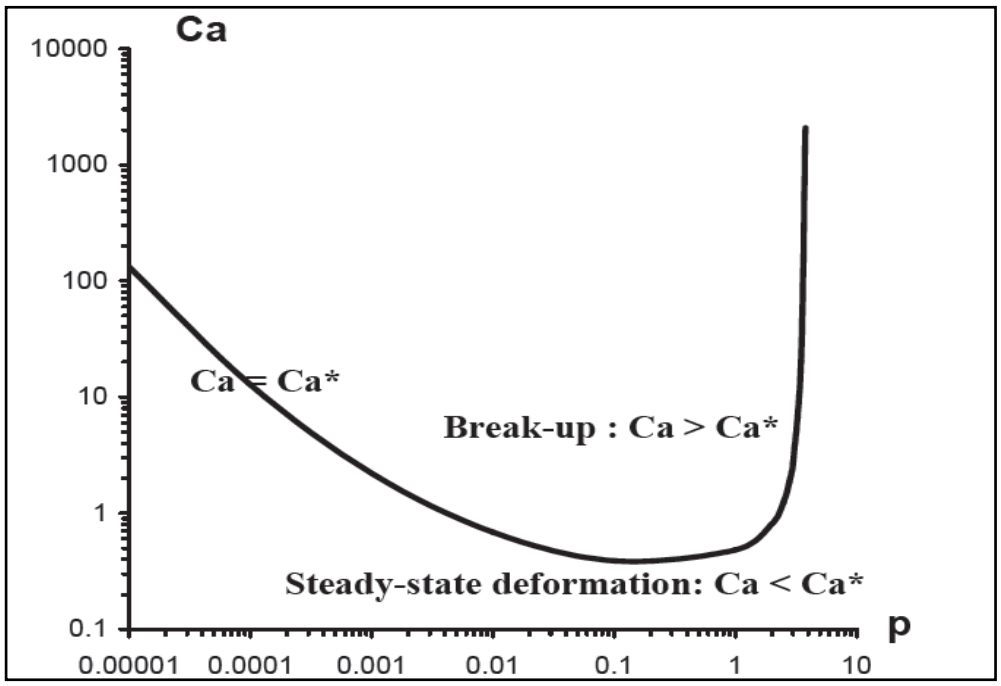

Figure C-1 Effet du rapport de viscosité « p » sur Ca_{cr} déterminé par Grace

D'une autre part, pour le cas d'un cisaillement simple, la rupture ne peut plus avoir lieu pour des systèmes ayant un rapport de viscosité supérieur à 4. En revanche, dans un écoulement élongationnel, la rupture des gouttelettes est observée quel que soit le rapport des viscosités.
De Bruijin donne une expression empirique permettant de calculer la valeur critique du nombre capillaire à partir du rapport des viscosités du mélange considéré :

Équation 4

$$Log(Ca_{crit}) = -0,506 - 0,0994\log(p) + 0,124(\log(p))^2 - \frac{0,115}{\log(p) - 0,6107}$$

Le mode de rupture et de la déformabilité de gouttelettes de polymère fondu dans un écoulement varie selon le rapport de viscosité et le nombre capillaire du système étudié. La figure C-2 montre 4 classes de déformation et de rupture d'une gouttelette. Dans le cas où aucun cisaillement n'est appliqué, la gouttelette présente une forme sphérique. Sous faible déformation, elle se déforme en forme d'ellipsoïde ; En revanche, pour des vitesses de cisaillement plus importantes, différents modes de rupture sont observés :

(a) Faible « *p* » : Rumsheidt & Mason ont montré que la goutte adopte une forme sigmoïdale (phénomène de Tip streaming)

(b) « *p* » = 1: Les auteurs ont constaté que la contraction de la goutte cesse d'être homogène et devient de plus en plus importante au centre (phénomène de striction). La gouttelette initiale se rompe en donnant naissance à deux gouttelettes filles.

(c) « p » = 0.7" et Ca > Ca*, la gouttelette se déforme sous forme cylindrique puis se rompe en des gouttelettes plus faibles.

(d) « p > 4 »: aucune rupture n'est observée.

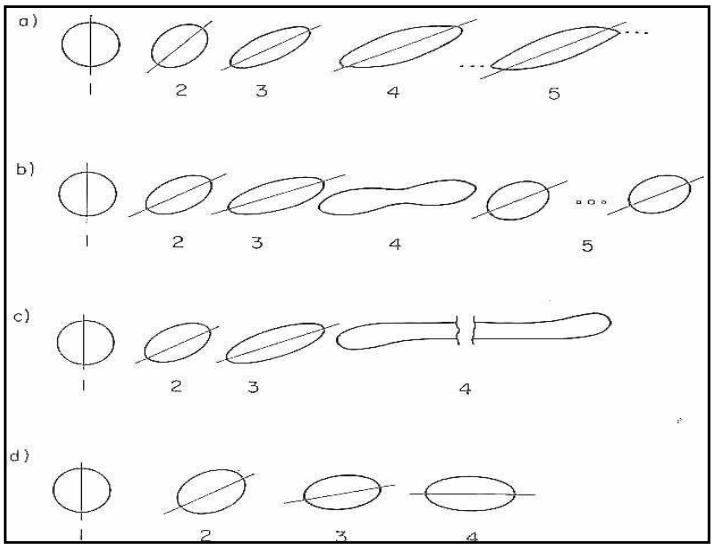

Figure C-2 Différents mode de déformation d'une gouttelette soumise à un cisaillement simple (a) p = $2*10^{-4}$; (b) p = 1; (c) p = 0.7; (d) p = 6

Dépendamment des valeurs de Ca, tant que Ca < $Ca_{cr,}$ les gouttes se déforment et atteignent une forme stable. L'énergie interfaciale domine. En revanche, si Ca > Ca_{cr}, elles se déforment de manière continue, deviennent instables puis se rompent suivant un des deux modes de rupture suivant :

- Pour de nombres capillaires légèrement supérieurs au nombre capillaire critique (Ca > $2Ca_{cr}$), les gouttelettes se déforment de manière affine dans un premier temps et se transforment en filaments.
- Pour des situations où le nombre capillaire est largement supérieur au Ca_{cr}, la goutte s'étire et adopte une forme fibrillaire avant de se fragmenter en plusieurs gouttelettes sœurs via les instabilités interfaciales. Il s'agit des instabilités de Rayleigh. L'élasticité des composants peut également contribuer à une augmentation de la taille des inclusions [3]

II Développement de la morphologie – Cas d'un mélange réactif

L'extrusion réactive représente une technique, fréquemment utilisée pour le contrôle de la phase de morphologie, phase de stabilisation ainsi que de l'adhésion interfaciale dans le cas des mélanges hétérogènes non miscibles.
La génération de la morphologie au cours de la transformation d'un mélange de polymères à l'état fondu représente le passage du mélange d'une taille macroscopique (granulés et /ou

poudres) en premier temps à une taille microscopique générée lors de l'étape de plastification de ce dernier. Pour une meilleure compréhension de l'influence du mélange réactif sur le développement de la morphologie, il est crucial d'examiner brièvement son développement dans le cas du mélange non-réactif. Une dépendance marginale de la taille de la phase dispersée avec le temps de mélange pour de larges intervalles de torques. En effet, la morphologie se développe au cours des premiers stades du mélange suite à un cisaillement des structures sous formes de feuilles suivi par une tension interfaciale conduisant à une rupture de ces dernières en des particules sphériques. L'effet de la présence d'un agent interfacial (copolymère bloc, compatibilisant) absorbé à l'interface matrice/gouttes d'un mélange de polymères altère considérablement l'évolution de la morphologie de ce dernier et par conséquent son comportement rhéologique durant sa mise en œuvre. Cet agent agit comme un agent tensioactif qui diminue la tension interfaciale du mélange. Il en résulte une réduction à la déformation des gouttes à l'interface. La déformation des gouttes sous l'effet d'un écoulement élongationnel en présence d'un agent tensioactif a été étudiée numériquement par Stone & Leal en 1990 ainsi que par Milliken et al. en 1993. Ces études ont montré que le mécanisme de déformation des gouttes est davantage gouverné par le profil de concentration du copolymère à l'interface suite à l'écoulement que par la diminution de la tension interfaciale. Ce profil de concentration résulte de la compétition entre deux facteurs antagonistes, d'un côté les molécules du copolymère sont repoussées par convection du centre de la goutte déformée vers ses deux extrémités en créant ainsi un gradient de concentration du copolymère à l'interface. De l'autre côté, les molécules de l'agent interfacial ont tendance à diffuser des extrémités vers le centre de la goutte afin de rétablir une distribution uniforme du copolymère au niveau de l'interface. Si la concentration locale du copolymère aux extrémités approche la concentration de saturation les molécules du copolymère auront tendance à diffuser vers l'équateur de la goutte afin de soulager ses extrémités, ce qui donne naissance à des contraintes de type Marangoni. Ces contraintes auront pour effet de stabiliser l'interface et par conséquent de limiter la déformation de la goutte. Toutefois, il convient de souligner l'influence des propriétés des systèmes sur la mesure de la tension interfaciale (différentes densités, différent ratio de viscosités, transparence, distribution de la masse moléculaire, température…). Pour les systèmes réactifs, il a été montré qu'un faible taux de réaction réduit fortement la tension interfaciale entre les polymères. Selon les travaux de Sundararaj, la tension interfaciale a été diminuée de moitié pour un mélange compatibilisé EPR -Anhydride maléique/PS-Amine.
Par conséquent, les travaux de recherche réalisés dans ce sens visent à comprendre les différents mécanismes relatifs à la déformation des gouttes afin d'établir des modèles qui seraient capables de prédire le comportement des mélanges sous écoulement et finalement prévoir les propriétés finales sans faire l'expérience. Sur le plan expérimental, différentes méthodes de détermination de la tension interfaciale sont développées dans la littérature.

III La tension interfaciale à l'état fondu

III.1 Méthodes de mesure

Les propriétés finales d'un mélange hétérogène de polymères sont intimement liées aux propriétés de ces composants, de leur morphologie générée au cours de leur mise en œuvre (distribution et dispersion des phases), et des propriétés de l'interface/interphase. Ainsi, dans le cas des systèmes multiphasiques (mélanges de polymères et alliages), l'étude de la tension interfaciale représente un paramètre – clé pour la caractérisation et la quantification des interactions présentes dans un mélange. Néanmoins, plusieurs techniques sont dispo-

nibles pour la détermination de la tension interfaciale. Le principe général de toutes ces techniques se base sur la balance entre une force motrice (Forces visqueuses, d'inertie ou gravitationnelles) et une résistance due à la force interfaciale, qui tend à minimiser l'aire de contact entre les différentes phases. De point de vue expérimental, il existe de nombreuses techniques de détermination dont deux types principaux se distinguent ; les méthodes à l'équilibre et les méthodes transitoires. La première famille contient « *la goutte pendante* », « *la goutte sessile* » ainsi que « *la goutte posée* ». Dans ce cas, la tension interfaciale est déterminée à l'état final au moment où le système atteint son état d'équilibre. Les méthodes transitoires sont plus rapides à mettre en œuvre, évitant ainsi la dégradation thermique des polymères. Parmi ces méthodes, nous pouvons citer « *la rupture d'un filament* », « *la rétraction de la gouttelette* déformée », « *la fibre enrobée* » et enfin « *la rétraction du disque* ». L'avantage majeur de ces méthodes réside dans la valeur de la tension interfaciale, plus proche de la réalité des mélanges. Ces méthodes reposent toutes sur l'observation microscopique de l'évolution de morphologie d'une phase minoritaire enrobée dans une matrice sous l'action de la température. Le principe consiste à mesurer le temps nécessaire à la phase minoritaire pour atteindre une morphologie stable (sphérique). Des calculs permettent alors de remonter à l'énergie interfaciale à l'état fondu.
Par ailleurs, il existe une autre méthode quelque peu singulière. Il s'agit d'une méthode rhéologique de cisaillement dynamique à faible amplitude de déformation. Le modèle de la tension interfaciale est basé sur le modèle d'émulsion de Palierne. Le comportement viscoélastique des polymères est pris en compte et les données sont représentatives de l'aire interfaciale totale du fait que la tension interfaciale est déterminée à partir de la relaxation de plusieurs gouttelettes plutôt qu'une gouttelette isolée. Cette méthode est lourde à mettre en œuvre et la précision sur la mesure reste assez faible. De par le matériel à notre disposition, nous avons décidé de mesurer la tension interfaciale de nos mélanges par la méthode de « *la rétraction de la gouttelette déformée* ».

III.1.1 Détermination de la tension interfaciale par la méthode de la « Rétraction de la gouttelette déformée » en utilisant la platine de cisaillement

Cette méthode repose sur l'enrobage d'une goutte de polymère entre deux films de l'autre polymère. Un bon enrobage de la goutte est nécessaire pour lui permettre de relaxer en une goutte sphérique. Cette méthode est utilisable sur une large gamme de viscosités.
Cette expérience a été mise en œuvre aussi bien sur des fluides newtoniens [8][9] que non newtoniens [10][11] et ce pour des études directes de la relaxation par analyse de la forme de la goutte, ou pour déterminer les tensions interfaciale. Il est nécessaire de réunir quelques conditions géométriques et optiques particulières pour pouvoir visualiser la morphologie de la goutte ou du mélange de polymères. La matrice doit être transparente. Dans le cas où les deux phases sont transparentes, les indices de réfraction respectifs doivent être suffisamment différents pour générer un bon contraste lors des observations. Leur différence de densité doit également être faible.

a) Descriptif du dispositif de cisaillement

Pour déterminer la tension interfaciale des mélanges multiphasiques, une platine de cisaillement LINKAM CSS 450 couplée à un microscope optique à transmission a été utilisée. Le schéma C-3 de la platine est présenté sur la Figure. Elle est constituée de deux vitres de Quartz parallèles entre lesquelles sera placé l'échantillon. Elle est pilotée par un ordinateur

utilisant le logiciel d'acquisition Linksys 1.41 pour les consignes de température, d'espacement entre lames et de déformation. Le dispositif présente les spécifications techniques suivantes :

- Température de l'ambiante à 450°C assurée par des plateaux chauffants en aluminium accolés aux vitres. Le système de chauffage est donc purement conductif.
- Vitesse de chauffage/refroidissement de 0,01 à 30°C/min. Les éléments mécaniques de la platine sont refroidis par un courant d'eau froide (20°C).
- Espacement entre les vitres variant entre 5 - 2500µm et modifiable à l'aide d'un moteur micrométrique.

L'observation de l'échantillon dans son épaisseur s'effectue à travers deux perçages de 5mm de diamètre réalisés dans les plateaux chauffants par transmission de la lumière. La zone d'observation est située à 7.5mm du centre de la vitre. Le cisaillement est appliqué par la rotation de la vitre inférieure à l'aide d'un moteur micrométrique alors que la vitre supérieure reste fixe.

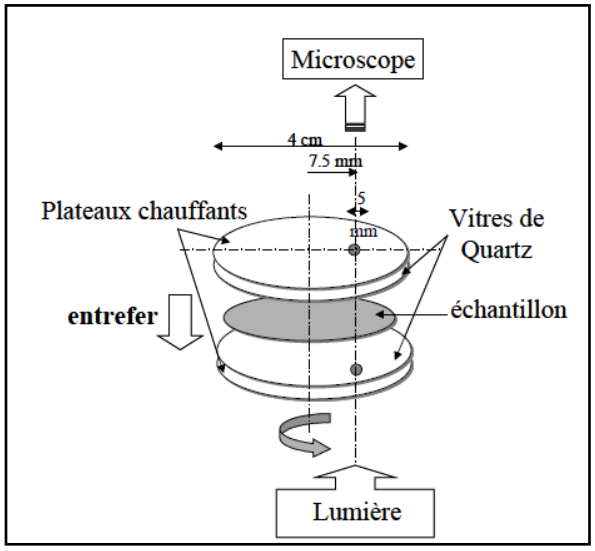

Figure C-3 Schéma de fonctionnement de la platine de cisaillement LINKAM CSS 450

La cellule Linkam est prévue pour être montée sur un microscope optique type équipé d'objectifs « longues focales » $\times 20$ et $\times 32$ permettant d'acquérir les images, qui serviront par la suite à l'analyse des phénomènes observés par le biais d'une caméra numérique CCD connectée au logiciel d'acquisition. Différentes auteurs ont déjà publié des travaux effectués sur ce dispositif. On peut citer par exemple Derayl et Cassagnau [12] qui ont choisi de travailler en mode écoulement à vitesse de cisaillement constant où ils ont montré la possibilité de d'obtenir des fibres relativement fines est calibrées à partir de gouttes de copolymère d'éthylène et d'acétate de vinyle dans une matrice de PDMS. En effet, une fois la morphologie désirée est atteinte, la température est changée provocant la cristallisation des fibres.

b) Mesure de la tension interfaciale

En utilisant la platine de cisaillement décrite ci-dessus, un saut en déformation est appliqué à une gouttelette de polymère fondue immergée dans une matrice polymère fondue. La relaxation de la gouttelette est alors enregistrée par la caméra optique jusqu'à ce que la goutte ellipsoïde retrouve sa forme d'équilibre sphérique. La valeur de la tension interfaciale est déduite des variations dimensionnelles de la gouttelette en fonction du temps de relaxation tout en connaissant la viscosité des constituants du mélange.

- Préparation de l'échantillon

L'échantillon-sandwich de polymères, de 500 µm à 1mm d'épaisseur, est préparé en faisant disperser des gouttelettes de polymère fondu à partir de poudre finement broyée entre deux films circulaires de matrice. Le système est ensuite porté à une température supérieure à la température de fusion (étape de plastification), la phase dispersée et la matrice devant être fondues. La préparation des échantillons pour la détermination de la tension interfaciale est schématisée comme suit (Cf figure C-4):

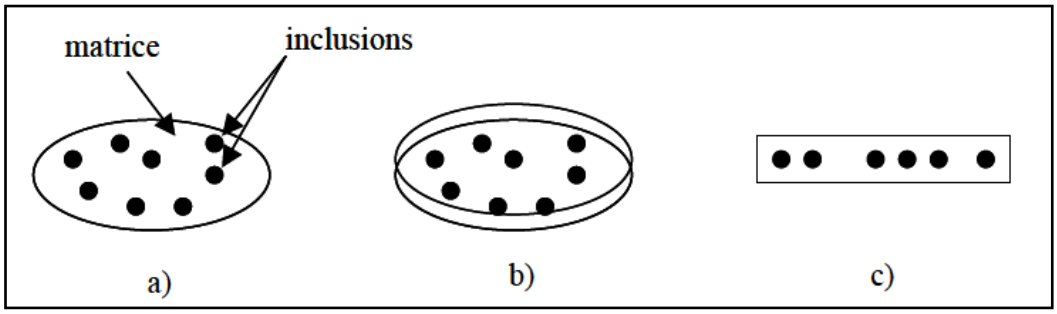

Figure C-4 Trois étapes pour la préparation de l'échantillon; a) dépôt de l'inclusion, b) assemblage du sandwich à température ambiante, c) fusion des polymères à haute température et enrobage de l'inclusion-coupe verticale de l'échantillon

L'étape (a) consiste à déposer la phase dispersée sous forme de poudre de manière homogène sur toute la surface d'un disque de matrice, à température ambiante.
L'étape (b) consiste à mettre le second disque de matrice sur les inclusions, à température ambiante. Une fois préparé, l'échantillon est introduit dans la platine de cisaillement et porté à haute température afin de plastifié l'ensemble phase dispersée-matrice. L'entrefer de la platine est ensuite modifié de façon à assurer une bonne cohésion entre la vitre supérieure et l'échantillon fondu. Cet ajustement de l'entrefer assure également un enrobage complet de la phase dispersée selon l'étape (c).

Après fusion, les particules de poudre sont soumises à un traitement de cisaillement pendant quelques secondes pour obtenir des gouttelettes sphériques bien définies. De courts filaments de polymères sont générés sous cisaillement. Lorsque le cisaillement est stoppé, les filaments se rompent en des multiples gouttelettes via les instabilités de Rayleigh. Parmi ces gouttelettes sphériques, une gouttelette isolée, non perturbée par une gouttelette voisine, est sélectionnée. Une succession de sauts de déformation est alors appliquée à cette gouttelette

jusqu'à ce qu'elle se déforme en ellipse de révolution. Dès l'arrêt du cisaillement, la relaxation de la gouttelette déformée est enregistrée par la caméra optique toutes les secondes.

- Méthode de calcul

Luciani et al et Siguillo et al proposèrent une expression pour décrire la relaxation de forme de goutte basée sur deux hypothèses : la tension interfaciale est la seule force motrice de la relaxation d'une goutte faiblement déformée et les propriétés rhéologiques des fluides ne varient pas pendant la mesure. Le traitement quantitatif est basé sur la théorie de Taylor (Eq.5) dans le cas des faibles déformations, qui a introduit un paramètre sans dimension D compris entre 0 (petites déformations) et 1 (grandes déformations):

Équation 5

$$D = D^\circ \exp - \left\{ \frac{40(p+1)}{(2p+3)(19p+16)} \frac{\alpha_{12}}{\eta_m R^\circ} t \right\} = D^\circ \exp\left\{ -\frac{t}{\tau_d} \right\} = \frac{L-B}{L+B}$$

D° est le paramètre de déformabilité au temps intial t=0, p le rapport de viscosité des constituants, η_m la viscosité Newtonienne de la matrice, R° le rayon initial de la gouttelette et α la tension interfaciale du mélange. Dans la limite des faibles déformations, la goutte déformée est généralement considérée comme un ellipsoïde dont l'axe majeur L est orienté avec un angle θ par rapport à la direction de la vitesse de déformation et B son axe mineur dans le plan vitesse/gradient de cisaillement.

Suivant cette analyse, le paramètre de déformation, D, décroît exponentiellement avec un temps caractéristique τ_d :

Équation 6 $$\tau_d = \frac{\eta_{eq} \bullet R^\circ}{\alpha_{12}}$$

La viscosité équivalente du mélange peut être déduite de l'expression suivante :

Équation 7 $$\eta_{eq} = \frac{(2p+3)(19p+16)\eta_m}{40(p+1)}$$

A partir des résultats expérimentaux, il suffit de tracer le logarithme népérien de D en fonction du temps. La pente de cette courbe donne accès au temps de relaxation τ_d de la phase dispersée. La connaissance des paramètres intrinsèques des composants permet ensuite de calculer la valeur de la tension interfaciale du mélange.

III.1.2 Détermination de la tension interfaciale par le « modèle de Palierne »

De nombreux modèles rhéologiques pour le domaine viscoélastique linéaire et à faibles déformations, ont été développés. Parmi lesquels on peut citer, le modèle d'Einstein, Le modèle d'émulsion d'oldroyd, le modèle de Choi et Schowalter et le modèle de Palierne.

Le modèle utilisé dans le calcul de la tension interfaciale de nos mélanges est celui de Palierne. Il s'agit d'une extension du modèle d'Oldroyd. Palierne a proposé une théorie prenant en compte la viscoélasticité des deux phases. Il tient également compte des effets de la distribution de la taille des inclusions.
Le modèle de Palierne décrit le module complexe du mélange à partir des modules de la phase dispersée et de la matrice:

Équation 8
$$G_b^*(\omega) = G^*_m(\omega)\frac{1+3\phi H(\omega)}{1-2\phi H(\omega)}$$

Avec

Équation 9
$$H(\omega) = \frac{4(\frac{\alpha}{R})\left[2G_m^*(\omega)+5G_d^*(\omega)\right]+\left[G_d^*(\omega)-G_m^*(\omega)\right]\left[16G_m^*(\omega)+19G_d^*(\omega)\right]}{40(\frac{\alpha}{R})\left[G_m^*(\omega)+G_d^*(\omega)\right]+\left[2G_d^*(\omega)+3G_m^*(\omega)\right]\left[16G_m^*(\omega)+19G_d^*(\omega)\right]}$$

Où G^*_b, G^*_m, G^*_d sont les modules complexes, en fonction de la fréquence, du mélange, de la matrice et de la phase dispersée, respectivement. Ce modèle permet d'estimer, à partir de données viscoélastiques des composants d'un mélange à l'état fondu, la tension interfaciale du système comme l'ont fait, par exemple, Lacroix et al. en 1997. Cette technique ne pourrait être utilisée que dans le cas où le plateau de G' aux faibles pulsations de fréquences est accessible dépendamment du torque et des intervalles de fréquences du rhéomètre. Pour des systèmes de viscosités élevés, le temps de relaxation pourrait être très élevé. Ainsi, la zone terminale se déplace vers les plus faibles fréquences. Ce qui est inaccessible expérimentalement. En outre, cette méthode rhéologique présente des difficultés expérimentales. Elle nécessite la préparation des mélanges par mélange mécanique ou en solution, la taille des particules est déterminée par microscopie électronique. L'erreur commise dans l'estimation de la taille des particules affecte directement la détermination de la tension interfaciale étant donné que les deux paramètres « R » et « γ » apparaissent dans l'expression du modèle. Certaines autres erreurs peuvent également provenir de la procédure d'ajustement.

References

[1] Taylor GI. The viscosity of a fluid containing small drops of another fluid. Proc. R. Soc. London, SER. A, **138**: 41-48. 1932.
[2] Taylor, GI. The formation of emulsions in definable Fields of flow. Proc. R. Soc. London, SER. A, **146**: p. 201-523. 1934.
[3] Mighri F, Ajji A, and Carreau PJ. Influence of elastic properties on drop deformation in elongational flow F. J. Rheo. **41**: 1183-1201. 1997.
[4] Acrivos A, Lo TS. Déformation and breakup of a single slender drop in an extensional flow, Journal of Fluid Mechanics, 86: 641-672.1978.
[5] Rallison JM. Note on the time-dependent deformation of a viscous drop which is almost spherical, Journal of Fluid Mechanics. 98: 625-633. 1980.
[6] Stone HA. Dynamics of drop deformation and breakup in viscous fluids. Ann. Rev. Fluid Mech., **26**: 95-102. 1994.
[7] Grace HP. Dispersion phenomena in high viscosity immiscible fluid systems and application of static mixers as dispersion devices in such systems. Chem. Eng. Commun. **14**: p. 225-227. 1982.
[8] Tjahjadi M, Stone HA, Ottino JM. Satellite and subsatellite formation in capillary breakup. J. Fluid Mech. **243**: p. 297-317. 1992.
[9] Tjahjadi M, Ottino JM, Stone HA. Estimating interfacial tension via relaxation of drop shapes and filament breakup. AIChE J., 1994. **40**: p. 385.
[10] Tretheway DC. Deformation and relaxation of Newtonian drops in planar extensional flows of a Boger fluid. J. Non-Newtonian Fluid Mech. **99**: p. 81-108. 2001.
[11] Sibillo, V, Simeone M, Guido S, Greco F, Maffettone PL. Start-up and retraction dynamics of a Newtonian drop in a viscoelastic matrix under simple shear flow. Journal of Non-Newtonian Fluid Mechanics. **134**: p. 27-32. 2006.
[12] Deyrail, Y. and Cassagnau, P., Phase deformation under shear in an immiscible polymer blend: Influence of strong permanent elastic properties. Journal of Rheology. **48**: p. 505-524. 2004.

Appendix D : Déformation de polymères

Le procédé de bi-étirage est un procédé de mise en forme complexe qui combine différentes phases de déformation du matériau.

Intérêts de l'orientation biaxiale des films à base de PLA

De nombreux intérêts se dégagent de l'orientation des films à base de PLA. Ils se résument par l'amélioration des propriétés physiques et mécaniques (brillance et transparence, bonnes propriétés de barrière, résistance aux chocs, obtention de très faibles épaisseurs…), l'obtention de films rétractables non thermo-fixés, l'obtention des films de stabilité dimensionnelle thermo-fixés et finalement par l'intérêt économique.

I Présentation d'ETIFI

ETIFI représente la machine de traction bi-axiale utilisée au sein du CEntre de Mise En Forme des matériaux (CEMEF) (Cf. figure D-1). Cette machine est constituée de deux axes de travail pouvant être pilotés soit de manière individuelle soit en leur appliquant la même consigne. Par conséquent, deux types de chargements peuvent être effectués : symétriques ou dissymétriques. Comme le montre la figure, ETIFI contient 4 liaisons glissières (système pour déplacer les traverses mobiles), 4 moteurs électriques asservis par un variateur de vitesse et 4 mors (système de fixation de l'éprouvette). Les moteurs sont capables de fournir des vitesses de déplacement de traverse allant de 10^{-3} mm/s à 100 mm/s et donc des vitesses de déformations allant de 10^{-4} s^{-1} à 10 s^{-1}. Dans la partie mécanique de la machine, 3 fours sont présents et se déplacent manuellement. Ils assurent des températures supérieures à 200°C en pulsant de l'air chaud. Au moment de l'essai, ils se positionnent sur la zone de travail et, par convection forcée, assurent une température homogène mesurée à l'aide d'un thermocouple placé à l'intérieur du four. L'originalité de cette machine se résume par le fait de pouvoir imposer des cycles thermiques (Chauffe, trempe à titre d'exemple) à notre échantillon en changeant manuellement les différents fours.

Toutefois, l'acquisition des données relatives au comportement de nos matériaux est assurée par des capteurs (de déplacement LVDT, de forces et de couples des moteurs) disposés sur chaque bras de la machine et par un thermocouple. Nous tenons à signaler que pour un pour un axe de travail composé de deux bras, nous avons un capteur de 500 N sur un bras et un de 5000 N sur l'autre.
ETIFI peut être donc pilotée de trois manières différentes : en vitesse, en position et en force. Dans notre étude, nous avons appliqué un asservissement en vitesse, un pilotage de type valeur fixe qui fournira une valeur fixe de vitesse pendant un temps « t » de séquence.

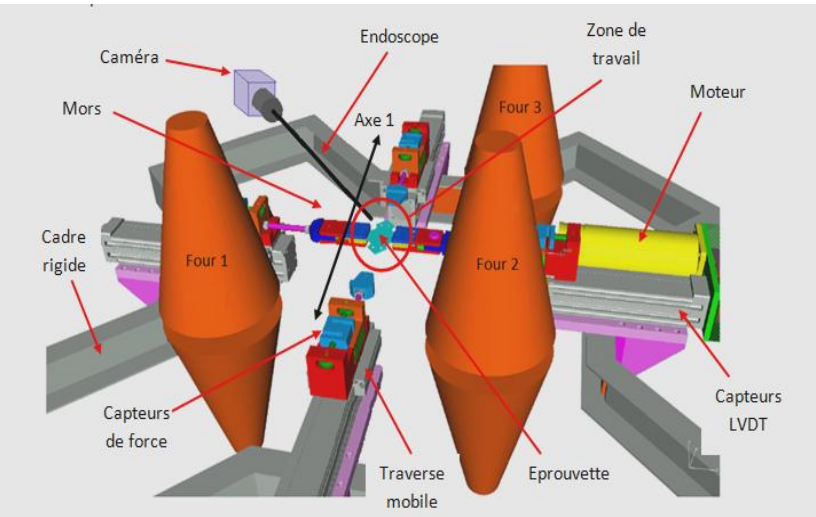

Figure D-1 Schéma représentatif d'ETIFI

I.1 Protocole expérimental

a) Conception de l'éprouvette

L'éprouvette est conçue de façon à être fixée par 4 mors ; C'est pour cette raison que les éprouvettes ont la forme d'une croix (Figures D-2 et D-3).

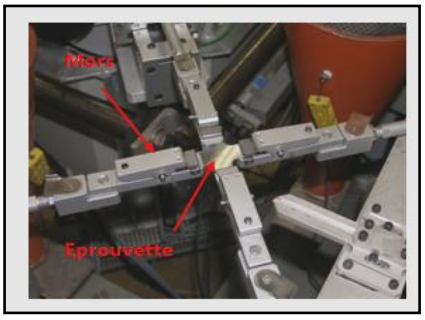

Figure D-2 Système de fixation de l'éprouvette

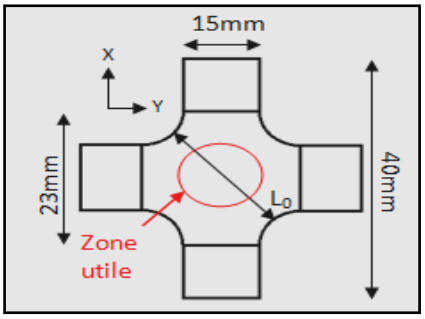

Figure D-3 Eprouvette en croix pour traction bi-axiale

C'est la zone utile de l'éprouvette (la diagonale) qui permet la localisation de la déformation au centre de l'éprouvette.

b) Description des sollicitations rencontrées

Historiquement, les cinématiques de déformation ont été définies relativement aux taux d'étirage, λ. Dans le cadre d'étirage uni-axial, ce paramètre est défini comme le rapport entre la longueur courante L et la longueur initiale L_0 de l'échantillon :

Équation 10 $$\lambda = \frac{L}{L_0}$$

Dans le cadre de bi-étirage, le taux d'étirage planaire ou de bi-orientation (TEP) est défini par le produit des taux d'étirage dans chacune des directions orthogonales d'étirage :

Équation 11 $$TEP = \lambda_{MD} \times \lambda_{TD}$$

Où MD désigne la direction machine ou axiale et TD représente la direction transverse, perpendiculaire à la direction machine.

Les courbes Contrainte/Déformation seront obtenus à partir des valeurs de force et de déplacement en utilisant la méthode globale de calcul :

Équation 12 $$\varepsilon_{x,y}(t) = \ln(\lambda) = \ln(\frac{l(t)}{l_0})$$

Équation 13 $$\sigma(t) = \frac{\sqrt{2} \times F(t)}{e_0 \times L_0 \times e^{-\varepsilon}}$$

Les capteurs de déplacement LVDT permettront le calcul de L(t) (Longueur de l'éprouvette), quant à la force F, elle sera donnée par les capteurs de force. L'épaisseur « e_0 » et la longueur « L_0 » constituent les dimensions de l'éprouvette.

Dans le but de travailler dans des conditions proches du procédé industriel, les paramètres d'essai ont été fixés comme suit :

a) Déformation uni-axiale de 1,2 Hencky (équivalent à λ ~3)
b) Vitesses d'étirage de 0,1mm/s, 1mm/s et 10 mm/s (équivalents respectivement à 0.004, 0.04 et 0.4 s-1)

c) Température d'essai T°= 75°C

D'un point de vue expérimental, les essais de biétirage font intervenir trois étapes successives :

- Une étape de chauffage de l'échantillon par convection, pendant 300 sec jusqu'à atteindre dans son épaisseur, une température homogène comprise entre sa température de transition vitreuse et sa cristallisation thermique.
- Une étape d'étirage isotherme à vitesse de déformation constante pendant un temps « t » dépendamment de la vitesse d'étirage.
- Une étape de refroidissement rapide à 25°C afin de figer la structure de l'échantillon et de limiter toute évolution microstructurale post-étirage. Une trempe efficace est ici recherchée dans le but de réaliser des analyses microstructurales aussi proches que possibles que celles pouvant être réalisées in situ.

Micro-mécanismes de déformation plastique et d'endommagement des polymères semi-cristallins

La connaissance précise des mécanismes de déformation et d'endommagement est nécessaire à l'analyse du comportement et des propriétés mécaniques du matériau. Dans cette partie, les mécanismes de la déformation plastique dans les polymères semi-cristallins sont succinctement décrits en considérant successivement la phase amorphe, la phase cristalline.

Les mécanismes de déformation des polymères semi-cristallins sont étroitement liés à la présence des deux phases, amorphe et cristalline. La phase amorphe peut être à l'état vitreux. Notons que la phase amorphe présente dans un milieu semi-cristallin peut présenter des caractéristiques quelques peu différentes d'un polymère amorphe massif correspondant en particulier à la température de transition vitreuse.

I Déformation plastique d'un polymère semi-cristallin / Mécanismes de déformation : généralités

Dans cette partie bibliographique, nous avons porté notre intérêt sur la déformation des polymères semi-cristallins. En général, la déformation plastique d'un matériau est un processus thermiquement activé. En effet, la température et la vitesse de déformation conditionnent ses propriétés mécaniques. L'étude de la dépendance de la déformation en contrainte, en température et en vitesse est d'une grande importance dans la compréhension du comportement plastique des matériaux et des mécanismes élémentaires.
L'échantillon PLA, comme tout autre polymère semi-cristallin est le siège de processus de mécanismes de déformation plastiques se propageant et entraînant une réduction de la cristallinité au début de la déformation sans détruire l'ordre cristallin. Parmi ces mécanismes nous pouvons citer :

a) *Glissement cristallographique [1][2][3]*

Le mécanisme le plus important pour la déformation plastique de cristaux polymères est le glissement cristallographique puisqu'il est capable de produire des déformations plus grandes que les autres mécanismes. Il est caractérisé par un plan (hkl) et une direction (uvw), qui identifient le système de glissement. Les plans de glissement sont le plus souvent ceux présentant une densité atomique élevée.

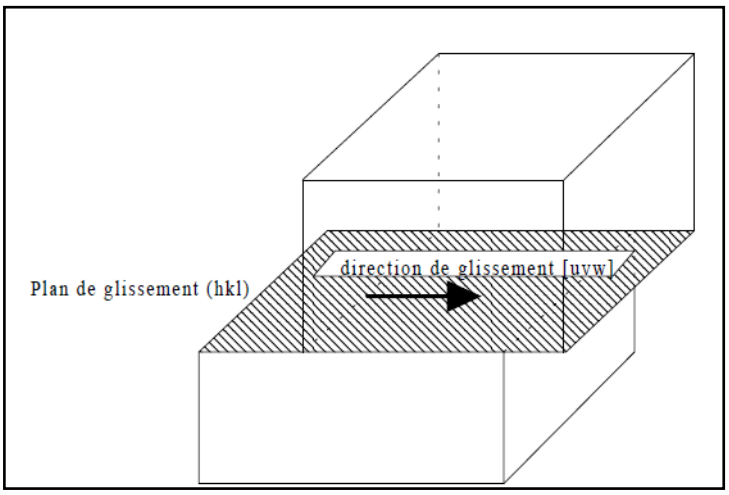

Figure D-4 Illustration du mécanisme de glissement cristallographique

Compte tenu des types de liaisons entre atomes (covalentes le long de la chaîne et Van der Waals entre chaînes voisines), on peut considérer que seuls sont potentiellement actifs les systèmes de glissement dont le plan contient l'axe de la chaîne. On pourra distinguer les glissements dans la direction de la chaîne (« *chain slip* »), qui sont les plus faciles, de ceux perpendiculaires aux chaînes (« *transverse slip* ») qui vont intervenir suite à l'orientation favorable de certains cristaux.

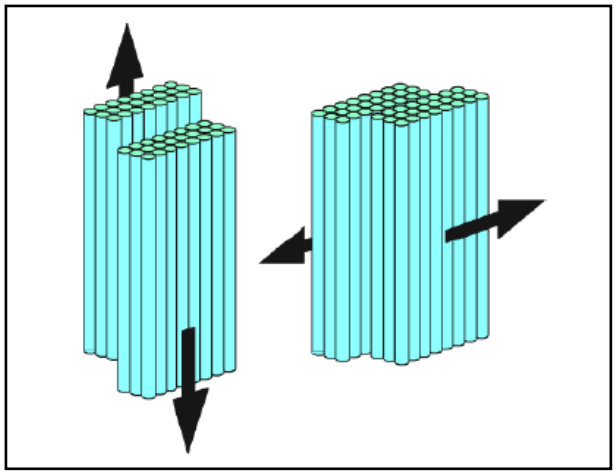

Figure D-5 Glissement parallèle et perpendiculaire aux chaînes macromoléculaires

Le glissement parallèle peut présenter deux aspects (i) le 'glissement homogène' où il intervient de manière égale pour tous les plans, et (ii) le 'glissement hétérogène' où seul un nombre réduit de plans sont concernés mais avec une intensité plus importante (Cf.figure D-5).

b) Transformation fibrillaire-Modèle de Peterlin

Pour de fortes déformations, ***Peterlin*** *[4][5]*a proposé le premier un modèle moléculaire pour décrire la transformation fibrillaire qui s'opère lors du passage de la striction sur le PEHD sans prendre en compte le rôle de la phase amorphe. Il suggère que la déformation des polymères semi-cristallins consiste en l'inclinaison des lamelles le cisaillement et la déformation plastique des cristaux et finalement la formation de microfibrilles. A savoir que cette approximation n'est pas valide pour les polymères semi-cristallins contenant une phase amorphe. Etant caoutchoutique, le rôle mécanique de cette phase se réduit à la transmission des contraintes d'une cristallite à l'autre par l'intermédiaire des molécules liantes. En outre, les macromolécules constituant la phase amorphe liées sont à l'origine de la création d'une force de retour vers l'état non déformé. Pour illustrer le déplacement des chaînes dans les zones amorphes interlamellaires, plusieurs auteurs ont utilisé un modèle simple de composition à deux phases, qui s'applique bien aux polymères semi-cristallins. Ce modèle met en jeu les deux mécanismes de déformation qui sont : [6]

- Glissement inter-lamellaire : Suite au cisaillement de la phase amorphe, les cristaux lamellaires glissent parallèlement les unes par rapport aux autres sous l'effet des contraintes appliquées (Figure D-6).
- Séparation inter-lamellaire : Ce phénomène se traduit par une séparation des lamelles cristallines suite à une application d'une contrainte de traction ou de compression perpendiculairement à la surface des lamelles cristallines ; dans ce cas, les chaînes macromoléculaires de la phase amorphe sont étirées ou compressées (Figure D-6).

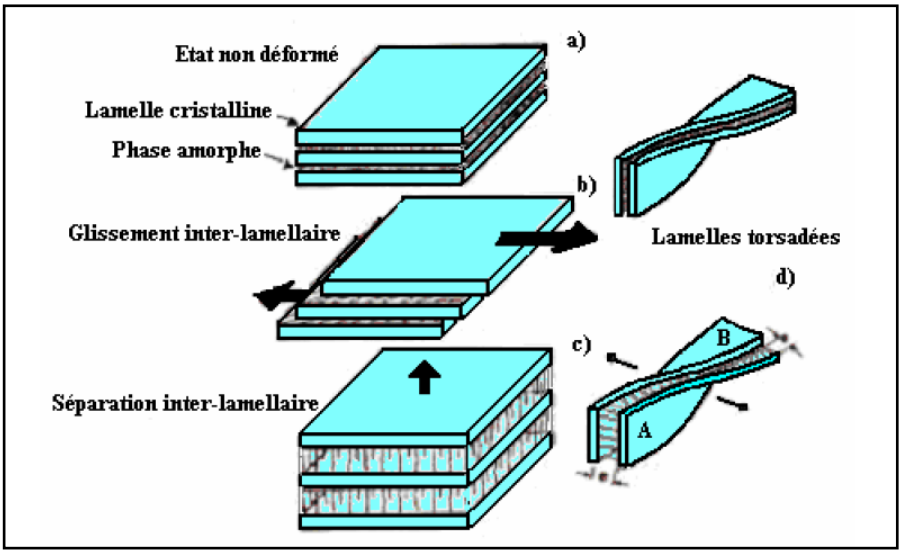

Figure D-6 Micro-mécanismes de déformation de la phase amorphe dans un polymère semi-cristallin

Dans le cas des lamelles cristallines torsadées, les deux mécanismes peuvent coexister au sein d'une même phase interlamellaire. D'où le modèle de ***Schultz*** [7][8] Ce modèle se décompose en trois étapes à partir de l'architecture initiale de deux lamelles séparées par une phase amorphe (modèle bicouche), comme le montre la figure D-7 :

- *Avant l'apparition de la striction* : Extension des molécules de liaison par séparation et glissement inter-lamellaire, puis basculement des chaînes par cisaillement cristallin homogène.

- *Apparition de la striction* : Fragmentation des lamelles par cisaillement hétérogène.

- *Après le passage de la striction* : Alignement des chaînes des nano-blocs cristallins dans l'axe de sollicitation, formation de la morphologie fibrillaire.

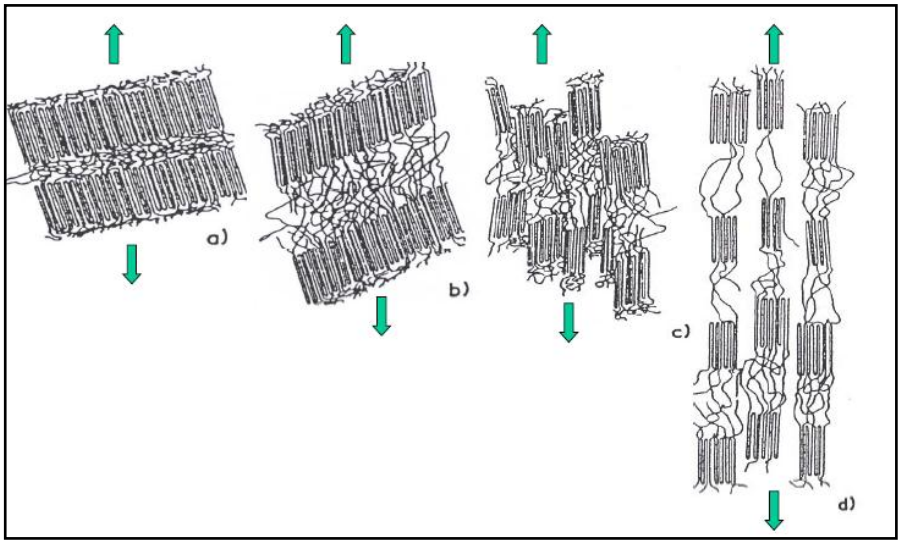

Figure D-7 Mécanisme de déformation des lamelles cristallines. a-état initial, b-extension des chaînes dans les lamelles, c-fragmentation des lamelles, d-alignements des blocs selon la direction du tirage

II Déformation plastique d'un polymère solides vitreux/ Mécanismes de déformation : généralités

Dans les polymères amorphes vitreux, lors de la déformation plastique, différents micro-mécanismes de plasticité permettant de dissiper de l'énergie peuvent être mis en jeu par le matériau. Deux mécanismes sont souvent été observés ; le cisaillement et le craquelage. Ces mécanismes sont compétitifs et leur observation va dépendre de la nature macromoléculaire du matériau et de la nature de chargement [9].

a) *Cisaillement [10]*

Le cisaillement est basé sur un phénomène de glissement. Il se manifeste par la propagation de bandes de cisaillement plus ou moins diffuses dans tout le matériau et qui s'opère sans variation du volume. Deux types de cisaillement ont été mis en évidence :

- Cisaillement localisé ou fine slip matérialisé par des bandes de 0.3 à 3µm de largeur. Ces bandes conduisent généralement à une rupture fragile.

- Cisaillement diffus ou 'coarse slip' formé par juxtaposition des bandes fines et courtes et développe de plasticité.

b) *Formation de craquelures ou « crazing »*

Les craquelures ressemblent à des petites fissures amorcées sur des sites de concentration de contrainte causées par des défauts (impuretés, porosités initiales, rayures en surface…) [11]. Elles se propagent perpendiculairement à l'axe de traction. Les deux surfaces libres de la fissure sont liées entre elles par une succession quasi-périodique de fibrilles comme le montre la figure D-8 [12]. Dans le cas des polymères amorphes vitreux, ce mécanisme représente un processus de cavitation et est accompagné par une variation du volume du fait de la création de micro-vides. Le mécanisme d'ouverture est à l'origine d'une croissance de ces cavités suivant l'axe de sollicitation. Dans les polymères semi-cristallins, les craquelures sont de petite dimension, leur propagation est gênée par les cristallites. A savoir que la structure spécifique de la craquelure lui confère un comportement cohésif malgré la cavita-

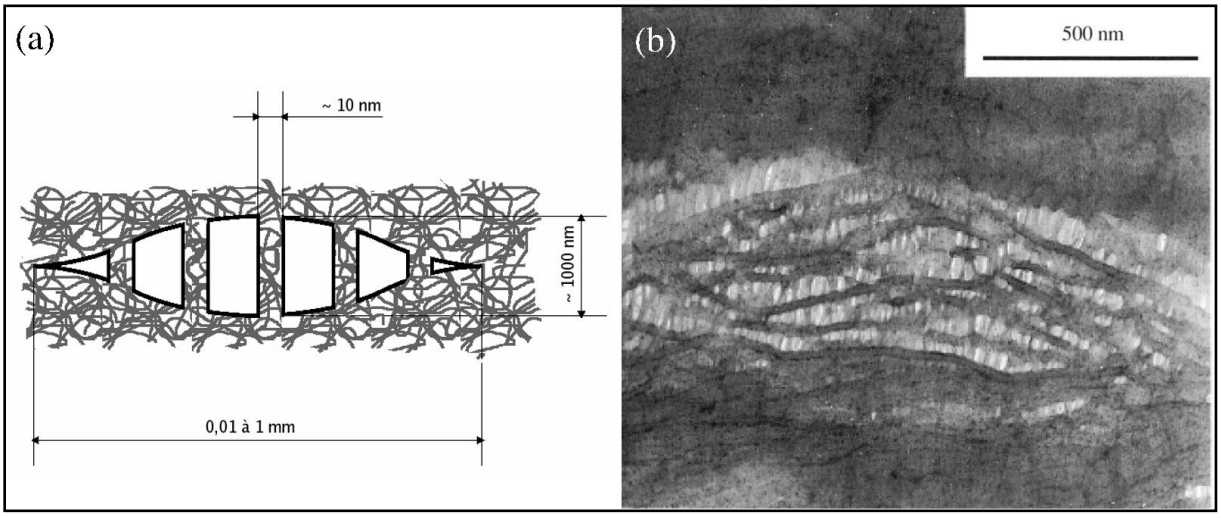

Figure D-8 a) Schéma d'une craquelure dans un polymère amorphe vitreux. (b) Image MET
tion.

III Apparition des instabilités plastiques à dans les polymères vitreux

Les procédés de mise en forme des polymères à l'état solide (thermoformage et étirage des films) sont affectés par des phénomènes d'instabilité plastique. Ces instabilités correspondent à différents mécanismes de localisation de la déformation à différentes échelles d'observation (i) Echelle microscopique (quelques nanomètres) : cascades de changements conformationnels des macromolécules, (ii) Echelle mésoscopique (quelques micromètres) : bandes de déformation et hétérogénéités intra-sphérolitiques, (iii) Echelle macroscopique (quelques millimètres) : striction généralisée ou striction localisée.

Ce phénomène contrôle l'aspect et les performances du produit final. Il est donc indispensable de comprendre les mécanismes à l'origine de l'instabilité plastique. Nous nous intéressons en particulier à l'initiation et à la propagation de la striction, sur lesquelles de nombreux auteurs ont travaillé. Ce mode d'instabilité se distingue par des bandes de cisaillement et des strictions obliques localisées (Figure D-9).

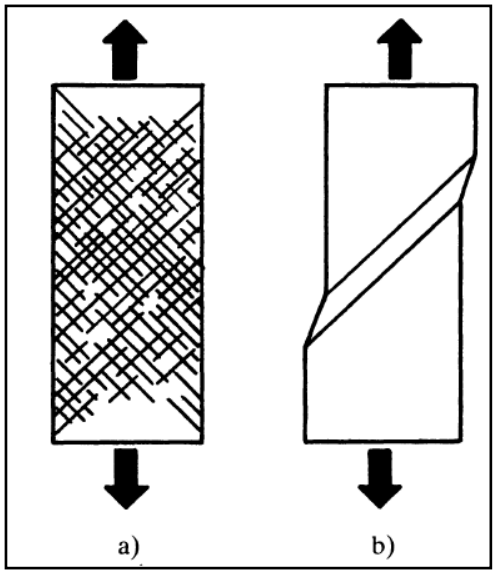

Figure D-9 Bandes de cisaillement (a) diffuses ou (b) localisées au cours de la traction d'un polymère vitreux

References

[1] Schirrer R. "Les craquelures dans les polymeres", Introduction à la mecanique des polymeres, 1ère edition. G'Sell C, Haudin, JM, France. 395-404. 1995.

[2] Young RJ, Bowden PB, Ritchie JM, Rider JG. Deformation mechanisms in oriented high-density polyethylene. Journal of Material Science. 8(1): 23-26. 1973.

[3] Young RJ, Bowden PB. Twinning and martensitic transformations in oriented high-density polyethylene. Philosophical Magazine. 29(5): 1061-1073. 1974.

[4] Peterlin A. Molecular model of drawing polyethylene and polypropylene. Journal of Materials Sciences. 6(6): 490-508. 1971.

[5] Petermann J, Kluge W, Gleiter H. Electron microscopic investigation of the molecular mechanism of plastic deformation of polyethylene and isotactic polystyrene crystals. Journal of Polymer Sciences. 17(6), 1043-1051. 1979.

[6] Langroudi AE. Etude de la déformation viscoélastique et plastique du PET amorphe et semi-cristallin, autour de la transition vitreuse, Thèse à l'INSA à Lyon. 202P. 1999.

[7] Schultz JM. Book review: Polymer materials science Prentice-Hall, Englewood Cliffs, NJ, Harrison. The Pennsylvania State University, 524 pages. 1974.

[8] Schultz JM. Review: deformation mechanisms in crystalline polymers. Polymer Materials and Sciences. 2034-2051. 1974.

[9] Labour T. Microstructure et comportement mécanique du polypropylène chargé, thèse à l'INSA de Lyon. 239 P. 1999.

[10] Schultz J. Mechanical behavior of semi-crystalline polymers. Polymer Materials science. New Jerse: Prentice hall. INC. 2-1: 513P. 1974.

[11] Plummer CJG, Cudré-Mauroux N, Kausch HH. Deformation and entanglement in semi-crystalline polymers. Polymer Engineering & Science. 34(4): 318–29. 1994.

[12] Kausch HH, Heymans N, Plummer CJ, Decroly P. Matériaux polymères : Propriétés mécaniques et physique. ISBN: 2-88074-415-6. 660 pages. 2001.

FOLIO ADMINISTRATIF

THESE SOUTENUE DEVANT L'INSTITUT NATIONAL DES SCIENCES APPLIQUEES DE LYON

NOM : AL-ITRY DATE de SOUTENANCE : Mardi 27 Novembre 2012

Prénoms : Racha

TITRE : Mélanges de polymères à base de Poly (acide lactique) : Structure/ Rhéologie/ Procédés de mise en forme

NATURE : Doctorat Numéro d'ordre :

Ecole doctorale : Ecole doctorale Matériaux de Lyon

Spécialité : Matériaux Polymères

RESUME : Ce travail de thèse porte sur l'étude des relations structure/procédés de mise en forme/propriétés finales de matériaux polymères à base de PLA/PBAT. Ces derniers sont destinés à l'emballage alimentaire en vue de remplacer le polyéthylène téréphtalate (PET). Cependant le PLA a certaines limites de processabilité par les technologies de la plasturgie. Le renforcement de ses propriétés à l'état fondu a été obtenu grâce à l'introduction d'un époxyde multifonctionnel capable de réagir avec les bouts de chaînes des polyesters. Aussi, des mélanges à base de PLA/PBAT ont été mis en œuvre en vue de conférer la ductilité au matériau final.

La première étape consiste en la compréhension des mécanismes de dégradation thermique et hydrolytique des deux polymères PLA et PBAT au cours des processus de mise en œuvre. En effet, la réaction d'extension des chaînes couplée au branchement induits par l'époxyde multifonctionnel palie cette dégradation. Les mécanismes d'extension de chaînes et de branchements sous-jacents ont été mis en évidence par l'analyse des énergies d'activation, des spectres de relaxation à l'état fondu ainsi que celle des grandeurs physico-chimiques en solution. En outre, les représentations de Van-Gurp-Palmen confirment la co-existence de chaînes macromoléculaires linéaires et aléatoirement branchées.

La seconde étape de ce travail a été dédiée à la compatibilisation des mélanges PLA/PBAT par ce même époxyde multifonctionnel. Des études expérimentales modèles basées sur la détermination de la tension interfaciale et la modélisation rhéologique ont montré le rôle majeur de compatibilisant induit par cet agent réactif. Ainsi, la diminution de la tension interfaciale confère à ces matériaux une meilleure cohésion interfaciale et une morphologie fine et homogène de la phase dispersée, accompagnée par l'amélioration des propriétés mécaniques.

L'étude des propriétés rhéologiques en cisaillement et en élongation des matériaux modifiés a permis de montrer une meilleure tenue mécanique à l'état fondu. Ainsi, une meilleure aptitude à l'extrusion gonflage a été démontrée en élargissant leurs cartes de stabilité.

Parallèlement à ces travaux, des études de bi-étirage des polymères seuls, de leurs homologues modifiés et de leurs mélanges montrent un durcissement structural, dû à la cristallisation induite sous déformation. Les morphologies cristallines ont été analysées finement par des méthodes calorimétriques et spectroscopiques.

Enfin, ces études ont été transposées à l'élaboration et à la compréhension des comportements d'une formulation industrielle complexe à base de PLA, PBAT et de farine céréalière plastifiée.

MOTS-CLES : Poly (acide lactique), Extension de chaînes, Branchement, Compatibilisation, Rhéologie, déformation bi-axiale, Extrusion-gonflage

Laboratoire (s) de recherche : Ingénierie des Matériaux polymères (IMP@INSA)

Directeur de thèse: MAAZOUZ Abderrahim
Co-encadrant de thèse : LAMNAWAR Khalid

Président de jury :

Composition du jury : BILLON Noëlle, Professeur (Mines-ParisTech, Sophia Antipolis)
GROHENS Yves, Professeur (Laboratoire d'Ingénierie des Matériaux de Bretagne)
BOUSMINA Mosto, Professeur (Académie Hassan II des sciences et techniques, Maroc)
CARROT Christian, Professeur (Université Jean Monnet, IMP@UJM, Saint Etienne)
LAMNAWAR Khalid, Maître de conférences (INSA de Lyon)
MAAZOUZ Abderrahim, Professeur (INSA de LYON)

Invités JANIN Claude, Docteur (Ulice/Limagrain, Clermont Ferrand)
LACRAMPE Valérie, Docteur (Toray Films Europ)